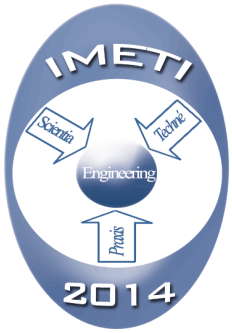

The 7th International Multi-Conference on Engineering and Technological Innovation

July 15 - 18, 2014 – Orlando, Florida, USA

PROCEEDINGS

Post-Conference Edition

Edited by:

Nagib Callaos
Hsing-Wei Chu
Belkis Sánchez
Michael Savoie
Andrés Tremante

Organized by

International Institute of Informatics and Systemics

Member of the International Federation for Systems Research (IFSR)

COPYRIGHT

The papers of this book comprise the proceedings of the conference mentioned on the title and the cover page. They reflect the authors' opinions and, with the purpose of timely disseminations, are published as presented and without change. Their inclusion in these proceedings does no necessarily constitute endorsement by the editors.

ISBN: 978-1-941763-12-4

PROGRAM COMMITTEE

Chairs: Hsing-Wei Chu (USA) and C. Dale Zinn (USA)

Adascalitei, Adrian	Gheorghe Asachi Technical University of Iaşi	Romania
Aguilar Torres, Fernando J.	University of Almeria	Spain
Al Obaidy, Mohaned	Gulf College	Oman
Al-Aomar, Raid	Jordan University of Science and Technology	Jordan
Amelink, Catherine	Virginia Tech	USA
Ariwa, Ezendu	London Metropolitan University	UK
Ashraph, Sulaiman	National University of Rwanda	Rwanda
Ayuga Téllez, Esperanza	Polytechnic University of Madrid	Spain
Barberà, Elena	Open University of Catalonia	Spain
Batos, Vedran	University of Dubrovnik	Croatia
Bekiaris, Evangelos	The Centre for Research & Technology, Hellas	Greece
Bernitzky, Dominik	Medical University of Vienna	Austria
Bönke, Dietmar	Reutlingen University	Germany
Braghin, Francesco	Polytechnic University of Milan	Italy
Bubnov, Alexey	Academy of Sciences and the Czech Republic	Czech Republic
Bye, Beverly J. D.	Stevenson University	USA
Cázares-Rangel, Víctor M.	Autonomous University of Nuevo Leon	Mexico
Chang, Maiga	Athabasca University	Canada
Chang, Wen-Kui	Tunghai University	Taiwan
Chen, Yuhua	University of Houston	USA
Cinquemani, Simone	Polytechnic University of Milan	Italy
Cubukcu, Feryal	Dokuz Eylul University	Turkey
Curran, Kevin	University of Ulster	UK
Dawoud, Dawoud S.	Victoria University	Uganda
Eby, Gulsun	Anadolu University	Turkey
Elmasry, Sarah	United Arab Emirates University	United Arab Emirates
Fúster-Sabater, Amparo	Institute of Applied Physics	Spain
Gangadharan, Sathya	Embry-Riddle Aeronautical University	USA
Gegner, Jürgen	University of Siegen	Germany
Gohil, Dipakkumar	Sardar Vallabhbhai National Institute of Technology	India
Guerlesquin, Gaël	Université de technologie Belfort-Montbéliard	France

Guijarro-Fuentes, Pedro	University of Plymouth	UK
Haggag, Mahmoud	United Arab Emirates University	United Arab Emirates
Hepdogan, Seyhun	University of Central Florida	USA
Hossain, Shazzat	Ryerson University	Canada
Iovan, Stefan	Romanian Railway IT Company	Romania
Izydorczyk, Jacek	Silesian University of Technology	Poland
Jazar, Reza N.	Royal Melbourne Institute of Technology University	Australia
Jesudoss, Auxeeliya	National University of Rwanda	Rwanda
Jingchao, Chen	University Donghua	China
Juanals, Brigitte	Université Paris Ouest Nanterre La Défense	France
Kawamura, Kimito	Asahi Group Holdings, Ltd	Japan
Klosowski, Piotr	Silesian University of Technology	Poland
Kobielarz, Magdalena	Wroclaw University of Technology	Poland
Koleva, Maria	Bulgarian Academy of Sciences	Bulgaria
Kothaneth, Shreya	Virginia Tech	USA
Kotnana, Ratnakar	National University of Rwanda	Rwanda
Kuipers, Ulrich	University of Applied Sciences Südwestfalen	Germany
Lahlouhi, Ammar	University of Biskra	Algeria
Lamastra Pacheco, Giovanna	Brazilian Institute of Capital Markets	Brazil
Lappas, Georgios	Technological Educational Institution of Western Macedonia	Greece
Lefevre, Thierry	Center for Energy Environment Resources Development	Thailand
Letia, Tiberiu	Technical University of Cluj-Napoca	Romania
Leuva, Dhawal	Embry-Riddle Aeronautical University	USA
Li, Longzhuang	Texas A&M University-Corpus Christi	USA
Li, Man-Sze	IC Focus Ltd.	UK
Litvin, Vladimir	California Institute of Technology	USA
López Román, Leobardo	University of Sonora	Mexico
Luh, Guan-Chun	Tatung University	Taiwan
Machado Caldeira, André	Sulamerica	Brazil
Mahdjoub, Morad	Université de Technologie Belfort-Montbéliard	France
Mauntz, Manfred	CMC Instrumnents GmbH	Germany
Mbobi, Aime Mokhoo	Centennial College	Canada
Minel, Jean-Luc	Université Paris Ouest Nanterre La Défense	France
Mohammadi, Farah	Ryerson University	Canada
Naddeo, Alex	University of Salerno	Italy
Nagai, Yasuo	Tokyo University of Information Sciences	Japan
Ngabonziza, Yves	The City University of New York	USA
Nožička, Jiří	Czech Technical University in Prague	Czech Republic
Oberer, Birgit	University of Klagenfurt	Austria

Okita, Yuji	Kanazawa Institute of Technology	Japan
Petit, Frédéric	Argonne National Laboratory	USA
Phillips, Steve	FEHRL Knowledge Centre	Belgium
Pillai, Krish	Lock Haven University of Pennsylvania	USA
Plasenzotti, Roberto	Medical University of Vienna	Austria
Priesler (Moreno), Miri	Ruppin Academic Center	Israel
Pursell, David	University System of Georgia	USA
Rai, Bharatendra K.	University of Massachusetts Dartmouth	USA
Reichman, Arie	Ruppin Academic Center	Israel
Resta, F.	Polytechnic University of Milan	Italy
Sagot, Jean-Claude	Université de Technologie Belfort-Montbéliard	France
Sala, Nicoletta	University of Italian Switzerland	Italy
Sathyanarayan, Priya	Embry-Riddle Aeronautical University	USA
Schaetter, Alfred	Pforzheim University	Germany
Schumacher, Jens	University of Applied Sciences Vorarlberg	Austria
Shiraishi, Yoshiaki	Nagoya Institute of Technology	Japan
Siddique, Mohammad	Fayetteville State University	USA
Singh, Harwinder	Guru Nanak Dev Engineering College	India
Skawinska, Eulalia	Poznan University of Technology	Poland
Soares Machado, María A.	Brazilian Institute of Capital Markets	Brazil
Staretu, Ionel	Transilvania University of Brasov	Romania
Sulema, Yevgeniya	National Technical University of Ukraine	Ukraine
Suzuki, Hiroshi	GE Energy	Japan
Suzuki, Takamasa	Kansai University	Japan
Tam, Wing K.	Swinburne University of Technology	Australia
Thundat, Thomas	University of Alberta	Canada
Vaida, Mircea-Florin	Technical University of Cluj-Napoca	Romania
Velázquez-Araque, Luís	Czech Technical University in Prague	Czech Republic
Vrána, Stanislav	Czech Technical University in Prague	Czech Republic
Williams van Rooij, Shahron	George Mason University	USA
Xeni, Elena	University of Cyprus	Cyprus
Yadav, S. M.	Sardar Vallabhbhai National Institute of Technology	India
Yamamoto, Hideki	Kansai University	Japan
Zainon Hamzah, Zaitul Azma	Putra Malaysia University	Malaysia
Zalewski, Romuald I.	Poznan University of Technology	Poland
Zaretsky, Esther	Hebrew University	Israel
Zobaa, Ahmed	University of Exeter	UK

ADDITIONAL REVIEWERS

Acma, Bulent	Anadolu University	Turkey
Acosta Rodríguez, José Á.	University of Seville	Spain
Albayrak, Y. Esra	Galatasaray University	Turkey
Andreev, Rumen	Bulgarian Academy of Sciences	Bulgaria
Aruga, Masahiro	Teikyo Heisei University	Japan
Badran, Omar	Al-Balqà Applied University	Jordan
Balas, Valentina	Aurel Vlaicu University of Arad	Romania
Barreiro, Joaquín	University of Leon	Spain
Barzev, Kiril	University of Rousse	Bulgaria
Batovski, Dobri Atanassov	Assumption University of Thailand	Thailand
Bayraktar, Emin	Paris Mechanics Institute	France
Bayraktar, Seyfettin	Yildiz Technical University	Turkey
Bhattacharya, Mithu	College of Business Administration, University of Detroit Mercy	USA
Bigan, Cristin	Ecological University of Bucharest	Romania
Bilich, Feruccio	University of Brasilia	Brazil
Brayner, Carlos	Federal University of Pernambuco	Brazil
Carrió Pastor, M. Luisa	Polytechnic University of Valencia	Spain
Challoo, Linda	Texas A&M University-Kingsville	USA
Chen, Jing-Heng	Feng Chia University	Taiwan
Chow, James	University Health Network	Canada
Chu, Hsing-Wei	Lamar University	USA
Del Valle, María	Universidad de Concepción	Chile
Delgado, Alberto	National University of Colombia	Colombia
Deng, Hepu	RMIT University	Australia
Devrim, Yilser	Atılım University	Turkey
Dijkstra, Jan	Eindhoven University of Technology	Netherlands
Doughan, Mahmoud	Lebanese University	Lebanon
Drid, Saïd	University of Batna	Algeria
El Kashlan, Ahmed	Academy for Science and Technology	Egypt
Elwany, Hamdy	Alexandria University	Egypt
Erbacher, Robert	Utah State University	USA
Federici, Stefano	University of Perugia	Italy

Fidan, Ismail	Tennessee Technological University	USA
Fiorini, Rodolfo	Politecnico di Milano	Italy
Frosch-Wilke, Dirk	University of Applied Sciences	Germany
Gallucci, Fausto	Eindhoven University of Technology	Netherlands
Garro, Alfredo	University of Calabria	Italy
Glowacki, Miroslaw	AGH University of Science and Technology	Poland
Goi, Chai Lee	Curtin University	Malaysia
Granovsky, Alex	Moscow State University	Russian Federation
Gujarathi, Ashish M.	Birla Institute of Technology and Science	India
Gutiérrez-Torres, C.	National Polytechnic Institute	Mexico
Hadzilias, Elias A.	National Technical University of Athens	Greece
Hardman, John	Florida Atlantic University	USA
Hassini, A.	Laboratory of Application and Analysis of Radiations	Algeria
Hassini, Abdelatif	University of Oran	Algeria
Hirz, Mario	Graz University of Technology	Austria
Ibrahim, Rahinah	Putra Malaysia University	Malaysia
Jang, Jongwook	Dongeui University	South Korea
Jastroch, Norbert	MET Communications	Germany
Jha, Ranjana	Netaji Subhas Institute of Technology	India
Jiang, Jinlei	Tsinghua University	China
Kaewarsa, Suriya	Rajamangala University of Technology Isan	Thailand
Kamrani, Ehsan	Polytechnic Montreal	Canada
Kannan, Rajkumar	Bishop Heber College	India
Kässi, Tuomo	Lappeenranta University of Technology	Finland
Khudayarov, Bakhtiyar	Tashkent Institute of Irrigation and Melioration	Uzbekistan
Komerath, Narayanan	Georgia Institute of Technology	USA
Li, Chengcheng	University of Cincinnati	USA
Li, Dayong	Shanghai Jiao Tong University	China
Li, Yu-Chiang	Southern Taiwan University	Taiwan
Lin, Chih-Ting	National Taiwan University	Taiwan
Lin, Chun Yuan	Chang Gung University	Taiwan
Liu, Tingyang Lewis	National Kaohsiung Normal University	Taiwan
Luqman, Chuah A.	University Putra Malaysia	Malaysia
Mahdoum, Ali	Centre de Développement des Technologies Avancées	Algeria
Mikhaylov, Ivan A.	University of Central Florida	USA
Mokhtari, A.	Versailles Saint-Quentin-en-Yvelines University	France
Morel, Eneas N.	National Technological University	Argentina
Moschim, Edson	State University of Campinas	Brazil
Navas, Luis Manuel	University of Valladolid	Spain
Neves, Luís F. F.	University of Louisville	USA
Olson, Richard C. L.	Enercon Services, Inc.	USA

Otto, Tauno	Tallinn University of Technology	Estonia
Popa, Rustem	University of Galati	Romania
Puslecki, Zdzislaw	Adam Mickiewicz University	Poland
Raj, Piyush	DNV GL	India
Reggiani, Luca	Politecnico di Milano	Italy
Ritter, Arthur	Stevens Institute of Technology	USA
Rodríguez L., Gloria I.	National University of Colombia	Colombia
Romero, Rosenberg J.	Autonomous University of the State of Morelos	Mexico
Ros, L.	Polytechnic University of Valencia	Spain
Rot, Artur	Wroclaw University of Economics	Poland
Rydhagen, Birgitta	Blekinge Institute of Technology	Sweden
Safarik, Pavel	Czech Technical University in Prague	Czech Republic
Sane, Vijay	American Institute of Chemical Engineers	India
Schmidt, Jon A.	Burns and McDonnell	USA
Serodio, Carlos	University of Trás-os-Montes and Alto Douro	Portugal
Skoko, Hazbo	Charles Sturt University	Australia
Song, Yulin	Memorial Sloan-Kettering Cancer Center	USA
Spina, Edison	University of Sao Paulo	Brazil
Šraml, Matjaž	University of Maribor	Slovenia
Sumaili, Jean Akilimali	Institute for Systems and Computer Engineering of Porto	Portugal
Süral, Haldun	Middle East Technical University	Turkey
Sutherland, Trudy	Vaal University of Technology	South Africa
Tobar, Carlos Miguel	Pontifical Catholic University of Campinas	Brazil
Travieso-González, Carlos M.	University of Las Palmas de Gran Canaria	Spain
Turcu, Cristina	Stefan cel Mare University of Suceava	Romania
Udén, Maria	Lulea University of Technology	Sweden
Vaganova, Natalia	Institute of Computational Mathematics and Mathematical Geophysics	USA
Verstichel, Stijn	Ghent University	Belgium
Virvilaite, Regina	Kaunas University of Technology	Lithuania
Vlasiou, Maria	Eindhoven University of Technology	Netherlands
Vukadinovic, Dinko	University of Split	Croatia
Wang, Ching-Huang	National Formosa University	Taiwan
Wen, Fuh-Liang	St. John`s University	Taiwan
Wolfengagen, Viacheslav	Institute for Contemporary Education JurInfoR-MSU	Russian Federation
Yang, Lei	Tongji University	China
Yoon, Changwoo	Electronics and Telecommunications Research Institute	South Korea
Zeman, Klaus	Johannes Kepler University Linz	Austria
Zhou, Zehai	University of Houston-Downtown	USA

ADDITIONAL REVIEWERS FOR THE NON-BLIND REVIEWING

Abramchuk, George H.	Measurement Technologies and Advanced Applications	Canada
Al-Hussein, Mohamed	University of Alberta	Canada
Begun, Siegfried	ETCOP Switzerland	Switzerland
Boubakeur, Ahmed	Ecole Nationale Polytechnique	Algeria
Casolo, Federico	Politecnico di Milano	Italy
Chávez, Gustavo	IEEE	El Salvador
Chen, Nan-Kuang	National United University	Taiwan
Chen, Ray	University of Texas, Austin	United States
Chou, Te-Shun	East Carolina University	United States
Cinquemani, Simone	Politecnico di Milano	Italy
Dao, Trung-Kien	Hanoi University of Science and Technology	Vietnam
Duan, Xuechao	Xidian University	China
Gyula, Horváth	University of Szeged	Hungary
Hafez, Bahaa	Texas A&M University	United States
Haralambopoulos, Dias A.	University of the Aegean	Greece
He, Haibo	University of Rhode Island	United States
Hundhausen, Martin	University of Erlangen-Nuremberg	Germany
Hwang, Sungho	Samsung	South Korea
Ibeas, Asier	Autonomous University of Barcelona	Spain
Ioana, Adrian	University Politehnica of Bucharest	Romania
Jastroch, Norbert	MET Communications	Germany
Jiménez Ferrero, María del C.	National Polytechnic Institute	Mexico
Kapley, Atya	National Environmental Engineering Research Institute	India
Khanduja, Gagandip Singh	L.C. Institute of Technology	India
Lee, Sung-Woon	Tongmyoung University	South Korea
Legnani, Giovanni	Università di Brescia	Italy
Li, Peng	East Carolina University	United States
Li, Ping	University of the Health Sciences	United States
Lijewski, Piotr	Poznan University of Technology	Poland
Luo, Ningsu	University of Girona	Spain

Marrone, Dan	Farmingdale State College	United States
Mendes, Francisca Dantas	University of São Paulo	Brazil
Merkisz, Jerzy	Poznan University of Technology	Poland
Moschim, Edson	State University of Campinas	Brazil
Nagai, Yasuo	Tokyo University of Information Sciences	Japan
Németh, Tamás	University of Szeged	Hungary
Raahemifar, Kaamran	Ryerson University	Canada
Rankin, Jeff	University of New Brunswick	Canada
Rao, Gottapu Sasi Bhushana	Andhra University	India
Rodríguez R., Ana Mª	University of Vigo	Spain
Safarik, Pavel	Czech Technical University in Prague	Czech Republic
Salah Morsy, Ahmed	Texas A&M University	United States
Sanches Silva, Ana T.	National Institute of Health Dr Ricardo Jorge	Portugal
Savaroglu, Gokhan	Eskisehir Osmangazi University	Turkey
Si Hong, Hoang	Hanoi University of Science and Technology	Vietnam
Solórzano, Edgar	IEEE	El Salvador
Stöhr, Michael	B.A.U.M	Germany
Thomas, Tg	Bits Philani	United Arab Emirates
Tomczyk, Andrzej	Rzeszow University of Technology	Poland
Vázquez, Laura	University of Vigo	Spain
Vázquez, Manuel	University of Santiago de Compostela	Spain
Yagoub, Mustapha	University of Ottawa	Canada
Yang, Haomiao	University of Electronic Science and Technology of China	China
Zakatistovs, Atis	Riga Business School	Latvia
Zayed, Tarek	Concordia University	Canada
Zhang, Guoping	Morgan State University	United States
Zhou, Qin	China University of Geosciences	China
Zsakó, László	Eötvös Loránd University	Hungary

The 7th International Multi-Conference on Engineering and Technological Innovation: IMETI 2014

HONORARY CHAIR
William Lesso

PROGRAM COMMITTEE CHAIRS
Hsing-Wei Chu
C. Dale Zinn

GENERAL CHAIR
Nagib Callaos

ORGANIZING COMMITTEE CHAIRS
Belkis Sánchez
Andrés Tremante

CONFERENCE PROGRAM MANAGER /
HARDCOPY PROCEEDINGS PRODUCTION CHAIR
Maria Sánchez

TECHNICAL CONSULTANT ON COMPUTING SYSTEM /
CD PROCEEDINGS PRODUCTION CHAIR
Juan Manuel Pineda

META REVIEWERS SUPPORT
Dalia Sánchez

SYSTEM DEVELOPMENT, MAINTENANCE AND DEPLOYMENT
Dalia Sánchez
Keyla Guédez

OPERATIONAL ASSISTANTS
Marcela Briceño

HELP DESK
Juan Esqueda

Special Track on Cybernetics and Information Technologies, Systems and Applications: CITSA 2014
In the Context of
The 7th International Multi-Conference on Engineering and Technological Innovation: IMETI 2014

HONORARY PRESIDENT
William Lesso

GENERAL CHAIR
Michael Savoie

ORGANIZING COMMITTEE CHAIR
José Ferrer

PROGRAM COMMITTEE

Chair: Hsing-Wei Chu (USA)

Agrawalla, Raman	Tata Consutlancy Services	India
Aguilar, José	University of the Andes	Venezuela
Bubnov, Alexey	Academy of Science of the Czech Republic	Czech Republic
Chang, Tsun-Wei	De Lin Institute of Technology	Taiwan
Fries, Terrence P.	Indiana University of Pennsylvania	USA
Głowacki, Mirosław	AGH University of Science and Technology	Poland
Halverson, Ranette	Midwestern State University	USA
Kim, Moo Wan	Tokyo University of Information Sciences	Japan
Kobayashi, Hideo	Mie University	Japan
Leu, Fang-Yie	Tunghai University	Taiwan
Leung, Lin	City University of New York	USA
Li, Xiangdong	City University of New York	USA
Liu, Chuan-Ming	National Taipei University of Technology	Taiwan
Martinez, Christopher	University of New Haven	USA
Mbobi, Aime Mokhoo	Centennial College	Canada
Mori, Kazuo	Mie University	Japan
Müller, Wilmuth	Fraunhofer IITB	Germany
Mundani, Ralf-Peter	Technical University of Munich	Germany
Naito, Katsuhiro	Mie University	Japan
Oya, Hidetoshi	University of Tokushima	Japan
Pawliczek, Piotr	AGH University of Science and Technology	Poland
Portnoy, Jacov	Ben-Gurion University of the Negev	Israel
Priesler, Miri	Ruppin Academic Center	Israel
Ramos, Ana Luísa	University of Aveiro	Portugal
Romanowska-Pawliczek, Anna	AGH University of Science and Technology	Poland
Simpson, William R.	Institute for Defense Analyses	USA
Sołtys, Zbigniew	Jagiellonian University	Poland

Su, Meng	Penn State University	USA
Thuo, Gikiri	Florida Agricultural and Mechanical University	USA
Zaretsky, Esther	The Academic College for Education Givat Washington	Israel

ADDITIONAL REVIEWERS

Ahmadi, Sohrab	University of Angers	France
Al. Obaidy, Mohaned	Gulf College	Oman
Almeida, Maria das Graças	Federal Center For Technological Education of Minas Gerais	Brazil
Amouzad Mahdiraji, Ghafour	University Putra Malaysia	Malaysia
Bigan, Cristin	Ecological University of Bucharest	Romania
Bouslimani, Yassine	University of Moncton	Canada
Capella H., Juan V.	Polytechnic University of Valencia	Spain
Chang, Herbert	National Yang-Ming University	Taiwan
Cingula, Marijan	University of Zagreb	Croatia
Collazos, César	University of Cauca	Colombia
Dash, Tirtharaj	Veer Surendra Sai University of Technology Burla	India
De Sitter, Jan	University of Antwerp	Belgium
Erkollar, Alptekin	University of Applied Sciences	Austria
Fesenko, Volodymyr	Kharkiv National University of Radio Electronics	Ukraine
Fu, Yujian	Alabama A&M University	USA
Fujita, Hamido	Iwate Prefectural University	Japan
Giannini, Franco	University of Rome Tor Vergata	Italy
Gómez Galán, José	Metropolitan University	Puerto Rico
Holgado, Otilia	Ministère de l'Agriculture, de l'Alimentation, de la Pêche	France
Imaña, José Luis	Complutense University of Madrid	Spain
Jang, Jongwook	Dongeui University	South Korea
Jayasuriya, Terrance Douglas	Institute of Engineering and Technology	Brunei Darussalam
Kamsin, Amirrudin	University of Malaya	Malaysia
Kaneko, Itaru	Tokyo Polytechnic University	Japan
Karimi, Bijan	University of New Haven	USA
La Rue, E	University of Pittsburgh	USA
Lee, In Soo	Kyungpook National University	South Korea
Lenuta, Alboaie	S. C. Axiologic Research S. R. L - IT Company	Romania
Liu, Ziping	Southeast Missouri State University	USA
Lu, Yun	Florida International University	USA
Maekawa, Mamoru	University of Electro-Communications	Japan
Matavulj, Petar	University of Belgrade	Serbia

Montabert, Cyril	Virginia Polytechnic Institute and State University	USA
Moshonas, Nikolaos	National Technical University of Athens	Greece
Müller, Ludìk	University of West Bohemia	Czech Republic
Musirin, Ismail	Universiti Teknologi Mara	Malaysia
Nahm, In Hyun	Sunmoon University	South Korea
Nutter, Brian	Texas Tech	USA
Odetayo, Michael	Coventry University	UK
Prokes, Ales	Brno University of Technology	Czech Republic
Prykarpatsky, Anatoliy	Ivan Franko Pedagogical State University	Ukraine
Reggiani, Luca	Politecnico di Milano	Italy
Rinaldi, Antonio M.	Università di Napoli Federico II	Italy
Roehrig, Christof	Univerity of Applied Sciences Dortmund	Germany
Rolland, Colette	Université Paris 1	France
Romagni, Susana	Metropolitan University	Venezuela
Rossini, Eugenio	Space Engineering SpA	Italy
Rot, Artur	Wroclaw University of Economics	Poland
San Feliu, Tomas	Polytechnical University of Madrid	Spain
Scheets, George	Oklahoma State University	USA
Schuller, Bjoern	Technische Universitaet Muenchen	Germany
Selby, Richard	Czech University of Life Sciences	Czech Republic
Shestakov, Nikolay	Kirensky Institute of Physics	Russian Federation
Shyr, Wen-Jye	National Changhua University of Education	Taiwan
Silva, Dante	Mapúa Institute of Technology	Philippines
Teixeira, Leonor	University of Aveiro	Portugal
Thomas, Djeisson	Pontifical Catholic University of Rio de Janeiro (PUC-Rio)	Brazil
Thurasamy, Ramayah	Universiti Sains Malaysia	Malaysia
Tsaur, Lih-Feng	Broadcom Inc.	USA
Tsaur, Woei-Jiunn	Inderscience Publishers	Taiwan
Wang, Wendy	San Jose State University	USA
You, Ah Heng	Multimedia University	Malaysia
Yusoff, Zulfadzli	Multimedia University	Malaysia
Zhou, Zehai	University of Houston-Downtown	USA
Zhuang, Yu	Texas Tech University	USA

ADDITIONAL REVIEWERS FOR THE NON-BLIND REVIEWING

Alencastro, Mario Sérgio Cunha	UNINTER	Brazil
Atchison, Martin	Monash University	Australia
Bhatia, Lovkesh	Punjabi University	India

Chen, Wuhua	Guangxi University	China
Figueiredo, Josiel M.	Federal University of Mato Grosso	Brazil
Hwang, Sungho	Samsung	South Korea
Kobayashi, Kentaro	Nagoya University	Japan
Koon, Mahindrapersad	University of Trinidad and Tobago	Trinidad and Tobago
Lee, Sung-woon	Tongmyoung University	South Korea
Mesaric, Josip	J.J. Strossmayer University of Osijek	Croatia
Rawlins, Marisha	University of Trinidad and Tobago	Trinidad and Tobago
Sima, Stanislav	Czech Education and Scientific Network	Czech Republic
Singh, Simranjeet	Punjabi University Patiala	India
Singh, Surinder	Sant Longowal Institute of Engineering & Technology	India
Tahara, Yasuyuki	University of Electro-Communications	Japan
Van Dyck, Colin	University of Mons	Belgium
Verma, Vinod K	Sant Longowal Institute of Engineering & Technology	India
Wang, Yanwu	Huazhong University of Science and Technology	China
Winfield Reyes, Ana María	Instituto Politécnico Nacional	Mexico
Yang, Haomiao	University of Electronic Science and Technology of China	China

Number of Papers Included in these Proceedings per Country

(The country of the first author was the one taken into account for these statistics)

Country	# Papers	%
TOTAL	**27**	**100.00**
Japan	4	14.81
Spain	3	11.11
El Salvador	2	7.41
Hungary	2	7.41
Mexico	2	7.41
United States	2	7.41
Brazil	1	3.70
Canada	1	3.70
China	1	3.70
Czech Republic	1	3.70
India	1	3.70
Iraq	1	3.70
Pakistan	1	3.70
Saudi Arabia	1	3.70
South Korea	1	3.70
Sweden	1	3.70
Venezuela	1	3.70
Vietnam	1	3.70

Foreword

Engineering activities are based on the development of new Knowledge (*Scientia*), new 'made things' (*Techné*), and/or new ways of working and doing (*Praxis*). *Scientia*, *Techné,* and *Praxis* are three important dimensions of a comprehensive conception of Engineering as a whole. Engineering, as *Scientia*, is mostly developed in academia; as *Techné,* is practiced in industry generating technological innovations; and as *Praxis,* is carried out in technical and non-technical organizations, supporting managerial activities and technical procedures, via methodical and methodological design and implementation. This is why Engineering provides one of the most solid academic and professional substrata for bridging among universities, industries and governments.

Publications and conferences related to Engineering are usually oriented to one of its three dimensions. While this is an adequate thing to do when disciplinary focus is sought, it does not represent Engineering as a whole and it misses the very important synergic relationships among the three kinds of engineering activities mentioned above. This is why a group of scholars, professionals, and consultants, in the field of engineering, considered the possibility of organizing a conference where presentations would not be reduced to one specific Engineering dimension, but would foster the participation of academics, practitioners, and managers in the three dimensions of Engineering, in the same conference, so they can synergistically interact with each other. A consequence of this purpose is the organization of The 7th International Multi-Conference on Engineering and Technological Innovation: IMETI 2014, where submissions were accepted for the presentation of:

- **New knowledge** (Engineering as *scientia*);
- **New products and services**, i.e. technological innovations (Engineering as *techné*);
- **New technical and managerial methods and methodologies** (Engineering as *praxis*);
- **New meta-engineering** (Engineering of Engineering activities) knowledge, innovations, and methodologies.

IMETI 2014 was organized and sponsored by the International Institute of Informatics and Systemics (IIIS, www.iiis.org), member of the International Federation for Systems Research (IFSR). The IIIS is a ***multi-disciplinary organization for inter-disciplinary communication and integration***, which includes about 4500 members. Consequently, a main purpose of the IIIS is to foster knowledge integration processes, interdisciplinary communication, and integration of academic activities. Based on 1) the transdisciplinarity of the systemic approach and its emphasis on *relationships* and *integrating* processes, and 2) the multi-disciplinary support of cybernetics' and informatics' concepts, notions, theories, technologies, and tools, the IIIS has been organizing multi-disciplinary conferences as a platform for fostering inter-disciplinary communication and knowledge integration processes.

Multi-disciplinary conferences are organized by the IIIS as support for both **intra-** and **inter-disciplinary** communication. Processes of intra-disciplinary communication are mainly achieved via traditional paper presentations in corresponding disciplines, while conversational sessions, regarding trans- and inter-disciplinary topics, are among the means used for inter-disciplinary communication. Intra- and inter-disciplinary communications might generate *co-regulative cybernetic loops*, via negative feedback, and *synergic* relationships, via positive feedback loops, in which both kinds of communications could increase their respective effectiveness. Figure 1 shows at least two cybernetic loops if intra- and inter-disciplinary are adequately related. A necessary condition for the effectiveness of Inter-disciplinary communication is an adequate level of **variety** regarding the participating disciplines. *Analogical thinking and learning processes* of disciplinarians depend on it; which in turn are potential sources of the creative tension required for cross-fertilization among disciplines and the generations of new hypothesis. An extended presentation regarding this issue can be found at www.iiis.org/MainPupose.

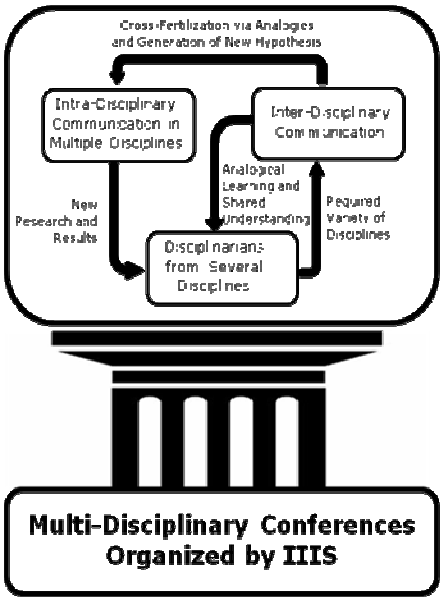

Figure 1

IMETI 2014 was organized jointly with other multi-disciplinary events with the purpose of providing a communicational forum to researchers, engineers, practitioners, developers, consultants, and end-users of computerized, communications, and/or control systems and technologies in the private and the public sectors. This multi-disciplinary forum provides the opportunity to share experience and knowledge by facilitating discussions on current and future research and innovation. Participants can explore the implications of relationships between new developments and their applications to organizations and society at-large. One of the primary objectives of IMETI 2014, and its collocated events, is to promote and encourage interdisciplinary cross-fertilization and knowledge communication. This might foster systemic thinking and practice, including the analogical thinking that characterizes the Systems Approach, which is, in most cases, the required path to logical thinking, scientific hypothesis formulation, and new design and innovation in engineering.

On behalf of the Organizing Committee, I extend our heartfelt thanks to:

1. the 125 members of the Program Committees from 35 countries;
2. the 224 additional reviewers, from 50 countries, for their **double-blind peer reviews**; and
3. the 82 reviewers, from 32 countries, for their efforts in making the **non-blind peer reviews**. (Some reviewers supported both: non-blind and double-blind reviewing for different submissions)

A total of 605 reviews made by 306 reviewers (who made at least one review) contributed to the quality achieved in IMETI 2014. This means an average of 9.92 reviews per submission (61 submissions were received). ***Each registered author had***

access, via the conference web site, to the reviews that recommended the acceptance of their respective submissions. Each registered author could also get information about: 1) the average of the reviewers evaluations according to 8 criteria, and the average of a global evaluation of his/her submission; and 2) the comments and the constructive feedback made by the reviewers, who recommended the acceptance of his/her submission, so the author would be able to improve the final version of the paper.

In the organizational process of IMETI 2014 (including the events organized in its context) about 61 papers/abstracts were submitted. These post-conference proceedings include about 27 papers, from 18 countries, that were accepted for presentation. We extend our thanks to the invited sessions organizers for collecting, reviewing, and selecting the papers that will be presented in their respective sessions. The submissions were reviewed as carefully as time permitted; it is expected that most of them will probably appear in a more polished and complete form in scientific journals.

This information about IMETI 2014 is summarized in the following table, along with the other collocated conferences:

Conference	# of submissions received	# of reviewers that made at least one review	# of reviews made	Average of reviews per reviewer	Average of reviews per submission	# of papers included in the proceedings	% of submissions included in the proceedings
WMSCI 2014	167	678	1052	1.55	6.30	116	69.46%
IMSCI 2014	90	324	580	1.79	6.44	48	53.33%
IMETI 2014	61	306	605	1.98	9.92	27	44.26%
CISCI 2014	120	518	1166	2.25	9.72	56	46.67%
TOTAL	**438**	**1826**	**3403**	**1.86**	**7.77**	**247**	**56.39%**

We are also grateful to the co-editors of these proceedings for the hard work, energy, and eagerness they displayed preparing their respective sessions. We express our intense gratitude to Professor William Lesso for his wise and opportune tutoring, for his eternal energy, integrity, and continuous support and advice as Honorary President of WMSCI 2014 and its collocated conferences, as well as for being a very caring old friend and intellectual father to many of us. We also extend our gratitude to Professor Belkis Sánchez, who brilliantly managed the organizing process. Special thanks to Dr. C. Dale Zinn, Professors Hsing-Wei Chu, Andrés Tremante, Michael Savoie, and Belkis Sánchez for chairing, or co-chairing the Program and/or the Organizing Committees of IMETI 2014 and/or the events organized in its context.

We also extend our gratitude to the following scholars, researchers, and professionals who accepted to deliver plenary workshops and/or to address the audience of the General Joint Plenary Sessions with keynote conferences.

Plenary Workshop, more details (abstracts and short bios) were included in the Conference Program booklet and at http://www.iiis.org/summer2014plenaryevents/

Professor Thomas Marlowe, Seton Hall University, USA, Department of Mathematics and Computer Science, Program Advisor for Computer Science, Doctor in Computer Science and Doctor in Mathematics

Dr. Susu Nousala, Aalto University, Finland, Researcher in Sustainable Design, and Research Fellow at the (Australasian Centre for the Governance and Management of Urban Transport) Faculty of Architecture- Buildi

Plenary Keynote Speakers, more details more details (abstracts and short bios) were included in the Conference Program booklet and at http://www.iiis.org/summer2014plenaryevents/

Professor Leonid Perlovsky, Harvard University and The Air Force Research Laboratory, USA

Professor Shigehiro Hashimoto, Kogakuin University, Japan, Associate to the President and Dean of Admissions Center, Doctor of Engineering and Doctor of Medicine Biomedical Engineering

Professor T. Grandon Gill, University of South Florida, USA, Director of the Doctorate of Business Administration

Dr. Jeremy Horne, President-emeritus, Southwest Area Division, American Association for the Advancement of Science (AAAS), USA

Dr. Karl H. Müller, Director of The Steinbeis Transfer Center New Cybernetics, Vienna, Austria and Professor at the University of Ljubljana, Slovenia

Professor Richard Segall, Arkansas State University, USA, Computer Information Technology

Professor Thomas Marlowe, Seton Hall University, USA, Department of Mathematics and Computer Science, Program Advisor for Computer Science, Doctor in Computer Science and Doctor in Mathematics

Dr. Ronald Styron, University of South Alabama, USA, Director of the Quality Enhancement Plan

Dr. Heidi Ann Hahn, Los Alamos National Laboratory, USA, Director of the Engineering Capability Development, Past President of the International Council of Systems Engineering (INCOSE) Enchantment Chapter

Dr. Robert Cherinka, MITRE Corporation, USA, Senior Principal Information Systems Engineer

Mr. Joseph Prezzama, MITRE Corporation, USA, Lead Communications Engineer, leads the program in support of the Chief Information Officer (CIO) for the United States Special Operations Command (USSOCOM)

Professor Mario Norbis, Quinnipiac University, USA, School of Business

Dr. Marta Szabo White, Georgia State University, USA, Associate Professor, Strategic Management, Director of the Robinson College of Business Honors Program, Director of Study Abroad Programs: Transition Economies and Business Mediterranean Style

Dr. Susan S. Nash, University of Oklahoma, USA, Director of Education and Professional Development, American Association of Petroleum Geologists

Dr. Matthew E. Edwards, Alabama A&M University, USA, Professor of Physics and Former Dean, School of Arts and Sciences

Dr. Russell Jay Hendel, Towson University, USA, Dept of Mathematics

Professor Tomas Zelinka, Czech Technical University in Prague, Czech Republic, Vice-Dean of the Faculty of Transportation Sciences

Dr. Fred Maymir-Ducharme, Executive Architect at IBM, USA, Defense & Space, and Adjunct Professor, University of Maryland University College (UMUC), USA

Dr. Jennifer Styron, University of South Alabama, USA, College of Nursing, Former Research Specialist and Distance Education Coordinator at The University of Southern Mississippi, USA

Associate Professor Adream Blair, University of Wisconsin, USA, College of Design, Architecture, Art and Urban Planning

Dr. Melinda Connor, Langara College- Vancouver Canada, Akamai University in Hilo Hawaii, and Science Advisor for the Spirituals for the 21st century project California State University Dominguez Hills, Former Director of Optimal Healing Research, University of Arizona, USA

Professor Sallyanne Payton, University of Michigan, USA, William W. Cook Professor of Law Emeritus, Professor of Art and Design Emerita University of Michigan Law School- Project Director

Many thanks to Drs. Dale Zinn**,** Sushil Archarya, Esther Zaretsky and professors Michael Savoie, Jorge Baralt, Hsing-Wei Chu, Mohammad Siddique, Andrés Tremante, Friedrich Welsch, Thierry Lefevre, José Vicente Carrasquero, Angel Oropeza, and Freddy Malpica for chairing and supporting the organization of conferences and/or special tracks in the context of, or collocated with, IMETI 2014. We also wish to thank all the authors for the quality of their papers, and the Program Committee members and the additional reviewers for their time and their contributions in the respective reviewing processes.

We extend our gratitude as well to María Sánchez, Juan Manuel Pineda, Leonisol Callaos, Dalia Sánchez, Keyla Guédez, Marcela Briceño, and Freddy Callaos for their knowledgeable effort in supporting the organizational process producing the hard copy and CD versions of the proceedings, developing and maintaining the software supporting the interactions of the authors with the reviewing process and the Organizing Committee, as well as for their support in the help desk and in the promotional process.

Professor Nagib C. Callaos, Ph. D.
IMETI 2014 General Chair
www.iiis.org/Nagib-Callaos

CONTENTS

Engineering Education

Technological Development and Innovation

Applications of Cybernetics and Informatics in other Scientific and Engineering Disciplines

Communications Technologies and Applications

Information and Computing Technologies

Communications Technologies and Applications

Disciplinary Research and Development

STRATEGIES TO ENHANCE THE ENZYMATIC GENERATION OF XYLOSE FROM CORN COB FOR XYLITOL PRODUCTION

Ana TORRADO-AGRASAR
Chemical Engineering Department, Faculty of Science, University of Vigo
Campus As Lagoas s/n, 32004 Ourense / Spain

Noelia PÉREZ-RODRÍGUEZ
Chemical Engineering Department, Faculty of Science, University of Vigo
Campus As Lagoas s/n, 32004 Ourense / Spain

Belinda PÉREZ-BIBBINS
Chemical Engineering Department, Faculty of Science, University of Vigo
Campus As Lagoas s/n, 32004 Ourense / Spain

Ana Belén MOLDES
Chemical Engineering Department, University of Vigo
Vigo, 36310 / EEI-Campus As Lagoas, Spain

José Manuel CRUZ
Chemical Engineering Department, University of Vigo
Vigo, 36310 / EEI-Campus As Lagoas, Spain

and
José Manuel DOMÍNGUEZ GONZÁLEZ
Chemical Engineering Department, Faculty of Science, University of Vigo
Campus As Lagoas s/n, 32004 Ourense / Spain

ABSTRACT

In this study, corn cob was evaluated as subtract and support for enzymatic hydrolysis of xylan into xylose for further fermentation into xylitol by *Debaryomyces hansenii*. Two strategies were considered, the use of enzymatic extracts produced *ad hoc* by solid state fermentation using *Aspergillus niger* strains, and the application of ultrahigh hydrostatic pressure (UHP) as a tool for enhancing the enzymatic reaction. The maximum levels of monosaccharides (xylose and glucose) achieved with *Aspergillus* extract were comparable to those obtained with commercial enzymes pointing out the apparent favorable effect of feruloyl esterase activity. Finally, the good results obtained for experiments conducted after UHP revealed that this pretreatment contributed in a great manner to enhance the activity of the enzyme.

Keywords: *corn cob, xylan, xylanases, feruloyl esterases, xylose, Aspergillus niger, ultrahigh hydrostatic pressure, Debaryomyces hansenii, xylitol*

1. INTRODUCTION

Corn cob is an interesting lignocellulosic subproduct obtained from maize, whose importance lies on the high production of this cereal as the main diet contributor on several countries. The high xylan content of corn cob, up to 30% [1], makes this waste a largely available renewable source of xylose, that can be employed as a feedstock for obtaining high value-added products by means of biotechnological processes. The production of xylitol by yeast fermentation is a good example of this strategy of valorization, whose successfulness depends on the extent of the corn xylan hydrolysis to xylose.

Although acid and hydrothermal treatments have shown good efficiencies, the mild conditions of the enzymatic hydrolysis offer the advantage of avoiding the generation of microbial inhibitors and toxic compounds as hydroxymethylfurfural and furfural coming from the thermal degradation of carbohydrates. Nevertheless, the complete enzymatic xylan hydrolysis is hindered by the chemical heterogeneity of the molecule and the complex structure of the lignocellulosic matrix.

Thus, corn xylans are heteropolysaccharides composed by a backbone chain of 1,4-linked β-D-xylopyranose units with variable and multiple branches of mono or di-saccharides mainly formed by xylose, arabinose, glucose, galactose and

glucuronic acid with different degrees of acetylation [2]. Additionally, the xylan fibers are highly cross-linked by diferulic bridges between side chain arabinoses through ester linkages, but they are also linked to the lignin matrix through similar ferulic and coumaric bridges. In consequence, the complete hydrolysis of the polysaccharide needs the action of different enzymes with complementary activities. Besides the main action of the endo-xylanases and β-xylosidase involved in the hydrolysis of the backbone chain, ancillary debranching enzymes are needed, including α-L-arabinofuranosidases, α-glucuronidase, ferulic acid esterase, α-galactosidase, feruloyl esterase and acetyl xylan esterase among others [3]. But, besides the presence of all the required enzymes, the efficiency of the process depends critically on the relative ratios between them, which also can differ depending on the xylan source. In effect, the existence of synergy between the enzymes can increase the rate and yield of the process, or even limit the total conversion of the polysaccharide. Three types of synergies have been described for the enzymes involved in hemicellulose hydrolysis [3]:

- homeosynergy: between the main-chain cleaving enzymes (endo- and exo-xylanases, and xylosidase)
- heterosynergy: between the main-chain cleaving and the debranching enzymes
- anti-synergy: when the action of one enzyme inhibits the action of another, e.g., when a debranching enzyme removes a side-chain whose presence is necessary for the main-chain cleaving enzyme.

The synergy between endo-xylanases and feruloyl esterases is not completely clear. Several studies report the synergistic effect of endo-xylanases on ferulic acid release by feruloyl esterase, but it does appear that the latter is not required for xylanase activity [3]. These observations are supported by the extremely poor activity of feruloyl esterases on insoluble ferulated xylan and by the fact that although diferulate cross-links hinder the enzymatic hydrolysis of lignocellulosic polysaccharides (mainly xylan), the degree of ferulate substitution of xylan seems not to affect the hydrolysis of the polysaccharide [4]. These authors also attributed the limited hydrolysis of xylan rich in diferulic bridges to inadequate concentrations of α-L-arabinofuranosidase and β-D-xylanosidase activities rather than to the presence of diferulates. Nevertheless, there are also studies describing the favorable effect of combining xylanases and feruloyl esterases on cellulose hydrolysis [5,6].

Consequently, considering the great importance of an adequate enzyme combination for the optimal hydrolysis of corn cob xylan, we propose the use of enzymatic extracts specifically produced for this purpose employing the same material to be further hydrolyzed as substrate for the culture of a ligninolytic fungus (*Aspergillus niger*) that posses the ability of expressing a broad spectrum of enzymes involved in xylan degradation [7]. Then, assays were made to compare the activity of *Aspergillus niger* extracts produced from corn cob by solid state culture, and some commercial enzymes. Finally, alternative pretreatments were also evaluated to improve the process. In summary, the aim of this work was to evaluate two strategies for the enzymatic hydrolysis of corn cob xylan as a source of xylose for xylitol production by *Debaryomyces hansenii*: the use of enzymatic extracts produced *ad hoc* by solid state culture using corn cob as substrate for *Aspergillus niger*, and the application of ultrahigh hydrostatic pressure (UHP) as a tool for enhancing the enzymatic reaction.

2. MATERIALS AND METHODS

Production of Aspergillus niger extracts by solid state fermentation

Corn cob was used as carbon source and support for solid state culture by *Aspergillus niger* CECT 2700. Milled (particle size < 5 mm diameter) corn cob (10 g dry weight) was placed in 250 mL Erlenmeyer flasks. A concentrated salts solution (containing 2.4 g/L $(NH_4)_2SO_4$; 3.0 g/L $NaNO_3$; 1.5 g/L KH_2PO_4; 0.3 g/L $CaCl_2.2H_2O$; 3 g/L yeast extract and 3 g/L glucose) was added to moisten the substrate to a ratio of 3.6 mL solution/g solid. After sterilization in autoclave at 100ºC for 1h, cultures were inoculated with 1 mL of a spore suspension prepared to provide a concentration of $1x10^6$ spores/g dry solid substrate. The cultures were incubated statically at 30 °C in a H_2O-saturated atmosphere for 5 days. Every 24 h the flasks were shaken by hand to prevent aggregation of solids. The crude enzymatic extract was prepared adding 10 mL of sterilized water/g of dry corn cob, and shaking at 200 rpm and 30ºC for 1 h. The extract was centrifuged at 4000 rpm for 10 min and the supernatant was filtered and frozen until use.

Commercial enzymes and activities

Corn cob hydrolysis was carried out with *Aspergillus niger* extract or using three commercial enzymes kindly provided by Novozymes (Denmark). **Table 1** shows the main enzymatic activities measured for all of them.

Table 1. Enzymatic activities of the *A. niger* CECT 2700 extract and the commercial enzymes used.

	Enzymes Activity			
Enzymes	**Xylanase[1] (U^5/mL)**	**Cellulase[2] (U^5/mL)**	**Cellobiase[3] (U^5/mL)**	**Feruloyl esterase[4] (U^5/mL)**
***A. niger* extract**	185	0.07	0.183	0.040
Ultraflo® L	2555	0.28	-	0.085
Pentopan	4396	-	-	-
Shearzyme	2265	0.30	0.011	-

1: measured with oat spelts xylan in 50 mM sodium phosphate buffer pH 6 at 50 ºC/10 min
2: measured with filter paper Whatman nº 1 in 50 mM citrate buffer pH 4.8 at 50 ºC/60 min
3: measured with cellobiose in 50 mM citrate buffer pH 4.8 at 50 ºC/30 min
4: measured with ethyl ferulate in 50 mM sodium phosphate buffer pH 6.0 at 40 ºC/30 min
5: µmol/min

Hydrolysis assays

The hydrolysis assays were performed in 250 mL Erlenmeyer flasks placing 10 g of milled corn cob (2 mm size) and 100 mL of liquid volume (containing 90 mL of sodium phosphate buffer pH 6 and 10 mL of the enzyme solution), with the exception of those cases where variable amounts of *Aspergillus niger* extracts were assayed. The incubation was performed at 37 ºC (except in the experiment with different temperatures), and 200 rpm.

Simultaneous or sequential hydrolysis and fermentation to xylitol

10 g of milled corn cob was placed in 250 mL Erlenmeyer flasks with 90 mL of distilled water containing peptone 5 g/L, yeast extract 3 g/L and malt extract 3 g/L, and sterilized in autoclave at 100 ºC for 1 h. Then, 10 mL of the enzyme (Ultraflo® L or the *Aspergillus niger* extract) was added for starting the hydrolysis of corn cob xylan. Three series of experiments were made by duplicate changing the time of inoculation, which consisted on 1 mL of 1 day old *Debaryomyces hansenii*:

-series A: simultaneous addition of enzyme and yeast
-series B: yeast inoculation 24 h after enzyme addition
-series C: yeast inoculation 48 h after enzyme addition

The conditions of incubation were 200 rpm and 37 ºC, with the exception of series B and C carried out with Ultraflo, that were incubated at 43 ºC during the first 24 and 48 h respectively.

Experimental conditions for UHP to enhance corn cob enzymatic hydrolysis

Each experimental unit consisted in 3 g of milled corn cob suspended in 24 mL of phosphate buffer 100 mM, pH = 6, and hydrolyzed with 5 mL of Ultraflo® L (Novozymes, Denmark) (**Table 1**). Four series were assayed by duplicate according to **Table 2**.

Table 2: Experimental conditions applied for the hydrolysis assays performed in combination with ultrahigh pressure treatment.

Series name	Thermal pretreatment (TP)	Ultrahigh Pressure Treatment (UHP)	Enzyme addition (E)
A	X	-	X (added after the TP)
B	X	X	-
C	X	X	X (added after the TP and before UHP)
D	-	X	X (added before UHP)

The thermal pretreatment (TP) was done in autoclave at 130ºC for 1 h. The Ultrahigh Pressure Treatment (UHP) was done at 200 MPa and 45ºC for 15 min in a laboratory high-pressure food processor unit (S-FL-850-9-W Stansted Fluid Power Ltd., Stansted, UK) equipped with a 120 mL vessel. In all cases the treated corn cob suspension was finally incubated at 45 ºC and 200 rpm in a lab shaker (Optic Ivymen System, Comecta S.A., distributed by Scharlab, Madrid, Spain) for 24 h to continue the hydrolytic process. Sampling was done just after the pressurization treatment ("t=0") or after the thermal treatment in case of series A, and 24 h after the incubation ("t=24 h"). In both cases 3.5 mL were taken, acidified immediately with 3.5 mL of 0.07M H_2SO_4 to stop the enzyme reaction, and centrifuged at 4,000 rpm for 10 min to recover the supernatant free of solids. Finally, xylose was measured by HPLC (Agilent, model 1200, Palo Alto, CA) using a refractive index detector with an Aminex HPX-87H ion exclusion column (Bio Rad 300 × 7.8 mm, 9 µ particles) with a guard column, eluted with 0.003 M sulfuric acid at a flow rate of 0.6 mL/min at 50ºC.

3. RESULTS AND DISCUSSION

a) ***Production of Aspergillus niger extracts by solid state fermentation***

First of all, a kinetic experiment was carried out using different concentrations of extract and corn cob previously subjected to heat pretreatments in autoclave at 130 ºC. Foreseeing that at this preliminary stage the conditions of operation were far from the optimal ones and therefore the levels of monosaccharides would be very low, the degree of hydrolysis was measured as the generation of reducing sugars to get a first view of the extract ability for breaking down the polysaccharide molecules. Despite the low xylanase activity of the fungal extract in comparison with the commercial enzymes (**Table 1**), the increasing levels of reducing sugars achieved with increasing enzyme concentrations, and the stability of the enzymatic extracts (reflected in low deceleration rates even after 60 h of incubation) showed the potential of this enzymatic mixture for xylan corn cob hydrolysis (**Figure 1**). Considering the very low cellulose and cellobiase activities in the fungal extract and the mild pretreatment applied to the substrate, no cellulose hydrolysis is expected.

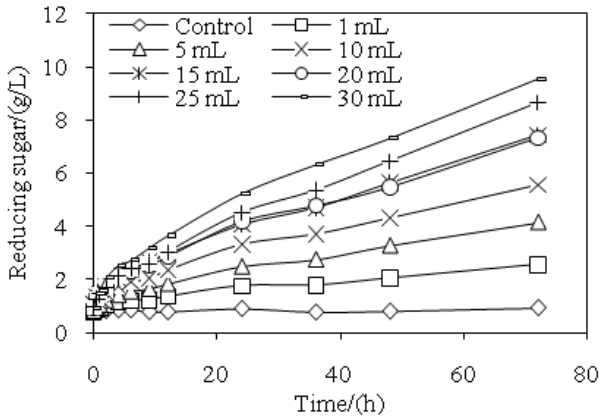

Figure 1 Reducing sugars generated from corn cob by different concentrations of the *A. niger* enzymatic extract.

Since the representation of the reaction rates calculated after 1 h of incubation (**Figure 2**) showed an almost linear dependence with the volume of enzyme, it is expected that increasing more the volume of the extract will provide better degrees of hydrolysis. The production of more concentrated extracts will be a better strategy to achieve higher levels of reducing sugars closer to the theoretical maximum for this corn cob concentration (around 30 g/L).

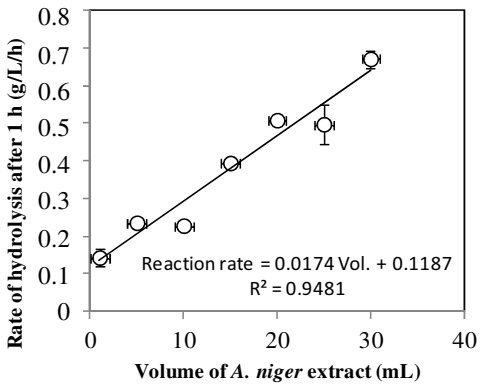

Figure 2 Dependence of the rate of corn cob hydrolysis, calculated after 1 h of incubation, with volume of *A. niger* extract.

Then, a new assay was performed comparing the *A. niger* extract (using a dose of 10 mL) with two commercial xylanases (Pentopan and Sherazyme) and a feruloyl esterase with high xylanase activity (Ultraflo) (**Table 1**). Three temperatures of incubation were assayed just in case that the enzymes had different optimal temperature reactions and any of them could be in disadvantage. The levels of reducing sugars generated in each case (**Figure 3**) clearly showed that the better degrees of hydrolysis were obtained with *Aspergillus* extracts and Ultraflo, both containing feruloyl esterase activity and the lowest xylanase activity in the case of the fungal extract. These results are interesting and need further study since the apparent favorable effect of the feruloyl esterase activity seems to be in contradiction with previous results [3] pointing to the independence of the xylanase activity with respect to the feruloyl esterase activity, and the poor performance of the feruloyl esterase on insoluble substrates, as commented before.

It is interesting to highlight the biphasic profiles of all the kinetics, which could be due to the progressive generation of oligosaccharides of lower molecular weight and increasing susceptibility to the enzymatic activities present in each case. More detailed studies identifying the chemical structure of the reaction products along the time of incubation will be necessary to asses this hypothesis.

A significant but low effect of the temperature of incubation was observed for both *Aspergillus* extract and Ultraflo. While the results obtained allowed defining 40 ºC as the optimal temperature for Ultraflo reaction in these conditions of operation, in the case of the fungal extract the better results were obtained at the lowest temperature assayed (37ºC), which could indicate even a lower optimal temperature.

Considering that 37 ºC is compatible with yeast growth, a final preliminary assay was done combining the enzymatic hydrolysis of corn cob with the *Aspergillus* extract or Ultraflo, and the microbial fermentation of the hydrolyzates with *Debaryomyces hansenii* to produce xylitol from the xylose released by the enzymes. Two operational strategies were assayed: yeast inoculation was done simultaneously with enzyme addition or sequentially 24 or 48 h after the start of the enzymatic process. Taking into account that the lag time for *D. hansenii* is around 24 h, this means that the highest substrate (mainly xylose) yeast consumption will start respectively after 24, 48 or 72 h after the beginning of the hydrolysis.

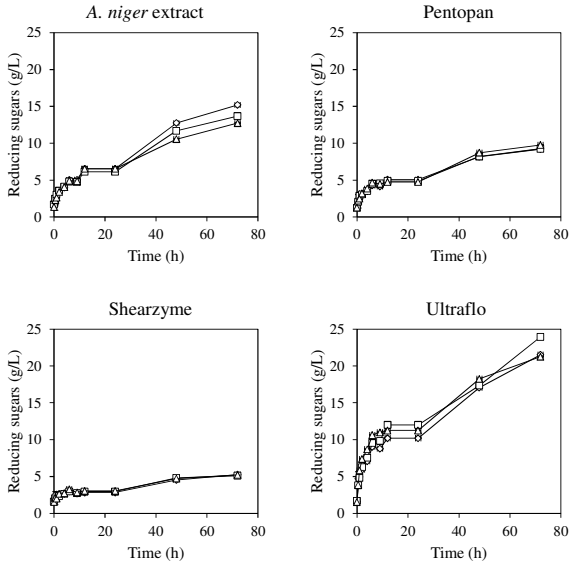

Figure 3 Degree of corn cob hydrolysis (measured as generation of reducing sugars) provided by the *A. niger* extract and three commercial enzymes at three temperatures of incubation: 37 (○), 40 (□) and 43ºC (▲).

The results obtained in **Figure 4** showed that xylose and glucose were produced simultaneously and almost in similar amounts by both enzymes, reflecting the joint action of all the enzymatic activities present in these extracts, which included cellulose and cellobiase activities (**Table 1**). Xylan debranching activity, which could contribute to glucose generation, was not analyzed. As it was expected, in all cases there was a peak of maximum glucose and xylose concentration in the culture medium as a result of the balance between the generation and consumption of the monosaccharides. Consequently, these peaks were higher and wider as the yeast addition was more delayed. Nevertheless, the xylitol production was very low in all cases because the levels of assimilable sugars in the culture medium were very low and mainly consumed for growth, and no xylitol trends were observed with regard to the simultaneous or sequential mode of operation. Previous optimization of the corn cob hydrolysis will be necessary for defining the optimal time of yeast addition.

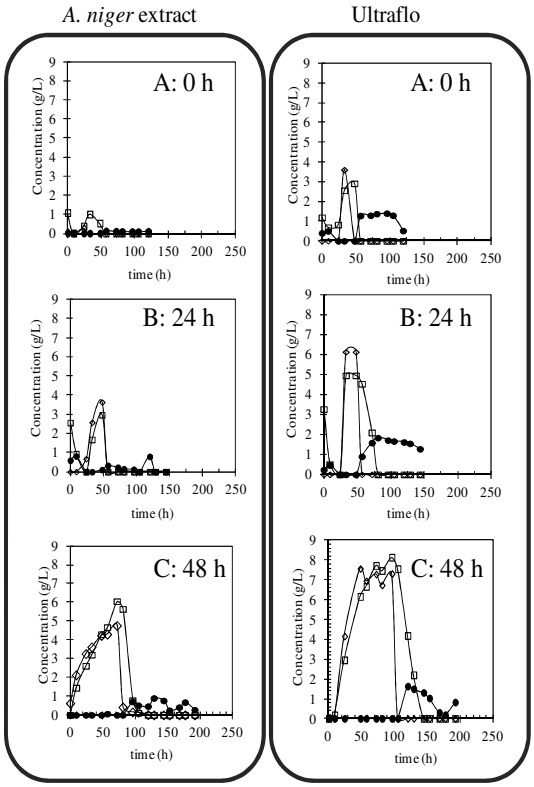

Figure 4. Glucose (◊) and xylose (□) consumption and xylitol (●) production in experiments of corn cob hydrolysis and fermentation with *Debaryomyces hansenii* performed at 37 ºC with an *Aspergillus niger* enzymatic extract or Ultraflo under three modes of operation: A, simultaneous addition of enzymes and yeast; B, yeast addition delayed 24 h with regard to enzymes; C, yeast addition delayed 48 h with regard to enzymes.

Although the maximum levels of monosaccharides achieved were always higher in the experiments made with Ultraflo, they were comparable to those obtained in the experiments made with the *Aspergillus* extract. Besides, it is interesting to stand out that they did not account for the big differences between the enzymatic activities between both enzymes used. While for Ultraflo the xylanase activity was one order of magnitude higher and the feruloyl esterase activity was twice the activity quantified in the *Aspergillus* extract, the maximum concentrations of glucose and xylose in the series with Ultraflo did not exceeded 1.7 times the values achieved in the experiments with the fungal extract. Therefore, these results suggest again the importance of the feruloyl esterase activity in the enzymatic hydrolysis of corn cob xylan, but the hypothesis of a better combination of different and complementary enzymatic activities in the fungal extract must be also considered as an important reason for its good performance towards corn cob, as commented before according to Grabber *et al*., [4]. A more detailed analysis of the enzymatic activities in the fungal extract will help to elucidate it.

b) UHP to enhance corn cob enzymatic hydrolysis

The main advantage of using enzymes for the generation of xylose from corn cob comes from the mild conditions of operation, which avoid the formation of undesirable by-products that can be inhibitory for the development of the yeast and toxic for human consumption. But, as well as the difficulties related to xylan heterogeneity for achieving high yields of hydrolysis, the high cost of enzymes makes necessary to maximize their action in order to make the process economically sustainable. Although the application of thermal and chemical pretreatments for opening the close structure of the lignocellulosic matrix is not so critical for hemicellulosic enzymatic hydrolysis than in the case of cellulose, they usually involve the xylan solubilization, which makes easier the accessibility of the enzymes. Nevertheless, these treatments operate under hard conditions of temperature, pH and pressure that lead to the generation of toxic compounds. In consequence, they must be avoided when working with enzymes.

The use of ultrahigh hydrostatic pressures (UHP), mainly applied in food processing for microbial and enzymatic inactivation as an alternative to thermal treatments in order to keep better the organoleptic and nutritional properties of the untreated food, has been recently assayed for enhancing the enzymatic hydrolysis and release of xylan in cellulosic fibers [8]. In this case, UHP was applied at low temperature (20ºC) as a "green" pretreatment before the enzymatic hydrolysis of bleached kraft pulp with xylanases. Working at an intermediate pressure (300 MPa) allowed increasing the rate and extent of the process 10 and 2 times respectively, which was attributed to the induced changes in the cellulose supramolecular structure [9], which made more accessible to enzymes the xylan immured in the cellulose interfibrillar space. On the other hand, the effect of high pressures on enzymes activity and stability is highly variable, causing inactivation or enhancement depending on the enzyme, substrate and physic-chemical conditions.

Considering all of that, we propose the use of ultrahigh hydrostatic pressures (UHP) simultaneously with the enzymatic treatment as a way for enhancing xylan hydrolysis in corn cob. A preliminary experiment was done with the commercial enzyme (Ultraflo) just to test the potential of the combined process operating at low pressures to avoid enzyme inactivation.

Figure 5 shows the comparison among the different experimental conditions assayed according to **Table 2**. Although the levels of xylose generated were low in all cases, they were considerably higher at both sampling times in the series subjected simultaneously to high pressure and enzyme.

Experiment B (TP + UHP), which was included as a control, allowed to discard any xylan hydrolysis due to the pressurization treatment only, while series A (TP + E) showed the poor performance of the enzyme after 24 h of incubation when only the thermal treatment previously was applied, which reflects the need for a stronger corn cob pretreatment for enhancing the activity of the enzyme. Consequently, the good results obtained for series C (TP + UHP + E) and D (UHP + D) reflect that, in some way, the application of high pressures contributed in a great manner to enhance the activity of the enzyme.

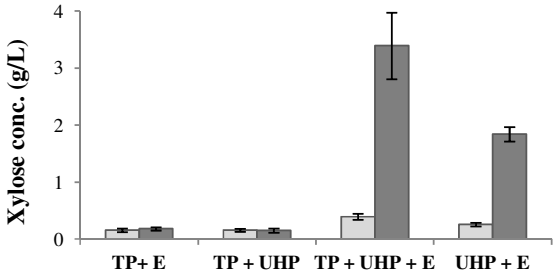

Figure 5. Xylose generated from corn cob subjected to the different treatments described in **Table 2**: TP, thermal pretreatment (130 ºC/1 h); UHP, ultrahigh hydrostatic pressure (200 MPa/45 ºC/15 min); E, Ultraflo addition. Bars in light grey correspond to samples taken just after the treatment, and bars in dark grey represent the results after 24 h of incubation at 45 ºC of the previously treated samples.

Considering that 200 MPa showed only a moderate effect on xylan hydrolysis when pressurization was employed as a pretreatment previous to the enzymatic treatment of *Eucalyptus globulus* bleached kraft pulp [8], it seems that the beneficial effect of UHP in this case could be mainly related to the enhancement of the enzymatic reaction by pressure. The better results obtained in series C with thermal pretreatment compared to series D without pretreatment are in agreement with this hypothesis. According with that, it is also noticeable the maintenance of the enzymatic activity after the pressurization.

4. CONCLUSIONS

In conclusion, although poor in terms of degree of corn cob hydrolysis, the results here obtained are promising and point to the interest of using enzymatic extracts for xylan hydrolysis that are specifically produced by microorganisms grown on the same material to be hydrolyzed. Additionally, although preliminary, these results give some indications about the potential of ultrahigh hydrostatic pressures as a way for enhancing the activity of the enzymes involved in xylan hydrolysis. Nevertheless, many questions and targets must be raised to confirm or discard this potential enzymatic tool. From a purely scientific point of view, it would be very interesting to study the existence in this case and the physicochemical nature of a coadyuvant effect of pressure on the enzymatic reaction of xylan hydrolysis that, as commented before, involves so many different activities and substrates. And, of course, from a more practical point of view it would be necessary to optimize the operational conditions to improve considerably the yield of the hydrolysis studying different combinations of pressure, temperature, time, type and concentration of enzymes, and application of additional pretreatments to help the process. Finally, it would be necessary to study the possible generation of by-products that could be undesirable for a posterior use of the hydrolyzates in microbial processes and for food purposes.

Acknowledgements

We are grateful to the Spanish Ministry of Science and Innovation for the financial support of this work (project CTQ2011-28967), which has partial financial support from the FEDER funds of the European Union.

5. REFERENCES

[1] R.A. Prade, "Xylanases: From biology to biotechnology", **Biotechnology and Genetic Engineering Reviews**, Vol. 13, 1996, pp. 120-131.

[2] A. Ebringerová, Z. Hromádková, J. Alfödi, V. Hříbalová, "The immunologically active xylan from ultrasound-treated corn cobs: Extractability, structure and properties", **Carbohydrate Polymers**, Vol. 37, 1998, pp. 231-239.

[3] J.S. Van Dyk, B.I. Pletschke, "A review of lignocellulose bioconversion using enzymatic hydrolysis and synergistic cooperation between enzymes-Factors affecting enzymes, conversion and synergy". **Biotechnology Advances**, Vol. 30, 2012, pp. 1458-1480.

[4] J.H. Grabber, R.D. Hatfield, J. Ralph, "Diferulate cross-links impede the enzymatic degradation of non-lignified maize walls", **Journal of the Science of Food and Agriculture**, Vol. 77, 1998, pp. 193-200.

[5] P. Yu, J.J. McKinnon, D.D. Maenz, A.A. Olkowski, V.J. Racz, D.A. Christensen, "Enzymic release of reducing sugars from oat hulls by cellulase, as influenced by *Aspergillus* ferulic acid esterase and *Trichoderma* xylanase". **Journal of Agricultural and Food Chemistry**, Vol. 51, 2003, pp. 218-223.

[6] M.G. Tabka, I. Herpoël-Gimbert, F. Monod, M. Asther, J.C. Sigoillot, "Enzymatic saccharification of wheat straw for bioethanol production by a combined cellulase xylanase and feruloyl esterase treatment". **Enzyme and Microbial Technology**, Vol. 39, 2006, pp. 897-902.

[7] N.N.M.E. Van Peij, M.M.C. Gielkens, R.P. De Vries, J. Visser, L.H. De Graaff, "The transcriptional activator XlnR regulates both xylanolytic and endoglucanase gene expression in *Aspergillus niger*". **Applied and Environmental Microbiology**, Vol. 64, 1998, pp. 3615-3619.

[8] S.C.T. Oliveira, A.B. Figueiredo, D.V. Evtuguin, J.A. Saraiva, "High pressure treatment as a tool for engineering of enzymatic reactions in cellulosic fibres", **Bioresource Technology**, Vol. 107, 2012, pp. 530-534.

[9] A.R.F.C. Ferreira, A.B. Figueiredo, D.V. Evtuguin, J.A. Saraiva, "High pressure pre-treatments promote higher rate and degree of enzymatic hydrolysis of cellulose", **Green Chemistry**, Vol. 13, 2011, pp. 2764-2767.

SIMULTANEOUS PRODUCTION OF BIOSURFACTANTS AND COAGULANTS-FLOCULANTS FROM TRIMMING VINEYARDS

Xanel VECINO
Chemical Engineering Department, University of Vigo
Vigo, 36310 / EEI-Campus As Lagoas, Spain

María PEREZ-AMENEIRO
Chemical Engineering Department, University of Vigo
Vigo, 36310 / EEI- Campus As Lagoas, Spain

Letricia BARBOSA-PEREIRA
Chemical Engineering Department, University of Vigo
Vigo, 36310 / EEI-Campus As Lagoas, Spain

Rosa DEVESA-REY
Defense University Center, Escuela Naval Militar,
University of Vigo, Spain

José Manuel DOMINGUEZ
Chemical Engineering Department, University of Vigo
Ourense, 32004 / Science Faculty, As Lagoas, Spain

Ana Belén MOLDES
Chemical Engineering Department, University of Vigo
Vigo, 36310 / EEI-Campus As Lagoas, Spain

and

José Manuel CRUZ
Chemical Engineering Department, University of Vigo
Vigo, 36310 / EEI-Campus As Lagoas, Spain

ABSTRACT

Trimming vineyards were hydrolysed with H_2SO_4 under selected conditions, in order to obtain hemicellulosic sugars that were neutralized with $CaCO_3$. Following the clarified hydrolysates were supplemented with nutrients, sterilized and used as carbon source in order to lactic acid as primary metabolite and biosurfactants as secondary metabolite, by using *Lactobacillus pentosus*. Once the fermentation was finished, biosurfactants were extracted from *L. pentosus cells* by using a solution containing 10mM KH_2PO_4/K_2HPO_4 and NaCl; whereas lactic acid was extracted from fermentation medium by using Amberlite IRA 400 in Cl^- form and desorbed with HCl Following in order to increase the pureness of lactic acid this was extracted from the aqueous solution by using isoamyl alcohol. Finally the lactic acid obtained biotechnologically was evaluated as coagulant-floculant to remove suspended solids from wastewater.

Keywords: renewable carbon source, lactic acid, bisourfactants, purification, coagulant-floculant

1. INTRODUCTION

The utilization of biotechnological processes to increase the environmental protection it is a good choice for the revalorization of agro industrial residues and for the production of biodegrable products. Nevertheless, for the application of biotechnological processes at industrial scale these has to be cost competitive with chemistry industry. From this point of view it is interesting to obtain various products simultaneously in the same biotechnological process. In this work the utilization of trimming vineyard is proposed as carbon source to obtain lactic acid that it has coagulant-floculant properties [1, 2], and biosurfactants in the same fermentation process using *L. pentous*. Trimming vineyards can be processed in acidic media (prehydrolysis) to convert the hemicellulose polysaccharides (xylan, mannan and galactan) into their correspondent monosaccharides (xylose, mannose and glucose) that can be fermented by *L. pentosus* to produce lactic acid and biosurfactants.

2. MATERIALS AND METHODS

Hydrolysis of trimming vineyards

Ground samples of trimming vineyards can be hydrolysed under selected conditions (3 % H_2SO_4, 15 min, 130 ºC, liquid/solid ratio 8:1 g/g) and the liquid phase, containing hemicellulosic sugars were neutralized with $CaCO_3$ to a final pH of 6.5 The $CaSO_4$ generated during this process can be precipitated and separated from the supernatant by filtration [3, 4].

Fermentation of hemicellulosic sugars from trimming vineyards by L. pentosus

The clarified hydrolysates obtained above, can be supplemented with nutrients (10 g/L of yeast extract and 10 g/L of corn steep liquid), sterilized and used directly as fermentation media. *L. pentosus* CECT-4023 T (ATCC-8041), obtained from the Spanish Collection of Type Cultures (Valencia, Spain) can be used in order to obtain lactic acid and biosurfactants following the protocol used in previous works [5]. During fermentation, it is important, in order to avoid product inhibition on *Lactobacillus pentosus,* neutralize the lactic acid produced, for example using NaOH 4M.

Extraction of biosurfactants

Once the fermentation is finish, cells can be recovered from the fermentation medium by centrifugation, and after washing twice in demineralized water, and resuspended in phosphate-buffer saline (PBS: 10mM KH_2PO_4/K_2HPO_4 and NaCl with pH adjusted to 7.0) biosurfactants can be obtained in the PBS. The extraction process can be carried out at room temperature, although if it were needed, biosurfactants can be obtained in absence of salt by increasing temperature up to 65 ºC. Following, bacteria can be removed by centrifugation [5, 6, 7]. These biosurfactants can be used in the bioremediation of contaminated soil [8].

Extraction and purification of lactic acid

Figure 1 shows the scheme for obtaining biosurfactants and lactic acid from trimming vineyards. Lactic acid can be recovered from the fermentation medium using anion exchange resins (for example Amberlite IRA 400, Amberlite IRA 96 or Amberlite IRA 67). Depending if resin is charged with Cl^-, OH^- or is freebase; lactic acid should be recovered from the resin using different solutions. Thus if resin is used in Cl^- form, lactic acid has to be recovered using HCl and lactic acid should be obtained in aqueous solution; whereas if resin is charged with OH^-, resin should be washed with NaOH and lactic acid should be recovered as sodium lactate [9, 10, 11]. Next in order to increase the pureness of lactic acid this can be extracted with isoamyl alcohol from water [12]. Following the organic and aqueous phases can be separated by decantation and the organic phase can be collected and evaporated under vacuum using rotatory evaporator to obtain purified lactic acid. In this work lactic acid was extracted from fermentation medium using Amberlite IRA 400 in Cl- form, using a liquid solid/ratio of 1/20 w/w and desorbed with HCl 1N. Lactic acid was analysed by HPLC using a Rezex RHM-Monosaccharide H+ Phenomenex column (mobile phase, H_2SO_4 0.01 M; flow rate, 0.4 mL/min; IR and UV detection).

Coagulation-Flocculation experiments

Water containing 500 NTU (Nephelometric Turbidity Units) of suspended solids was treated with 1 g/L of $AlCl_3$ or lactic acid obtained biotechnologically in a Jar Test Flocculation system (Velp Scientifica). The first measurements were taken after 1,5 h and then at 2, 3 and 5 h. The turbidity reduction—expressed as NTU—was measured in a turbidimeter. Distilled water was used as a blank and experiments were run in triplicate.

3. RESULTS AND DISCUSSION

Lactic acid as coagulant –flocculant

After fermentation of hemicellulsoic sugars from trimming vineyards about 18 g/L of lactic acid can be produced. This lactic acid, obtained in the process described in **Figure 1,** can be used as coagulant to remove suspended solids from wastewater [1, 2]. Other authors have proposed the utilization of calcium sulphate as flocculant to reduce sedimentation basin water turbidity [13]. Using calcium sulphate at doses of 350 to 700 mg/L the turbidity of unstirred sedimentation basin water was reduced to 50 NTU by Przepiora et al. [13] within 3h, starting with a turbidity of 400 NTU. These results are comparable with those obtained when lactic acid is used as coagulant–flocculant. **Figure 2** shows the percentage reduction of NTU (nephelometric units) of water after treatment with lactic acid obtained biotechnologically, in comparison with $AlCl_3$, the most common coagulant-flocculant used nowadays. It can be observed that lactic acid gave percentages of turbidity reduction close to $AlCl_3$. In this case water contained 500 NTU was treated with 1 g/L of lactic acid; and it was observed that after 3 h of starting the coagulation-flocculation process more than 90% of suspended solids were removed from water.

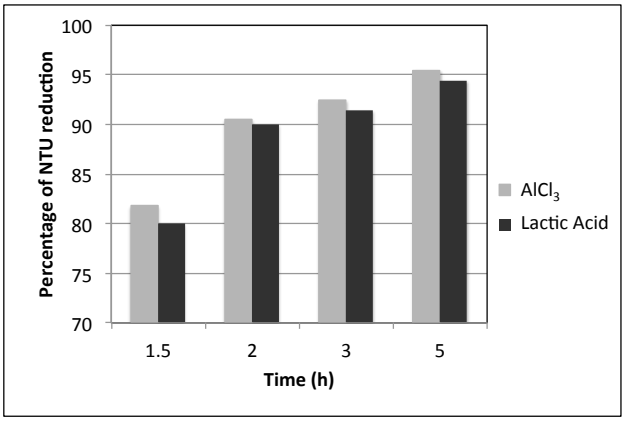

Figure 2. Percentage of NTU reduction, in the water, at different times, in presence of lactic acid or $AlCl_3$.

Production of biosurfactants from trimming vine-shoots

Following the procedure showed in **Figure 1**, trimming vine shoots can be hydrolysed in order to obtain hemicellulosic sugars that after neutralization suppose an interesting carbon source for lactic acid and biosurfactant production. These biosurfactants are cell bound to the plasmatic membrane of *lactobacillus pentosus* cells and they can be extracted with

buffer phosphate using reduced concentration of salt. Thus from hemicellulosic sugars containing 18 g/L of xylose and 10 g/L of glucose, 11 mg/L of biosurfactants were obtained, when the extraction medium contained 0,9 % of NaCl; whereas when the extraction was carried out in absence of salt about 9 mg/L of bisourfactants were extracted from the *lactobacillus pentosus* cells. This biosurfactant can reduce the surface tension of water about 16 units.

4. CONCLUSIONS

Agricultural residues, like trimming vineyards, can be used during biotechnological process as carbon source for obtaining valuable products like lactic acid and biosurfactants. Thus, less non-renewable carbon sources will be needed to obtain this kind of products contributing to a sustainable development.

ACKNOWLEDGMENT

The authors wish to thank to the Spanish Ministry of Economy and Competitiveness (project CTM2012-31873) and Vecino X. is grateful to the University of Vigo for her predoctoral contract.

5. REFERENCES

[1] Devesa-Rey, R., Fernández, N., Cruz, J.M. and Moldes A.B. Optimization of the dose of calcium lactate as a new coagulant for the coagulation–flocculation of suspended particles in water. **Desalination**, Vol. 280, 2011, pp. 63–71.

[2] Devesa-Rey, R., Bustos, G., Cruz, J. M., and Moldes A. B. Evaluation of non-conventional coagulants to remove turbidity from water. **Water Air Soil Pollut.**, Vol. 223, 2012, pp. 591–598.

[3] Bustos, G., Moldes, A.B., Cruz, J.M., and Domínguez J.M. Production of fermentable media from vine-trimming wastes and bioconversion into lactic acid by *Lactobacillus pentosus.* **J Sci Food Agric.**, Vol. 84, 2004. pp. 2105–2112.

[4] Moldes, A. B., Bustos, G., Torrado, A., and J. M. Domínguez. Comparison between Different Hydrolysis Processes of Vine-Trimming Waste to Obtain Hemicellulosic Sugars for Further Lactic Acid Conversion. **Appl Biochem Biotechnol.**, Vol. 43, 2007, pp. 244–256.

[5] Portilla-Rivera, O., Torrado, A. and Domínguez J. M. Stability and emulsifying capacity of biosurfactants obtained from lignocellulosic sources using Lactobacillus pentosus. **J. Agric. Food Chem.**, Vol. 56, 2008, pp. 8074−8080.

[6] Moldes, A.B., Torrado, A.M., Barral, M.T. and Domínguez J.M. Evaluation of biosurfactant production from various agricultural residues by *Lactobacillus pentosus*. **J. Agric. Food Chem.**, Vol. 55 (11), 2007, pp. 4481-4486.

[7] Vecino, X., Devesa-Rey, R., Cruz, J.M. and Moldes A.B. Study of the synergic effects of salinity, pH and temperature on the surface active properties of biosurfactants from *Lactobacillus pentosus*. **J. Agric. Food Chem.,** Vol.60 (5), 2012, pp.1258-1265.

[8] Moldes, A.B., Paradelo, R., Rubinos, D., Devesa-Rey, R., Cruz, J.M., and Barral M.T. Ex Situ Treatment of Hydrocarbon-Contaminated Soil Using Biosurfactants from Lactobacillus pentosus. **J. Agric. Food Chem.,** Vol. 59 (17), 2011, pp. 9443-9447.

[9] Moldes, A.B., Alonso J.L., and Parajó, J.C. Resin selection and single-step production and recovery of lactic acid from pretreated wood. **Appl. Biochem. Biotechnol.**, Vol. 95 (2), 2001,pp. 69-81.

[10] Moldes, A.B., Alonso, J.L. and Parajó J.C. Recovery of lactic acid from simultaneous saccharification and fermentation media using anion exchange resins. **Bioprocess Biosyst Eng.**, Vol. 25, 2003, pp. 357–363.

[11] Gullón, B., Alonso, J.L., and Parajó J. C. Ion-Exchange Processing of Fermentation Media Containing Lactic Acid and Oligomeric Saccharides. **Ind. Eng. Chem. Res.**, Vol. 49, 2010, pp. 3741-3750.

[12] Uslu H., Bayat, C., Gökmen, S. And Yorulmaz, Y. Reactive extraction and LSER model consideration of lactic acid with tripropylamine+ organic solvent systems from aqueous solution at room temperature **Desalination**, Vol. 249, 2009, pp. 694–698.

[12] Przepiora, A., Hesterberg, D., Parsons, J.E, Gilliam, J. W., Cassel, D. K., Faircloth, W. Calcium sulfate as a flocculant to reduce sedimentation basin water turbidity. **J. Environ. Qual.** Vol. 26, 1997, pp. 1605–1611.

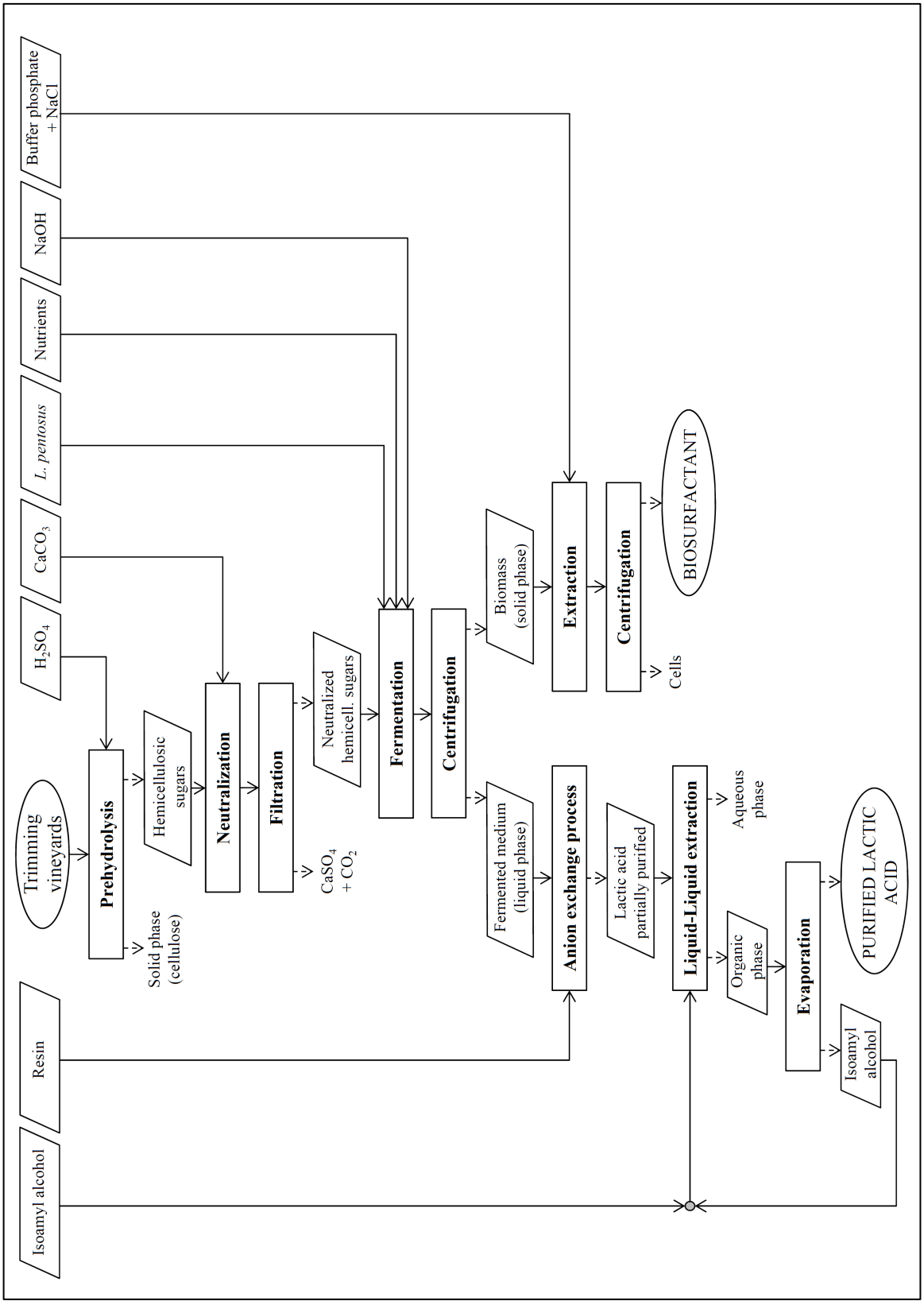

Figure 1. Scheme of simultaneous production of biosurfactants and lactic acid from trimming vineyard.

EFFECT OF SOIL LOADING AND pH DURING BATCH SOLVENT EXTRACTION OF FLUORENE FROM SOIL USING A LIPOPETIDE BIOSURFACTANT AQUEOUS SOLUTION

Xanel VECINO
Chemical Engineering Department, University of Vigo
Vigo, 36310 / EEI-Campus As Lagoas, Spain

Rosa DEVESA-REY
Defense University Center, Escuela Naval Militar,
University of Vigo, Spain

José Manuel DOMINGUEZ
Chemical Engineering Department, University of Vigo
Ourense, 32004 / Science Faculty, As Lagoas, Spain

José Manuel CRUZ
Chemical Engineering Department, University of Vigo
Vigo, 36310 / EEI-Campus As Lagoas, Spain

and

Ana Belén MOLDES
Chemical Engineering Department, University of Vigo
Vigo, 36310 / EEI-Campus As Lagoas, Spain

ABSTRACT

In this work a lipopeptide biosurfactant, obtained from an agro industrial residue, was used as washing agent to remove fluorene from soil. Soil extraction carried out with biosurfactants is more environmental friendly tan those extraction based on volatile solvents or chemical surfactants. Thus, in order to find the best operational conditions, the effect of soil loading and pH during batch solvent extractions were studied by using different solid/liquid ratios and pH. We found that generally a decreasing soil:solution ratio resulted in a higher extraction efficiency. Thus when the solid/liquid ratio was fixed at 1/50, 100 % of fluorene was extracted from soil at pH 6.

Keywords: bisourfactants, lipopeptide, soil, PAHs, bioremediation

1. INTRODUCTION

Polycyclic aromatic hydrocarbons (PAHs) compounds are considered in carcinogenic, mutagenic, and teratogenic compounds [1,2]. Thus, in 2008, 28 PAHs have been identified as priority pollutants by the National Waste Minimization Programme, in a project funded by US Environment Protection Agency [3].

In previous works [4], a biosurfactant obtained from *L. pentosus* was used to improve the spontaneous biodegradation of octane in soil; observing that after 15 days of starting the bioremediation experiment, biosurfactants from *L. pentosus* reduced the concentration of octane in the soil to 58.6 % or 62.8 %, for soil charged with 700 and 70.000 mg/kg of hydrocarbon respectively. It can be speculated that the removal of octane from soil should be easier than the elimination of fluorene because octane is linear hydrocarbon with a low molecular weight, whereas fluorene is a polycyclic aromatic hydrocarbon.

The aim of this research was to evaluate the feasibility of biosurfactants contained in an agricultural residue for the removal and biodegradation of polycyclic aromatic hydrocarbons (PAHs) from contaminated soil. Batch extraction experiments were carried using different soil loadings and pH.

2. MATERIALS AND METHODS

Contamination of soil

Farming soil, collected from a 0-20 cm deep layer in Carballo-Coruña (Spain) was contaminated with 500 mg/L of fluorene. Before contamination, soil was sieved at a particle size lower than 1mm. Following, soil samples, 2.5 g, were contaminated with 1 mL of a solution containing 1.25 mg of fluorene/mL of acetone. Fluorene was dissolved in acetone in order to produce an homogeneous distribution of fluorene in soil. Following, the contaminated soil, at a final concentration of 500 mg/L of fluorene, was stirred vigorously for 30 min to promote homogeneous distribution of fluorene. Soil samples were left to rest for 48 h at 28 ºC to eliminate acetone in a shaker at 150 rpm.

Elemental analysis of soil

Soil was analyzed using a Fisons-EA-1108 CHNS-O (Thermo Scientific). Previously to analysis soil was submitted to thermo catalytic decomposition. Analyses were carried out by triplicate.

Desorption of fluorene from soil within a water-soil-biosurfactant system

Soil samples (0.5 to 2.5 g) were saturated with 25 mL of an aqueous solution, containing a lipopeptide, within pH 3-6.

Following, the water-soil-biosurfactant system was kept under agitation at 150 rpm for 24 h. The soil sample was removed from the solution by centrifugation at 1350 x g for 30 min. To determine the amount of fluorene removed from the samples, the concentration of fluorene in the supernatant was analyzed by spectrophotometry at 254 nm. The wavelength was chosen based on the maxima absorbance values of fluorene. The percentage of fluorene eliminated was calculated based on the content of initial fluorene applied to the soil and the final fluorene concentration in the aqueous phase. Soil samples, also were washed with 25 mL of water in absence of biosurfactant and the percentage of fluorene extracted, was used as control.

Because fluorene has low solubility in water the calibration curve was obtained by dissolving fluorene in acetonitrile: water (1:1). Thus, the aqueous supernatants from samples also were dissolved in acetonitrile: water (1:1) before measuring it in the spectrophotometer at 254 nm.

3. RESULTS AND DISCUSSION

The maxima concentration of PAHs that can be achieved in the solvent solution is 10 mg/L; 30 mg/L and 50 mg/L corresponding to the assays containing 0.5 g, 1.5 g and 2.5 g of soil respectively. **Table 1** shows the solid/liquid ratio used in the different assays as well as the maxima concentration of fluorene that can be achieved in the aqueous phase.

Table 1. Maxima fluorene concentrations that can be extracted by the aqueous solution, containing the biosurfactant, under different soil loadings.

Amount of soil (g)	Solid /liquid ratio (g/mL)	Maxima concentration of fluorene in the aqueous phase (mg/L)
0.5	1/50	10
1.5	1/16.6	30
2.5	1/10	50

Results obtained in this work, showed the ability of biosurfactant to increase the apparent solubility of fluorene in the aqueous phase, and significantly enhanced its biodegradation within 24 hours at the lower solid/liquid ratio (1/50).

The extraction of fluorene to the aqueous phase, containing the biosurfactant, was found to be rapid (within 1 h). **Figure 1** shows the percentage of fluorene extracted after one hour at the lower, intermediate and higher soil loading, at different pH: 3, 4, 5, and 6. It can be observed that 1/50 solid/liquid ratio rendered the maximum percentage of extraction (100%) in comparison with higher solid liquid ratios, where the maximum percentage of extraction was about 46 % and 27 % using 1/16.6 at pH 6 and 1/10 solid/liquid ratio at pH 6 respectively. It is important to point out that the maximum percentages of extraction were achieved at pH 6 in all the experiments. These results are in concordance with those reported by other authors. Thus, Pannu et al. [5] found that a pH within the range of 4–8 highest oil recovery from soil was achieved (more than 90%); whereas the highest PAH extraction efficiency occurred at pH of 6–7.

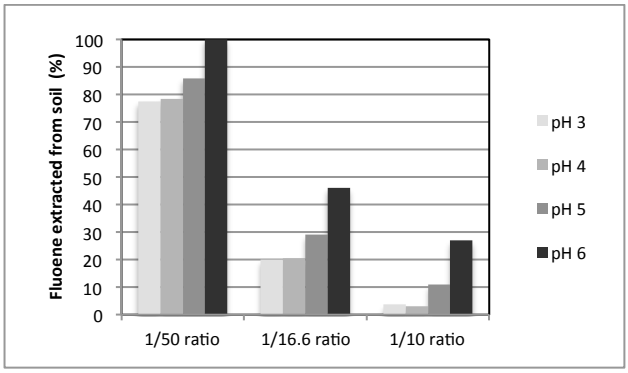

Figure 1. Percentage of fluorene eliminated from soil at different soil loading and different pH.

In addition **Figure 2** shows the concentration of fluorene in the aqueous phase containing the lipopeptide biosurfactant after 24 hours of starting the extraction process. It was observed that lower solid/liquid ratios not only improved the extraction of fluorene from soil, but also increased the biodegradation or elimination of PAH from the aqueous phase after longer bioremediation times.

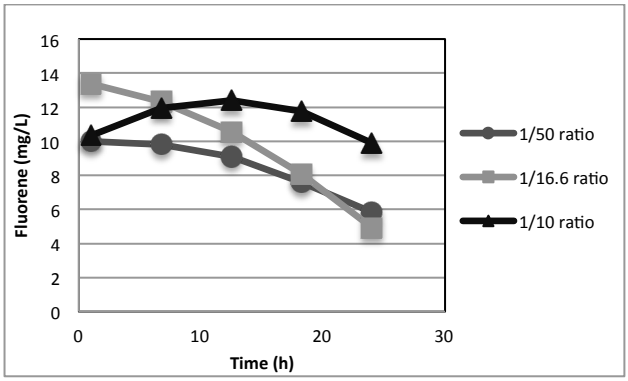

Figure 2. Biodegradation of fluorene in the aqueous solution, corresponding to the fluorene eliminated from soil under different solid/liquid ratios at pH 6, in presence of biosurfactant.

In this work, percentages of fluorene extraction were similar to those obtained by other authors using synthetic surfactants like Triton X-100, Tween 80 and Brij 30 [6-8].

4. CONCLUSIONS

The results from this study indicate that aqueous solution containing biosurfactants obtained from an agricultural residue is appropriate as washing agent as well as biodegradation enhancer for the detoxification of PAHs contaminated soil. The extraction and biodegradation of PHAs from soil was increased using low solid/liquid ratios around: 1/50 (g of soil/ mL of biosurfactant aqueous solution).

ACKNOWLEDGMENT

The authors wish to thank to the Spanish Ministry of Economy and Competitiveness (project CTM2012-31873) and Vecino X. is grateful to the University of Vigo for her predoctoral contract.

5. REFERENCES

[1] J. Santodonato. Review of the estrogenic and antiestrogenic activity of polycyclic aromatic hydrocarbons: relationship to carcinogenicity. **Chemosphere**, Vol. 34, 1997 pp. 835–848

[2] C.E. Bostrom, P. Gerde, A. Hanberg, B. Jernstrom, C. Johansson, T. Kyrklund, A. Rannug, M. Tornqvist, K. Victorin and R. Westerholm. Cancer risk assessment, indicators, and guidelines for polycyclic aromatic hydrocarbons in the ambient air. **Environmental Health Perspectives**, Vol. 110, 2002, pp. 451–488.

[3] Yap, C. L., Gan, S. and Ng H. K. Application of vegetable oils in the treatment of polycyclic aromatic hydrocarbons-contaminated soils. **Journal of Hazardous Materials**, Vol. 177, 2010, pp. 28-41.

[4] Moldes, A.B., Paradelo, R., Rubinos, D., Devesa-Rey, R., Cruz, J.M. and Barral, M.T. Ex situ treatment of hydrocarbon-contaminated soil using biosurfactants from Lactobacillus pentosus. **Journal of Agricultural and Food Chemistry,** Vol. 59, 2011, pp. 9443-9447.

[5] Pannu, J.K., Singh, A. and Ward, O.P. Vegetable oil as a contaminated soil remediation amendment: application of peanut oil for extraction of polycyclic aromatic hydrocarbons from soil. **Process Biochemistry**, Vol. 39, 2004, pp. 1211–1216.

[6] Zhu, H., Aitken, M.D. Surfactant-enhanced desorption and biodegradation of polycyclic aromatic hydrocarbons in contaminated soil. **Environ. Sci. Technol**. Vol. 44, 2010, pp. 7260-7265.

[7] Hussein, T.A., Ismail, Z.Z. Desorption of selected PAHs as individuals and as a ternary PAH mixture within a water-soil-nonionic surfactant system. **Environ. Technol,** Vol. 34, 2013, pp. 351-361.

[8] Singh, A.K., Cameotra, S.S. Efficiency of lipopeptide biosurfactants in removal of petroleum hydrocarbons and heavy metals from contaminated soil. **Environ. Sci. Pollut. R.** Vol. 20, 2013, 7367-7376.

Optimization of a Compact Thermal Model For a Ball Grid Array (BGA) Package Using Experimental Data

Magdy ABDELAAL
Communication & Networks Engineering Department, Prince Sultan University
P.O.Box No. 66833 Rafha Street, Riyadh 11586, Saudi Arabia

and

Tayaz FAKHRY, Farah MOHAMMADI
Department of Electrical and Computer Engineering, Ryerson University
Toronto, ON, M5B 2K3, Canada

ABSTRACT

This paper presents generation of a compact thermal model of a Ball Grid Array (BGA) based on experimental results obtained from infrared (IR) camera system with the optimization process, so that the steady state and transient thermal behaviors of the package may be predicted fast with required accuracy. The optimization algorithm selected for compact model generation was Gauss-Newton and Levenberg-Marquardt methods which are well known as a fast and high performance method of multidimensional optimization using MATLAB.

Keywords: Compact Thermal Model, Ball Grid Array (BGA), infrared (IR) camera system, Optimization

1. INTRODUCTION

More component density in electronic boards, more speed of VLSI circuits and unwillingly more power dissipation of fast electronic devices seem to be bundled together. Dramatic increase of applications of such circuits and devices, urges the thermal analysis and power management studies of such systems a vital design requirement. The amount of dissipated power by the chip is directly related to its temperature which is a crucial parameter in electrical behavior of electronic components, circuit performance, and reliability of the electronic system. Thermal analysis is an important part of modern electronic design thus that enables the designer to calculate the critical thermal variables as key factors in electrical analysis and accurate performance estimation. In general, there are three levels of thermal analysis: component, package or system level. Depending on the level of the design an electronic designer is engaged with, one of these analyzing levels must be chosen that gives out only the sufficient and relevant information about the thermal behavior of the subject of the thermal analysis [1,2].

In many cases of thermal analysis most of the information provided as the detailed model is unnecessary for the consumer because it includes the thermal characteristics of undesired locations. A smaller model that is capable of calculating only the hot spots, the temperatures and heat fluxes at some desired locations can help the designer to perform the thermal analysis much more easily and quickly with the required accuracy. Such model is called Compact Thermal Model (CTM). CTM can be generated from the detailed numerical model or the experimental data. This thesis focuses on generation of CTM at package level using experimental test.

The key to successful experimental test (for the purpose of thermal analysis) is the ability to obtain comprehensive and accurate prediction of temperature gradients influencing the quality of electronic products under near real-time operating conditions. However, the commonly used method of gathering these temperature gradients using thermocouples is limited by the large number of points to be monitored and the small size of the components being measured. Connecting tens to hundreds of thermocouples is very time consuming. In addition, thermocouples can act as heatsinks and conduct away heat, affecting the accuracy of measurements since the action of the heatsink may lower device temperatures.

Infrared (IR) thermal imaging system is a method which addresses the above-mentioned issues by providing comprehensive two-dimensional temperatures gradients of components under test [3,4]. This is accomplished without the need to make contact with the components. Therefore, the thesis focuses on generation of CTM at package level using experimental testing data obtained from infrared thermal imaging system.

2. THERMAL ANALYSIS OF ELECTRONIC PACKAGES BY INFRARED (IR) CAMERA

A recent infrared thermography setup for thermal analysis of electronic packages was proposed by [3] in 2009. The measurement setup is used to perform two types of analysis a) steady state analysis, b) transient analysis. In steady state analysis, after switching the power ON, a time interval is given to the system to reach its steady state condition. This is due to the fact that oil based heat-sink takes some period of time to completely cover the whole surface of the device under test (DUT) and remove the heat homogenously. To perform transient analysis on the DUT, an abnormal stress is imposed to a system in the form of different load work conditions.

The major apparatus used in the proposed experimental setup include an FLIR infrared camera system, data acquisition system, digital thermometer, infrared transparent oil (Aldrich oil), oil pump and power supply. A typical measurement setup is shown in figure 2.5. The measurement setup is capable of capturing up to 420 frames per second (fps) with a 10μm 10μm spatial resolution, and it can be applied to multiple chips with relative simplicity. The IR camera frame rate can be increased up to 10 KHz as long as the bandwidth of the camera stays under 1GB/s.

2.1 Infrared Camera

The infrared camera used in this measuring setup is a FLIR SC4000 camera (Fig. 1) which is a high-speed, high-resolution, high sensitivity, science-grade infrared camera with Gigabit Ethernet, Camera Link and USB interfaces for maximum flexibility and performance. With a 320 × 256 pixel Indium Antimonide (InSb) detector, the ThermoVision SC4000 camera offers unmatched

resolution and thermal sensitivity. An extremely sensitive detector and high speed read out design, provide the camera with extraordinary image quality for the most demanding applications. A typical temperature distribution of a DUT with a cooling fan is shown in Fig. 2. The thermocouple installed under the heat-sink (LO1) indicates temperature of 52.3°C.

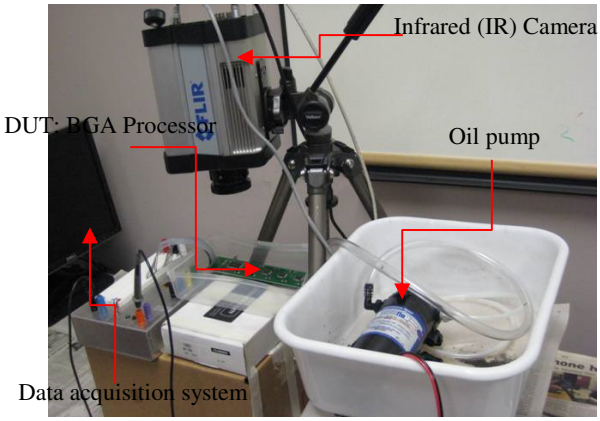

Fig. 1: Typical Test Setup

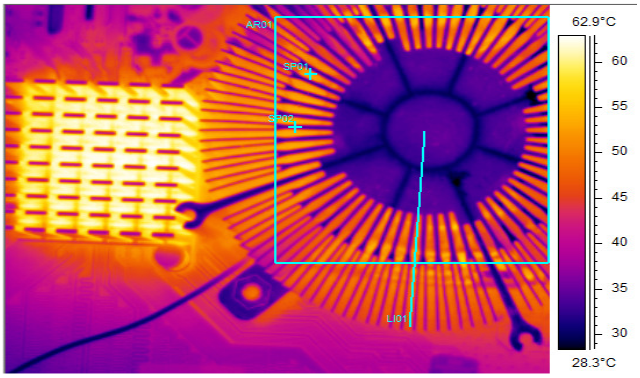

Fig. 2: Typical Temperature Distribution of the DUT with Air Cooling.

2.2 Data Acquisition System

The data was captured and analyzed using the integrated data acquisition system of the optical system, supported by PC-based ThermaCAM Researcher software for data acquisition, analysis and reporting. ThermaCAM Researcher software contains powerful measurement and analysis functions for extensive temperature analysis, including isotherms, line profiles, area histograms and image subtraction capability. The acquired input data were recorded in real time for subsequent analysis using this software package. Additionally, the SC4000 camera system has an optional Software Development Kit (SDK) for custom programming and interfacing to the camera.

2.3 Software and computing tools

Various hardware and software pieces are required to obtain a compact thermal model of a package. These tools were applied to the experimental test setup, various coding programs, execution and running the experimental case studies post-processing analysis.
Three different categories of software were applied in this work: Experimental test software is those related to the programming of a BGA. ModelSim and Quartus II [5] module is used to run the BGA in a way that the circuitry and as such the BGA, drives a current into the circuit and by calculating the power of the BGA and having the temperature profile of the device under test (DUT) and tracking the junction temperature so the static and dynamic compact thermal model may be obtained.
Then, infrared (IR) camera system's dedicated software is discussed as part of the data acquisition system (section 2.2). The last category is mathematical and post-processing software to obtain the compact thermal model for a BGA. An algorithm was developed in MATLAB to calculate the proper values for the RC network. These values are optimized by a cost function and optimization algorithm. The optimization algorithm was based on the Gauss-Newton and Levenberg-Marquardt methods.

3. PARAMETERS FOR THE BGA TEST CONFIGURATION

Temperature profile were collected from the BGA (CYCLONE II FPGA Development Kit ALTERA, Fig. 3) [6,7]) using the software development kit (SDK) of the IR camera and Verilog and Quartus II instruction code. Selected parameters for the BGA test configuration is listed in Table 1.

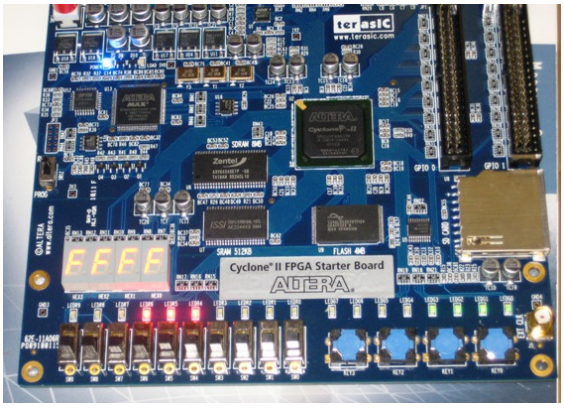

Fig. 3: Device under Test (DUT) - BGA Electronic Package

Table 1: Parameters for the BGA Test Configuration.

Configuration Parameter	Description
DC Voltage Supplier	7.5 Volts
IR Camera constants: Speed	30 f/s- 2700 frames
IR Camera constants: Pixels	320□256
IR Camera constants: Distance	30 cm
Oil Pump distance	30 cm, identical level
Heat-sink flow	Laminar
Fixed Emissivity	0.92
Average Ambient Temperature	23.3 □C

4. DYNAMIC COMPACT THERMAL MODEL

Process of generating the compact thermal model for a BGA is illustrated in the flowchart shown in Fig. 4. First the frames corresponding to the temperature profiles of the surface of the BGA are obtained via the SDK. To perform the procedure of fetching the frames, the software application of Visual C++ was used. This developed program looked for the X and Y coordinates of a specific element (in this case the junction temperature) in a raw data file obtained by SDK. Then a resistor network topology representative of the experimental data was calculated. The transient or time dependent dynamic model of a package is generated by calculating the resistors' and capacitors' value by optimization method.

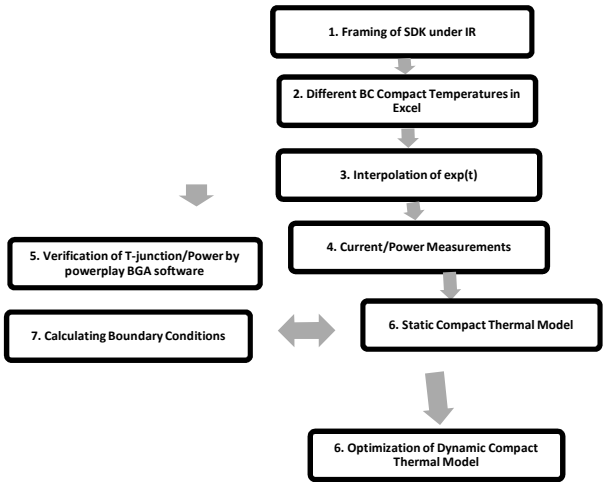

Fig. 4: Flowchart of Generating the Compact Thermal Model for a BGA.

4.1 Definition of a RC Dynamic Compact Thermal Model

The topology of the RC network illustrated in Fig. 5 was used for the BGA package. This RC network includes a total of seven resistors and seven capacitors. Each capacitor represents a particular part of the package thermal mass.
Using node voltage analysis, the governing equation of solving network is:

$$[C]\frac{d}{dt}[T(t)]+[G][T(t)]=[P(t)] \quad (2)$$

where [C] and [G] represent the thermal capacitance and the thermal conductance matrix, respectively.
is the temperature vector, and is the nodal loads and sources which express the heat source connected to the junction node and boundary conditions applied to the external nodes.

Equation (2) is a set of 14 linear differential equations. Equation (2) has been transferred from time domain to frequency domain by Fourier transform.

$$[T(\omega)]=(j\omega[C]+[G])^{-1}[P(\omega)] \quad (3)$$

Equation (3) is the definition of the RC network dynamic compact model.
Under steady state conditions all capacitors are fully charged and model is only a resistor network. Therefore, the matrix C is null. The obtained results from detailed model can be used to calculate the matrix G of equation (2). We assume a constant nodal dissipation (p(t)) of 0.25 watts for steady state analysis. For dynamic analysis, power dissipation is a step function with magnitude equal to 0.25 watts.

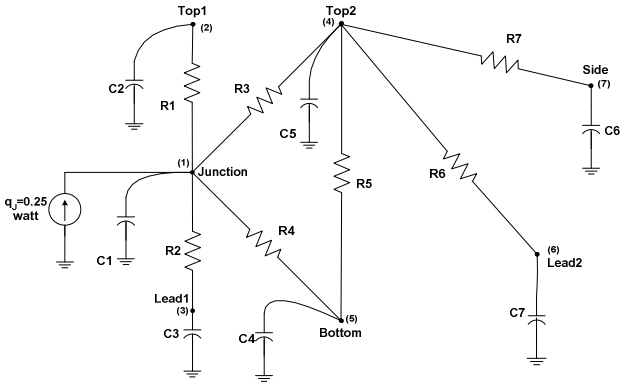

Fig. 5: Dynamic Compact topology for the BGA package.

4.2 Optimization Method

The method of computing resistors and capacitors is performed by an optimization algorithm. An optimization algorithm has been developed in MATLAB [8] to calculate the proper values for these parameters. Their values are optimized by a cost function and optimization algorithm. The optimization algorithm was based on Gauss-Newton and Levenberg-Marquardt methods which are well known as a fast and high performance method of multidimensional optimization. This is one of the most popular and widely used methods of multi-variable our multi-dimensional optimization which belongs to the class of direct search optimization methods because it doesn't use derivatives of variables. The optimization algorithm tries to find the best values of parameters so a cost function representing the deviation between the compact and detailed model is minimized. The cost function is defined as:

$$COST=\sum_{i=1}^{N}\sum_{k=1}^{n}\left(\frac{\left|Tj_i^d(\omega_k)\right|-\left|Tj_i^c(\omega_k)\right|}{\left|Tj_i^d(\omega_k)\right|}\right)^2 \quad (4)$$

where N=58 is the number of boundary conditions,
n=512 is the number of samples in time domain or frequency domain,
$\left|Tj_i^d(\omega_k)\right|$ is the magnitude of the Fourier transform of the ith Junction temperature obtained from experimental test,
$\left|Tj_i^c(\omega_k)\right|$ is the magnitude of the Fourier transform of the ith Junction temperature calculated by compact model.

A summary of the resistors' and capacitors' values of dynamic compact thermal model is listed in Table 2.

Table 2: Static & Dynamic Compact Thermal Models for a BGA Obtained.

Capacitance – Dynamic Compact Model (j/K)	Admittance – Static Compact Model (K/W)
0.088	54.353
0.026	116.34
1.8057	106.56
0.0015	4.87
0.00042	3.77
0.04	87.70
0.00024	4.39

4.3 Validation

Verification of the compact model is the process of comparing its results to the experimental results and calculating the relative error percentages. According to the criterion proposed in [9] we can consider the generated model a valid Compact Thermal Model if its relative difference with respect to the experimental results does not exceed certain agreed value for predetermined parameters such as junction temperature. As proposed in [9], the relative errors must not exceed 10% and as long as thermal variables predicted by compact model show relative errors with respect to experimental test less than this predetermined value, the generated compact model is validated and is acceptable. Table 3 shows the junction temperature relative errors for four applied boundary conditions obtained from dynamic analysis. It's clear that all of the errors are less than 10% criterion accepted in this work.

Table 3: Junction temperature comparison

Case	Compact Model	Experimental	Difference
1	41.1	43.9	6.6%
2	37.2	40.1	7.4%
3	32.2	34.8	7.8%
4	24.6	25.7	3%

5. Conclusion

A methodology for generation of static and dynamic compact thermal model using an experimental infrared measurement technique was presented. This method was applied for a Ball Grid Array (BGA). In this work, coupling the IR thermography measurement with the optimization process to generate a compact thermal model was performed. The experimental setup is capable of performing steady state and transient analyses. The optimization process was developed by using an optimization block in order to calculate and optimize the boundary conditions required for the compact thermal modeling. Based on the obtained results, it can be concluded that the dynamic thermal behavior of BGA package can be described by generated dynamic compact model. This model is capable of calculating the temperatures and heat fluxes at some desired locations which can help the designer to perform the thermal analysis much faster and easier with the required accuracy.

ACKNOWLEDGEMENT

The authors would like to acknowledge the supports provided by National Science and Engineering Council of Canada (NSERC) and Ryerson University.

REFERENCES

[1] C. Gillot, Y. Avan, N. Cezac, G. Poupon, C. Schaeffer, and E. Fournier, “Silicon Heat Pipes Used as Thermal Spreaders”, IEEE Trans. on Components and Packaging Technologies, Vol. 26, No. 2, June 2003.

[2] F.A. Mohammadi and S. Sharifian Attar, “Development of an Electro-thermal Simulation Tool for Integrated Circuits”, Canadian Journal of Electrical and Computer Engineering (CJECE), Vol. 33, Issue 3, 2008.

[3] F. Farrokhi, F.A. Mohammadi “Temperature and Power Measurment of Modern Dual Core Processor by Infrared Thermography”, Proceeding of the IEEE International Symposium on Circuits and Systems (ISCAS2010), pp. 1603 - 1606, Paris, France, May 30- June 02, 2010.

[4] Wan Jiuqing, Li Xingshan, "PCB infrared thermal imaging diagnosis using support vector classifier," Intelligent Control and Automation, 2002. Proceedings of the 4th World Congress on, vol.4, no., pp. 2718- 2722 vol.4, 2002 doi: 10.1109/WCICA.2002.1020010.

[5] Navabi, Zainalabedin.: Digital design and implementation with field programmable devices, 2004.

[6] ALTERA Corporation, “CYCLONE II Device Family Datasheet”, February 2008.

[7] http://www.altera.com/literature/ug/ug_cii_starter_board.pdf, Last Accessed in February 17, 2011.

[8] The MathWorks Inc., MALAB R2011 Copyright 1984-2011 http://www.mathworks.com/

[9] Clemens J. M. Lasance, "Two Benchmarks to Facilitate the Study of Compact Thermal Modeling Phenomena," IEEE Transactions on Components and Packaging Technologies, VOL. 24, No. 4, December 2001.

MASS DISTRIBUTION EFFECTS ON FLUTTER CHARACTERISTICS AS RESULT OF SAWTOOTH

Abid A. Khan
Institute of Space Technology, Pakistan, 44000
E-mail: khan.abid@ist.edu.pk
Nadeem S. Khan
National University of Sciences & Technology, Pakistan, 24090
E-mail: nadeem@gatech.edu

ABSTRACT
Flutter clearance is a critical phase of prototype aircraft qualification for airworthiness in designed flight envelope. Flutter problems experienced on an aerodynamic surface (horizontal tail) during wind tunnel testing and subsequent flight testing of whole aircraft were investigated. In order to address the observed problem, number of methods were studied and evaluated to optimize the design for flutter safe flight. This paper deals with an experimental investigation on the effect of flutter characteristics induced by the saw tooth cut on a scale model of wing tail with an aim to change the mass distribution. This paper presents the experimental setup, the results obtained and the analysis of the designed modification for the purposes of enhancing the flutter speed.

1. INTRODUCTION

Flutter is a self-excited oscillation of an aerodynamic surface and its associated structure caused by the interaction of the aerodynamic, inertial and elastic characteristics of the components involved [1]. High speed aircraft are more susceptible to flutter although it can even be observed on home built aircraft. At speeds below the flutter speed, oscillations will be damped. However, at flutter speed, un-damped oscillations will persist with constant amplitude. The divergent behavior can occur within a few cycles or with very little velocity increment above flutter speed which results in in damage or destruction of structure.

Flutter may be caused by the coupling of two or more structural modes [2]. These coupled modes may be wing bending and torsion, wing bending-control surface hinge torsion, wing torsion-fuselage bending, or horizontal/vertical tail-fuselage modes. With the increase in speed, frequency of some modes remains stable and these modes do not interact with any other structural mode. However, frequency of other modes change as speed is increased and they tend to interact with each other. At certain velocity (V_f), the modal damping of a mode goes to zero, which becomes an onset condition for flutter.

The first flutter incident was recorded on a Handley Page 0/400 a twin engine biplane bomber in 1916. Since then a remarkable progress in flutter flight testing techniques with advances in computational methods, has been reported as efforts in flutter prediction. Historical overview of the testing techniques [3], advances in test data analysis [4] and overview of flight flutter testing research at NASA [5] sum up the efforts in this direction till end of last century. However, a number of publications in the last decade further advanced the research in predicting the phenomena through simulation and computational techniques [6-14].

Realizing catastrophic behavior of flutter, a lot of research as efforts to delay or avoid the excitement has been published. Use of advanced materials to meet high flutter speed requirements with minimum weight, without strength penalty is one of the useful techniques being implemented [15]. Reconfiguration of aerodynamic surfaces [16-18], study of reducing non-linearities [19, 20] and change in mass distribution through addition of balance weights [21] are some other important research study areas in the field. Effect of local structural alterations during the process of design optimization [22, 23] was studies in the last decade and alterations to the control actuators and associated considerations in aero-servo elastic analysis resulting from different order state space models [24, 25] have already been researched.

There are authors who have also proposed useful methods for investigation and suppression of flutter in turbo-machinery [26, 27]. In addition the flutter occurrences are also distressing civil engineers as its application on bridge construction is complex and a lot has been published in this regards [28, 29].

2. AIRCRAFT FLUTTER WTT

Evaluation of flutter performance of all critical aircraft surfaces vis-a-vis design through conduct of wind tunnel tests, on scale model, at different speeds is a routine procedure during aircraft development. These tests are performed to determine the airspeed, frequency and damping of potential aircraft flutter to verify analytical flutter computations. During these tests, flutter speed of horizontal tail was found to be low. Detail analysis of test results revealed that damping of the horizontal tail was found to be 14% during ground vibration testing as compared to flutter model which had very low damping of approximately 6%. This caused substantial decrease in the rotational stiffness of the horizontal tail on flutter model. It was therefore, decided to further investigate the flutter characteristics during tail flutter testing.

Horizontal Tail Flutter Test

A low speed flutter wind tunnel test on of the horizontal tail was thus conducted for further investigations. During these tests, a model of scale 1:2 was used for determining the flutter frequency for different bending and torsional stiffness, angles of attack and varying values of free play of attachment shaft. The data so obtained during 35 wind tunnel runs was considered essential for evaluation and comparison of flutter speed and frequency determined through computational work using Finite Element Method.

Additional Tests. During the tests flutter speed for the model was recorded close to 38 m/s. An additional task of changing the configurations of test model with addition of balance weights at different locations and use of stiffer springs was also accomplished which gave positive results and flutter speed went over 38 m/s. The flutter speed went into an acceptable range with torsional stiffness increase by 25% and introduction of balance weight of 4Kg at the root of horizontal tail. In addition to the change in balance weights another technique which is not very common for flutter optimization was selected for studying its effect on the flutter characteristics.

3. SAW TOOTH DESIGN

The structural design although not very common, but has been successfully used on F-15 aircraft for weight reduction [30]. The saw tooth shown in Fig-1, is being used for curing flutter problems and eliminate buffet for the aircraft. The planform developed with saw tooth cut not only generates vortices and delays flow separation at high angle of attack but has been claimed to positively impact the flutter velocity.

Figure 1: Horizontal Tail on F-15 Aircraft

Saw Tooth Implementation Scheme

Two tail models with 1:2 scale were prepared for testing. First model was tested in its original shape as shown in figure 2 whereas, second model as shown in figure 3 was modified for saw tooth cuts of different sizes tabulated in table 1. A total of three different saw tooth areas were tested for determining the effects of saw tooth on flutter characteristics.

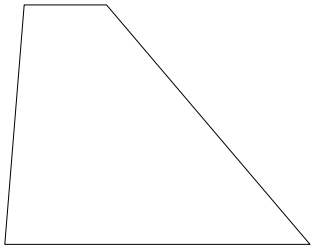

Figure 2: Horizontal Tail Planform

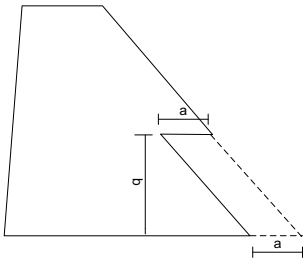

Figure 3: Saw Tooth Cuts

Table 1: Leading Edge Saw Tooth

Case	a (mm)	b (mm)	Area (mm^2)	% Area of Saw Tooth
1	300	450	135000	5.87
2	250	550	137500	5.98
3	250	650	162500	7.06

Flutter Tests with Saw Tooth

Model 2 with three different saw tooth areas as given in table 1 were tested. A total of 30 wind tunnel test runs were conducted to verify the effect of modification on the flutter speed. Figure 4 below shows the placement of model in the wind tunnel whereas, figure 5 shows

different saw tooth cut configurations of the horizontal tail model.

Test Results. Flutter speed and frequency were recorded for model # 2 (with saw tooth) during wind tunnel testing so that these parameters can be compared with already available values recorded for model # 1 (without saw tooth) and analytically computed results.

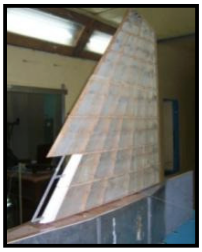

Figure 4: Tail Model in Wind Tunnel

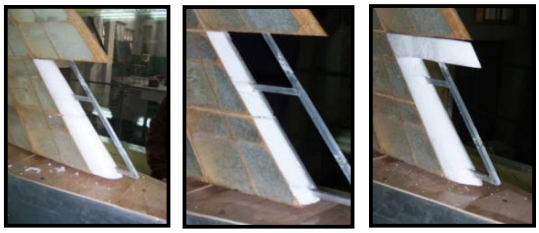

Figure 5: Wind tunnel testing

Analytical computations performed on the model for comparison showed that an increase of 10% in flutter speed at 2% damping was possible by use of saw tooth design. Damping and frequency correlations in torsion mode are published in the literature [31-33] and same can be used for analysis of the results.

The test runs verified that the flutter speed increases with the use of saw tooth modification on horizontal tail model. The increase noted through the tests was only 7%, which was lower than the analytically computed values of 10%. The detailed test results for the both the models are tabulated in table 2. A number of test runs were performed during testing however, only average parameter value for each configuration has been mentioned in the table for analysis.

4. ANALYSIS

The figure 3 shows that saw tooth modifications are quadrilateral areas with dimension 'a' as depth in the aircraft longitudinal direction whereas 'b' as length in the aircraft lateral direction. The test results reveal that introduction of saw tooth cut at the tail's leading edge increased the flutter speed. The maximum increase is observed with a deeper saw tooth (larger dimension 'a'). However, increase in flutter speed was maximum when saw tooth area was 5.87% which reduced when it was increased to 5.98% and 7.06 %. Therefore, reduction in the effective area of the horizontal tail leads to lower values of flutter speed.

Table 2: Saw Tooth Test Results

S No	Flutter Speed (m/s)	Flutter Frequency (Hz)	Remarks
1	33.5	3.80	Model 1 without saw tooth
2	37.5	3.99	Model 2 with saw tooth case 1
3	36.3	3.95	Model 2 with saw tooth case 2
4	35.5	4.00	Model 2 with saw tooth case 3

The advantages of saw tooth cut modification will adversely affect the aerodynamic characteristics of the aerodynamic surface. One of the direct effects is moving of the aerodynamic Center of Pressure (CP) towards the trailing edge. This change will affect the loading pattern on the horizontal stabilizer thus exerting increased loads on the actuator. This will thereby necessitate the alteration/ replacement of the actuator to cater for the modified hinge moment. In case the induced changes are not responded through other alterations, additional deflection of horizontal tail will be required to maintain the pitching characteristics of the aircraft.

5. CONCLUSIONS

The test results has validated the fact that introduction of saw tooth design (optimum area) will positively impact the flutter characteristics of aerodynamic surface. However, the maximum change observed in the flutter speed is approximately 10%. The change will be accompanied with other adverse effects therefore, it is not a desired scenario to achieve the result solely by means of incorporating the saw tooth cut. Flutter speed can be effectively improved by several means that alter the unsteady aerodynamic characteristics of an aerodynamic surface. However, various factors are to taken into consideration once deciding which method to be actually implemented. The final decision may include the degree of ease of adoption and the cost factor. Saw Tooth design can be adopted for increase in flutter speed. However, reduction in the surface area of tail will have other adverse effects necessitating the alterations in related hardware design, such as replacement of actuator.

References

[1] LE, C.F.I., *FLUTTER, BUZZ, AND DIVERGENCE*. NASA Space Vehicle Design Criteria. Vol. SP 8003. 1964: NASA.

[2] De Langre, E., *Frequency lock-in is caused by coupled-mode flutter.* Journal of fluids and structures, 2006. 22(6): p. 783-791.

[3] Kehoe, M.W., *A historical overview of flight flutter testing*. Vol. 4720. 1995: National Aeronautics and Space Administration, Office of Management, Scientific and Technical Information Program.

[4] Cooper, J., et al., *Advances in the analysis of flight flutter test data.* Advanced Aeroservoelastic Testing and Data Analysis, 1995: p. 13-1.

[5] Brenner, M.J., R.C. Lind, and D.F. Voracek, *Overview of recent flight flutter testing research at NASA Dryden*. Vol. 4792. 1997: National Aeronautics and Space Administration, Office of Management, Scientific and Technical Information Program.

[6] Kheirandish, H., G. Beppu, and J. Naicamichi, *Computational investigation of wing flutter.* International Journal of Computational Fluid Dynamics, 1999. 12(3-4): p. 279-290.

[7] Cai, C.S. and P. Albrecht, *Flutter derivatives based random parametric excitation aerodynamic analysis.* Computers & Structures, 2000. 75(5): p. 463-477.

[8] Leyland, P., et al., *Fully Coupled Fluid-Structure Algorithms for Aeroelasticity and Forced Vibration Induced Flutter.* Revue Européenne des Éléments Finis, 2000. 9(6-7): p. 763-803.

[9] Gee, D., *Numerical continuation applied to panel flutter.* Nonlinear Dynamics, 2000. 22(3): p. 271-280.

[10] Chamara, P. and B. Coller, *A study of double flutter.* Journal of fluids and structures, 2004. 19(7): p. 863-879.

[11] Moosavi, M.R., A.R. Naddaf Oskouei, and A. Khelil, *Flutter of subsonic wing.* Thin-Walled Structures, 2005. 43(4): p. 617-627.

[12] Haddadpour, H. and R.D. Firouz-Abadi, *Evaluation of quasi-steady aerodynamic modeling for flutter prediction of aircraft wings in incompressible flow.* Thin-Walled Structures, 2006. 44(9): p. 931-936.

[13] Hémon, P., E. De Langre, and P. Schmid, *Experimental evidence of transient growth of energy before airfoil flutter.* Journal of fluids and structures, 2006. 22(3): p. 391-400.

[14] Wei, T., S. Zhongke, and C. Jie, *Aircraft Flutter Modal Parameter Identification Using a Numerically Robust Least-squares Estimator in Frequency Domain.* Chinese Journal of Aeronautics, 2008. 21(6): p. 550-558.

[15] Guo, S.J., J. Bannerjee, and C. Cheung, *The effect of laminate lay-up on the flutter speed of composite wings.* Proceedings of the Institution of Mechanical Engineers, Part G: Journal of Aerospace Engineering, 2003. 217(3): p. 115-122.

[16] Ibrahim, R. and S. Castravete, *Flutter suppression of a plate-like wing via parametric excitation.* Nonlinear Dynamics, 2006. 46(4): p. 387-426.

[17] Zhang, W. and Z. Ye, *Effect of control surface on airfoil flutter in transonic flow.* Acta Astronautica, 2010. 66(7–8): p. 999-1007.

[18] Yu, M. and H. Hu, *Flutter control based on ultrasonic motor for a two-dimensional airfoil section.* Journal of Fluids and Structures, 2011.

[19] Tang, D. and E. Dowell, *Effects of geometric structural nonlinearity on flutter and limit cycle oscillations of high-aspect-ratio wings.* Journal of fluids and structures, 2004. 19(3): p. 291-306.

[20] Ding, Q. and D.-L. Wang, *The flutter of an airfoil with cubic structural and aerodynamic non-linearities.* Aerospace Science and Technology, 2006. 10(5): p. 427-434.

[21] Khan, A.A., A.M. Khan, and N.S. Khan, *Mass distribution effect of flutter characterstics*, in *The 5th International Multi conference on Engineering and Technological Innvoation*2012: Orlando, FL, USA. p. 44 - 49.

[22] Livne, E. and G.D. Blando, *Reduced-order design-oriented stress analysis using combined direct and adjoint solutions.* AIAA journal, 2000. 38(5): p. 898-909.

[23] Livne, E. and G.D. Blando, *Design-Oriented Frequency Response of Structural Dynamic Systems Using Combined Direct and Adjoint Reduced- Order Approximations.* AIAA journal, 2003. 41(7): p. 1377–1385.

[24] Brenner, M.J., *Actuator and Aerodynamic Modeling for High-Angle of- Attack Aeroservoelasticity.* AIAA Paper, 1993. 93: p. 1419.

[25] Brenner, M.J., *Aeroservo-elastic Modeling and Validation of a Thrust- Vectoring F/A-18 Aircraft.* NASA. Tech. p 3647, 1996. 96.

[26] Sun, X. and S. Kaji, *Control of blade flutter using casing with acoustic treatment.* Journal of fluids and structures, 2002. 16(5): p. 627-648.

[27] Ekici, K., R.E. Kielb, and K.C. Hall, *The effect of aerodynamic asymmetries on turbomachinery flutter.* Journal of Fluids and Structures, 2013. 36(0): p. 1-17.

[28] Matsumoto, M., et al., *Flutter instability and recent development in stabilization of structures.* Journal of Wind Engineering and Industrial Aerodynamics, 2007. 95(9–11): p. 888-907.

[29] Ge, Y.J. and H.F. Xiang, *Computational models and methods for aerodynamic flutter of long-span bridges.* Journal of Wind Engineering and Industrial Aerodynamics, 2008. 96(10–11): p. 1912-1924.

[30] Shelton, J. and P. Tucker. *Minimum weight design of the F-15 empennage for flutter*. in *AIAA, ASME, and SAE, Structures, Structural*

Dynamics, and Materials Conference, 16 th, Denver, Colo. 1975.

[31] Farhat, C., K. Pierson, and C. Degand, *Multidisciplinar Simulation of the Maneuvering of an Aircraft.* Engineering with Computers, 2001. 17: p. 16-27.

[32] Farhat, C., P. Geuzaine, and G. Brown, *Application of a Three-Field Nonlinear Fluid Structure Formulation to the Prediction of the Aeroelastic Parameters of an F-16 Fighter.* Computers & Fluids, 2003. 32: p. 3-29.

[33] Geuzaine, P., et al., *Aeroelastic Dynamic Analysis of a Full F-16 Configuration for Various Flight Conditions.* AIAA Jounal, 2003. 41(3): p. 363-371.

Micro-siting/positioning of wind turbines: introducing a multi-criteria decision analysis framework

Heracles Polatidis
Dept. of Earth Sciences, Uppsala University
Campus Gotland Visby, 621 67, Sweden

and

Stefan Ivanell
Dept. of Earth Sciences, Uppsala University
Campus Gotland Visby, 621 67, Sweden

ABSTRACT

In the context of wind energy planning the wind turbine micro-siting/positing issue refers to the optimal placement and arrangement of individual turbines in a wind farm. Different approaches have been proposed for tackling this problem in the literature including several types of optimization techniques, generic & meta-heuristic algorithms and applications of realistic models of integrated economic performance of wind farms, among others. In this article we propose Multi-Criteria Decision Analysis (MCDA) techniques as a complement to current practices for identifying an initial compromise solution to the problem of wind turbine micro-siting. After a short literature review on contemporary methods for micro-sitting/positioning of wind turbines in a specific site, and an introduction to the MCDA methods, we highlight the potential usefulness of MCDA methods in siting wind turbines in a certain terrain as a complement to current practices. We finally argue that MCDA methods could account for the inclusion of a number of socio-environmental parameters in the relevant process that was not apparent so far.

Keywords: Wind Turbines, Micro-sitting, Multi-Criteria Analysis, Wind project development.

1. INTRODUCTION

In the context of wind energy planning the wind turbine micro siting/positing problem refers to the optimal placement and arrangement of individual turbines in a wind farm. Different approaches have been proposed for tackling this problem in the literature with linear & non-linear optimization techniques and the use of Generic Algorithms (GAs) prevail together with the more recent implementation of meta-heuristic algorithms and applications of realistic models of integrated economic behavior of wind farms. The whole process is actually a challenging subject involving fluid dynamics and decision making and could play a crucial role in local wind energy planning.

Nevertheless, the methods used so far focus in optimizing a number of rather restricted parameters related to maximizing total electricity production and minimizing initial investment and overall life-cycle cost. In order to achieve this, specific criteria used for positioning individual wind turbines in a predefined site are the minimization of the wake effect, minimization of distance to access roads and electrical infrastructure, minimization of total land requirements and land cost, maximization of operational safety and the minimization of the topographic effect among others. Nonetheless, these criteria afford limited consideration to other environmental and social issues that may also be present as elements which can be included in the optimal micro-design for wind farms. In particular, factors such as visual impact, noise production, bird disturbance, biodiversity loss, impact on wild-life & habitats and the shadow effect, inter alia, can be studied during the micro-siting of turbines in a wind farm. In this way, it would be possible to assess and mitigate even further the particular local impact of the wind project on the environment.

It may therefore be an imperative, that new complementary to the already existent planning tools would be developed to identify the preferred micro-siting and design option for a wind project, balancing different, sometime intangible, environmental and social/cultural issues as well as functional, technical and economic requirements.

In this article we propose Multi-Criteria Decision Analysis (MCDA) techniques as appropriate for finding an initial compromise solution to the problem of wind turbine micro-siting. MCDA deals with the process of making decisions in the presence of multiple objectives. The goal is to choose among several alternatives using a number of decision criteria. In most cases, there is no alternative that performs better than all of the others according to all selected criteria; therefore, the solution must be a compromise. MCDA methods aid the process of identifying this compromise solution. The use of MCDA techniques has a long history in renewable energy and environmental planning and decision analysis and provides a comprehensive methodological framework for integrated evaluation and appraisal MCDA applications include areas such as (renewable) energy, manufacturing, services, medical, public policy, transport, environmental management, etc. In the context of this paper, MCDA methods may aim to help identifying a distribution of wind turbines in a given terrain in such a way that wind is captured more effectively while satisfying several criteria/constrains on economic, social, environmental and resource-based issues.

The paper unfolds as follows. First we provide a literature review that deals with issues such as methods and techniques for micro-sitting/positioning of wind turbines in a specific site, appropriate criteria, related constraints and objectives of the process. Then we continue with a short introduction to MCDA methods and their applications in energy and environmental planning and wind farm design and decision analysis in particular. Subsequently, we highlight the potential usefulness of MCDA methods in siting wind turbines in a certain terrain as

a complement to current practices. We finally argue that MCDA methods could account for an integrated framework for the inclusion of socio-environmental parameters in the relevant process of micro siting of wind turbines that was not apparent so far. The purpose of this paper is not to provide for such a MCDA framework for wind turbines micro-sitting, but rather to highlight its necessity and potential usefulness.

2. LITERATURE REVIEW

Current practices in micro-sitting of wind turbines

The micro-siting of wind turbines in a given site has recently attracted a lot of consideration due to the growing progress of wind energy [1]. This trend has led to the development of wind farms in areas of greater orographic complexity, raising doubts on the use of simple, linear, mathematical models of fluid dynamics, and basic micro-economic models for optimal positioning of wind turbines [2]. Nevertheless, micro-sitting of wind turbines is one of the several issues that a developer/planner has to tackle in identifying the appropriate overall design of a wind farm. Other design attributes include the identification of the optimal site in a given area, the number of wind turbines to be installed, the type of wind turbines, the technical specifications, grid connection, accessibility, the need to avoid excessive turbulence, environmental issues, operational safety, etc. Each of these attributes could be further decomposed into a number of sub-attributes. For example appropriateness of a site could incorporate issues such as average wind speed, direction of wind, legislative restrictions, suitability of soil and terrain, local topography, and so forth while the assessment of the wake effect could incorporate issues such as wind direction, turbulence level, atmospheric stability conditions etc. The production, maintenance and turbine lifetime also highly depend on the farm layout and farm control systems. To optimize a farm considering layout, cable costs and foundation costs in relation with maintenance and lifetime estimation is very complex. Still, it is apparent that the wind turbine micro-sitting problem is in fact only a part of the wider issue of local wind farm planning and the level and complexity of analysis can be extremely high [3]. Thus, even in the case of the most simplified objective function (maximization of the annual energy production), the optimization problem cannot be solved by classical optimization techniques [4]. To cope with this problem, most authors have used type of meta-heuristics techniques which have proved to be efficient when searching for the optimal solution to this problem [1, 4]. These type of techniques could include GAs [5, 6, 7, 8], several optimization methods [9] and other integrated economic models of wind farm performance [10, 11], among others.

Mosseti et al, 1994 were actually the first to develop, apply and propose a methodology for identifying the optimal wind turbine distribution at a given site by mans of a GAs. The purpose of their paper was to investigate the feasibility of GAs by analyzing the results obtained in some simple applications. The rather basic parameters they optimized included the maximization of energy production and the minimization of installation costs [5].

Grady et al, 2005 employed a GA in order to obtain optimal placement of wind turbines for maximum production capacity while limiting the number of turbines installed and the land occupied by each wind farm. They tested their approach in three distinct cases, namely unidirectional uniform wind, uniform wind with variable direction and non-uniform wind with variable direction. Results also included, total power output, efficiency of power output and optimal number of turbines for each configuration out of the many they included in the analysis, among others [6].

Marmidis et al, 2008 proposed an approach based on a more general statistical and mathematical method to appropriately arrange wind turbines in a given farm. As a test case, a square site is subdivided into 100 square cells that can be possible turbine locations and as a result, the program concluded the optimal arrangement of the wind turbines in the wind park, based on Monte Carlo simulation [10].

Very recently Gonzales et al, 2014 provided an excellent review on recent developments in the optimal wind turbine micro-sitting problem. In their paper they list 148 articles and they highlight the main aspects which need to be taken into consideration when facing the overall issue of local wind farm design. In addition they propose potential areas of further research that include the need to provide for in-depth analysis of the computational costs required by each optimization method used, the necessity to explicitly account for different types of uncertainties in project development, the consideration of different conflicts of interest that may emerge and the requisite to take into account environmental issues such as visual impact and noise disturbance [4].

Since a considerable number of these latest factors can be analyzed by means of MCDA methodologies, we subsequently shortly introduce the main families of MCDA techniques and their applications in energy and environmental planning and management.

An introduction to Multi-Criteria Decision Analysis

In decision-aiding for energy-environmental planning, in particular, several alternatives are analyzed in terms of multiple non-commensurate criteria, and many different stakeholders, with conflicting preferences, are involved [12]. For energy planning, there exists a need to select and rank the most favorable projects because energy resources are scarce and there are limited financial means available. It is necessary, therefore, to select a reliable methodology and to rank energy development projects according to a variety of objectives and criteria. MCDA methods are considered a realistic approach to such a complex choice problem.

Several different multi-criteria methods have been applied to energy and environmental issues. The key approaches can be classified based on the type of decision model they apply. The main categories of methodologies include [13]:

(A) Outranking methods, such as the ELECTRE and the PROMETHEE families [14, 15, 16, 17, 18]
(B) Value/Utility-based methods, such as the Multi-Attribute Utility Theory (MAUT) [19], the Simple Multi-Attribute Rated Technique (SMART) [20], the Analytic Hierarchy Process (AHP), that can be also found in Other methods according to different categorizations [21] and the most elementary multi-criteria technique the Simple Additive Weighting (SAW)
(C) Interactive - programming methods [22, 23, 24]
(D) Other methods like NAIADE [25], FLAG [26] and SMAA [27] among others.

The first category (A) is the so-called Outranking methods. These methods use pair-wise comparisons between potential alternative actions aiming to build an outranking relation between them. These methods are not bounded into a rigorous mathematical model but, providing further exploitation and processes, deduce to support the Decision-Maker (DM) in finding a what could be called "good" decision, depending on the available information.

The second category (B) is the Value System approach (American School). Its purpose is to build a value-utility function that aggregates the DM's preferences on the evaluation criteria. This formula provides a quantitative mode that guides the DM in reaching his decision. These methods have the advantage to be based in a fully-defined mathematical problem that can eventually formulate a complete preorder of the possible actions. Nonetheless, in many cases, they lack of a realistic representation of reality since the overall preferences on a standpoint are only modeled with severe difficulty by a unique function.

The third category (C) includes the interactive-programming methods. They are based on a kind of procedure that consists of an alteration of stages of computation and discourse. In the beginning the analyst establishes an initial solution. The DM acts in response by providing additional data regarding his preferences. This supplementary information is then introduced into the model in the next calculation stage. The procedure is repeated until the DM feels that he/she has reached an acceptable solution.

Finally the rest of the methods (category D) are just different types of techniques that actually cannot be easily sorted in one of the above mentioned categories.

The use of MCDA techniques has a long history in energy planning and provides a sound methodological framework for (renewable) energy evaluation and appraisal [28, 29, 30]. For example, when developing a renewable energy source, one of the important issues is the degree of exploitation of the source. Is the maximum possible number of wind turbines going to be installed? Should a decision be made to proceed with caution, installing a limited number each time and examining the consequences? A number of conflicting factors, technological, economic, environmental, social, risk, etc., must be taken into account, especially in places where limited exposure to similar projects, may lead to local opposition that might jeopardize future developments [31].

3. MCDA AS A COMPLEMENT TO CURRENT PRACTICE FOR WIND TUIRBINE MICRO-SITTING

It is quite evident that, so far, a number of rather restricted parameters are taken into consideration when positioning wind turbines in a certain site. Factors such as visual impact, impact on birds, other wild life and habitats, noise disturbance, impacts to particular sites of interest like archeological sites & traditional villages/settlements, change of rural life-style, local societal habits and old-style landscape character etc. are sometimes hard to quantify and are often neglected from the analysis. Nevertheless, the expected further augmented need for wind resources exploitation would somehow mandate that care continues to be taken to ensure that wind turbines are sited and designed so that adverse effects are minimized, and that areas which are highly valued for their landscapes and scenery are given due protection [32].

These additional parameters/criteria could be taken into account in the micro-sitting process of wind turbines via the inclusion of MCDA methodologies in the planning process as a complement to currently used techniques. By those means the inherent uncertainties associated with any type of project development, the sensitive environmental parameters like for example the visual impact to specific nearby sites of interest and the different local societal preferences, among others could be considered (Fig. 1).

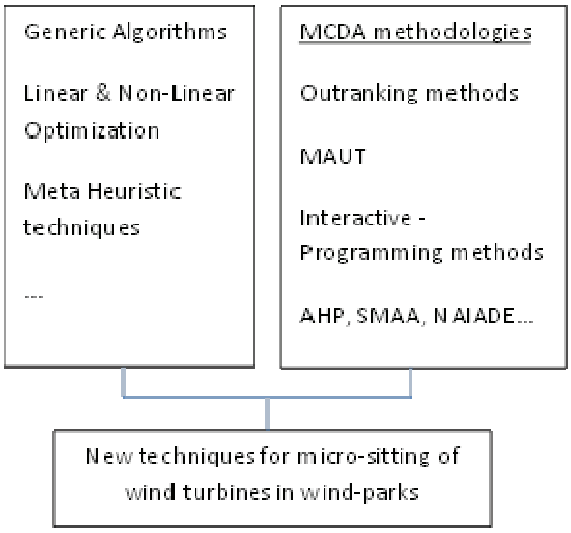

Fig. 1: MCDA methods as complement to current techniques for wind turbine micro-sitting

In particular, MCDA methods could aid in (Fig. 2):

- the treatment of uncertainty via threshold values, probability distributions, fuzzy sets and belief functions [13].
- the addressing of the visual impact to a particular nearby site of interest as it could be assessed for example via the method found in [33].
- the inclusion of different local societal values and viewpoints via the preference elicitation exercise when assessing pertinent criteria weights [13].
- the identification of a final proposal that could manage the conflicts raised between all the above parameters via the iteration process in the searching for a group compromise solution [31].

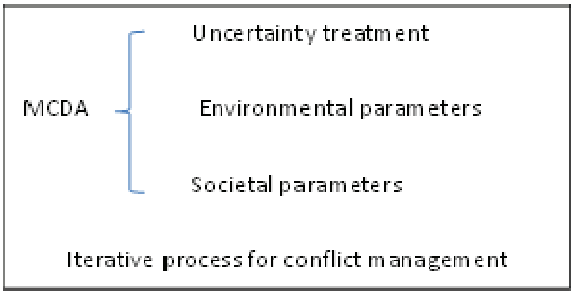

Fig. 2: Potential particular contribution of MCDA techniques in the process of wind turbine micro-sitting

Particularly during this process of iteration, different societal perceptions of landscape and visual impact could also be taken into consideration and a visually balanced, simple and consistent image could be better identified.

4. CONCLUSIONS

Micro-sitting/positioning of wind turbines in a given site refers to the process of optimizing total energy production of an entire wind park and at the same time take into account a number of environmental, economic, societal, technological etc. constraints by suitable placement of individual wind turbines. Several assessment tools and various techniques have been used to date to tackle this issue. In most cases, however, current approaches concentrate on optimizing particular criteria that are usually related to technical and economic issues, for example the analysis of the interactions between wind turbines, and often give little attention to environmental and other wider societal parameters that are also pertinent. Furthermore, it is usually the case that the attributes taken into account are studied in isolation and it seems that a wider framework to provide for an integrated type of optimization is missing. In this paper we introduce MCDA methodologies as a complement to current approaches of wind turbine micro-sitting. Several specific features of MCDA methods like their ability to explicitly account for project uncertainty, environmental parameters, societal values and conflict management may render these techniques quite applicable to the problem of micro-positioning of wind turbines. Nonetheless, the development and application of such a planning framework still remains a future research priority.

9. REFERENCES

[1] Ch.Wan, J. Wang, G. Yang, H. Gu, X. Zhang, "Wind farm micro-sitting by Gaussian particle swarm optimization with local search strategy", **Renewable Energy**, Vol. 48, 2012, pp. 276-286.

[2] J.M.L.M. Palma, F.A. Castro, L.F. Ribeiro, A.H. Rodrigues, A.P. Pinto, "Linear and nonlinear models in wind resource assessment and wind turbine micro-sitting in complex terrain", **Journal of Wind Engineering and Industrial Aerodynamics**, Vol. 96, 2008, pp. 2308-2326.

[3] R.C. Bansal, T.S. Bhatti, D.P. Kothari, "On some of the design aspects of wind energy conversion systems", **Energy Conversion and Management**, Vol. 43, 2002, pp. 2175-2187.

[4] J.S. Gonzales, M.B. Payan, J.M.R. Santos, F. Gonzalez-Longatt, "A review and recent developments in the optimal wind-turbine micro-siting problem", **Renewable and Sustainable Energy Reviews**, Vol. 30, 2014, pp. 133-144.

[5] G. Mosetti, C. Poloni, B.. Diviacco, "Optimization of wind turbine positioning in large windfarms by means of a generic algorithm", **Journal of Wind Engineering and Aerodynamics**, Vol. 52, 1994, pp. 105-116.

[6] S.A. Grady, M.Y. Hussaini, M.M. Abdullah, "Placement of wind turbines using genetic algorithms", **Renewable Energy**, Vol. 30, 2005, pp. 259-270.

[7] A. Emani, P. Noghreh, "New approach on optimization in placement of wind turbines within wind farm by generic algorithms", **Renewable Energy**, Vol. 35, 2010, pp. 1559-1564.

[8] J.S. Gonzalez, A.G.G. Rodrigez, G.C. Mora, J.R. Santos, M.B. Payan, "Optimization of wind farm turbines layout using an evolutive algorithm", **Renewable Energy**, Vol. 35, 2010, pp. 1671-1681.

[9] A. Kusiak, Z. Song, "Design of wind farm layout for maximum wind energy capture", **Renewable Energy**, Vol. 35, 2010, pp. 685-694.

[10] G. Marmidis, St. Lazarou, E. Pyrgioti, "Optimal placement of wind turbines in a wind park using Monte Carlo Simulation", **Renewable Energy**, Vol. 33, 2008, pp. 1455-1460.

[11] J.S. Gonzalez, A.G.G. Rodrigez, G.C. Mora, J.R. Santos, M.B. Payan, "Overall design optimization of wind farms", **Renewable Energy**, Vol. 36, 2011, pp. 1973-1982.

[12] R. Lahdelma, P. Salminen, J. Hokkanen, "Using Multicriteria Methods in Environmental Planning and Management", **Environmental Management**, Vol. 26, 2000, pp. 595-605.

[13] H. Polatidis, D. Haralambopoulos, G. Munda, R. Vreeker, "Selecting an appropriate Multi-Criteria Decision Aid Technique for renewable energy planning", **Energy Sources, Part B: Economics, Planning, and Policy**, Vol. 1, 2006, pp. 181-193.

[14] B. Roy, Ph. Vincke, "Multicriteria analysis: survey and new directions", **European Journal of Operational Research**, Vol. 8, 1981, pp. 207-218.

[15] B. Roy, "The outranking approach and the foundations of the ELECTRE methods", **Theory and Decision**, Vol. 31, 1991, pp. 49-73.

[16] B. Roy, M. Present, D. Silhol, "A programming method for determining which Paris metro stations should be renovated", **European Journal of Operational Research**, Vol. 24, 1986, pp. 318-34.

[17] J.P. Brans, Ph. Vincke, "A preference ranging organization method The PROMETHEE method for MCDM", **Management Science**, Vol. 31, 1985, 647-656.

[18] J.P. Brans, Ph. Vincke, B. Mareschal, "How to select and how to rank projects: The PROMETHEE method", **European Journal of Operational Research**, Vol. 24, 1986, pp. 228-238.

[19] R. Keeney, H. Raiffa, **Decision with Multiple Objectives: Preferences and Value Trade-Offs**, New York: John Wiley & Sons, 1976.

[20] D. von Winterfeldt, W. Edwards, **Decision Analysis and Behavioral Research**, Cambridge: Cambridge University Press, 1986.

[21] Th. L. Saaty, **The Analytic Hierarchy Process**, New York: McGraw – Hill, 1980.

[22] M. Zeleny, **Multiple Criteria Decision Making**, New York: McGraw-Hill, 1982.

[23] R. Steuer, **Multiple criteria optimization: theory, computation and application**, New York: Wiley, 1986.

[24] Ph. Vincke, **Multicriteria decision aid**, New York: Wiley, 1992.

[25] G. Munda, **Multicriteria evaluation in a fuzzy environment. Theory and applications**, Heidelberg: In: Ecol. Econ. Physica-Verlag, 1995.

[26] P. Nijkamp, R. Vreeker, "Sustainability assessment of development scenarios: methodology and application to Thailand", **Ecological Economics**, Vol. 33, 2000, pp. 7-27.

[27] R. Lahdelma, J. Hokkanen, P. Salminen, "SMAA – Stochastic Multiobjective Acceptability Analysis", **European Journal of Operational Research**, Vol. 106, 1998, pp. 137–143.

[28] J. Siskos, Ph. Hubert, "Multi-criteria analysis of the impacts of energy alternatives: A survey and a comparative approach", **European Journal of Operational Research**, Vol. 13, 1983, pp. 278-299.
[29] F.A. Lootsma, P.G.M. Boonekamp, R.M. Cooke, F. Van Oostvoorn, "Choice of a long-term strategy for the national electricity supply via scenario analysis and multi-criteria analysis", **European Journal of Operational Research**, Vol. 48, 1990, pp. 189-203.
[30] J.P. Huang, K.L. Poh, B.W. Ang, "Decision Analysis in Energy and Environmental Modeling" **Energy**, Vol. 20, 1995, pp. 843-855.
[31] D. Haralambopoulos, H. Polatidis, "Renewable energy projects: structuring a multi-criteria group decision-making framework", **Renewable Energy**, Vol. 28, 2003, pp. 961-973.
[32] Scottish Natural Heritage, **Sitting and Designing windfarms in the landscape, Version 1**, Inverness, December 2009, available at: www.snh.org.uk
[33] L-I. Tegou, H. Polatidis, D. Haralambopoulos, "A multi-criteria framework for an isolated electricity system design with Renewable Energy Sources in the context of Distributed Generation: the case study of Lesvos island Greece", **International Journal of Green Energy**, Vol. 9, 2012, pp. 256-279.

VLSI Design and Verification of a CMOS Inverter Using the Tanner EDA: A Case Study

Nian Zhang, Juan F.R. Rochac, Esther Ososanya, Wagdy Mahmoud, and Samuel Lakeou
University of the District of Columbia
Department of Electrical and Computer Engineering
4200 Connecticut Ave. NW
Washington, DC, 20008 USA
nzhang@udc.edu, jrochac@udc.edu, eososanya@udc.edu, wmahmoud@udc.edu, slakeou@udc.edu

ABSTRACT

Although the Tanner EDA has been widely used in many universities, there is lack of a shareable publication, document, or tutoring video on VLSI design and verification. Few online tutorials or tutoring video are quite outdated. They either cannot be used for step-by-step guideline, or they only cover part of the entire design flow, which doesn't meet designer's need.

The lack of up to date publication or document has caused a huge barrier for universities to teach a VLSI lab. Due to a severe discrepancy in procedure and parameter setting, instructors have to report technical cases to the Tanner EDA technical support center, and then spend significant time troubleshooting problems with the remote assistance from the Tanner engineers. This has greatly affected the progress of lab teaching and student learning. Therefore, there is an urgent need to create and disseminate a shareable publication or document on VLSI design and verification with the latest version of Tanner EDA.

This paper promotes the needs of a comprehensive study on the newest version of Tanner Tools Pro v16.0 (released in 2013), a state-of-the-art CAD tool for VLSI design. An inverter is used as a proof-of-concept example to go through the major VLSI design flow, including schematic capture, pre-layout simulation, physical layout, extract, design rule check (DRC), and layout vs schematic (LVS). For each step, not only the most challenging and crucial parts are addressed, but also the most different parts from the outdated online tutorial are explained in detail with necessary snapshots. Other universities and designers will find it an invaluable document, which ensures an efficient and fast VLSI design and verification.

Keywords: VLSI Design and Verification, CMOS Inverter, Tanner EDA

1. INTRODUCTION

To keep up with the phenomenal growth in very large scale integration (VLSI) technologies, it is critical for higher education institutions to teach the most competitive computer-aided design (CAD) tools in the market [1][2][3].

Tanner EDA (electronic design automation) is one of the leading EDA industries in the world. It is a powerful and productive analog and mixed-signal ICs design suite that drives innovation for analog IC, mixed signal, and MEMS design [4]. One of the most appealing features is that it provides with Windows based IC design tools, which makes it easy to use. Four tools are integrated in this suite.

- S-Edit: schematic capture tool
- T-Spice: SPICE simulation engine integrated with S-edit
- L-Edit: physical design tool
- LVS: layout vs schematic verification tool

2. MOTIVATION AND CHALLENGES

The education of VLSI design laboratory with Tanner EDA faces challenges. Although the Tanner EDA has been widely used in many universities, there is lack of a sharable publication, document, or tutoring video on VLSI design and verification for students. Few online tutorials or tutoring are quite outdated, since Tanner Tools EDA has major releases every 12-18 months. The tutorials or video that can be found on the internet were written before 2011 [5][6][7][8][9][10]. They either cannot be used for step-by-step guideline due to significant difference from the newest version of Tanner EDA, or they only cover a small part of the entire design flow.

The lack of up to date document has caused a huge barrier for universities to teach a VLSI lab. Due to a severe discrepancy in procedure or parameter setting, instructors have to report technical cases to the Tanner technical support center, and then spend significant time troubleshooting the problem with the remote assistance from the Tanner engineers. This will greatly affect the progress of lab teaching and student learning. Therefore, there is an urgent need to create and disseminate a shareable publication or document on VLSI design and verification with the latest version of Tanner EDA.

This paper promotes the needs of a comprehensive exploration on the newest version of Tanner Tools Pro v16.0 (released in 2013), a state-of-the-art CAD tool for VLSI design. A CMOS inverter is used as an example to go through the major VLSI design flow, including schematic capture, pre-layout simulation, physical layout, extract, design rule check (DRC), and layout vs schematic (LVS). For each step, not only the most challenging and crucial parts are addressed, but also the most different parts from the outdated online tutorial are explained in detail with

necessary snapshots. This effort would provide other universities or designers with an invaluable document to ensure an efficient and fast VLSI design and verification.

The remaining of the paper is organized as follows. Section III describes the schematic design. Section IV illustrates the pre-layout simulation. Section V explains the layout design. Section VI depicts the design rule check (DRC), Section VII describes extract, Section VIII explains the layout vs schematic (LVS), and Section IX gives the conclusions.

3. SCHEMATIC DESIGN

Schematic Design establishes the general scope, conceptual ideas, the scale and relationship of the various program elements. The primary objective of schematic design is to arrive at a clearly defined feasible concept based on the most promising design solutions. It consists of the following fundamental elements.

- Open S-edit platform
- Create a new design
- Add libraries to the design
- Create a new view (under menu Cell)
- Add devices, input & output ports, and supply device (VDD) and a ground device (GND)
- Add a voltage source to provide voltages to VDD and GND

A complete schematic design of an inverter is shown in Fig. 1.

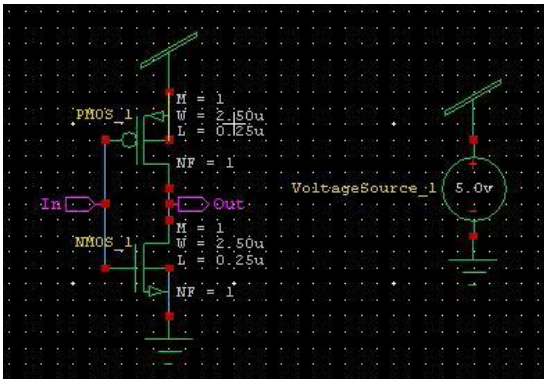

Fig. 1 Circuit schematic of an inverter cell.

4. PRE-LAYOUT SIMULATION

After schematic design, designers have to conduct a pre-layout simulation to check whether their design match with the specification requirement. Assume transient analysis is performed. It includes the following fundamental elements.

- Start S-edit platform
- Open the Inverter design
- Open menu Setup SPICE Simulation, select Transient/Fourier Analysis.
- Select the Generic 250nm library file in the Library Files field. Importantly, TT should be manually added in the end, i.e. Generic_250nm.lib TT, as shown in Fig. 2. It is important to specify the library or model file. Since each MOS transistor symbol fabricated in a different technology will behave differently. Only when a technology process is specified, the MOS transistor symbol can be associated to that process and behavior accordingly.

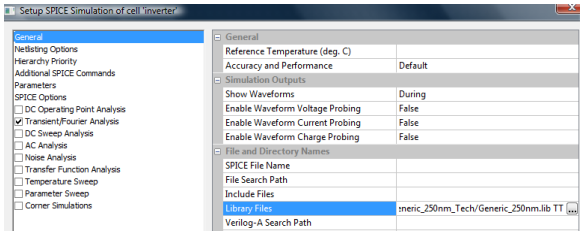

Fig. 2 Make selection of simulation type and set the library files in the Setup SPICE Simulation window.

- Create a pulse voltage source, V2. Under Spice Elements, select voltage source, modify the interface as Pulse. Set the period to 20ns. Drag a Net Label on the higher end of the pulse voltage source, and call it the same name as the input port, i.e. IN.
- To observe the input and output voltages, under Spice Commands, select print voltage, modify the interface to Voltage and create a new instance at the input & output ports. A complete simulation mode circuit schematic is shown in Fig. 3.

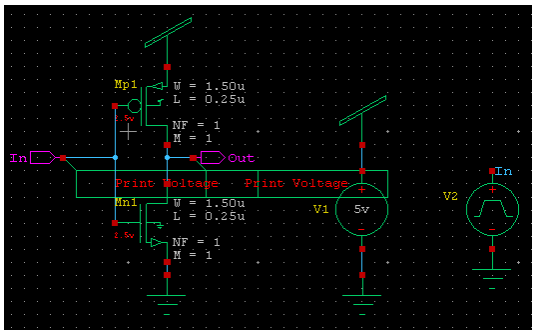

Fig. 3 Simulation mode circuit schematic.

- Run the T-spice simulation. The results of the pre-layout simulation are shown in Fig. 4.

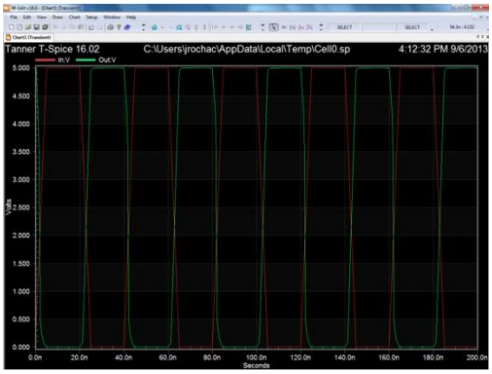

Fig. 4 Pre-layout simulation of an inverter.

5. LAYOUT DESIGN

A layout-design of an IC refers essentially to the three-dimensional character of the elements and interconnections of an IC. There is a continuing need for the creation of new layout designs which reduce the dimensions of existing integrated circuits and simultaneously increase their functions. It consists of the following fundamental elements.

- Open L-edit platform.
- Create a new design. Select TDB as the Technology Reference.
- Add libraries to the design.
- Import Technology.
- Create a new view (under menu Cell).
- Draw the layout.

After adding libraries, all the layers will be added to the layer palette. Designers may use these layers to draw the layout. But designers still have to import technology to your layout design, i.e. Generic_250nm_TechSetup.tdb. Later when you perform DRC check or LVS check, the standard rule set will be checked to see if they have been violated or not. A complete layout of an inverter is shown in Fig. 5.

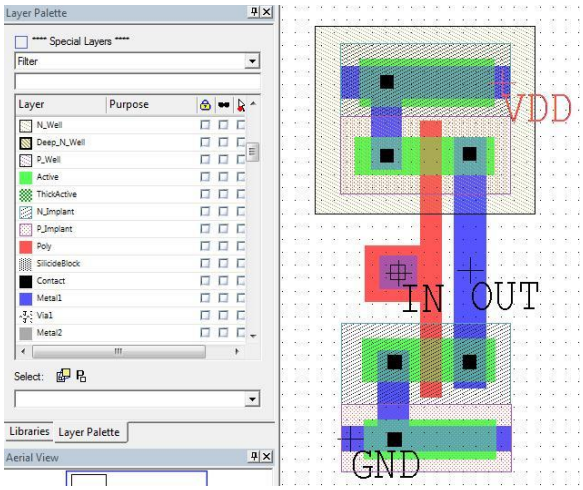

Fig. 5 Layout design of an inverter cell.

6. DESIGN RULE CHECK

Design Rule Check (DRC) is the area of electronic design automation (EDA) that determines whether the physical layout of a particular chip layout satisfies a series of recommended parameters called design rules. Design rule checking is a major step during physical verification on the design. Design rules are a series of parameters provided by semiconductor manufacturers that enable the designer to verify the correctness of a mask set. Design rules are specific to a particular semiconductor manufacturing process.

Check the DRC Standard Rule Set and run the DRC check. After running DRC, if there is no error that means the design satisfies design rule check, as shown in Fig. 6. Otherwise, check on each rule that is violated, and then go to the location that is circled or marked by bold solid circle or line to fix them.

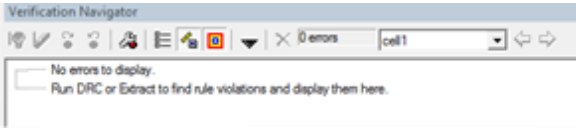

Fig. 6 No error in the DRC rule check.

Usually, the most common errors can be fixed by moving the two layers apart, or adjust the contact size according to the rule.

7. EXTRACT

To verify the functionality and timing of this inverter, the SPICE netlist from the layout needs to be extracted. The extracted view allows designers to run LVS (layout vs schematic). It consists of the following elements.

- Setup extract.
- Unselect HiPer Verify options.
- Extract netlist from the layout.

In the Setup Extract window, use the technology setup from Generic_250 nm.ext file. Designers will see that a SPICE extract output file. i.e. cell1.spc will be generated (in the same folder with their layout) after running the extraction. In addition, if designers do not have HiPer Verify license, they won't be able to use Hierarchical or background settings in Setup Extract. Instead, designers should uncheck all the options under "HiPer Verify" options, as shown in Fig. 7.

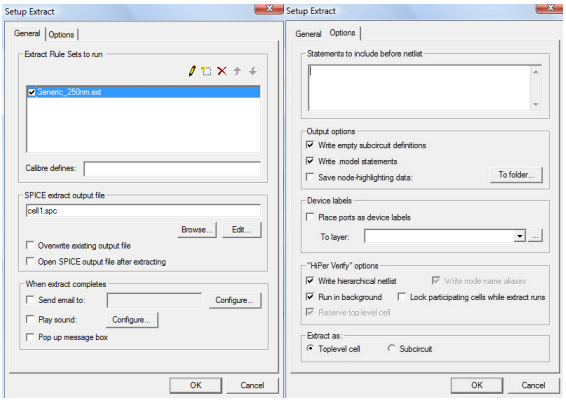

Fig. 7 The Setup Extract window. The left figure shows the definition file under the General tab. The right figure shows the HiPer Verify setting under the Option tab.

8. LAYOUT VS SCHEMATIC (LVS)

The Layout Versus Schematic (LVS) is the class of EDA verification software that determines whether a particular integrated circuit layout corresponds to the original schematic or circuit diagram of the design. LVS verification involves:

1. Extraction: The software program takes a database file containing all the layers drawn to represent the circuit during layout. It then runs the database through many area based logic operations. Area based logical operations use polygon areas as inputs and generate output polygon areas from these operations. These operations are used to define the device recognition layers, the terminals of these devices, the wiring conductors and via structures, and the locations of pins (also known as hierarchical connection points).
2. Reduction: In the time of reduction the software combines the extracted components into series and parallel combinations if possible and generates a netlist representation of the layout database. A similar reduction is performed on the "source" schematic netlist.
3. Comparison: The extracted layout netlist is then compared to the netlist exported from the circuit schematic. If the two netlists match, then the circuit passes the LVS check and a message will come "Circuits are equal". The procedure includes the following elements.

- Open LVS platform
- Create a new LVS setup file
- Export SPICE netlist of the schematic from S-Edit. Use this SPICE file for schematic netlist.
- Use the SPICE netlist from previous extraction for layout netlist. The SPICE netlist extracted from the layout and the exported SPICE netlist from the schematic are shown in Fig. 8.

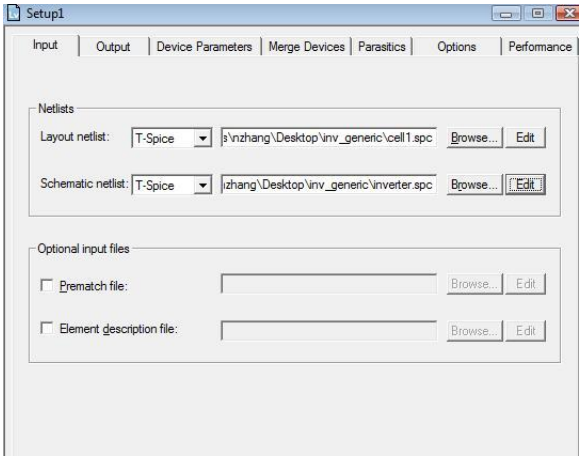

Fig. 8 Layout Versus Schematic (LVS) setup. The SPICE netlist extracted from the layout and the exported SPICE netlist from the schematic are the two inputs.

- Run the verification.

If everything matches, designers will see a report window that says "Circuits are equal" in red, as shown in Fig. 9. If they don't match, it will show which line in the SPICE file is wrong.

```
************************* FINAL RESULT ****************************

Circuits are equal.
Run time: 0:00 (min:sec)
```

Fig. 9 Layout Versus Schematic (LVS) result. The two circuits are proved to be equal.

9. CONCLUSIONS

This paper thoroughly investigated the design flow of a proof-of-concept CMOS inverter using the latest version of Tanner EDA, i.e. Tanner Tools v16.0, a state-of-the-art CAD tool for VLSI design. It filled in the gap between the outdated tutorials and the up to date document about the latest Tanner EDA. The major VLSI design flow components, including schematic design, pre-layout simulation, physical layout, extract, design rule check (DRC), and layout vs schematic (LVS) were completely explored. For each step, not only the most challenging and crucial issues were addressed, but also the most different parts from the outdated online tutorials or videos were explained in detail with necessary snapshots. This effort would provide other universities and designers with an invaluable document to ensure an efficient and fast VLSI design and verification. In the future, this shareable document will be updated and disseminated on a regular basis to keep up with advances in Tanner EDA technology.

In addition, the proposed study will leverage the key success factors for fresh engineering graduates by equipping them with a rich set of skills to overcome the challenges caused by emerging techniques and rapid changing products.

10. REFERENCES

1. S. Sharma, S. Azeemuddin, M. Anwar, "A Self Learning VLSI Lab along with Web-Based Platform to Design Schematics and Layouts," **2011 IEEE International Conference on Technology for Education (T4E)**, vol., no., pp.205,207, 14-16 July 2011.
2. K. Vanitha, C. A. Sathiya Moorthy, "Implementation of an integrated FPGA based automatic test equipment and test generation for digital circuits," **2013 International Conference on Information Communication and Embedded Systems (ICICES)**, vol., no., pp.741,746, 21-22 Feb. 2013.
3. Chun Zhao, W. Zhang, C. Z. Zhao, K. L. Man, T. T. Jeong, J. K. Seon, Y. Lee, "Standard cell library establishment and simulation for scan D flip-flops based on 0.5 micron CMOS mixed-signal process," **2011 International SoC Design Conference (ISOCC)**, vol., no., pp.306,309, 17-18 Nov. 2011.
4. Tanner EDA, http://www.tannereda.com/.
5. Design and Simulation of Inverter with Tanner Tool, http://www.manishapattanaik.in/Manual/INVERTER_WITH_TANNER_TOOLS.pdf.
6. Guide to the Tanner EDA v12.6 Design Tools for use in designing, simulating, and laying out ICs, http://www.coe.montana.edu/ee/andyo/EELE414/information/Guide_to_TannerEDA_for_VLSI.pdf.
7. Tanner EDA L-edit (Layout Editor), Tufts University, http://www.tufts.edu/~rwhite07/PRESENTATIONS_REPORTS/ledit.pdf
8. Get Started with L-Edit, UC Santa Barbara, http://www.engr.ucsb.edu/~sumita/courses/Courses/ME141B/LEditGettingStarted.pdf
9. Creating an Inverter using S-Edit, Brown University, http://scale.engin.brown.edu/classes/EN1600S08/tutorials/sedit_tutorial.htm.
10. S-Edit Inverter, http://www.youtube.com/watch?v=qM9neB5wnCo.

Analysis of Thermo-Mechanical Coupling Characteristics and Structural Design of Rotary Liner Hanger Bearing in Ultra-Deep Well Drilling

Weiqing Li
School of Engineering and Technology, China University of Geosciences (Beijing)
Beijing, 10083, China
Department of Mechanical and Aerospace Engineering, The Ohio State University
Columbus, 43210, USA

and

Jianchong Wang
School of Engineering and Technology, China University of Geosciences (Beijing)
Beijing, 100083, China

ABSTRACT

The bearing is a key part of the rotary liner hanger in the drilling engineering of ultra-deep wells and complex wells. However, bearings are limited by the design space, heavy loads (more than 60 tons), and extreme working conditions (e.g., high temperature, high pressure and muds). The load capacity and service life of bearings are always the primary bottlenecks for the development of rotary liner cementing technology. By applying a combination of theory analysis and simulation and experiment techniques, we discuss in this paper the working conditions, contact theory of complex interface, thermo-mechanical coupling characteristics, failure mechanism, and structure optimization of bearings. The optimization improves the load capacity and service life of bearings. The research result of the thermo-mechanical coupling characteristics will provide a practical and theoretical basis for a set of design rules for bearings in ultra-deep well drilling engineering.

Keywords: Bearing, Contact Theory, Thermo-mechanical Coupling, Ultra-deep Well Drilling, Rotary Liner Hanger Bearing.

1. INTRODUCTION

In ultra-deep and complicated well drilling, well cementing is the most important step of drilling engineering. Cementing quality directly affects the operational integrity of the well. The application of rotating liner hanger cementing can meet this requirement effectively. After the liner is laid down and the hanger is set, the liner begins to rotate by the power from the top drive. This method is beneficial to the liner reaching the design position in complicated conditions, such as in resistance conditions, small gap wells, high-angle wells, and horizontal wells. This method is also helpful for improving displacement efficiency and cementing quality.

The bearing is a key part of the rotary liner hanger. In the liner drilling and cementing process, the bearing has to carry the weight of the entire liner. However, the size of the bearing is small because of borehole size restrictions. A special bearing is needed that can function under heavy loads (more than 60 t axial force and more than 600 N•m torque) and extreme working conditions, such as high temperature (more than 120 °C), high pressure, and mud. Therefore, the bearing should not only ensure an extremely heavy load and a certain rotary torque but should also have a certain service life (more than 20 h). The load capacity and service life of bearings are the primary bottlenecks in the development of rotary liner cementing technology.

The technology of rotating liner hangers was developed in the 1920s. Rotating liner hangers have since received increasing attention because of its advantages in cement engineering and various types of rotary liner hanger have been developed (1, 2, 3, 4, and 5). However, research on the rotary liner hanger bearing is relatively slow because of its complex working conditions and the high cost of experiments, thus restricting the development of this type of bearing. Two early patents (6, 7) provide a type of bearing structure. However, this bearing cannot meet present drilling requirements in complicated field conditions and ultra-deep wells because of structural and working principle drawbacks. Ma (8) developed a bearing that has been applied to some field drillings; however, this bearing has a load capacity and service life that do not meet practical requirements. One report (9) showed that huge losses were caused in 15000 oil and gas wells because of the low quality of well cementing in China.

By applying a combination of theory analysis and simulation and experiment techniques, we discuss in this paper the working conditions, contact theory of complex interface, thermo-mechanical coupling characteristics, failure mechanism, and structure optimization of bearings. First, this paper presents the structural design of the bearing based on Hertz theory. Secondly, thermo-mechanical coupling analysis was applied and the structure of the bearing was optimized on the basis of the analysis results. Finally, experiments were conducted to verify the effectiveness of the optimization. The optimization improves the load capacity and service life of the bearing. The results of the simulation experiments show that the load capacity of the designed bearing is significantly increased. The research result will provide a practical and theoretical basis for making a set of design rules for this type of bearing.

2. STRUCTURE DESIGN BASED ON HERTZ THEORY

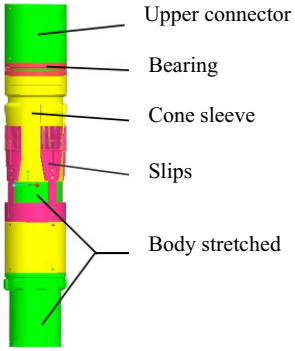

Figure 1. Location of the bearing

The location of the bearing at work is shown in Fig. 1. During cementing, the slips move upward and rest on the outer casing of the cone sleeve with the outer diameter enlarged through the cone of the sleeve. The bearing is set on the cone sleeve, and axial force from the stretched body is applied to the bearing via the upper connector.

Thus, the bearing has to work under a bad condition, such as heavy axial load (60 t to 75 t), high temperature (120 °C to 150 °C), mud (density is 1.2 g/cm^3 to 1.8 g/cm^3, particle size is 200 mesh to 400 mesh) and certain torque (600 N • m to 1200 N • m)

The following assumptions were made to simplify the complex design conditions into feasible design conditions.

(1) The bearing only has an axial load (the small torque is calculated by using the adjustment coefficient as compensation).

(2) The rollers are controlled by the raceway of the seat ring when the bearing rotates.

Under these assumptions, the mathematical models of the maximum contact stress between the rollers and raceway of the seat ring and the mathematical model of the rated load were established.

The maximum contact stress between the roller and trace could be calculated on the basis of Hertz theory.

$$\sigma_{\max} = \frac{2Q}{\pi bLwe}, \tag{1}$$

where Q is the total axial load carried by the bearing, b is the half width of the roller contact surface, and L_{we} is the effective length of the roller.

Given the steel roller bearing, the half width of the contact area is expressed as follows:

$$b = 3.35 \times 10^{-3}\left(\frac{Q}{Lwe\sum\rho}\right)^{1/2}. \tag{2}$$

When the assumption is ideal contact, the curvature is calculated as follows:

$$\sum\rho = \frac{2}{Dwe(1-\gamma_i)}. \tag{3}$$

$$\gamma_i = D_{we}\cos\psi / D_{pw}. \tag{4}$$

where D_{we} is the pitch circle diameter of the roller, γ_i is the shear strain, ψ is the half cone angle of the roller, D_{pw} is the pitch circle diameter of the bearing.

The rated load was calculated as follows:

$$C_{oa} = 220 \times (1 - \frac{D_{we}\cos\alpha}{D_{pw}})ZL_{we}D_{we}f_af_b\sin\alpha, \tag{5}$$

where C_{oa} is the basic rated static load of the bearing, D_{we} is the pitch circle diameter of the roller, D_{pw} is the pitch circle diameter of the bearing, α is the bearing contact angle, Z is the number of rollers, L_{we} is the effective length of the roller, f_a is the material factor, and f_b is lubrication factor.

The result of the structure design based on the work conditions and Hertz Theory was in Fig. 2. The result is composed of 01 (seat ring), 02 (shaft ring), 03 (roller), 04 (retainer), and 05 (sealing gasket).

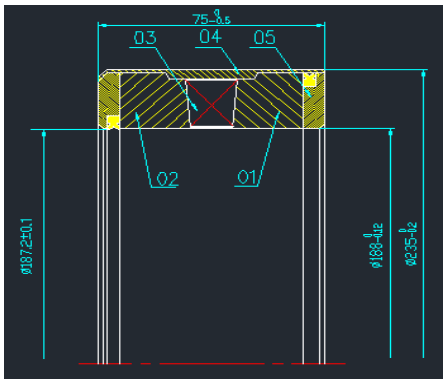

Figure 2. Structure of the bearing

This structure was designed by simplifying assumptions that do not exactly match the actual conditions. Conducting many experiments to determine if the designed bearing meets the requirements of the drilling engineer is unreasonable because of the huge trial costs. Thus, this paper conducted a series of static and thermo-mechanical coupling simulations to find defects and improve the structure and parameters.

3. STATIC SIMULATION

The bearing needs to function at extreme heavy loads because of the limitation of the design space in the well dimension. Thus, the bearing needs to have high static-load bearing capacity. When the bearing structure was designed, static load and maximum contact stress based on Hertz theory were considered. However, Hertz theory is based on the contact of the ideal roller and bearing raceway (10). In practice, accurately calculating the contact deformation of two contact bodies and simplifying the end effect in finite length line contact are difficult (11, 12). Therefore, some assumptions must be simplified to apply classical theory. This approach introduces a certain bias to the design conditions and actual working conditions. This paper introduced static simulations to analyze the contact stress and deformation of the bearing and optimize the parameters on the basis of the results.

(1) 3D FEM model

Contact analysis is a type of highly nonlinear analysis and is characterized by high amounts of calculations (9). To obtain a satisfactory accuracy and reasonable calculation scale, the model needs to reflect the actual structure of the important mechanical properties of the bearing and have a low number of simple units. By considering the symmetry, this study applies 1/40 of the whole bearing in the analysis (Fig. 3).

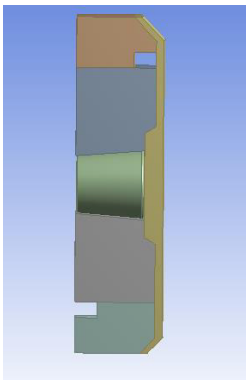

Figure 3. 1/40 model of bearing

(2) Material Properties

The properties of the materials are shown in Table 1.

Table 1. Material properties

Element	Material	Young's modulus (GPa)	Poisson's ratio	Yield Strength (MPa)	Tensile strength (MPa)
Roller	ZGCr15	206	0.3	1667-1814	———
Shaft ring	ZGCr15	206	0.3	1667-1814	———
Seat ring	ZGCr15	206	0.3	1667-1814	———
Sealing gasket	H62	100	0.34	110	360
Retainer	20CrMnTi	206	0.3	835	1030

(3) Unit selecting and meshing

Meshing is an important step in the development of the FEM model, and factors such as quantity, quality, density, interface and demarcation point, layout, unit order, displacement coordination, node, and element numbers need to be considered. In this paper, local meshes were refined three times so that both accuracy and analysis speed can met the requirements. The meshed model is presented in Fig. 4, which shows that the mesh of the contact area is the most intensive.

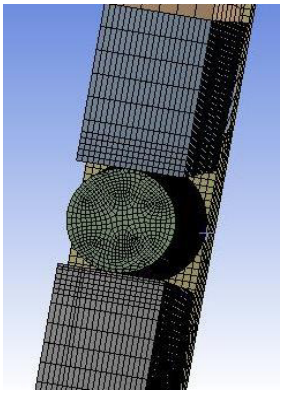

Figure 4. FEA model after meshing

(4) Creation of Contact Pairs

Contact analysis has two issues. One issue is the presence of an unknown contact area before solving the problem. This issue should be resolved because the contact area will change with load, material, boundary conditions, etc. The other issue is that most contact problems need to calculate friction, which is nonlinear in most conditions, and achieving convergence is difficult.

Surface–contact–surface has several advantages, including applicability in a large sliding friction and large deformation. This approach also has no restrictions in rigid surface shape. A variety of modeling control such as binding contact, adjustment of initial penetration contact, and translation of contact surface can be used. Therefore, surface–contact–surface was applied in this paper. Roller was considered a rigid surface. Seat ring and shaft ring were considered flexible surfaces. The contact pairs shown in Table 2 include two frictional contacts and five frictionless contacts.

Table 2. Definition of contact pairs

Location of the contact pair	Type of contact	Coefficient of friction
Shaft ring and roller	Frictional	0.1
Shaft ring and upper washer	Frictionless	____
Shaft ring and retainer	Frictionless	____
Seat ring and roller	Frictional	0.1
Seat ring and lower washer	Frictionless	____
Seat ring and retainer	Frictionless	____
lower washer and retainer	Frictionless	____

A contact problem is a highly nonlinear problem. Some problems such as rigid displacement, results divergence, contact separation, and contact penetration may appear. This paper adjusted the contacts continuously according to the flowchart (Fig. 5) until the result reached the optimal solution.

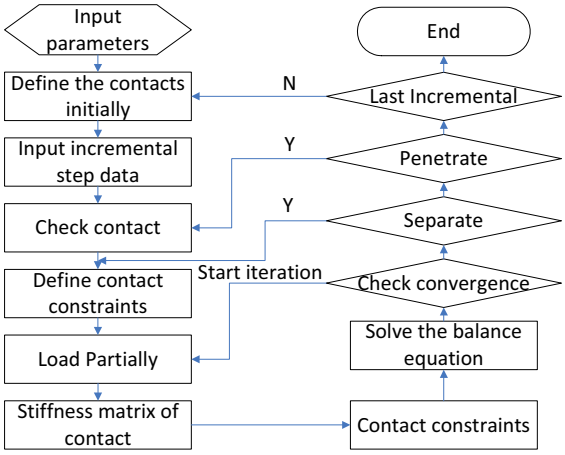

Figure 5. The Flowchart of adjusting contact

Selection of the contact calculation: an FEM generally includes the Lagrange multiplier method, penalty function method, augmented Lagrange multiplier method, and Lagrange multiplier perturbation method (13). Considering the advantages and disadvantages of these four algorithms, as well as the 3D characteristics of the bearing contact problem and calculation accuracy and convergence problems (13, 14), this paper chose the Lagrange multiplier method.

(4) Static simulation result and improvement

Figs. 6, 7, and 8 show the analysis results of the bearing based on Hertz theory when the axial load is 65 t and torque is 750 N•m.

Fig. 6 shows the stress distribution on the bearing. The maximum stress is 3058.5MPa and is located at the contact area between the roller and shaft ring. The contact stress not only causes bearing deformation (Fig. 7) bus also causes roller radial displacement. The radial displacement produces a certain pressure on the bearing retainer. The retainer was squeezed and has a large deformation because it is a type of thin-walled part.

Fig. 7 shows the bearing deformation. The maximum deformation is located at the contact area between the retainer and upper sealing gasket near the area notch of the sealing ring. The bearing deformation is approximately 0.2 mm. These deformations will have a significant influence on the sealing effect, thus leading to the entrance of mud into the bearing and significantly increasing the bearing wear.

Fig. 8 shows the shear stress distribution on the bearing. The maximum shear stress is 2192.7 MPa, which is much smaller than the stress. Therefore, the influence of certain torque is smaller than the heavy axial load.

Figs. 6 and 7 show that one of the causes of bearing failure is heavy axial load, which causes significant stress and deformation. Deformation influences the sealing effect.

The structural design based on Hertz theory cannot meet the requirements of drilling engineering. The following improvements were made on the basis of the analysis results to solve the above-mentioned problem:

(1) Applied full complement tapered roller instead of cylindrical roller bearing to increase axial load carrying capacity.

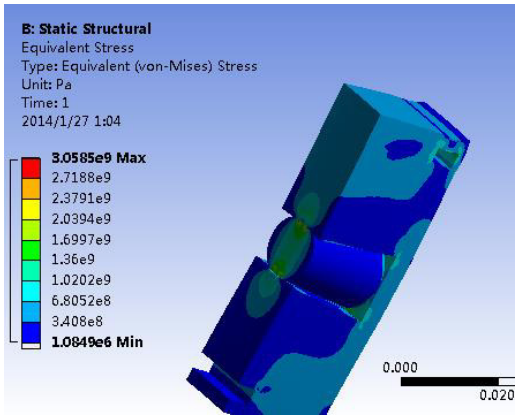

Figure 6. Stress distribution of bearing before improvement

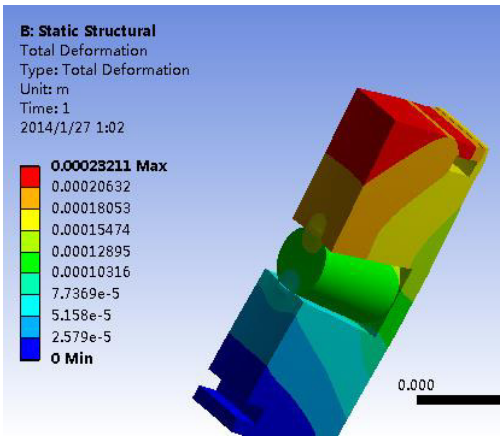

Figure 7. Deformation of bearing before improvement

(2) Rationally designed the cone angle of the roller to ensure that the rollers run in a pure rolling type along the raceway.

(3) Designed the roller with convexity to improve the bearing stress distribution and avoid stress concentration.

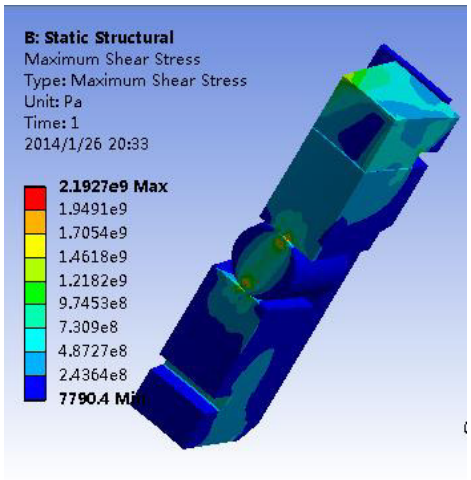

Figure 8. Distribution of shear stress before improvement

(4) Add a 45° chamfer with a width of 6 mm on the upper sealing gasket on the basis of 6 mm radial dimension. This measure can improve the sealing characteristics because the seal groove almost has no axial force, thus reducing the amount of deformation of the upper sealing gasket and retainer.

Figs. 9 and 10 show the analysis results of the bearing after the structural improvement. Fig. 9 shows that the maximum stress is 2676.9 MPa, which is 381.6 MPa less than the result before improvement. The stress of the notch of the sealing ring on the upper sealing gasket is reduced to 12.8 MPa.

Fig. 10 shows the bearing deformation after structural improvement. The deformation is located at the contact area between the retainer and upper sealing gasket near the notch area of the sealing ring and is approximately 0.12mm. The deformation is reduced by 40%, which is beneficial to the sealing characteristics. Although the maximum deformation inside the upper sealing gasket is 0.06 mm larger than the result before improvement, the result is acceptable because the interference fit between the upper sealing gasket and shaft is needed.

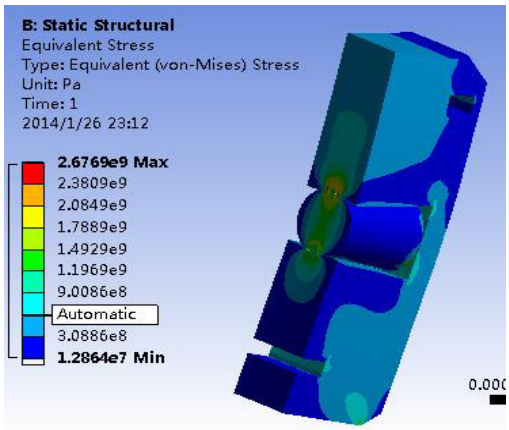

Figure 9. Stress distribution of bearing after improvement

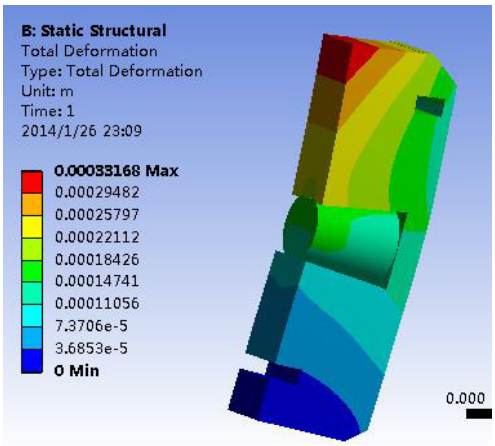

Figure 10. Deformation of bearing after improvement

4. THHERMO-MECHANICAL COUPLING SIMULATION

Bearings are applied in heavy load and high-temperature conditions; thus, the increase in temperature significantly influences the carrying capacity, clearance, and fatigue life of

bearings. The main heat source of the bearing used in this study originates from the temperature of the deep well, the heat of the sliding friction between adjacent rollers, the pure rolling friction between rollers, and the seat ring and shaft ring. The primary locations that produce heat are at the contact surface of the roller, seat ring, and shaft ring. This study adds the temperature influence to the simulation by thermo-mechanical coupling analysis to match the analysis with the actual working conditions.

The temperature analysis of the bearing is complex and is based on the calculation model of frictional heat, the heat-transferring model, and the ambient temperature. Some research has been conducted to solve these problems. Palmgren (15) proposed an empirical formula for the friction torque of the viscosity and rolling bearing under overall load. Jones (16) analyzed the friction and friction torque at the raceway area with consideration to the spin slide. Harris (17) proposed a network computing method to analyze the temperature distribution of a bearing system. Haidong Ren (18) amended Harris's empirical formula and developed a mathematical model for high-speed bearing friction torque. Michael Flouros (19) developed software to calculate the temperature of the outer ring of the ball bearing in an aero engine. Gonzalez-Perez (20) proposed an FEM to consider the torsional effect

An indirect method was applied in this study because it is more effective than the direct method in analyzing highly nonlinear problems. First, a steady-state thermal analysis was conducted to calculate the heat transfer and convection. Then static simulation was introduced to the result of the steady-state thermal analysis to analyze the thermo-mechanical coupling influence on the contact stress and deformation of the bearing. A temperature boundary condition was established on the outer side of the retainer because the primary heat was from the drilling well. The temperature was set to 150 °C. The internal temperature of the bearing was set to 25 °C, which is the initial ambient temperature. Heat convection coefficient with air was set on the small end of the roller, internal of the shaft ring, seat ring, outside of the roller and retainer.

The thermodynamic properties of the bearing can be seen from the simulation results of the steady state under the condition that the temperature in the down hole was 150 °C, and the bearing was under normal atmospheric temperature (25 °C). Figs. 11 shows the temperature gradient is low in the internal structure of the bearing during thermal analysis. After the heat reaches the steady state, temperature distribution shows a decreasing trend from the retainer ring to the adjust ring. The

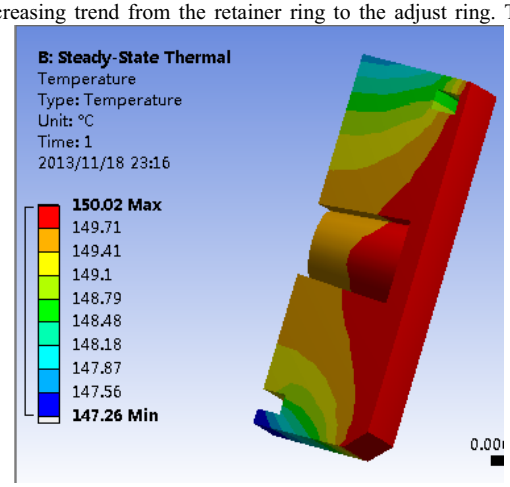

Figure 11. Temperature distribution of steady-state

Fig. 12 shows that the maximum heat flux appears in the upper and lower ends of the bearing. The heat flux in the middle is small because of the small temperature difference.

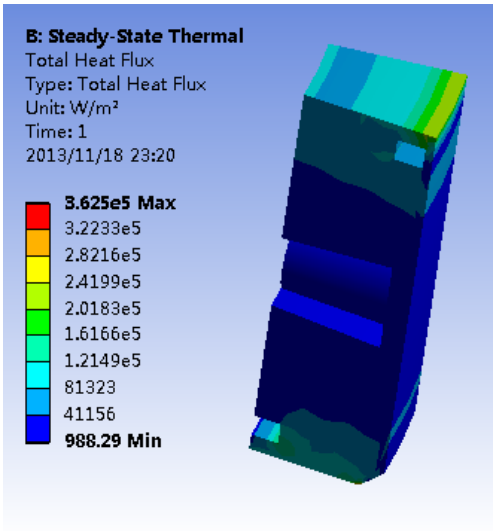

Figure 12. Heat flow distribution of steady-state

The time required to reach the steady state is short; thus, this study introduces static analysis to the result of the steady-state thermal analysis to simulate the thermo-mechanical coupling characteristic of the bearing. Figs. 13 and 14 show the results of the thermo-mechanical coupling simulation.

Fig. 13 shows that the maximum stress is 2695.5 MPa, which is 18.6 MPa bigger than the result without considering the influence of temperature. High temperature reduces the carrying capacity of the bearing.

Fig. 14 shows the bearing deformation with consideration to the thermo-mechanical coupling. The deformation is located at the contact area between the retainer and upper sealing gasket near the notch area of the sealing ring and is approximately 0.14 mm, which is 0.02 mm bigger than the result without the influence of temperature. The increased deformation had certain adverse effects on the sealing characteristics. Fig. 14 shows that the bearing deformation from heat can partly offset the maximum displacement because of the mechanical deformation of the bearing.

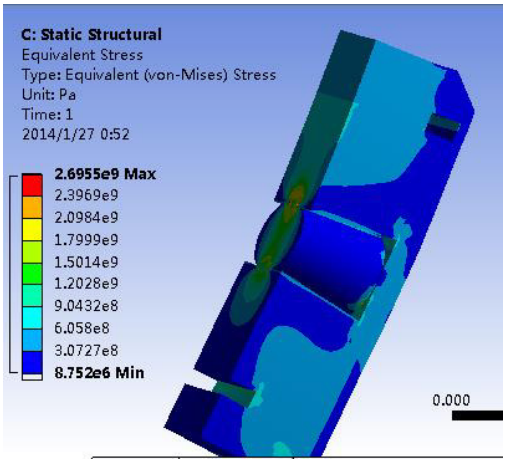

Figure 13. Stress distribution of thermo-mechanical coupling simulation

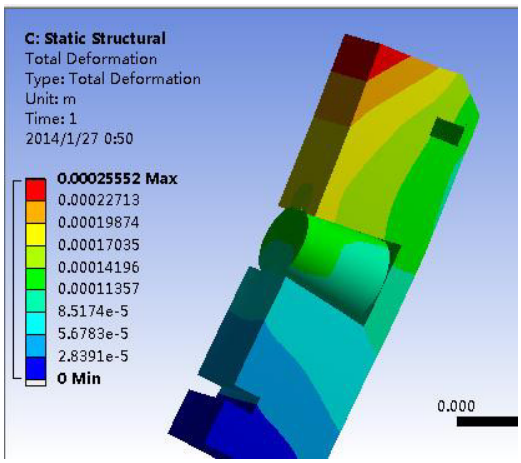

Figure 14. Deformation distribution of thermo-mechanical coupling simulation

On the basis of the simulation results, some design rules for this type of bearing can be concluded:

(1) High-temperature environments have a certain influence on the contact stress of the bearing. The maximum contact stress with consideration to the role of the temperature field is bigger than the maximum contact stress without consideration to the role of the temperature field. Thus, the rated load should be increased 10% more than the rated load on the basis of Hertz theory when designing this type of bearing because of high temperature.

(2) High-temperature environments have a certain influence on bearing deformation and affect the sealing performance of the bearing. Thus, certain sealing measures must be used to prevent the entrance of mud into the bearing and abrasive wear. One possible approach is to select the bearing material with high strength, hardness, and abrasion resistance characteristics.

(3) High-temperature grease should be applied to meet the bearing operating temperature, which often reaches 120 °C to 150 °C.

5. EXPERIMENT

Some experiments were conducted to verify the results of the structure optimization and thermo-mechanical coupling simulation.

Four developed bearings were tested in this study on a test machine (Fig. 15). Two bearings were the bearings designed on the basis of the Hertz theory, and two bearings were optimized on the basis of the simulation results. The carrying capacity and service life were tested in water and mud.

Figure 15. The machine to test developed bearing performance

Table 3 shows the result of the bearing based on Hertz theory and Table 4 shows the result of the bearing optimized on the basis of thermo-mechanical coupling simulation. Table 3 shows that the service life of a bearing is only 7.5 h when damaged. Table 4 shows that one bearing works 31.5 h in water, whereas the other bearing works 21 h in mud. After a series of optimization and improvements, the bearing is able to meet the drilling engineering requirements: serve 20 h on the condition of heavy axial load (60 t to 75t), high temperature (120 °C to 150 °C), mud (density is 1.2 g/cm^3 to 1.8 g/cm^3), and certain torque (600 N • m to 1200 N • m).

Table 3. Experimental result of bearing before optimization

Bearing No.	1	2
Medium	Water	Mud (1. .06g/cm^3)
Axial Load(t)	65	65
Torque(N • m)	600	750
Time (Hour)	7.5	7.5
Result	Roller fragmentation; Pits appear in the surface of raceways;	Roller fragmentation; Pits appear in the surface of raceways; Shaft ring and seat ring fracture

Table 4. Experimental result of bearing after optimization

Bearing No.	1	2
Medium	Water	Mud (1. .06g/cm^3)
Axial Load(t)	65	65
Torque(N • m)	600	750
Time (Hour)	31.5	21
Result	Roller fragmentation; Pits appear in the surface of raceways	Roller fragmentation; Pits appear in the surface of raceways Shaft ring and seat ring fracture

The experiments also verify the effect of the result of simulation. Figs. 16, 17, and 18 show several typical failure modes.

Figure 16. Roller dropped off the bearing

Figure 17. Pits and fractures appeared on the Surface of raceway

The dropping off of the roller from the bearing (Fig. 16) is consistent with the simulation results stating that the maximum stress is located at the contact area between the roller and shaft ring (Figs. 6, 9, and 13). Contact stress not only causes bearing deformation and bus also caused the radial displacement of the rollers (Figs. 7, 10, and 14).

The failure of pits and fractures appear on the surface of raceways (Fig.17), and the failure of roller fragmentation

Figure 18. Roller fragmentation

(Fig.18) are related to the location of the maximum stress and fatigue flaking because of roller radial displacement.

These experiments verify the feasibility of researching the characteristics of rotary liner hunger bearing by simulating the thermo-mechanical coupling characteristics. The simulation research provides a solution to the high cost of the drilling to some extent.

6. CONCLUSION

This paper discusses the working conditions, contact theory of complex interface, thermo-mechanical coupling characteristics, failure mechanism, and structure optimization of the rotary liner hunger bearing. The following conclusions are obtained.

(1) The rotary liner hanger bearing is limited by the design space and operates under heavy loads conditions (more than 60 t); thus, the bearing needs to have a high ability to withstand high static loads.

(2) Operating ambient temperature and mud have significant influences on the carrying capacity and serve life of the bearing.

(3) The failure mechanism of the bearing is fracture mechanism under the control of heavy load, temperature, and abrasive wear.

(4) The bearing developed in this paper has been tested on the test machine. The result shows that the structure optimized bearing can meet the requirements. Every part of the bearing is intact when the load is 65 t and torque is 600 N • m in a water medium or 750 N • m in a mud medium for 20 h.

(5) Some designing rules are concluded on the basis of the research results of the thermo-mechanical coupling characteristics (see 3).

Conducting many experiments is impractical because of the high cost. Analysis thermo-mechanical simulation is a feasible method on studying the characteristic of rotary liner hanger bearing in ultra-deep well drilling engineering.

7. ACKNOWLEDGMENTS

This project was supported by the Fundamental Research Funds for the Central Universities (265201304), China Scholarship Council (201306405002), and Design Innovation and Simulation Laboratory at Ohio State University.

8. REFERENCES

[1] Lindsey, H.E., and Jr., Durham, K.S., "Field Results of Liner Rotating During Cementing", **Society of Petroleum Engineers**, 1987, 2(1), pp. 9-14.

[2] Allwin, R. P. "Optimizing Stress Distributions in Rotating Liner Hangers", **ASME Journal of Energy Sources Technology**, 1990, pp. 14-18.

[3] Mota, J., Campo, D. and Menezes. J., et al, "Rotary Liner Drilling Application in Deepwater Gulf of Mexico", **Proceedings of SPE/IADC Drilling Conference**, 2006, pp. 753-762.

[4] Kunning, J., Wu, Y.F., Thomson, I. J., et al, "Non-retrievable Rotating Liner Drilling System Successfully Deployed to Overcome Challenging Highly Stressed Rubble Zone in a GOM Ultra-Deepwater Sub-Salt Application", **Proceedings of SPE Annual Technical Conference and Exhibition**, 2009, pp. 3430-3441.

[5] Jimenez, C., Soto, S., Leon, A., et al, "New Liner-Hanger Technology Improves Safety and Reduces Non-Productive Time in Deviated High-Temperature Wells in South Central Venezuela", **Proceedings of SPE Annual Technical Conference and Exhibition**, 2009, pp. 1999-2010.

[6] Louis M. Scalzi, "Bearing for liner-hanger assembly", U.S., US4190300, 1980.

[7] Juan A. Garcia, "Seal Bearing Apparatus", U.S., US4033640, 1977.

[8] Yonggang K., Yongan S., and YongChan Zh., et al, "A Rotating Liner Hanger Bearings", China, CN201826788U, 2011.

[9] Krantz T. L., "On Calculation Methods and Results for Straight Cylindrical Roller Bearing Deflection, Stiffness and Stress", **Proceedings of the ASME 2011 International Design Engineering Technical Conferences & Computers and Information in Engineering Conference**, 2011, 8, pp. 25-36

[10] Qiu, L., Parejko, J., "Raceway Curvature Effect Analysis and Optimum Design on Ball Bearing Life Performance", **ASME/STLE 2004 International Joint Tribology Conference, Parts A and B**, 2004, pp. 757-764.

[11] Wei, T., **Logging Evaluation of the Quality of Oil and Gas Well Cementing**, Beijing: Petroleum Industry Press, 2010.

[12] Tian, B., **Thermal - Mechanical Finite Element Analysis of Rolling Mill Bearing System**, Wuhan University of Science and Technology, 2010.

[13] Hertz, H., "On the Contact of Rigid Elastic Solids and on Hardness", **Miscellaneous Papers**, 1896, 1(1), pp. 163-183.

[14] Yan, Y. X., Zhu, C.,Hang, L. X., et al, "Lab-Built Pulse Arc Evaporator", **Journal of Vacuum Science and Technology**, 2004, 24, pp. 94 -96.

[15] Palmgren A., "Ball and Roller Bearing Engineering", **Burbank**, 1959, pp. 137-145.

[16] Jones, A. B., "Ball Motion and Sliding Friction in Ball Bearing", **Journal of Basic Engineering (ASME Trans)**, 1959, 81(1), pp. 1-12

[17] Harris,2001,**Rolling bearing analysis, John Wiley**

[18] Ren, H.D., Yang, B. Y. and Wei, P., "The Prediction of Dynamic Friction Torque for Aerospace High Speed Bearings", **Lubrication Engineering**, 2008, 2 (33), pp. 54 - 108.

[19] Michael, F., "Correlations for Heat Generation and Outer Ring Temperature of High Speed and Highly Loaded Ball Bearings in an Aero Engine", **Aerospace Science and Technology**, 2006, 10, pp. 611-617.

[20] Gonzalez-Perez, I., Roda-Casanova, V., Fuentes, A., et al, "A Finite Element Model for Consideration of the Torsional Effect on the Bearing Contact of Gear Drives". **ASME Journal of Mechanical Design**, 2012, 134, pp. 1-8.

New FACTS Equipment in an Enhanced Version of Smart Grids

The Magnetic Gate

Julio Enrique Posada C.
EIII Transmission & Distribution of Energy
San Salvador, El Salvador, C.A.

ABSTRACT

This work is a qualitative proposal of new device FACTS, which aims to repowering the "Smart Grids", to a higher level than currently achieved. The existing FACTS that are covering the role of power flow control have the disadvantages of the use of electronic devices, generating excessive heat and harmonics injected into the network. These devices are expensive and its regulation is binary: zero flow or total flow. This proposal offers a more versatile power flow control from zero to one hundred percent. Smart grid will no longer need to have a Relay Counseling Center, will be sufficient for communication between the points involved in the network by pilot wire or other means available to control and protect the network. In combination with phasor measurement units (PMUs) in form of "Observation Incomplete" will not be necessary to have approximation techniques to estimate the variations caused by the dynamics of demand.

Keywords: Camera Ready, Meter Reading, Power Generation, Dispatch, Power Demand, Power System Protection.

I. INTRODUCTION

This work is a qualitative proposal of new device FACTS, which aims to repowering the "Smart Grids", to a higher level than currently achieved. The existing FACTS that are covering the role of power flow control have the disadvantages of the use of electronic devices, generating excessive heat and harmonics injected into the network. These devices are expensive and its regulation is binary: zero flow or total flow. This proposal offers a more versatile power flow control from zero to one hundred percent. Smart grid will no longer need to have a Relay Counseling Center, will be sufficient for communication between the points involved in the network by pilot wire or other means available to control and protect the network. In combination with phasor measurement units (PMUs) in form of "Observation Incomplete" will not be necessary to have approximation techniques to estimate the variations caused by the dynamics of demand.

II. NOMENCLATURE

FACTS: Flexible Alternating Current Transmission System.
MFC: Magnetic Field Control.
CT: Current Transformer.
CVT: Capacitor Voltage Transformer.
CPU: Control processor unit.

III. FOREWORDS

This paper is a qualitative proposal and is not intended to present a design with detailed drawings, but rather an idea or concept of equipment that, based on knowledge and basic principles of electricity and magnetism, combined with some concepts of "Smart Grid" make sense for this proposal.

Therefore, the section five "basic calculations" shows just that, basic calculations with elementary formulation. The widespread use of Magnetic Gate (MAG) although does not cover the total current benefits of "Smart Grid" to manage the load, will improve to a higher level than currently hold.

FACTS equipment that currently cover the function of regulatory of power flow, have the disadvantages of the use of electronic devices, such as excessive heat generated and the injection of harmonics in the network, they require the respective filters.

This, without taking into account what those machines are expensive and offer them the regulation is binary: zero flow or total flow, or "all or nothing". The MAG provides a regulation of the power flow on a more versatile scale, being able to control it from zero to one hundred percent.

Furthermore, it is unnecessary the Counseling Center Relays, will be enough the communication between the MAGs associated with each circuit breaker, through pilot wire or some other means available. Therefore, due to fewer crossed and analyzed data, the laborious task of considering whether an event is really a failure, will be less complicated and will be carried out more quickly.

Using MAG in combination with PMUs is available measurement readings in mode "Observation Incomplete" and will require no approximation techniques for estimating the variations caused by the demand dynamics, because the MAG operating in "floating mode" as discussed further below, the network automatically and gradually rearrange these variations. Incomplete observation could be used only for measuring voltage and current signals of the network in some specific points in the network.

IV. DESCRIPTION OF EQUIPMENT

The MAG is a FACTS device controller bidirectional power flow, proposed to: regulate the power flow at a given point of a transmission system, eliminate instability events, protect the system against failures short-circuit on transmission lines and correct the power factor on a particular node where there is no provision of capacitor banks or where its necessary greater accuracy of the correction already made. Its operation has a greater versatility that the mechanisms currently used and will be very useful when for some reason, we want to have control load flow retaining it (in whole or in part) at any point, in order to divert the flow of power at our convenience elsewhere in the system.

The protection of existing power systems for the transmission lines (main and backup) currently held by relays of: distance, differential, earth fault, overload, etc. will become part of the backup protection, moving completely to the MAG main protection function. Moreover, the protection of substations on the inside (transformers, capacitor banks, buses, etc.) remains protected by the current schema.

The author presents his work at the qualitative level but shows some calculations assuming the MAG works as a reverse current transformer.

MAG is a series of coils (coils 2) connected in series or in parallel, feeding a magnetic field within a flexible armor used as a second coil (coil 1) by circulating the field around the line current of so, that the current induced by the field as opposed to circulate the line current, annulling this totally or partially. The author has called this arrangement of coils 1 and 2 as "Magnetic Cannon (MAC)" which is the main part of the MAG. (Figure 1)

The coils 2 of MAC may be interconnected in series or in parallel depending on the amount of current that is available to feed them. Hereafter this document will assume the serial interface.

The MAC will be operated in automatic mode intelligently by the MFC, which is basically formed by a power supply, a switch to make changes to the interconnection of the coils 2 and a CPU which analyzes and decides the actions to take. (Figures 2, 3 and 4)

The CPU may need to have with the help of some PMUs (for incomplete observation) in the network or otherwise, place a simplified unit type of them in each CPU of each MFC to monitor and process the parameters of the corresponding node. Each MFC receive signals from the associated measuring equipment (current and potential transformers) as well as information from the surrounding MFC.

When a load current flows from one node to another through a transmission line, such current leaves the first node and then enters the second node. In the event of line failure, events happen otherwise, the current will be from both nodes to any intermediate point of the line to feed such failure.

Determining the point of failure may be effected as follows. Simulations should be performed three phases to ground faults at the midpoint of the "n" lines of the system; the percentage of short circuit current contribution of the two nodes who feed the fault must be tabulated for each one.

The percentage will be the same power contributions to the magnetic coils of the coils 2 of each MAC, in each of the two adjacent nodes when a real fault occurs at the midpoint of the line; then the MACs will strangle and keep fixed the current flow. Variations arising from real faults of this percentage, represents the separation proportionally from the midpoint of the real fault is happening.

For this reason and because the strangulation floating in the two circuit breakers that feed the failure will not allow the TCs rise above its magnetization curve, preventing the protective relay tripping execute their function; will be the MFCs of both points of to determine fault, to interrogate each other about the direction of current flow. Having detected the fault, the MFCs will send an endorsement signal trip their respective relays to be these which isolate the failed line from the system.

Simplifications

Basically, the MAG acts as the inverse of a current transformer (CT^{-1}) where, for simplicity: is omitted the use of the equivalent circuit, it has been assumed zero leakage flux and the value of the impedance of the primary assumes the same value as its resistance.

Another approach to be taken into account is that the number of turns of the coil 1 equals the number of primary turns N1 for the case of a transformer. This is because really, the primary driver has no loop around the armature, but the armature has a winding around the primary conductor.

Finally, it is assumed that the current and line voltage are exactly in phase with the secondary signals of the current and voltage transformers respectively. Since it is likely that this requirement is not met, appropriate adjustments shall be made by some means or with the assistance of the PMU mentioned above.

V. MAG OPERATION

Magnetic Gate can be operated in manual mode and automatic mode. We must first set the parameters to be monitored by the MFC, in their intensity. This may be choosing the level 1 for slight variations caused by natural changes in demand. The Level 2 for medium changes due to events of instability. Finally, level 3 for the abrupt changes caused by failure of any transmission line of the system.

Manual Operation Mode
Manual mode, in turn, can be used in fixed mode and power factor correction mode.

Fixed Mode Operation
The Load Dispatch Centre fixed the MAG at a predetermined maximum value of flow of primary current in a circuit breaker system, which can reduce the flow in any case. This, is a way to modify the distribution of natural load flow and force the system to behave the way our best interest.

Power Factor Correction Mode
In manual mode, the "Load Dispatch Centre" also can correct the power factor on a particular node in the network. For these we need to perform the two following steps in all lines and in all the breakers of each line, that feed the node where will be improved the power factor. Step one through the MFC, we sliding the angle of the current flow between the signals in the coils 2 and the secondary current of the CTs. Step two is to make a current injection at the node in question, from the adjacent nodes. This current will be consumed by the reactive impedance on the line and the process is equivalent to an artificial modification of the "Ohm's Law" in phasor form. (Figures 5, 6, 7, 8, 9 and 10)

The current injection procedure to correct the power factor applies only for emergencies. This is for example, when a capacitors bank is failed. This requires that at least two generation nodes on each side (left and right or up and down) of the node to correct PF, increase the voltage in order to that neighboring lines of that node, inject current through the MAG of each Gas Circuit Breaker (GCB) involved according to Figure 5.

This injection of current is achieved by manipulating the magnetic fields in the MAG circuits, each of the two ends of each transmission line connecting to the node where it is desired to correct the power factor. Manipulation should generate a magnetic field in the same direction of the field generated by the line current when the current is injected into the node where it is desired to correct the power factor.

Otherwise, the manipulation should generate a magnetic field in the opposite direction of the field generated by the line current when the current is injected from the node where it is desired to correct the power factor.

Automatic Operation Mode
The automatic mode is used in three versions: floating, instability detection and line protection.

Floating Mode
The MAG measure level variation caused by a natural dynamic load flow in a transmission system and allows the strangulation to rearrange slowly.

Detection Mode Instability
Under this mode, the MAGs measure the variation in level 2, freezes in fixed mode all points with that level, eliminating the oscillations of the power flow that occurs during these events. At the same time determine which is the point of greatest instability and causes (if it's necessary) the trip of corresponding MAG generator linked to that point.

Line Protection Mode
All MAGs near the point of failure, detects variations in level 3 and immediately freezes the flow of current in a maximum value. The two MAGs associated with circuit breakers that feed fails, send the signal to trip endorsement for relays to be them who separate the failed line from the system. The new form to identify the point of failure will be according to the direction of current contributions from the two nodes involved in the fault location. (Figure 11)

VI. BASIC CALCULATIONS

Known Variables. Available values are for a line that transmits 100 MW at 115 kV in three phases:

- Primary current I_1 (500 amperes)
- Primary wire resistance R_1 (0.1 Ω/km)
- Primary turns N_1 (100)
- Secondary turns N_2 (10,000)

Unknown Variables. The variables to be calculated are:

- Primary voltage V_1
- Secondary current I_2
- Secondary voltage V_2

Formulae Used:

- $N_1 I_1 = N_2 I_2$ (1)
- $V_1 = I_1 R_1$ (2)
- $V_1 I_1 = V_2 I_2$ (3)
-

Values obtained in normal condition:

- V_1 = 0.05 volts/meter
- I_2 = 5.0 amperes
- V_2 = 5.0 volts

Values obtained in short-circuit condition for 40 kilo-amperes:

- V_1 = 4.0 volts/meter
- I_2 = 400 amperes
- V_2 = 400 volts

The estimated data: number of primary and secondary turns (100 and 10,000 respectively) and the value of primary lead wire resistance (0.1 ohm per kilometer) produce values V1, V2 and I2 for normal and short-circuit condition, reasonably acceptable.

VII. ALTERNATIVE FOR THE MAGNETIC CANNON.

We can replace the Magnetic Cannon using a set of coils (attenuation coils) with winding concentric donut-shaped, but different from the toroidal arrangement, but so that the magnetic field generated in the armature in the center of the donut (where circulates the primary current) induces a reverse flow current to such primary current, annulling totally or partially. (Figure 12)

VIII. REFERENCES

[1] Stanley H. Horowitz, Arum G. Phadke y Bruce A. Renz, "The Future of Power Transmission" IEEE Magazine, Taking Measure of the Smart Grid around the World, marzo-abril 2010.

[2] Enrique Santacana, Gary Rackliffe, Le Tang y Xiaoming Feng, "Getting Smart" IEEE Magazine, Taking Measure of the Smart Grid around the World, marzo-abril 2010.

[3] C. Russell Mason, "The Art and Science of Protection Relays" Mexico: C.E.C.S.A. 1980, pp. 131-138.

[4] Vembu Gourishankar, "Electromechanical Energy Conversion" Mexico: R.S.I. 1969, pp. 36-40.

IX. CONCLUSIONS

In this case we wish to control an electric power in the range of 100 megawatts or more, by means of a magnetic gate of a few watts. If we see the example of a hydroelectric dam with a reservoir of 10 square kilometers and a 50 meter hydraulic head over the discharge pipe. Then we have that the energy required to close a valve in the pipe, is exactly the same as that required for close the valve, in case that the reservoir 100 kilometer square (10 times higher of stored energy). The same applies to the current flowing in the primary transmission line, since the energy involved, being channeled in this case by an electrical conductor, is particularly "quantized" and therefore easily controllable.

In both cases, the energy necessary to close a mechanical valve, and the energy required to close a magnetic valve; is small compared with the energy they are handling.

X. PHILOSOPHICAL METHOD USED FOR DEVELOPMENT OF THIS WORK: "VECTOR-GUIDE IN PROCESSES FOR SOLUTIONS NON EXISTING (GPS VECTOR)"

The philosophy of developing THE GPS VECTOR, consisting of descriptive works that serve as basis for designers and engineers can develop some device proposed. This philosophy is based on a presentation prepared by the author (Julio E. Posada), developed and exposed in 2004 in El Salvador during the Eleventh National Congress of Engineering, CONIMEIRA XI; with a paper "CONVERSION OF SUPERIOR EDUCATION, FOR ACCELERATED DEVELOPMENT OF TECHNOLOGY".

Any paper developed by the method above described, basically states the following precepts:

- All Great Discoveries are based on Basics Concepts of Science. If a discovery is made with advanced technology and high-level knowledge, then it is not a discovery is but an extension of a previous discovery.
- Developing a GPS VECTOR based on basic concepts of science, serves as a platform for development teams to implement it and produce a mechanism that, in these moment DO NOT EXISTS, but will contribute to the development of mankind.
- All Intellectuals has the ability to make great discoveries in any branch of science, always they were provided with the basic knowledge related to that discovery.

- The basic knowledge can be transferred without much effort from one individual to another, through daily contact between them. This phenomenon is called by the author as *Contamination of Knowledge*. Corporations should allow their scientists in the various branches of science; contaminate information to colleagues or workers fellows, who have the same or different specialties, to promote the acquisition of basic knowledge of a specific topic, on individuals working within the factories or labs.

- To give further impetus to the concept of Contamination of Knowledge, corporations must build libraries compendia of basic concepts with minimal use of equations and numerology, such that everybody of its employees may acquire a concept related to a mechanism currently preparing or, enforce any idea he has come to mind, to find conceptual support for successfully carrying out its mission. These libraries compendia of basic concepts may be structured on a corporate level in the first instance, but could be extended to local or federal government, in order to promote the nationwide (or worldwide) development of technology more quickly.

The "Vector GPS" concept, in addition to indicate a futuristic event, offers the appropriate and necessary technology to carry out the mentioned event. On the other hand, "Science Fiction" indicates the futuristic event but do not offers the technology that really allows conducting to the event.

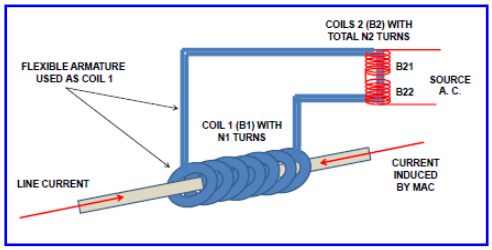

Figure 1. Magnetic Cannon.

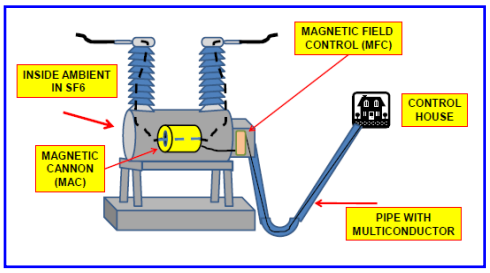

Figure 2. Overview of Magnetic Gate and Parts

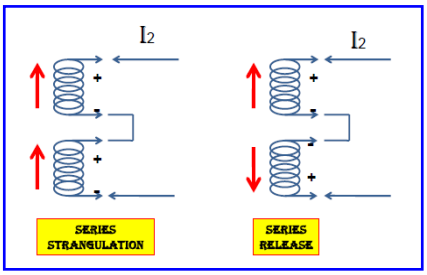

Figure 3. Interconnection of Coils

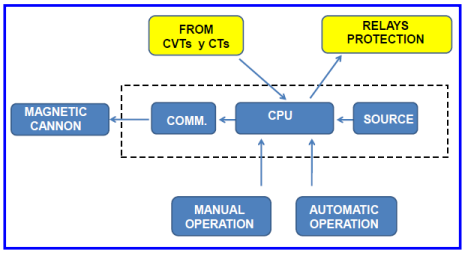

Figure 4. Interconnection Diagram of Parts of the MAG

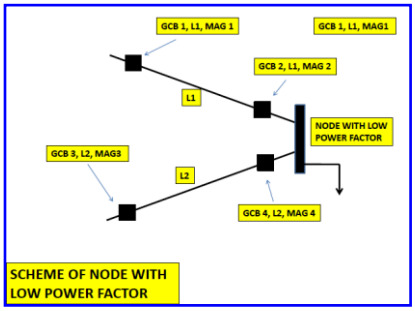

Figure 5. Scheme of a node with low power factor

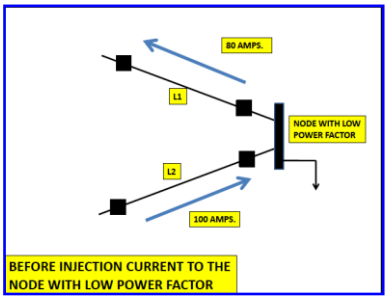

Figure 6. Before injection current to the node with low power factor

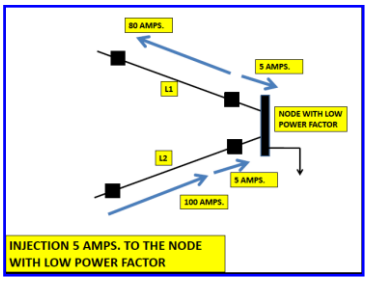

Figure 7, Injection 5 amps. To the node with low power factor

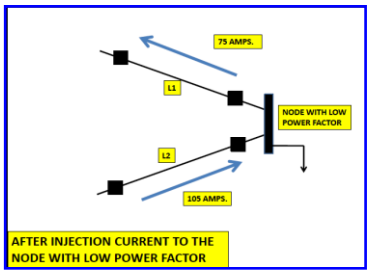

Figure 8. After injection current to the node with low power factor

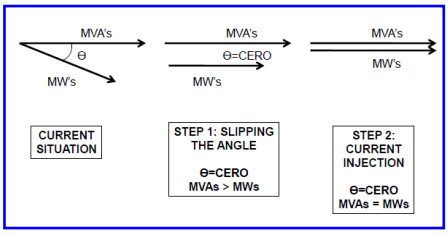

Figure 9. Steps to follow in all lines and in all the breakers of each line, that feed the node where will be improved the power factor

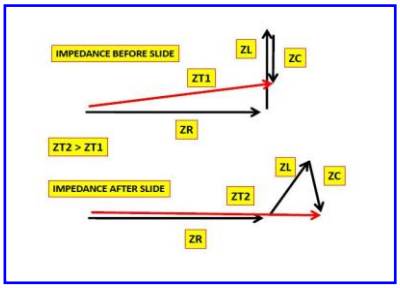

Figure 10. Artificial Equivalent Modification of the Ohms Law

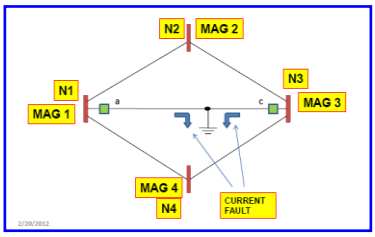

Figure 11. A current flowing toward the center (between the two circuit breakers) line from two adjacent nodes, it indicates failure

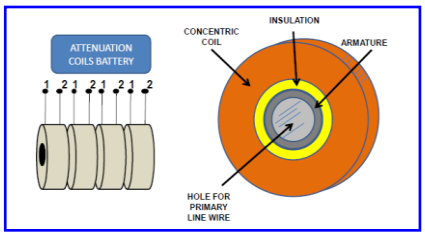

Figure 12. Alternative for Magnetic Cannon.

ATTENUATOR OF SEISMIC MOVEMENTS IN HIGH-RISE BUILDINGS

Julio Enrique Posada C.
EIII Transmission & Distribution of Energy
San Salvador, El Salvador, C.A.

ABSTRACT

This summary describes conceptually the "Attenuator of Seismic Movements ASM" which is an approach for a solution that reduces the risk of personal injury and property damage in high-rise buildings during a seismic event. Not intended to present structural calculations of high-rise buildings, but only to present a guide for calculators and designers to get the result proposed here, which is to reduce the oscillation of a building due to a seismic. Although this proposal is aimed to high-rise buildings, it can be adapted perfectly to any type of building over ten floors.

Keywords: Camera Ready, Motors Batteries, Half-Cycle, Oscillation, Vibration.

I. INTRODUCTION

During a seismic, a building of great height oscillates according to its natural frequency. The frequency are subject to the type of construction, or its dead weight, type of materials used, live loads, height, building morphology (dimensions) etc. From structural study we obtain a pattern of oscillation which would stand out one or more antinodes. These antinodes are the opposite to nodes or inflection points, in other words, antinodes are the points where the amplitude of oscillation is greater. Studies will determine where the most convenient points to install the motors batteries are, but until the study will be performed, we assume that the antinodes are the ideal location to install the motors batteries. (Figures 1, 2 and 3)

II. FORCED VIBRATION GENERATION

Each ASM has a battery of eight motors with its axis out of balance by a flywheel that contains a weight pooled, at an angle no greater than ten degrees. This is in order to produce vibration during operation of them, and thereby to transmit power to building by way of "impact load", when it is subjected to a seismic. The secret of this energy transfer is that the vibration is forced to hit harder, in the half-cycle in which the unbalanced weight is against to the instantaneous movement of the building. Otherwise the half cycle, in which the unbalanced weight is in favor of the building instant motion, the vibration is forced to beat with less force. (Figure 4)

III. SWAP POSITIVE-NEGATIVE IN FORCED VIBRATION

As an example to define the forced vibration, take the case of a set of motors with 1800 RPM and a seismic of 75 cycles per minute. This means that for every cycle of the seismic, we will have 24 cycles in the motors. Redefining, for each half cycle of the seismic, we have 12 half cycles on the motors. This is an advantage because we have the opportunity to accumulate 12 strokes of each motor to confront one seismic stroke. It should be noted that during the half cycle that the unbalanced flywheel is in favor of the instantaneous motion of the seismic, the vibration is attenuated by providing lower voltage to the stator windings of the motors. (Figures 5 and 5.1)

IV. ENERGY DELIVERY THROUGH FORCED VIBRATION

The weight of the unbalanced flywheel will be calculated according to the structure of the building, its natural frequency. The transfer of power from the motors must occurs as opposed to ground motion at a given moment and in proportion to their amplitude; by means of a series of pulses or shocks caused by the vibration, from of the unbalance flywheel, during operation of the mentioned motors. The motors type

we choose will depend on the available range, whose characteristics suit the purpose best way to achieve optimal attenuation. Some of these features would what type of motors has less time in his start from zero to nominal speed. The governor will know when swapping between positive and negative forced vibration, through two magnetic points that send a signal to the governor to exchange the type of forced vibration.

It is possible that in real operation, there will be a small slip of the vector resulting from the forced vibration, about fifteen or twenty degrees; so in this case, the time that marks semi cycles must adapts to this phenomenon in order to counteract the movement seismic. (Figure 6)

V. INTRODUCTION AND REMOVING A RESISTANCE TO FORCE VIBRATION

One way (among others) to program the forced vibration positive permutation to forced vibration negative, is placing a magnetic point 90 degrees behind the unbalanced weight and placing another magnetic point ahead 90 degrees of unbalanced weight. Thus, the flywheel 360 has been divided into two halves of 180 degrees each. Whenever the magnetic flywheel points pass through a third magnetic point which is fixed relative to the rotating flywheel, a sign of change between positive and negative forced vibration shall executed. This signal of change will trigger the thyristors 1 and 2, which produce a bypass on a resistor in series with the stator windings of the motor, to increase the speed, or failing; a resistor is inserted in the same windings, reducing its velocity. (Figure 7)

VI. COUNTERING THE SEISMIC

Each battery must consist of 8 electrical motors with horizontal axis, and although the power on each motors depends on the previous calculations (structural study), it is estimated that they will be between 100 and 200 HP each. Each level of the building where these batteries will be located must be segmented into four quadrants; the most convenient configurations are square shape and the rectangular shape (although this method can be adapted to any type of polygon). Shall be allocated two motors for each of the four quadrants, These pair of motors are located to operate on a coordinate axis, in a plane at a given floor of the building, previously selected. (Figures 8 and 9)

VII. CONTRIBUTION FROM EACH OF EIGHT MOTORS OF A BATTERY TO COUNTER THE SEISMIC

The eight motors of a given battery, contribute with the pulses generated by their vibration, to counteract the effects of the seismic motion in the building. Any direction as to adopt a seismic may be countered by the attenuator through "Floor Control System" consisting of: the motion sensor, the governor, the thyristor trigger circuit and circuit of assignment intensities; all these acting on motors. The circuit of assignment intensities allows the thrust vector of the motors may follow the seismic thrust vector. (Figures 10, 11, 12 and 13)

VIII. CONTROL SYSTEM IN EACH BATTERY

Each motors battery will be commanded by a governor, who in turn receives information from a movement sensor, which basically is seismograph with transducers with low power electrical signals outputs.

The Seismic will be detected by the movement sensor and sending to governor, which will analyze the following three variables: 1) intensity or amplitude of oscillation of the building due to seismic, 2) movement frequency oscillation of the building due to seismic, and 3) the direction and orientation of the oscillation of the building due to seismic.

The motion sensor will send the information to the governor for the purpose to mitigate the effect of the seismic on the building, and on the basis of the three measured variables, shall emits following attenuation commands on the motors chosen (not necessary the eight) to counteract the oscillation of the building due to seismic:

1) Assign the speed (intensity) of the motors, direction and orientation of the opposing force.

2) Assign to each motors the half-cycles in which shall operate with positive or negative forced vibration, according to the oscillation frequency of the building from the seismic movement. (Figure 14)

IX. PRIORITY ON THE ASSIGNMENT OF VELOCITY

The priority in the assignment of the velocities is, for the case of positive velocity, the bigger of them. Moreover, in the case of negative velocity, the priority is for the minor of the absolute value of them. (Fig. 15)

X. STARTING THE SYSTEM

Step 1, as a preamble to a seismic event, invariably precedes a series of imperceptible movements for humans; then Step 2 , other movements appears on the threshold of human perception; and finally Step 3, occurs movements clearly perceptible by human.
The starting protocol will be as follows: Step 1, start of two motors in "No load mode" (using clutch) in a battery; Step 2, start of other two motors in "No load mode"; and Step 3, take the load (unbalanced flywheel) of the four motors operating in "No load mode".
Then the control system does the rest.

XI. MOTORS BATTERIES LOCATION

The location of a motors battery at antinodes could not produce better attenuation. Therefore, by simulation must be sought the optimal location that offers the best attenuation. To achieve this optimal location, it is necessary that during the simulations, the first bank be located at various positions (floors) and chooses the one that best results occur.
Then, still during the simulation, it must explore the need for a second or more motors batteries, according to the cost benefit ratio.
Furthermore, alternative ways to generate the forced vibration would, reverse instantly (within about 1 millisecond) of the stator fields or, fields manipulation of the rotor fields utilizing synchronous motors. Thus we would obtain a braking pulse.

XII. PHILOSOPHICAL METHOD USED FOR DEVELOPMENT OF THIS WORK: "VECTOR-GUIDE IN PROCESSES FOR SOLUTIONS NON EXISTING (GPS VECTOR)"

The philosophy of developing the GPS VECTOR, consisting of descriptive works that serve as basis for designers and engineers can develop some device proposed. This philosophy is based on a presentation prepared by the author (Julio E. Posada), developed and exposed in 2004 in El Salvador during the Eleventh National Congress of Engineering, CONIMEIRA XI; with a paper "CONVERSION OF SUPERIOR EDUCATION, FOR ACCELERATED DEVELOPMENT OF TECHNOLOGY".

Any paper developed by the method above described, basically states the following precepts:

- All Great Discoveries are based on Basics Concepts of Science. If a discovery is made with advanced technology and high-level knowledge, then it is not a discovery is but an extension of a previous discovery.

- Developing a GPS VECTOR based on basic concepts of science, serves as a platform for development teams to implement it and produce a mechanism that, in these moment DO NOT EXISTS, but will contribute to the development of mankind.

- All Intellectuals has the ability to make great discoveries in any branch of science, always they were provided with the basic knowledge related to that discovery.

- The basic knowledge can be transferred without much effort from one individual to another, through daily contact between them. This phenomenon is called by the author as *Contamination of Knowledge*. Corporations should allow their scientists in the various branches of science; contaminate information to colleagues or workers fellows, who have the same or different specialties, to promote the acquisition of basic knowledge of a specific topic, on individuals working within the factories or labs.

- To give further impetus to the concept of Contamination of Knowledge, corporations must build libraries compendia of basic concepts with minimal use of equations and numerology, such that everybody of its employees may acquire a concept related to a mechanism currently preparing or, enforce any idea he has come to mind, to find conceptual support for successfully carrying out its mission. These libraries compendia of basic concepts may be structured on a corporate level in the first instance, but could be extended to local or federal government, in order to promote the nationwide (or worldwide) development of technology more quickly.

The "Vector GPS" concept, in addition to indicate a futuristic event, offers the appropriate and necessary technology to carry out the mentioned event. On the other hand, "Science Fiction" indicates the futuristic event but do not offers the technology that really allows conducting to the event.

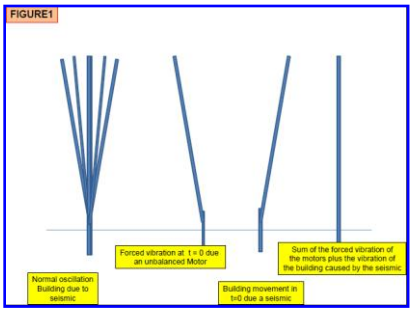

Figure 1, Combining seismic movements with the motor movements, it counteracts the movement of the building

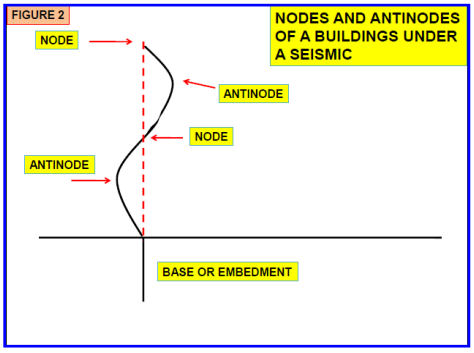

Figure 2, Locating Nodes and Antinodes

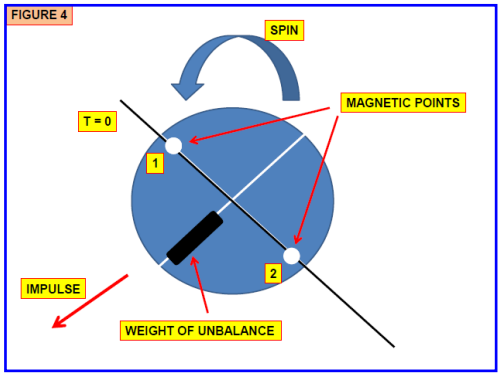

Figure 3, Flywheel Unbalanced

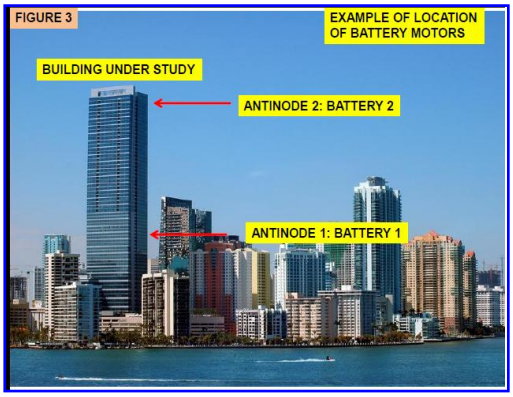

Figure 4, Location Estimated Antinodes

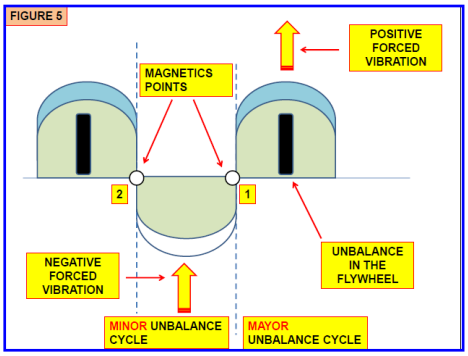

Figure 5, Beat Cyclic of Motors

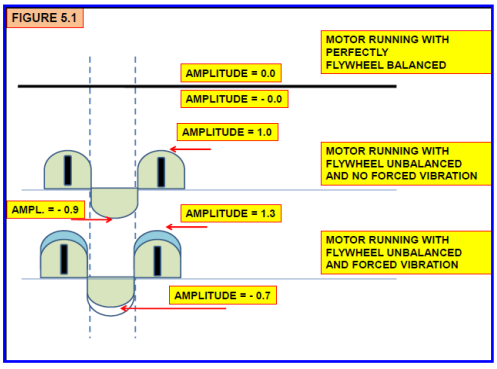

Figure 5.1, Forced Vibration in General Form

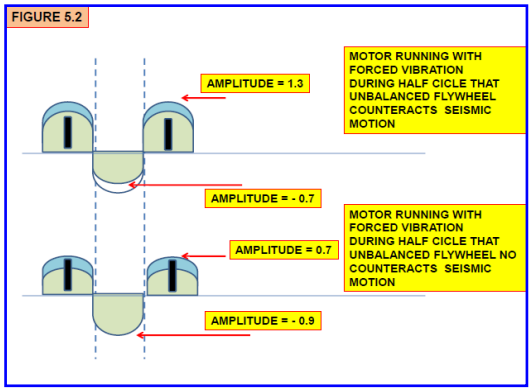

Figure 5.2, Forced Vibration in General Form

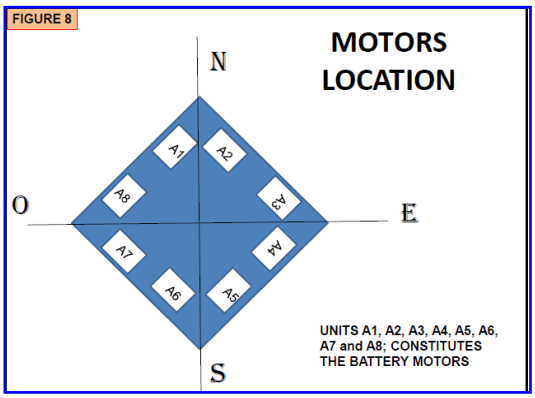

Figure 8, Physical Arrangement of the Motors Battery

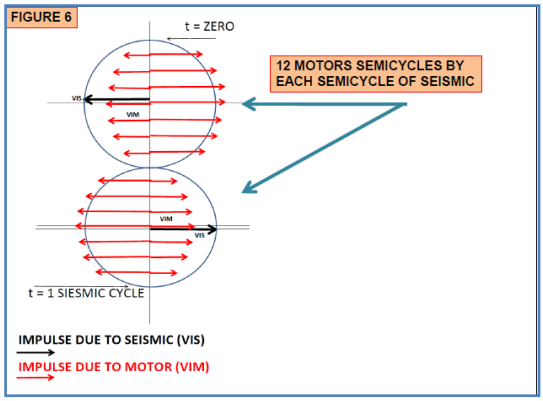

Figure 6, a seismic cycle contains 12 cycles of the motors (in this case)

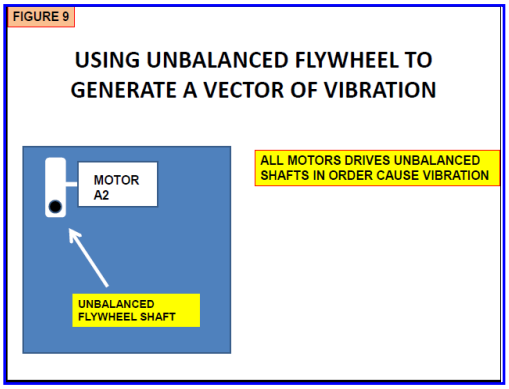

Figure 9, Vibration Motorized Unit

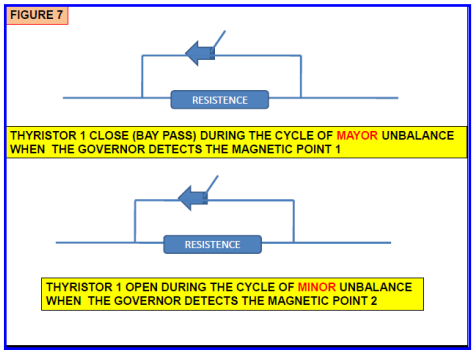

Figure 7, Boost and attenuation of Motors strokes

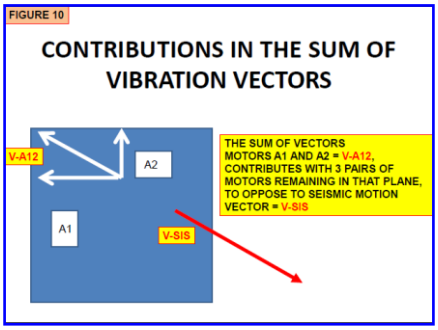

Figure 10, Contribution of Motors against seismic

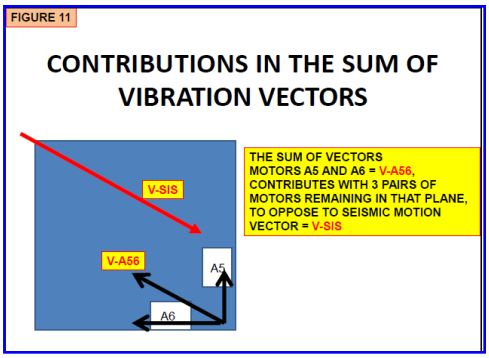

Figure 11, Contribution from other Motors against the Seismic

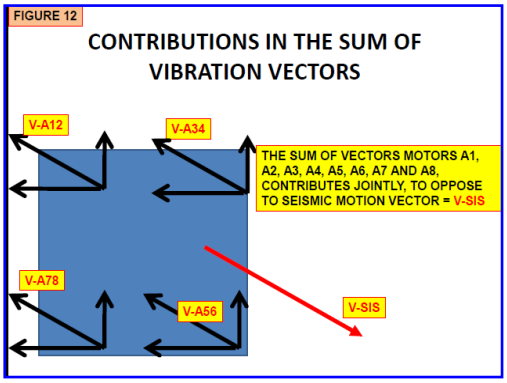

Figure 12, Contribution from the Eight Motors against the Seismic

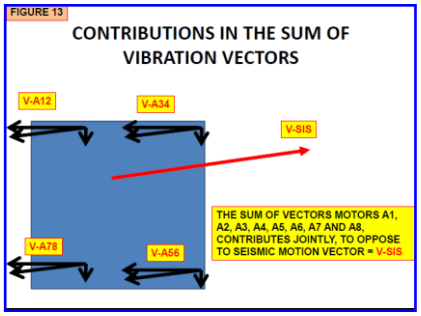

Figure 13, Contribution of the Eight Motors against the Seismic (other direction)

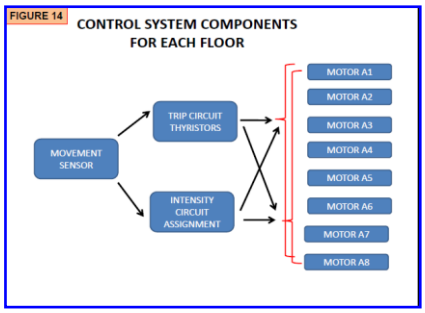

Figure 14, Interaction between Components of the Control

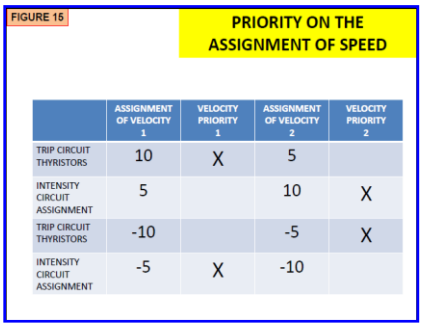

	ASSIGNMENT OF VELOCITY 1	VELOCITY PRIORITY 1	ASSIGNMENT OF VELOCITY 2	VELOCITY PRIORITY 2
TRIP CIRCUIT THYRISTORS	10	X	5	
INTENSITY CIRCUIT ASSIGNMENT	5		10	X
TRIP CIRCUIT THYRISTORS	-10		-5	X
INTENSITY CIRCUIT ASSIGNMENT	-5	X	-10	

Figure 15, Priority of the Assignment of Speed

Dynamic Policy Investigation for Infrastructure Rehabilitation

Roozbeh RASHEDI and Tarek HEGAZY
Department of Civil and Environmental Engineering, University of Waterloo
Waterloo, N2L3G1, Canada

ABSTRACT

Civil Infrastructure assets are essential to support a nation's economy and the welfare of its citizens. Despite their importance, the condition of the civil infrastructure in North America is much lower than acceptable levels, with investment backlog being huge in size. Furthermore, recent requirements for encouraging sustainable development and promoting public private partnerships (PPPs) have added additional complexities to policy making in the domain of infrastructure rehabilitation to reduce backlog. Although a large body of knowledge has been accumulated in the past decade on infrastructure management, little or no efforts have focused on strategic policy-making, considering the dynamic interactions among policies, rehabilitation decisions, and resulting infrastructure performance. This paper thus presents a framework to analyse the impact of strategic policies such as budget levels and PPP options, on backlog accumulation, infrastructure condition, and sustainability performance. The framework uses System dynamics (SD) to test the effectiveness of various policy scenarios on the long-term performance of infrastructure assets, and ultimately improve the economics of the costly infrastructure rehabilitation.

Keywords: Policy Investigation, Strategic Decision-Making, Infrastructure Management; System Dynamics

1. INTRODUCTION

Civil Infrastructure, such as roads, highways, transportation systems, water/sewer networks, schools, etc., are among the most important assets that directly impact a nation's economy and quality of life [1]. Despite their importance, the condition of the civil infrastructure in North America is much below acceptable levels. America's infrastructure report cards, for example, show little condition improvement from 2005 to 2013 [2], while the investment needed to bring the infrastructure to satisfactory level has dramatically increased from $1.6 trillion to $3.6 trillion during this time (Figure 1). The majority of the existing infrastructure was constructed decades ago and has been rapidly deteriorating due to aging, constant use, and exceeded capacity. To sustain infrastructure safety and operability, regular maintenance, repair, and rehabilitation (often refer to as MR&R) are necessary. However, due to the insufficient pubic funding for these actions, backlog keeps accumulating over time and causes a major challenge for asset managers. The need to improve infrastructure condition and reduce backlog are not the only challenges that asset managers are facing today. New regulations for sustainable development also increase the complexity of infrastructure management. In 1987, the World Commission on Environment and Development [3] defined sustainable development as "a process in which the exploitation of resources, the direction of investments, the orientation of technical development, and institutional changes are all in harmony and enhance both current and future potential to meet human needs and aspirations". As such, all the life cycle decisions of the infrastructure, including MR&R, has to account for environmental, social, and economical impacts. To help with this process, researchers (e.g., [4] and [5]) and different agencies (e.g., Infrastructure Canada; United States Environmental Protection Agency (EPA)) have introduced guidelines for sustainable developments [6]. In addition to sustainability, Public Private Partnership (PPP) has been viewed as an attractive method for procuring large and complex public infrastructure projects. This approach introduces additional complexities to the infrastructure decision-making process.

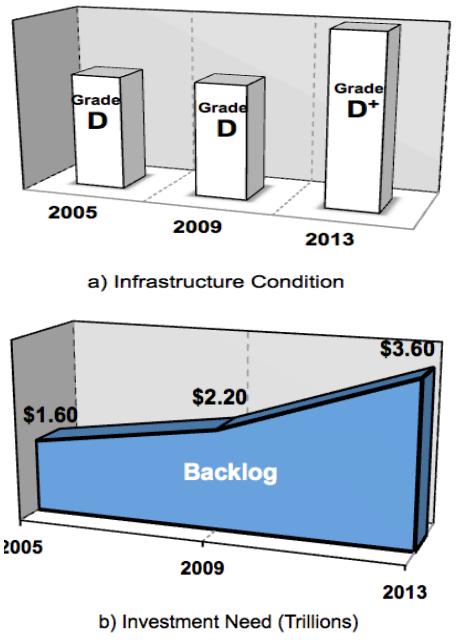

FIGURE 1 Infrastructure condition and backlog (U.S.)

Using PPP decreases the infrastructure backlog, optimizes risk and resources, and brings innovation into the infrastructure projects [7, 8]. These advantages make PPP a popular project delivery method for municipalities. In Canada, more than $27.1 billion is invested in different PPP infrastructure projects, such as schools, public transit, local roads, hospitals, or wastewater programs, in the period between 2009 and 2011 [8]. According to the World Bank, many developing countries have also encouraged the private sector to participate in infrastructure facilities, and between 1990 and 1999, more than 30 developing countries have had at least one project completed by the private sector [9, 10, 11].

Although a large body of knowledge has been accumulated on infrastructure management, few efforts focused on the dynamic interactions among infrastructure-related parameters and on developing decision support systems for policy analysis. This paper proposes an integrated framework to analyse the impact of different strategic policies on the infrastructure serviceability, backlog accumulation, and sustainability.

2. PROPOSED POLICY INVESTIGATION FRAMEWORK

The proposed framework considers three of the main interrelated aspects of strategic asset management including: (1) Financial performance and infrastructure backlog accumulation [12, 13, 14]; (2) Sustainability related issues [4, 15] and (3) Type of public private partnership (PPP) [9, 16, 17]. These aspects are integrated within a holistic strategic model that investigates the impact of sustainability policy, budget policy, and PPP policy on asset performance and backlog accumulation. As shown in Figure 2, the proposed policy investigation framework has four interrelated modules: (1) sustainability; (2) physical infrastructure; (3) life cycle cost analysis (LCCA); and (4) policy analysis. Accordingly, the framework considers the dynamic interactions within and among these modules, and can be used to provide policymakers with a clearer understanding of the long-term impact of their policies.
As shown in Figure 2, there are many interactions among different modules of the strategic policy investigation, and between the key strategic variables within each module. First, an effort was made to identify the main parameters that decision-makers, managers, and engineers in the selected asset domain (e.g., educational facilities) consider as key parameters that affect each module. For example, considering the physical infrastructure module, the related strategic variables include as asset condition, asset deterioration, level of service (LOS), serviceability limits, renewal actions, deterioration transition probabilities, improvements effects of different renewal actions, etc. To analyse and study the interactions among these parameters, the system dynamics (SD) simulation approach can be then used as an effective tool to capture the dynamics of complex systems [18, 19]. System dynamics uses the method of causal loop diagraming to study key parameters and the underlying feedback structure of the system. A causal loop diagram (CLD) consists of variables connected by links denoting the causal influences among them. Casual links show effects of variables on each other by link polarities. A positive link polarity (+) implies that "if a cause increases, the effect increases above w2hat it would otherwise have been" and vice versa. Similarly, a negative link polarity (-) means "if the cause increases, the effect decreases below what it would otherwise have been" and vice versa [19].

For instance, considering the key parameters (variables) within the physical infrastructure module, a CLD can be developed as shown in Figure 3. In the presented CLD, asset deterioration is linked to asset condition by a negative link polarity. Based on the aforesaid definition of negative polarity, this causal link simply implies that more deterioration results in lower asset condition scores. Another negative link also connects asset condition to asset deterioration, which indicates that by decreasing the asset condition deterioration rate increases (i.e., assets in poor conditions have higher deterioration rates). The combination of these links then creates a positive (or reinforcing) feedback loop as depicted by Figure 3. Positive loops cause growth or decays. In the case of asset condition, a cycle is established in which infrastructure deterioration occurs at an accelerated rate (the accelerated process of deterioration has been reported in different infrastructure related literature, e.g., [1]).

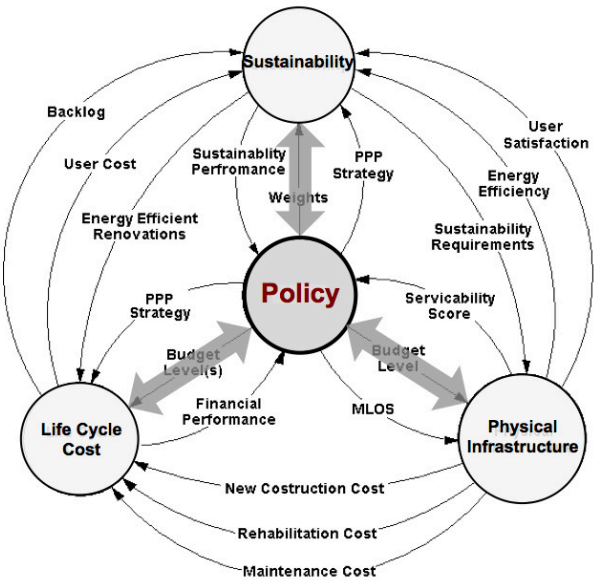

FIGURE 2 Strategic policy investigation framework

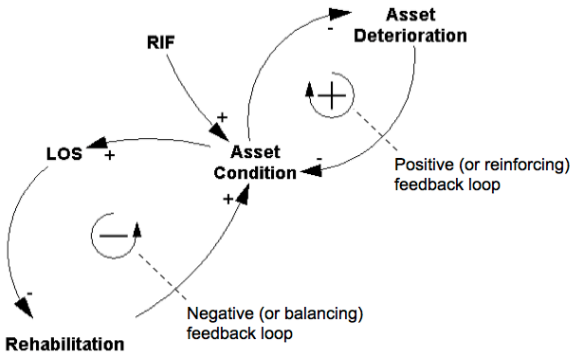

FIGURE 3 A Causal Loop Diagram example

On the other hand, improving asset condition increases the level of service, which is presented by a positive link between the two variables. By increasing the LOS the number of renewal actions will decrease (i.e., a negative link). If the number of renewal actions decreases then asset condition decays (i.e., positive link). This behavior, as depicted in Figure 3, represents a negative (or balancing) feedback loop. Negative loops cause self-balancing behaviors that lead to equilibriums. The negative loop in Figure 3 suggests that the number of renewal actions is adjusted based on the observed LOS to keep the asset condition within an acceptable serviceability level depending on the importance of the assets (determined by RIF), which is a very common renewal approach in the area of asset management.

The CLD (mental representation) models will be then translated into to stocks and flows (simulation components) to create an SD model. Stocks and flows along with CLDs are the two central components of dynamic system theory. Stocks are accumulations that characterize state of the system and generate information upon which decisions and actions are based [19]. Flows, on the other hand, are activities and actions that generate quantities or information that accumulates in the stocks over time. Considering the key variables in Figure 3, asset condition can be represented by a stock that accumulates the state of conditions over time (Figure 4). On the other hand, asset deterioration can be then represented by an outflow that decreases the stock value (i.e., causes condition to decay), while renewal actions can be represented by an inflow that increases the stock value (i.e., improves the condition). Flows can cause increase (i.e., inflow) or decrease (i.e., outflow) in the state of stock variables. The net flow into the stock is the rate of change of the stock. Hence, the behavior of stocks and flows can be determined using Eq. (1).

$$\text{Stock}(t) = \int_{t_0}^{t} [\text{Inflow}(s) - \text{Outflow}(s)]ds + \text{Stock}(t_0) \qquad (1)$$

where Inflow(s) represents the value of the inflow at any time *s* between the initial time to and the current time *t*.

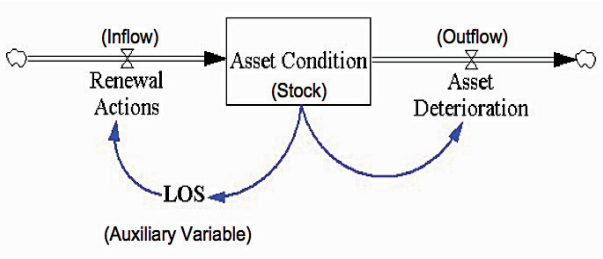

FIGURE 4 A Stock & Flow Diagram example

Equivalently, the net rate of change of any stock, its derivative, is the inflow minus the outflow, defining the following differential equation:

$$d(\text{Stock})/dt = \text{Inflow}(t) - \text{Outflow}(t) \qquad (2)$$

Based on Figure 4 and Eq.1, the system starts with an initial condition CI_0 (i.e., $\text{Stocl}(t_0)$). Deterioration is then acts as an outflow, which reduces the condition over time and renewal actions can increase the stock variable over time based on the number of repair interventions.

3. CASE STUDY

A case study of educational facilities from the inventory of the Toronto District School Board (TDSB), which administrates a network of more than 550 school buildings, has been used within the proposed framework for policy-making. The key strategic variables have been identified based on reviewing literature about each module (physical, LCCA, sustainability, and policy), previous research on TDSB asset network, and other guidelines and documents from the TDSB. These four modules involve a total of 27 key strategic variables as shown in Table 1. Based on the possible causal effects of each parameters on the others detailed causal loop diagrams are developed for each module and then integrated and refined through numerous rounds of logic test and comparison to make sure that all major interactions are captured.

To validate the identified parameter and the dynamics among them, causal trees were generated to test different layers of relations within the proposed system (Figure 5). The CLDs are then mapped into an overall stock and flow SD simulation model with integration between different modules. Figure 6 shows the overall structure of the strategic SD model for the TDSB case study. The model is intended to consider the whole inventory of existing assets at the strategic level, and as such, it models deterioration from a system-level view (i.e., electrical, mechanical, architectural, and etc.).

TABLE 1 Key strategic parameters

Modules	Key Variable	*Assumptions/Comments*
Physical Infrastructure	Asset Condition	*Based on field condition assessment [0 – 100].*
	Asset Deterioration	*Uses a Markovian process. TPMs are assumed to be available.*
	Rehabilitation	*1) Full Replacement; 2) Major Rehab.; & 3) Minor Rehab.*
	No. of Assets	*Number of assets in a certain condition states (A, B, C, and D).*
	Total No. of Assets	*Total number of existing assets.*
	RIF	Relative Importance Factor *obtained from surveys among experts.*
	Level of Service (LOS)	*Calculated based on asset condition.*
LCCA	Total Available Budget	*Sum of public and private investments.*
	PPP Payments	*Based on an agreed interest rate, invested amount, and duration.*
	Rehabilitation Budget	*Total available budget minus the payments to private sector.*
	Rehabilitation Cost	*Cost of each rehabilitation actions.*
	User Cost	*Public fees and tolls (assumed to be increased by using PPP).*
	Total Life Cycle Cost	*Sum of rehabilitation cost and payments over strategic period.*
	Infrastructure Backlog	*Budget deficit to bring all critical assets to acceptable condition.*
	Financial Performance	*Function of expected backlog and TLCC [0 – 100].*
Sustainability	Environmental Impact	*Determined based on energy efficiency.*
	Social Impact	*Determined based on user satisfaction.*
	Economical Impact	*Determined based on financial performance.*
	Energy Efficiency	*Based on asset condition and the percent of assets in good condition.*
	User Satisfaction	*The social impact of the infrastructure, based on assets' LOS.*
	Sustainability Performance	*Determined based on environmental, social, and economic impacts.*
Policy	Budget Level	*Percentage of budget allocated to a certain asset category.*
	Pubic Investment	*Rehabilitation budget set by government.*
	Private Investment	*Investment from private sector.*
	PPP Duration	*The duration of private sector investment (e.g., year 1 to 10).*
	Interest Rate	*Annual rate of return or interest for the private investment.*
	No. of Payments	*Number of annual payments to private sector.*
	Sustainability Weights	*Weights for environmental, social, and economical effects.*

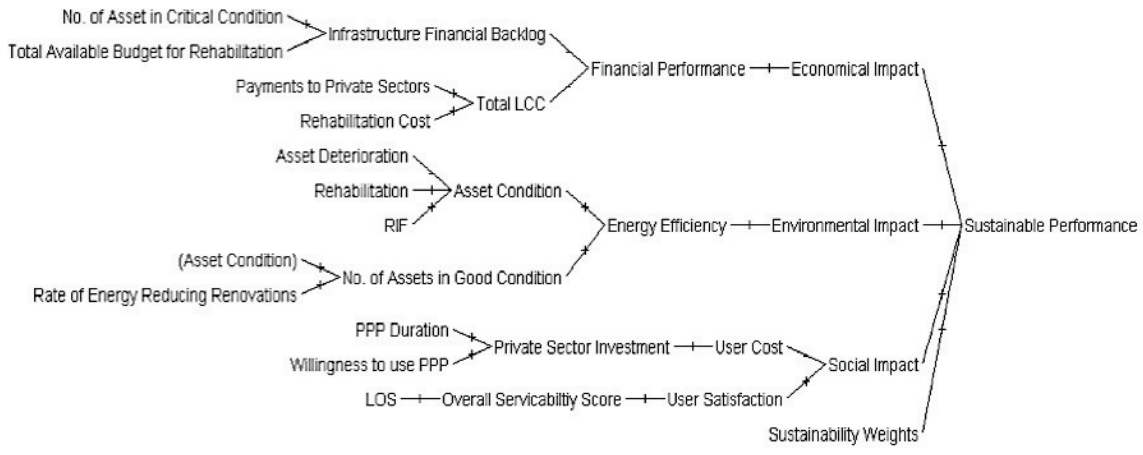

FIGURE 5 A causal trees example associated with the sustainable performance

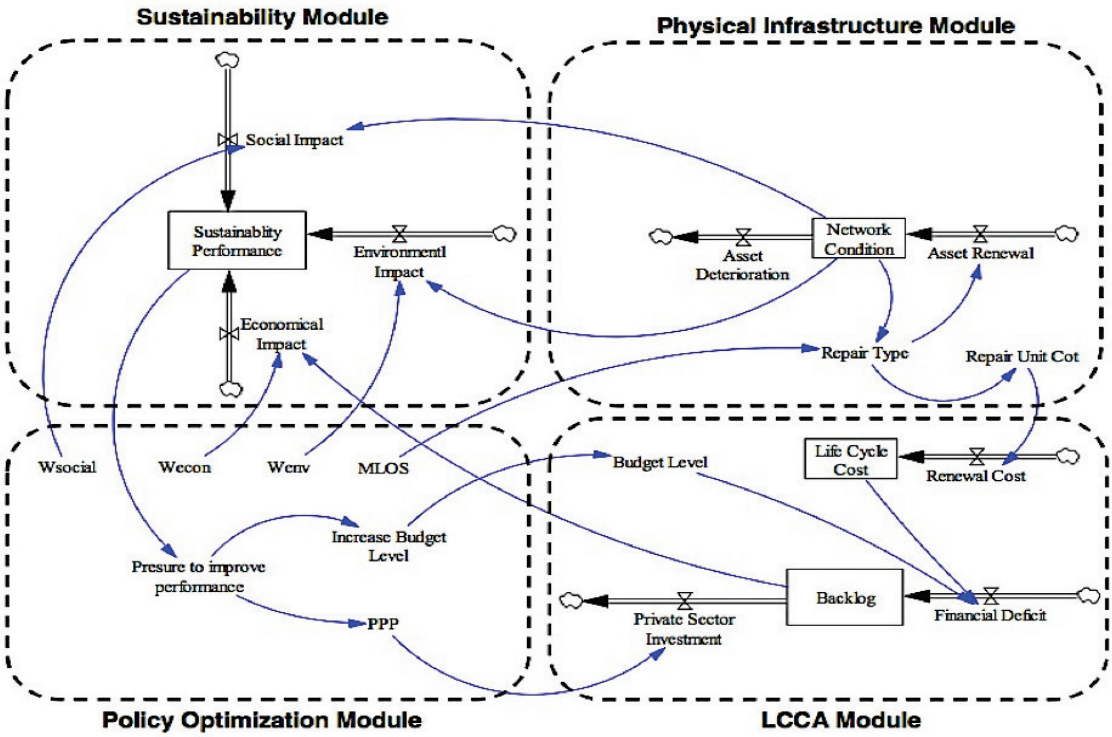

FIGURE 6 Overall structure of the strategic SD model

4. EXPERIMETATION AND RESULTS

The SD model is utilized to conduct experiments by varying different policy-related parameters and examining the SD results of a 50-year simulation. As an example of the possible outcomes of the proposed model, different policy scenarios related to budget distribution have been tested by varying the values of the percentage of total available annual budget which is allocated to different categories of assets based on their condition. Three categories of assets have been identified based on the condition indices associated with different asset components from TDSB. These categories include: assets in good condition or category B, assets in average condition or category C, and asset in critical condition or category D. The percentage of budget allocated to these categories is then represented as $\%B_B$, $\%B_C$, and $\%B_D$, respectively. In this experiments, an annual rehabilitation budget of $5M/year (with no private investment) has been used. Four policy scenarios have been investigated, as shown in Table 2. The first scenario allocates the available rehabilitation budget only to critical assets. The second scenario distributes the available budget equally among the three categories. The third scenario allocates more budget to critical assets, while the fourth scenario allocates more budget to assets in average condition (Category C). Each scenario is a separate experiment with its associated parameter values defined in the SD model, while maintaining the behavior of focus aspects (e.g., The results are shown in Figure 7. Although allocating more budget to rehabilitate critical assets (Scenario1) is a common practice, simulation results revealed that this policy results in the highest backlog, the lowest condition, and the lowest sustainable performance. The second scenario (distributing available budget equally), on the other hand, is the best strategy among the four proposed policies. As shown in Figure 7 the second scenario shows the lowest backlog accumulation, highest overall asset condition amongst the four proposed policy scenarios. As demonstrated by this example, the proposed framework is an effective tool to study the long-term behavior of the system and to avoid misperceptions about the effectiveness of policies such as Scenario 1 in the domain of infrastructure management.

TABLE 2 Budget distribution policy scenarios

Scenario	%Budget Allocated to Category B ($\%B_B$)	%Budget Allocated to Category C ($\%B_C$)	%Budget Allocated to Category D ($\%B_D$)
1) Critical Only	0%	0%	100%
2) Equal Dist.	33.3%	33.3%	33.3%
3) More to D	25%	25%	50%
4) More to C	25%	50%	25%

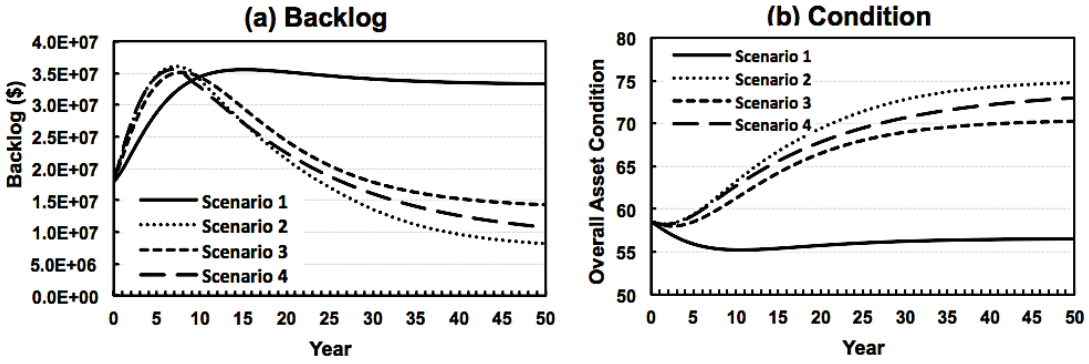

FIGURE 7 Simulation results for different budget distribution polices

5. CONCLUDING REMARKS

This paper presented a novel strategic policy investigation framework for infrastructure rehabilitation and management. The proposed framework utilizes system dynamics simulation techniques as an effective method for policy optimization. The model has four integrated modules for analysing the main interactions among physical infrastructure, life cycle cost, sustainability, and strategic policies of asset managers. The framework proved to be promising in analysing long-term performance of an infrastructure network considering different what-if scenarios. The framework is also capable of demonstrating the dynamics amount different aspects of asset management. Using this model enables asset managers to investigate the effectiveness of their strategic decisions and acquire better understanding of the impacts of strategic decision-making process.

6. REFERENCES

[1] Hudson, W.R., Hass, R., & Uddin, W. (1997). **Infrastructure Management**. McGraw- Hill, New York, USA.

[2] **America's Infrastructure Report Cards**, (ASCE) http://www.infrastructurereportcard.org/ Accessed 2009 – 2013.

[3] World Commission on Environment and Development (1987). **Our Common Future**, Oxford University Press, New York.

[4] Ugwu, O. O., Kumaraswamy, M. M., Wong, A., & Ng, S. T. (2006a). Sustainability appraisal in infrastructure projects (SUSAIP): Part 1. development of indicators and computational methods. **Automation in Construction**, 15(2), 239-251.

[5] Ugwu, O. O., Kumaraswamy, M. M., Wong, A., & Ng, S. T. (2006b). Sustainability appraisal in infrastructure projects (SUSAIP): Part 2: A case study in bridge design. **Automation in Construction**, 15(2), 229-238.

[6] ISI (2011). Draft of the envision assessment system, version 1.0. Institute for Sustainable Infrastructure, http://www.sustainableinfrastructure.org/ Accessed September 14, 2012.

[7] Sanchez, R.M. (1998). Feasibility Evaluation Model for Toll Highway. Ph.D. Dissertation, the University of Texas at Austin, Austin, TX.

[8] PPP Canada 2013. http://www.p3canada.ca/ Accessed January 2013.

[9] Roger, N. (1999). Recent Trends in Private Participation in Infrastructure. Public Policy for the Private Sector, **The World Bank Group**. Private Sector and Infrastructure Network, Note No. 196.

[10] World Bank Group. (1999). The Private Sector in Water Competition and Regulation. **The World Bank Group**, Washington, D.C.

[11] World Bank (2003). http://www.worldbank.org Accessed January 2013.

[12] Sklar, D. (2004). Principles of Asset Management – The Holistic Model. Energy Pulse: **Insight, Analysis and Commentary on the Global Power Industry**.

[13] Mirza, S. (2008). Canada's infrastructure deficit a sad legacy for future generations. special report: the need for alternate revenue, Municipal leader, 32-34.

[14] Evdorides, H., Nyoagbe, C. E., & Burrow, M. P. N. (2012). Strategies to clear road maintenance backlog. **Proceedings of the Institution of Civil Engineers: Municipal Engineer**, 165(4), 205-213.

[15] Australian Asset Management Collaborative Group (AAMCoG) (2012). **Guide to Integrated Strategic Asset Management**, Version 2.0, March 2012.

[16] Levy, S. M. (2008). Public-private partnerships in infrastructure. **Leadership and Management in Engineering**, 8(4), 217-230.

[17] Too, E. G. (2010). A framework for strategic infrastructure asset management, **Engineering Asset Management Review**, 2010, 1, 31-62

[18] Forrester, J. W. (1961) **Industrial Dynamics**. Cambridge: MIT Press; Currently available from Pegasus Communications: Waltham, MA.

[19] Sterman, J. (2000). **Business Dynamics:** Systems Thinking and Modeling for a Complex World. Boston: Irwin/McGraw-Hill.

ANALYSIS OF AIR FLOW PAST AND THROUGH THE 2415-3S AIRFOIL FOR AN UNMANNED AERIAL VEHICLE WITH INTERNAL PROPULSION SYSTEM

L. Velázquez-Araque[1*], Luis. D. Mendoza[1] and J. Nožička[2]

[1] Department of Mechanical Engineering, National University of Táchira, San Cristobal, Venezuela.
luis.velazquez@unet.edu.ve

[2] Department of Mechanical Engineering, Czech Technical University in Prague, Prague, Czech Republic.

ABSTRACT

This paper deals with the prediction of velocity fields on the 2415-3S airfoil which will be used for an unmanned aerial vehicle with internal propulsion system and in this way analyze the air flow through an internal duct of the airfoil using computational fluid dynamics. The main objective is to evaluate the effect of the internal air flow past the airfoil and how this affects the aerodynamic performance by means of lift and drag forces. For this purpose, three different designs of the internal duct were studied; starting from the base 2415-3S airfoil developed in previous investigation, basing on the hypothesis of decreasing the flow separation produced when the propulsive airflow merges the external flow, and in this way obtaining the best configuration. For that purpose, an exhaustive study of the mesh sensitivity was performed. It was used a non-structured mesh since the computational domain is three-dimensional and complex. The selected mesh contains approximately 12.5 million elements. Both the computational domain and the numerical solution were made with commercial CAD and CFD software, respectively. Air, incompressible and steady was analyzed. The boundary conditions are in concordance with experimental setup in the AF 6109 wind tunnel. The k-ε model is utilized to describe the turbulent flow process as followed in references. Results allowed obtaining velocity contours as well as lift and drag coefficients and also the location of separation and reattachment regions in some cases for zero degrees of angle of attack on the internal and external surfaces of the airfoil. Finally, the selection of the configuration with the best aerodynamic performance was made, selecting the option without curved baffles.

INTRODUCTION

According to the evolution of Unmanned Aerial Vehicles (UAV), several investments have been increasing every year, especially in the field of aerodynamic characteristics which can be obtained through wind tunnel tests.

This paper is part of a project which consists in the design of a solar UAV with internal blowing propulsion system; using computational fluid dynamics (CFD) on the 2415-3S airfoil, transport equations are aimed to be solved and also an accurate mesh refinement to obtain three-dimensional velocity fields. The evaluation of the effect of the air flow through and past the airfoil on the aerodynamic behavior is one of the objectives of this paper; this air flow in actual conditions will be generated by a ducted fan located in the fuselage of the UAV. The analysis involved the comparison of two configurations of the internal design of the airfoil: with and without curved baffles. Another important result will be the numerical flow visualization by means of three-dimensional streamlines. The whole process is described in the following sections.

OVERVIEW OF THE ANALYSIS MODEL

The aim of this research is to analyze the behavior of the air flow at the internal cavity of the 2415-3S airfoil and predict possible zones of flow separation at the suction surface of this airfoil. A three-dimensional numerical simulation by using CFD will be performed to obtain velocity fields and also streamlines of the flow.

AIRFOIL TESTED

The 2415-3S airfoil has been designed for the UAV focusing on several parameters of common commercial UAV's manufactures such as total wingspan, weight, flight velocity and others. It comes from a NACA four digits family airfoil, the NACA 2415 (Figure 1). It has an abrupt step on the suction side, located at 30% of the chord from the leading edge. This step simulates the blowing propulsive outlet of the wing in normal flight conditions.

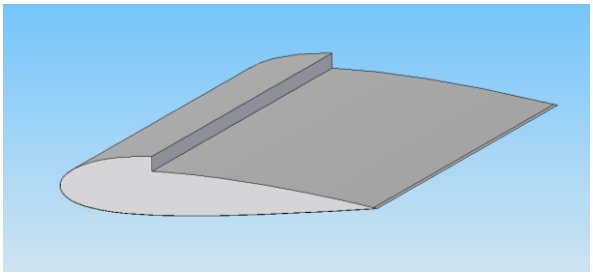

Figure 1. 2415-3S Airfoil

In a previous investigation [1] a two-dimensional numerical solution of the flow field past the 2415-3S was obtained as seen in Figure 2.

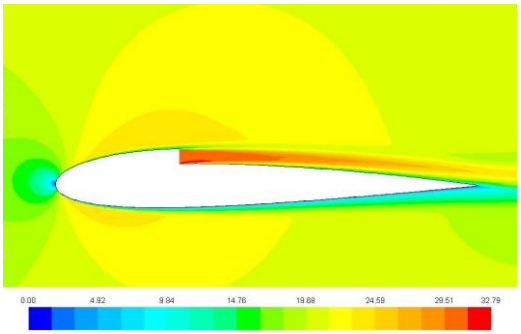

Figure 2. Velocity contours of the 2D numerical simulation of the 2415-3S airfoil at 0° of angle of attack (AOA) [2]

It is possible to observe in Figure 2 the zone of highest velocity just next to the step which simulates the propulsive outlet. No presence of regions with a velocity of 0 m/s besides the stagnation point at the leading edge, therefore no regions of separation were observed. Now the purpose is to validate those results with a three-dimensional numerical simulation and also including the analysis of the flow through the internal cavity of this airfoil because that is how the air will be supplied to the wings in the actual situation. For this purpose, an exhaustive analysis of two configurations of the internal cavity is performed.

Below, it is possible to see two configurations of the airfoil's internal cavity. In Figure 3, a smooth rounded cavity outlet is shown (model A); this shape is intended to smooth the flow that comes from the ducted fan. Then, Figure 4 shows a cavity with a straight outlet (model B); this shape is intended to lead the flow tangential to the airfoil's suction surface.

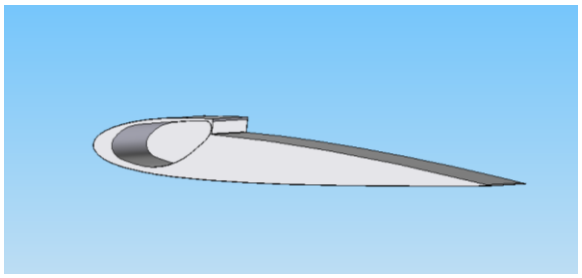

Figure 3. 2415-3S airfoil with a smooth rounded cavity outlet (model A)

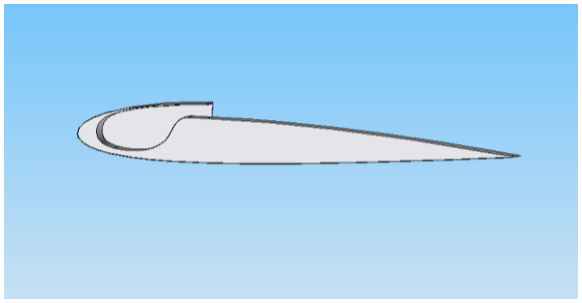

Figure 4. 2415-3S airfoil with a smooth straight cavity outlet (model B)

COMPUTATIONAL DOMAIN

Something very important in this part is the choice of the domain, because it is formed by real borders such as the upper and lower surfaces of the airfoil and also by imaginary borders which enclose the external environment [4]. A virtual wind tunnel was made to enclose the airfoil as seen in Figure 5. The domain extends from 1 chord lengths upstream to 5 chord lengths downstream also 1 chord lengths above and below the airfoil, having a width of 2 chord lengths; these dimensions are based on the actual wind tunnel AF 6109 located at the aerodynamics Laboratory at the University of Tachira.

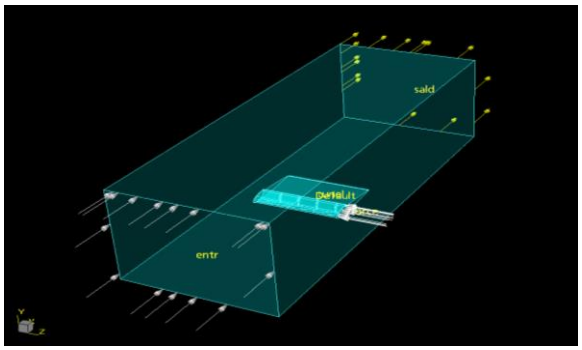

Figure 5: Computational domain for the numerical simulations

DISCRETIZATION OF THE DOMAIN

The geometry shown in Figure 5 is discretized using an unstructured mesh of approximately 12.5 million elements after performing a mesh sensitivity study; this mesh has been also supplemented with very small elements in the vicinity of the surface of the airfoil forming a boundary layer. References when creating the mesh were followed [3]. The domain was created by using *Solid Edge* commercial CAD software and the mesh was created by using *ANSYS CFX* commercial CFD software as seen in Figure 6. Single meshes were created for each internal cavity configuration.

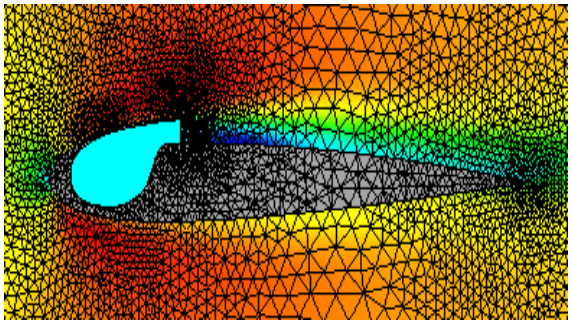

Figure 6: A mesh used for the numerical simulation

The complexity of the 2415-3S airfoil's internal cavity turns the meshing process complex as well since very small volumes or cells are generated and thus increasing the mesh density and then the computing time.

BOUNDARY CONDITIONS

At the inlet of the tunnel, it is specified the air absolute velocity magnitude of 20m/s and also its components; in this case the velocity is parallel to the horizontal axis; therefore it does not have any component in the ordinates. Likewise, at the inlet of the airfoil's internal cavity, air absolute velocity magnitude of 20m/s was set. The upper and lower surfaces of the airfoil are set as walls. At the outlet it is specified the pressure as the atmospheric pressure. For the lateral walls of the domain they are set as symmetry.

TURBULENCE MODEL

The k-ε model is derived from the Navier-Stokes equations and it is one of the simplest complete models of turbulence with two-equation models in which the solution of two separate transport equations allows the turbulent velocity and length scales to be independently determined. The standard k-ε model falls within this class of models and has become very used for practical engineering flow calculations. It is a semi-empirical model. It is robust, economic, and presents reasonable accuracy for a wide range of turbulent flows.

RESULTS AND ANALYSIS

Air at 25ºC, incompressible and stationary is simulated with a Reynolds number of $2x10^5$. In Figures 7 and 8 it is possible to see the air flow behavior at the internal cavity of the 2415-3S airfoil by means of streamlines.

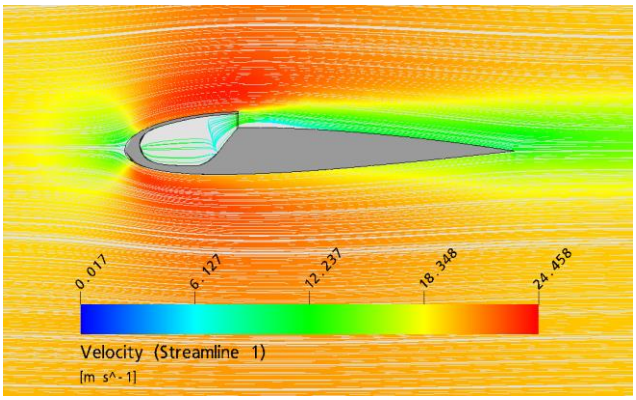

Figure 7. Flow streamlines past model A (rounded cavity outlet)

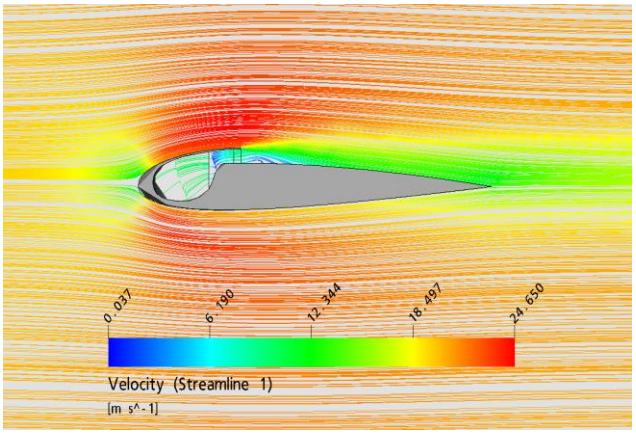

Figure 8. Flow streamlines past model B (straight cavity outlet)

It is possible to observe in Figure 7 that the cavity with a rounded outlet (model A) although it increases the forced air flow inlet area, tends to produce certain separation due to its curvature. Figure 8 shows that the cavity with a straight outlet (model B) produces less separation of flow in a small degree which enhances the airfoil's aerodynamic behavior. Therefore this model was chosen.

Below, Figures 9 and 10 show the velocity field and streamlines along the whole 2415-3S airfoil's suction surface.

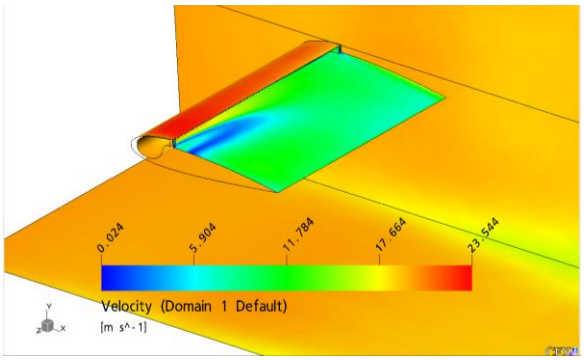

Figure 9. Surface velocity field past the 2415-3S airfoil (model B)

In Figure 9 it is possible to see that the air flow is attached to almost the whole airfoil's suction surface, however there is a zone where the velocity is very close to 0m/s which may indicate that the flow is probably detached and may lead to a separation region.

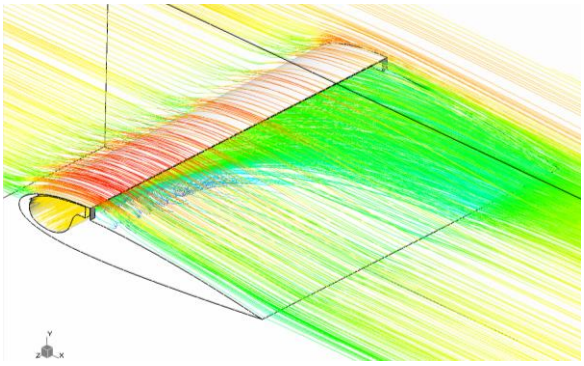

Figure 10. Air flow streamlines past the 2415-3S airfoil (model B)

Air flow streamlines in Figure 10 are now confirming that there is a separation region close to the airfoil's forced air inlet, Inside this region, it is possible to observe that the adverse pressure gradient causes a reversed flow and this becomes into a counter-rotating vortex.

Starting from this model, a baffle was placed inside the internal cavity of model B in order to redirect the forced air flow to minimize the flow separation on the suction surface; in this configuration, the baffle was placed halfway the span leading to model C. It is important to mention that making this new configuration, the meshing process is even more complex increasing the computing time.

Below, Figures 11 and 12 show the velocity field and streamlines along the 2415-3S airfoil's suction surface with the internal baffle.

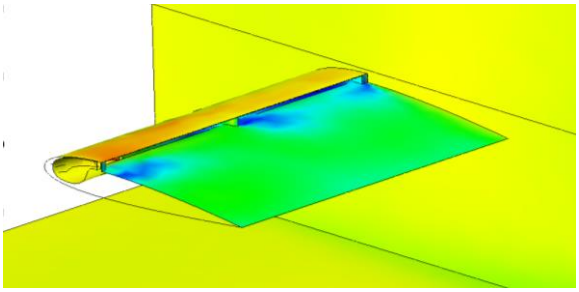

Figure 11. Surface velocity field past the 2415-3S airfoil (model C)

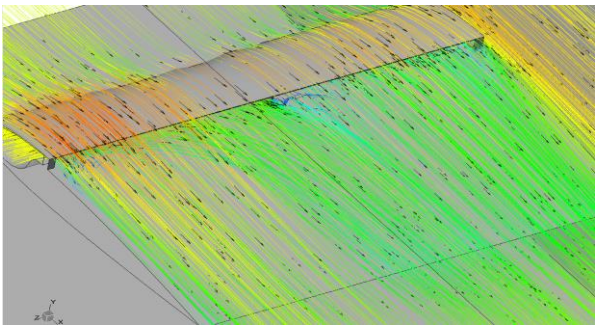

Figure 12. Air flow streamlines past the 2415-3S airfoil (model C)

Figure 11 shows the presence of certain zones of flow separation (deep blue color). Observing Figure 12, it is possible to notice that the internal baffle also generates certain recirculation. The force air flow tends to return due to the pressure drop that the rest of the flow provokes when passing along the baffle at the internal cavity.

In order to develop another feasible solution, model C was modified placing three curved baffles in an equidistant array and smaller than the one used previously leading to model D as seen in Figure 13.

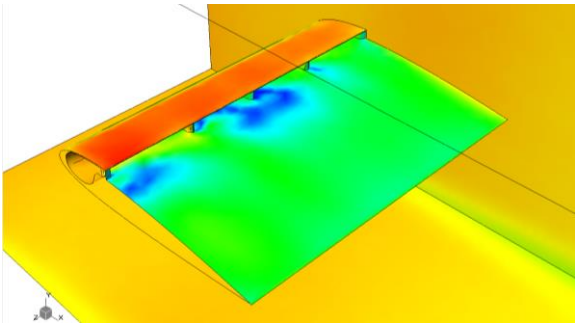

Figure 13: Surface velocity field past the 2415-3S airfoil (model D)

Likewise the previous case, it is possible to observe that placing more baffles within the 2415-3S airfoil's internal cavity, more recirculation and separation regions are obtained. This due to part of the flow that goes to the airfoil's surface tends to return at the outer edge of the baffle because of the pressure drop.

Later, a new internal design is introduced (model E), without curved baffles but modifying the 2415-3S airfoil's internal cavity in such a way to redirect as best as it gets the forced air flow towards the suction surface and minimize the flow separation as shown in Figure 14.

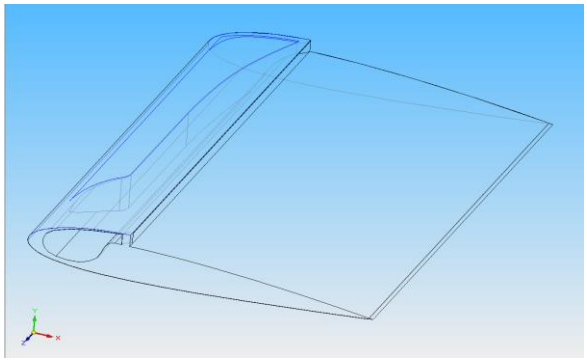

Figure 14. 2415-3S airfoil without internal curved baffles (model E)

In Figure 15 it is possible to see that the locations with the lowest velocity are smaller than the ones obtained with previous models. However it is still present. Therefore model D is the most adapted so far with respect to the other analyzed models because it is clear that this latter modification presents smaller separation regions on the 2415-3S airfoil's suction surface.

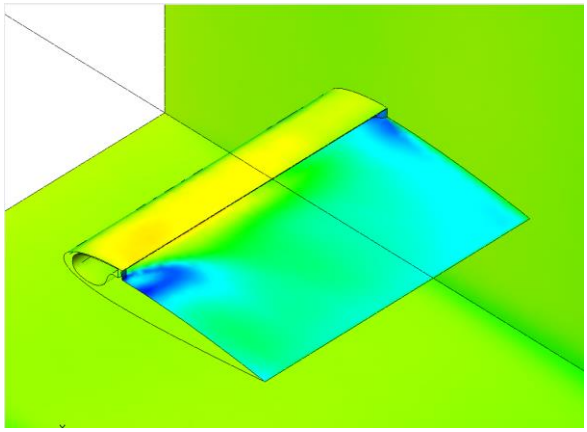

Figure 15. Surface velocity field past the 2415-3S airfoil (model E)

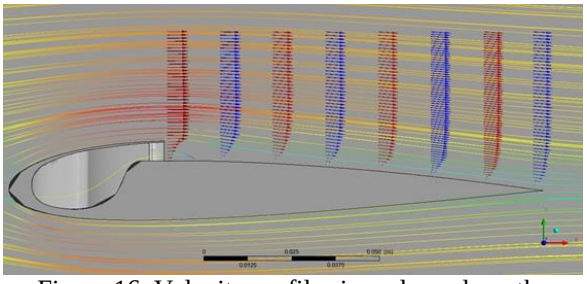

Figure 16. Velocity profiles in a plane along the supper surface (model E).

In Figure 16 it is shown several velocity profiles past the propulsive outlet along the 2415-3S model E airfoil. These profiles are located in a plane at 20 mm from the cavity inlet and spaced 15 mm each other. Almost all of these profiles show a parabolic shape which means no separation of flow.

Figure 17 shows an isometric view of a plane containing several velocity profiles. Notice the first profile which presents some velocity vectors that are not aligned with the airflow direction mainly due to the change of the velocity direction.

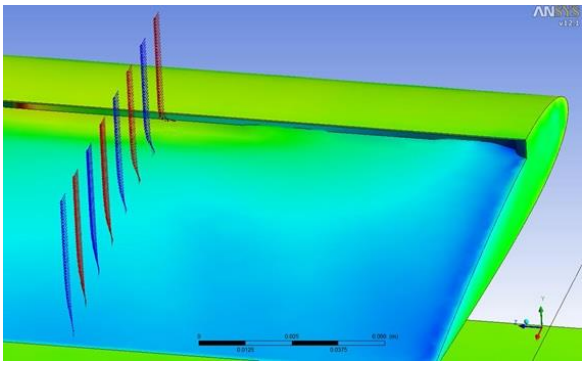

Figure 17. Velocity profiles in a plane along the supper surface (model E).

In Figure 18 it is possible to see three-dimensional streamlines past the propulsive outlet. The external airflow has been hidden for a better view. Although there is a very strong change of the air velocity direction, the flow still remains attached to the upper airfoil surface.

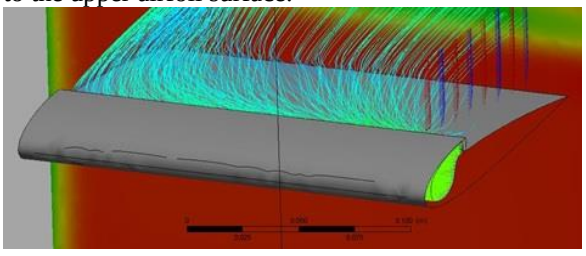

Figure 18. Three-dimensional streamlines past the propulsive flow past model E.

CONCLUSION

By means of the use of computational fluid dynamics it has been possible to obtain the flow field of air past and through the internal cavity of a new designed airfoil, the 2415-3S. It was also possible to obtain the location of separation regions in some cases. Five configurations were analyzed through an exhaustive comparison of the flow field by means of velocity contours and streamlines turning out that the aerodynamic performance of the configuration without internal curved baffles (model E) shows the best aerodynamic performance among the other three proposed configurations.

FUTURE WORK

Since this work is part of the development of the unmanned aerial vehicle with internal propulsion, a lot of work still needs to be done, however concerning airfoils, which was the scope of this work, new questions have been found according to obtained results and several aspects can be investigated focusing on:

- Obtaining numerical aerodynamic coefficients such as lift drag and pitching moment.
- Validation of numerical results by testing experimentally the selected 2415-3S airfoil configuration and study its aerodynamic performance in terms of the flow distribution for efficient propulsion.

REFERENCES

[1] Velazquez-Araque L. (2013): ¨Development of an Airfoil for an Unmanned Aerial Vehicle¨, LAP LAMBERT Academic Publishing ISBN-13: 978-3659332623.

[2] Velazquez-Araque L., Nožička J (2012).: ¨Numerical Analysis of Flow past an Airfoil for a Solar Powered Unmanned Aerial Vehicle with Internal Propulsion System¨, Proceedings of The 23rd International Symposium on Transport Phenomena. Auckland, New Zealand.

[3] Velazquez-Araque L., Nožička J. (2012): ¨Computational Simulation of the Flow past an Airfoil for an Unmanned Aerial Vehicle¨, Proceedings of The 5th International Multi-Conference on Engineering and Technological Innovation: IMETI 2012. Orlando, USA.

[4] Jeandrevina G., Saccoa C., Paolettib C. and Preidikmanc S. "Simulación numérica utilizando CFD de los ensayos en túnel de viento de una pala de generador eólico en condición de operación rotor estático".

LUDIC TEACHING OF STATISTICS AT A HIGHER LEVEL: COMBINATORIAL ANALYSIS CASE

Francisco Casanova del Angel
SEPI of the ESIA, ALM Professional Unit, Polytechnic National Institute. fcasanova@ipn.mx

and

María Elena Rosas Sánchez
ESIA Structures Academy, ALM Professional Unit, Polytechnic National Institute. malenars@ipn.mx

Abstract

This work makes an academic-didactic contribution based on teaching practice at a higher level in engineering schools, with the objective to achieve actual assimilation by students. Learning elements were modified, focusing on development of skills and self-confidence of each student. Learning strategies different from traditional ones were promoted, resulting in the students adapting games. Therefore, the educational environment was improved, and learning was supported through teamwork and a deeper knowledge of the topic.

Keywords: learning, teaching, skills and competence.

1. Introduction

Among the most complex and frequent problems teachers face throughout the teaching-learning process at a higher level is that the student assimilates the behavior of physical phenomena, since comprehension of their basic foundations is difficult, as the relationship between mathematics and mechanical phenomena is not immediate. How could there be a way to relate those concepts in order to lead to significant learning? Which is the best way to relate theory and practice in order to achieve such learning? In order to answer these questions, an objective of this work is to contribute to achieving learning with a different and innovative proposal, through application and adaptation of board games and other didactic contributions. From 2009, when a new educational model entered into effect at the National Polytechnic Institute in Mexico, the index of failing students fluctuated from 50% through 60%, which generated the need to carry out proposals based on features of student population related to factors influencing their school life.

A theory to better understand the significant learning concept is that focused particularly on scientific concepts teaching-learning processes based on students' concepts in daily life, and considers that every learning situation may be studied along two axes: i) learning by the student (significant or by memory), and ii) teaching strategy (guided or autonomous reception and discovery). Students show, individually, stories, comics, poems, acrostics and songs based on specific topics included in the subject. [3]

2. Implementation

For instance, let us see one of the ludic developments of the unit corresponding to combinatorial analysis of the statistics subject. It must be underlined that this is not the only development carried out by students.

From a conceptual point of view, combinatory is a branch of mathematics, belonging to the discrete mathematics area, which studies enumeration, construction and existence of configuration properties satisfying certain established conditions. There is no clear classification of a sub-area, but all of them share certain overlapping degree among them, as well as with other branches of discrete mathematics. In

extremal combinatorics, the approach is to determine how large or small a collection of objects should be in order to satisfy a previously established condition. Combinatorics is about the number of various manners to consider sets based on elements of a given set, respecting certain rules such as order, repetition, and partition.

How did the students develop the topic and application? They read the theory about combinatorial analysis. They looked for a real implementation, well known in daily life, focusing on the history of its development and marketing. They got deeper into its mechanism (disassembling several Rubik's cubes in order to understand it). They studied the algorithms (which were not fully understood at first) and, based on their solutions, they made one, Figure 1.

3. History and mechanism of Rubik's cube

Rubik's cube was invented by sculpture and architecture professor Ernő Rubik in 1974, as a school tool to help his students understand tri-dimensional objects.

A standard cube is 5.7 cm long on every side, Figure 2. The puzzle includes 26 pieces or small cubes. Each piece includes an internal hidden extension interconnected to other cubes, while allowing them to move to different positions; however, the central piece of each of the 6 faces is a single cube, for which reason it stays compact but it may be easily manipulated.

There are 6 central pieces showing a single-colored face, twelve two-colored edge pieces and eight three-colored vertex pieces. The relative position of such cubes regarding the others may be altered turning the cube 90°, 180° or 270°, but the relative position of the color of the sides regarding the other pieces may not be changed: it is determined by the relative position of the central cubes.

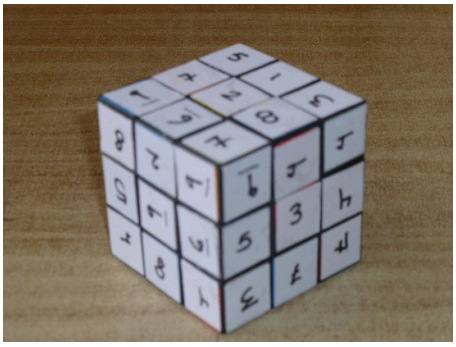

Figure 1. Rubik's cube made by students

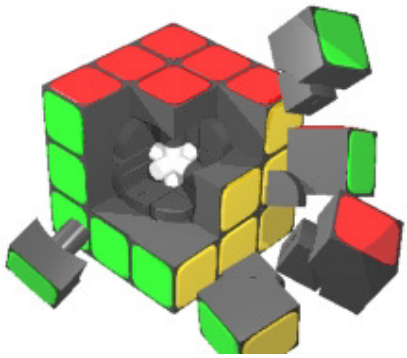

Figure 2. Rubik's cube mechanism

3.1. Algorithms

In terms of Rubik's cube fans, a memorized sequence of movements with a desired effect on the cube is called algorithm. Such terminology is derived from the mathematical use of *algorithm,* a preset of well-defined, ordered and finite instructions or rules which allow to carry out an activity through successive steps. Every method to solve the cube uses its own set of algorithms, which may be used to get the cube closer to be solved. The original Rubik's cube had no marks on the central faces and, therefore, solving it did not require to properly orient such central faces. Theoretically, a cube may be solved even with the central pieces rotated, but solving this adds a challenge. To mark the central parts of a Rubik's cube increases difficulty, as the set of possible distinguishable configurations is expanded. There are $4^6/2$ (2 048) ways to orient the central

parts, since parity of vertices implies an even number of simple movements of such.

3.2. Solving and Notation

Many fans of Rubik's cube use a notation developed by David Singmaster to write a sequence of movements: the "Singmaster notation". Its relative nature allows algorithms to be written in a way that such may be applied regardless of which side is appointed as higher or how colors are organized in a given cube.

- *F* (front): the side in front of the person
- *B* (back): the side opposite to the front
- *U* (up): the side on top or on the higher part of the front side
- *D* (down): the side opposite to the higher part, under the cube
- *L* (left): the side directly to the left of the front
- *R* (right): the side directly to the right of the front
- *f* (two front layers): the side in front of the person and the corresponding middle layer
- *b* (two back layers): the side opposite to the front and the corresponding middle layer
- *u* (two layers upward): the higher side and the corresponding middle layer
- *d* (two layers downward): the lower side and the corresponding middle layer
- *l* (two left layers): the side to the left of the front and the corresponding middle layer
- *r* (two right layers): the side to the right of the front and the corresponding middle layer
- *x* (rotate): rotate the whole cube on *R*
- *y* (rotate): rotate the whole cube on *U*
- *z* (rotate): rotate the whole cube on *F*

There exists the custom to solve a Rubik's cube within the less time possible. There is a series of speed-cubing competitions in the world.

4. Discussion of Results

Works shown prove that, with the knowledge to work in teams, individual results are potentialized and enhanced. Negative experiences are deeply rooted in most students, who feel their capacity to be minimized when working in teams. With due instruction and practice, any person may overcome his/her difficulties to be part of a team.

Collaborative educational experience in the classroom, described above, is a good practice, as it is based on the principles to promote good relations among students, as well as between the student and the teacher, thus developing reciprocity and cooperation. Activities were used to invite to build knowledge, permanent feedback was provided, and time was devoted to the corresponding task. Diversity and various ways to work among students were respected. Here, the role of the teacher is crucial, since he/she is the main promoter of the work.

This development of skills, due to its complexity and importance, allows three command levels. First, it is the responsibility of people in the team to carry out tasks, comply with the terms and consider that common objectives are of first priority regarding individual objectives. Second, it assumes more participation and involvement for the team's efficiency, not only participating formally in demanded tasks, but also being interested on good understanding and harmony among the team members, collaborating in order that members may learn and value each other. Leadership of the team requires to organize, to show initiative to move others and positively influence them, these being the third level of competence's command. In order to know and assess learning and progress along these three levels, we must focus on these markers: task carried out, participation, organization and social

value granted to the task carried out with others. [4]

The innovating process developed was related to solving a problem, this being understood as a situation making difficult to obtain something, for which reason it was necessary to find the means to allow us solving it. This was significant in order to know, structure and characterize the problem, as well as identifying required strategies. Board games were made, stories and comics were created, and this became collective knowledge, which was applied to improve educational processes, helping the student to understand fundamentals of structures. [5]

5. Conclusions

Among results obtained throughout the development of educational research herein presented, the following stand out:

- Most participants considered that the innovation process was motivating, which demonstrates that the impact of innovation in the teaching-learning process is relevant and support educational processes.
- With the new educational models implemented in the Mexican educational system, to prepare new strategies contributing to achieve institutional goals for education at a higher level became necessary. This new activity enhanced learning of students, since their work could be achieved in team and new skills to understand fundamentals of the subject were developed.
- The role of the teacher changes when he/she becomes promoter and provider of learning, since he/she develops new methods, techniques and activities to promote building knowledge among the students, as well as linking contents taught with personal and social experiences.

Acknowledgments

This article and its didactic research were developed with part of the time of Research Projects IPN-SIP 20130805 and 20141056.

Bibliography

[1] **Programa de Desarrollo Institucional**. (**2001**). Instituto Politécnico Nacional. México.

[2] **Instituto Politécnico Nacional**. (**2002**). *Un nuevo modelo educativo para el IPN*. México.

[3] **Rosas Sánchez, M. E**. (**2010**). Contribución académica a la licenciatura en ingeniería civil. XVIII Congreso Nacional de Ingeniería Estructural. (2010). León, Guanajuato. México.

[4] **Villa, A y Poblete, M**. (**2007**). *Aprendizaje basado en competencias, una propuesta para la evaluación de las competencias genéricas.* Bilbao. Ediciones Mensajero.

[5] **Fuentes Agustí, Marta**. (**2001**). Naufragar en Internet. Ed. Virtual Educa. México

A Case Study Design of Border Gateway Routing Protocol Using Simulation Technologies

Chengcheng Li
School of Information Technology
University of Cincinnati
Cincinnati, OH 45221
Chengcheng.li@uc.edu

ABSTRACT

This paper presents a case study that is designed to teach students hands-on experience on designing and implementing Border Gateway Protocol (BGP). This case study was used as a final project in a senior level computer networking class to evaluate students' understanding of key networking concepts and proficiency of configuring and implementing a wide range of network technologies. Through doing the BGP project, students reviewed and learned other foundational networking topics other than BGP, including Interior Gateway routing Protocols (IGPs), IPv6, switching, load balancing, policy based routing, and access control. Students had the chance to explore the rich features of BGP attributes to manipulate routes between the autonomous systems in a network simulation lab environment. This BGP case study comprehensively review the key knowledge unites of the networking class and can be used as an assessment tool evaluating students' understanding and overall performance.

Keywords: Network Modeling, Simulation, Emulation, Virtualization, BGP

1. INTRODUCTION

BGP is the dominating Exterior Gateway Protocol used today. It is exclusively developed for routing data traffic on the Internet and has been used to build the backbone networks of the Internet Service Providers (ISP). BGP is currently in the fourth version since its release in 2005. The design of BGP is significantly different from that of the IGPs, such as RIP, EIGRP, OSPF, and ISIS which are usually briefly discussed in college level networking classes. BGP are able to advertise networks without having an active interface in these networks. In other words, BGP routers are capable of advertising a huge amount of routing information to their peers or neighbors without having the reachability of these networks verified. In fact, the BGP routing table can contain tens of thousands of routes as the number of routes on the Internet has been grown exponentially over the years, especially after IPv6 has been adopted. BGP routers on the boundaries of the ISP networks propagate all the routes in their BGP table to the BGP peers, generating huge network traffic and demanding large computing and storage resources. Therefore, BGP needs to be enabled with care. With limited knowledge of BGP, inexperienced system administrators may redistribute the BGP or the Internet routes into enterprise networks. Doing so can quickly bring down the entire network, because many routers do not have the sufficient storage or processing capacity for the huge amount of BGP routing information traffic, causing devastating network outage. And it is usually unnecessary for all the routers to learn all the routes on the Internet except for the gateway or autonomous boundary routers. BGP is not enabled on an enterprise network unless this network is in a mulithoming or transit autonomous system (AS), in which there are more than one exits to the ISPs for load balancing and fault tolerance. For most small and mid-sized

enterprise networks, BGP is not needed. However, BGP is the only routing protocol that provides loop-free interdomain routing between AS's. Mastering BGP concepts and configuration process is a must have skill for network engineers working for the ISPs.

BGP is a path vector protocol with a routing algorithm similar to that of distance vector protocols. But the convergence time of BGP may take from seconds to hours because there are constant large amount of route changes on the Internet, and we certainly don't want the Internet, triggered by all these changes, to be updated very frequently. Otherwise, the internet will be very unstable and the network bandwidth will be wasted on exchanging unnecessary routing information. BGP uses a rich set of parameters to manipulate the route attributes and therefore prioritizes certain routes over the others. The network engineers have a full control over choosing the optimal routes for data traffic. However, obtaining proficiency of configuring these attributes needs practice and comprehensive understanding of BGP processes and concepts. The field engineers may need to take several courses in BGP before actually having a hands-on on the production ISP networks.

2. CASE STUDY DESIGN

BGP is introduced in many networking classes, but seldom is discussed in detail due to its complexity. Additional on-the-job training is usually required for the system engineers and administrators before they work for the ISPs. It is considered a difficult task to simulate the internet traffic in a lab environment. BGPlay provides a web interface to demonstrate real time BGP traffic between AS's on the Internet [1]. But the configuration functionality is not provided. There are BGP simulation and modeling tools based on NS-2 (Network Simulator) [2][3], supported by an NSF grant. Both ns-BGP and BGP++ provide BGP extensions to NS-2 for BGP traffic simulation [4][5]. However, these NS-2 extensions have a steep learning curve and require programming and scripting skills that many IT students don't have.

An open source network simulation and modeling toolkit was introduced in the author's previous research that incorporates lab activates that covers a wide range of network concepts from routing, switching, security, IT services, QoS, VoIP, multicasting, IPv6, to IT infrastructure design and implementation. A BGP project was designed as the final project for a senior network class. And it's completely implemented by using the tools that are installed either one students' personal laptops or a cloud lab hosted on our "Sandboxes" supported by Vmware vSphere.

Diagram 1 shows four routers representing AS2000, an enterprise network, and AS 1000, an ISP network. AS2000 uses the proprietary EIGRP routing protocol as its IGP. AS1000 uses OSPF, a hierarchical IGP commonly used by ISPs. More than one physical links between the routers are used to provide load balancing and redundancy. This lab sets up a multihoming topology with more than one exits of the enterprise network facing the ISP. Students are required to configure the network from both the enterprise and the ISP's engineers' perspectives to implement correct routing policies and route traffics through the desired routing paths.

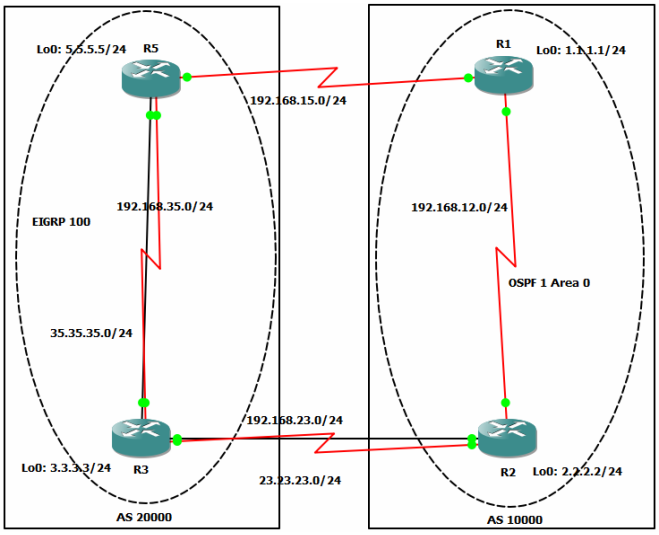

Diagram 1. Network Topology of BGP Case Study

The network concepts and individual steps of the project were discussed during the class lectures accompanying with instructor lab demonstrations. Students are required to examine the default behaviors of BGP and write them into a report with the screenshots and explanations of the routing and BGP tables. There are two routes for R5 to reach 192.168.12.0/24, the network inside the AS1000, one through R1 and the other through R3. By default, R5 uses R1 to reach 192.168.12.0/24 because the routes learned from R1- an eBGP neighbor is preferred to R3 – an iBGP neighbor when other attributes of these two routes remain the same. Based on the project requirements, students working as the system administrator of the ISP, need to change the BGP attribute of 192.168.12.0/24 on R1 so that R5 prefers R3 to get there. And then the students need to work as the system administrator of AS2000, the enterprise network, and change the route attributes three times only on R5 to change the route preferences between R3 and R1. The final report would include the configuration process and detailed descriptions of BGP attributes that were modified. The correctness of the project implementation can be conveniently verified through examining the BGP and routing tables. Diagram 2. is a screenshot extracted from a sample student report. The highlighted fields show that this student correctly modified the default attributes multiple times for R5 to take R1 or R3 as the next hop to reach 192.168.12.0/24 network.

The network concepts that this project covers in an upper computer networking class is summarized in Table 1.

Network Concepts	Implementation
IP Scheme Design	Design the IP networks for efficient use of given IP space.
IGP Implementation	Configure EIGRP, OSPF areas, and load balancing; use virtual interfaces as routing sources for better stability of routing updates
eBGP	Provide TCP connections for BGP peers; modify the multi-hop behavior
iBGP	Use virtual interface for routing sources; use the next-hop-self on the AS boundary routers to provide a routable address for the iBGP peers
Propagate Routes through BGP	Advertise and verify BGP routes
Traffic Identification and Isolation	Create access control lists to identify data traffics and apply them to the inbound or outbound directions of the correct interfaces
Policy Based Routing	Create route policies based on the lab requirements for BGP route manipulation. The attributes that are used in this project include but not limited to weight, route origin, multi-exit discriminator, and AS path

Table 1. Network Concepts and Skills Covered by the BGP Case Study

Network	Next Hop	Metric	LocPrf	Weight	Path
r> 1.1.1.0/24	1.1.1.1			0	10000 i
*> 2.2.2.0/24	1.1.1.1	65		0	10000 i
*> 3.3.3.0/24	35.35.35.3	409600		32768	i
r>i5.5.5.0/24	3.3.3.3	409600	100	0	i
*> 35.35.35.0/24	0.0.0.0	0		32768	i
* i	3.3.3.3	0	100	0	i
* 192.168.12.0	1.1.1.1	500	300	0	10000 10000 10000 10000 i
*>i	3.3.3.3	0	100	255	10000 i

Diagram 2. The BGP Table from a Sample Student Submission

3. FINDINGS AND DISCUSSIONS

Based on the end-of-semester survey, the majority of the students claimed that the project is very challenging but also a great learning experience to comprehensively review the networking concepts learned through the semester. Instructor lab demonstration and in-class hands-on teaching are critical components for some of them finally complete the project. Two third of the class find the lab environment is easy to set up and stable to use. They also appreciate the online lab as a backup option, supported by the university's VMware vSphere cloud infrastructure. The average time for the students to complete the project is between 12 to 16 hours which is the appropriate workload for the grade weight assigned to the project. The project can be easily extended to cover other advanced topics in computer networking based on the needs from different concentrations of IT curricula. A design of an advanced project is provided below.

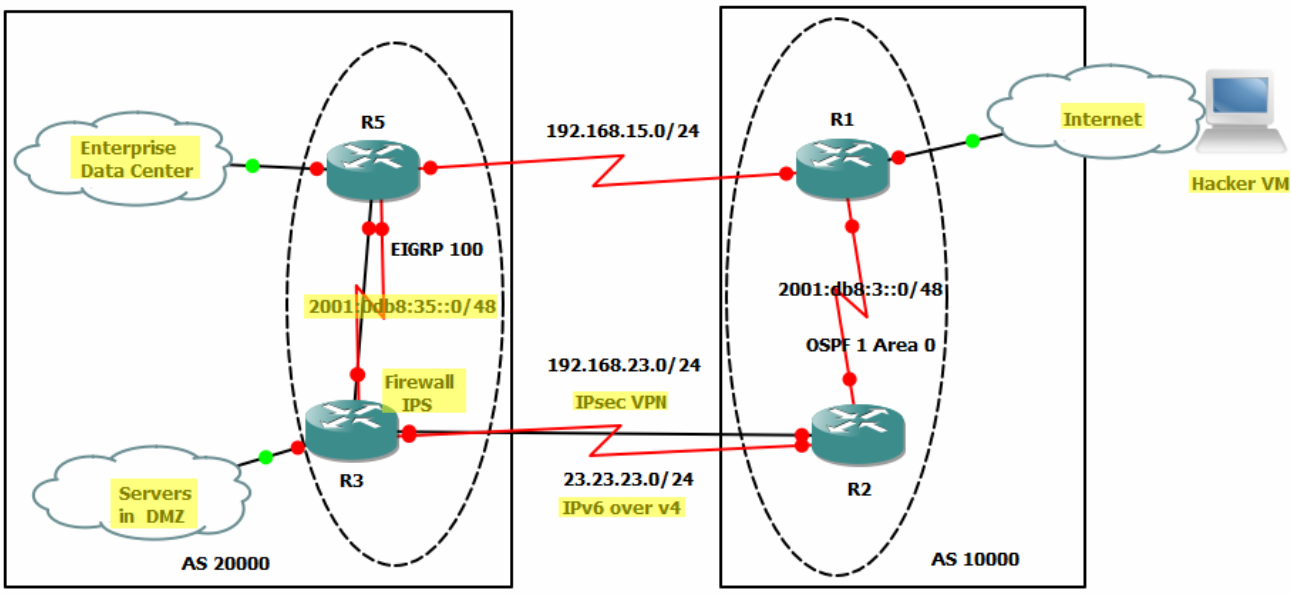

Diagram 3. Extended Project Design to Cover IPv6, Cybersecurity, and Server Virtualization

In the extended project design, dual stack of IP protocols needs to be implemented to route both IPv4 and IPv6 traffics. BGP configuration also needs to be modified to support IPv6. R3 is redesigned to provide firewall, IPS, and VPN services for secure connections to the resources in the enterprise network. An IPsec VPN tunnel can be constructed between R3 and R2. VirtualBox Linux virtual machines will be installed and connected to R3 and R5 to simulate the servers and datacenters that should be isolated and protected by the firewall. Another virtual machine connected behind R1 will simulate hacking activities to test the IPS and Firewall on R3.

4. CONCLUSIONS

This paper summarizes the design and implementation of a BGP case study project used in a senior computer networking class for the students to have a comprehensive review of key networking concepts, especially in Policy Based Routing on BGP route optimization which is usually neglected in IT curricula due to the complexity of the protocol and the difficulty of simulating the BGP process in a lab environment. The BGP project can be implemented on the students' personal laptop computers with a set of open source network emulation and simulation tools. Students find the project is challenging and relative to their learning goals. The lab setup and material can be easily adopted by other IT curricula. The contents and objectives of this project can be extended to cover many networking concepts, providing students valuable hands-on experience that is required by IT employers.

5. ACKNOWLEDGEMENT

This research is based upon work supported by the National Science Foundation Grant No. 0837722.

6. REFERENCES

[1] Cortese, P.F.; Di Battista, G.; Moneta, A.; Patrignani, M.; Pizzonia, M., "Topographic Visualization of Prefix Propagation in the Internet," IEEE Transactions on Visualization and Computer Graphics, vol.12, no.5, pp.725-732, Sept.-Oct. 2006

[2] Qun, Z.A.; Wang Jun, "Application of NS2 in Education of Computer Networks," International Conference on Advanced Computer Theory and Engineering, 2008. ICACTE '08, pp.368-372, 20-22 Dec. 2008

[3] Rahimi, M.J.; Parveen, S.; Morshed, M.; Khan, M.R.; Sarker, P., "Development of the smart QoS

monitors to enhance the performance of the NS2 Network Simulator," 2010 13th International Conference on Computer and Information Technology (ICCIT), pp.137-141, 23-25 Dec. 2010

[4] Gill, R.; Paul, R.; Trajkovic, L., "Effect of MRAI timers and routing policies on BGP convergence times," 2012 IEEE 31st International Performance Computing and Communications Conference (IPCCC), pp.314-323, 1-3 Dec. 2012

[5] Raghavan, V.; Riley, G.; Jaafar, T., "Realistic Topology Modeling for the Internet BGP Infrastructure," IEEE International Symposium on Modeling, Analysis and Simulation of Computers and Telecommunication Systems, 2008. MASCOTS 2008, pp.1-8, 8-10 Sept. 2008

Teaching string processing by using XML

László MENYHÁRT
Department of Media & Educational Informatics, Eötvös Loránd University
Budapest, 1117, Hungary

ABSTRACT

In my opinion there are real, practical problems which are very important in teaching. I propose that we use XML to teach string processing. In this article I present my approach and a suggested curriculum. I tested my own framework implemented in Lazarus IDE with two groups at ELTE. I gave some XML processing problems to my students with which they solved string processing function. I carried out an assessment, which is also analyzed here. I found that students enjoyed more these practical problems than fictive theoretical problems of the previous years' courses.

Keywords: Teaching, string processing, XML.

1. INTRODUCTION

The subject of my PhD is XML. I am teaching at the Eötvös Loránd Science University (ELTE) where I had some courses about string processing, because at ELTE we use similar curriculum to the mentioned one in [7]. I found that the base algorithms are not too interesting for the students. These theoretical problems come from the course's book [5]. That is why I tried to create some new practices. I selected the topic from the area of XML. The SAX parsing is a simple sequential string processing method which is used to present the importance of this course. This common problem is solved by a lot of implementation or we can create a simplistic application, too.
I worked out a curriculum which is presented here, and I had a chance to test it in two groups where the students filled out a questionnaire. There was no control group who learned the same without XML. I compared their productivity and their impressions with the previous years' courses. Their feedbacks prove that students enjoyed more the practical problems than the theoretical, separate, simple tasks. This article and its appendices are available on the [1] URL.

2. CURRICULUM

I created a new topic for this course with practices based on my idea. Now I present lesson plans for two 90 minute lessons, and the hand-out which is useful for teachers and students as well.

Two lessons plan

First lesson

- Introduction (Booting and filling the first part of the questionnaire) – 5 minutes
- XML review – 15 minutes
  - HTML. What is difference between HTML and XML? What does it do? Why do we use it?
  - String file: readability, processability, …
  - Well-formed
    - Now we expect another restriction, because in this way we can handle it more easily: "Very well"-formed
- Processing XML – 10 minutes
  - DOM
    - tree data-structure
  - SAX (in more detail)
    - startDocument, endDocument, startElement, endElement, findCharacters others unmanaged events
- Reviewing SAX_template – 15 minutes
  - Downloading and unzipping
  - Running SAX_example
  - Reviewing surface, types, variables and functions of SAX_template
- Practice 1 – 25 minutes
  - Implementation of SAX parsing
    - Designing of "event-functions": How can we create a table?
    - Coding into the SAX_template
- Practice 2 – 20 minutes
  - Implementation of getAttributeValue
    - Theorem of Linear searching
    - Coding into the SAX_template
- Homework
  - Continue and finish the code

Second lesson

- Introduction (Booting and review of the previous lesson) – 5 minutes
- Practice 3/a. – 20 minutes
  - Design 'parseXML' function
- Practice 4/a. – 20 minutes
  - Design co-procedures and helpers
- Practice 4/b. – 20 minutes

  - Implementation of co-procedures with coding into the SAX_template
- Practice 3/b. – 22 minutes
  - Implementation of parseXML with coding into the SAX_template
- Fill the second part of the questionnaire – 3 minutes
- Homework
  1. Continue and finish the code!
  2. Rewrite SAX_handler to generate a "list" instead of a "table".
  3. Implement readCDATASection
  4. How can we generalize the parseXML procedure? Modify it for every (not only very-well formed) XML file!

Regarding another idea the order is changed. On the first coding lesson students implement the functions based on the given algorithms and only on the second lesson can they understand the motivation (read XML processing).
So we introduced the class with XML and SAX processing. Students implemented their own application into the framework.

XML and its processing

XML is a well-known technology [2]. That is why I do not write about it in this article. It is processed by DOM (Document Object Model) as a tree-structure [3] or with SAX (Simple API for XML) [4]. The second philosophy looks at the XML document as a sequential text file. This part is available more detailed in [1].

SAX_template

I created an application with GUI in Lazarus IDE because it was defined on this course, so it is given. This complete application was emptied to a template into which students had to code only the main parts. So it was prepared for the students. Delphi can be a good choice for developing GUI application, but then this template's code must be converted to Delphi's special language.

Download

The first reference [1] contains all required matters for the testing.

3. FRAMEWORK

Important files

- unit1.pas: Main program to be displayed. Do not modify!
- saxunit.pas: It contains the general parsing procedure and the co-functions.
- SAX_handler.inc: It contains the event-functions

Users view

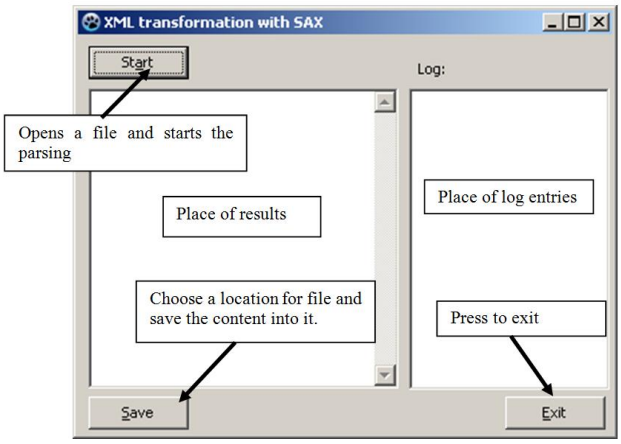

Figure 1: View of the template application

Types

We defined a new type for storing the name and value of the attribute.

```
TAttribute=Record
  name:String;
  value: String;
end;
```

An element can have more attributes, so we store them in an array.

```
TAttributeArray=Array(1..100:TAttribute)
```

We handle the count field to use the array as a list.

```
TAttributeList= Record
  count:integer;
  item:TAttributeArray;
end;
```

Variables

The main variables in the SAX class are the generated text, the log and the text file which has XML content.

```
parsedStr,log:String;
f_xml:TextFile;
```

Co-variables

We need some other variables to read forward a character or to collect the characters.

```
ch:Character;
s1,s:String;
```

We manage the name and value of attributes detached and in a list, too.

```
ename,value: String;
att_list:TAttributeList;
```

We must find the position of "=" (the equal sign) character.

```
p: integer;
```

We will use a variable for the loop.

```
i: integer;
```

Notify the end of the tag or node.

```
endoftag,endofnode:Boolean;
```

Procedures and functions

We need getter/setter functions to reach the main variables.

```
setString(fs: String);
setLog(fs: String);
getString: String;
getLog: String;
```

We want to append strings to the main variables.

```
addString(fs: String);
addLog(fs: String);
```

The next procedure makes the general XML processing.

```
parseXML(fname: String);
```

The previous procedure needs the following co-functions.

```
readForwardACharacter: String;
readToLess: String;
readToGreater: String;
readAWord(endoftag:   Boolean;endofnode:
Boolean): String;
readCDATASection: String;
readAttributesTo(att_list:TAttributeList
; endofnode: Boolean);
```

The next 5 procedure will be overwritten as event-functions. These are in SAX_handler.inc file.

```
startDocument;
endDocument;
startElement(ename:
String;attr_list:TAttributeList);
endElement(ename: String);
findCharacters(value: String);
```

The following is a co-function for parsing the attributes in the opening tag.

```
getAttributeValue(attr_list:TAttributeLi
st;aname: String): String;
```

The implemented algorithms are available in [1]. Students got only the frame of these functions. The task was creating the bodies of every function.

4. OPINIONS AND QUESTIONNAIRE ANALYSIS

I established two groups at ELTE, both of which had two lessons. The students were on a minor BSc informatics teaching course. This course is for students who will be teachers. Their informatics subject will be the second one beside the main subject. The name of the course is "Programming Fundamentals (M1,M2)" [6].

The first group was the control group, which did not get the hand-out [1]. The second group received it. Independently from this I think the second group was more active and more inquisitive. The first group was not able to answer the question: "Which tags must be written to define a table in HTML?". The answer would have been: table, tr, and td. Their knowledge of HTML is too high and they felt the question is too simple. Or they were not so active and they hated the new teacher, with new methodologies.

In the first year I tried to use these methods on one lesson for two groups but at that time we did not have enough time to implement the algorithms. We have time only for discussion of the algorithms (3/a, 4/a) without implementing the functions (4/b, 3/b) in the first group. These identifiers refer to the lesson plan practices. (see Chapter 2.) Within the second group there were teams of 2-3 people, each team was coding functions but they were unable to run the complete application. Every team implemented one function isolated from others. Students were more efficient with this "mini project" methodology.

This has been confirmed by the results of the questionnaire. My colleagues and I recorded the minutes at the checkpoints during the lessons and the timing was kept. Based on these findings I recommend two lessons for this topic.

I asked the students to fill out the following questionnaire. It contained three parts. The first part of the questionnaire was filled at the beginning of the lesson. Part one is designed for self-analysis of student's knowledge of the topics

1. Your result of "Web-development 1." (if no mark, leave blank)
2. Knowledge of HTML (according to you)
3. Knowledge of XML before the lesson
4. Knowledge of XML parsing before the lesson
5. Knowledge of Pascal programming language
6. Knowledge of Lazarus IDE

"Web-development 1." is an optional subject in the first semester on the topic of HTML knowledge. The answers could be these:

1. insufficient; not …
2. sufficient
3. medium; pass for …
4. good
5. excellent; very …

The second part of the questionnaire was filled at the end of the second lesson. Questions were these:

1. Attention level during the lessons
2. Knowledge level at the end of the lesson. (How do you feel?)
3. How do you rate this topic?
4. How do you rate the order of the lessons?
5. How do you rate the teacher's knowledge?
6. How do you rate the teacher's presentation style?
7. Rate the template application's ease of appearance
8. Rate the template application's ease of usability
9. Rate the template application's ease of implementation
10. Rate the ease of implementation of SAX parsing (create "event-functions")
11. Rate the ease of implementation of getAttributeValue (linear searching theorem)
12. Rate the ease of implementation of parseXML (complex task, requiring more thinking / thought-provoking)
13. Rate the ease of implementation of co-functions (easier, "more precisely" task)

The answers should be the same as the previous ones.

Finally the third part of the questionnaire contained two questions that could be answered in free text.

1. What did you like on the lesson?
2. What did you NOT like on the lesson?

The result file (5_results_hu.xlsx) is attached into the [1]. I present here my conclusions:

- Their knowledge of HTML is medium (3)
- They had no XML knowledge (1.175)
- Pascal programming language is known moderately (2.8)
- Lazarus IDE knowledge is low (1.85)
- Their attention was held well (3.8)
- They learned something (2.5)
- About the lesson
  - The topic is good (4,05)
  - The order of the lesson is good (3.9)
  - The teacher's knowledge was good (4.65)
  - The teacher's presentation style was good (4.15)
  - These questions were rated well by the second group (0.7). They could work from the hand-out. It worked!
- The template application is good (4.01). It was preferred by the second group, too.
- The rating of SAX parsing was better by 0.5 in the second group (3.3).
- The implementation of getAttributeValue was medium (3.05). They did not know the linear searching algorithm. If they had, it would have been only a coding exercise.
- The last two exercises were rated not so good (3). We could only review these on the first lesson and one week later it was forgotten.
- So we can see that medium HTML knowledge is enough for understanding XML and performing transformations to HTML.

I regret that – but unfortunately – I forgot to take a vote about the next question: "Do you think this course should be included in the next semester or not? (Y/N)"

Here I would like to share some answers from the free texts.

Answers to the first question:

1. "Practical tasks"
2. "The basic idea of the HTML transformer"
3. "The topic itself."
4. "Acquisition of new knowledge"
5. "The application was very funny and 'cute'!"
6. "I learned more interesting new things, which will be useful."
7. "At last we learned meaningful things on an example which can be used in life!"

Answers from students to the second question:

1. "Unfortunately I was late 40 minutes"
2. "There was a lot of background information so not everything could be understood."
3. "The speed. I was not prepared to use other applications and there were some problems with my Linux. (She had her own laptop and she did not use the computer in the lab.)"
4. "It required a bit too much complex knowledge. The framework program was more complex as well. The development required even more knowledge. But at least it was interesting. More like this!"
5. "It was a bit fast, but I was awfully tired. Maybe this was the problem. :)"

These answers confirm that the students need practical problems to practice on instead of dry theoretical examples.

5. CONCLUSIONS

In this paper I presented a new idea for teaching string processing by using XML, the lesson plan is available and I analyzed the questionnaire that was completed during the two test-lessons. The presentation, the lesson plan, the questionnaire, the hand-out, the results and the applications are available on the URL [1]. I received confirmation that the students are more interested in spectacular examples than the fictional, theoretical, unnatural ones. Unfortunately till now I did not find other schools where string processing would be taught with XML parsing examples.

6. REFERENCES

[1] László MENYHÁRT, Additional materials for this article "Teaching string processing by using XML", http://xml.inf.elte.hu/articles/TeachingStringProcessingWithXMLAndAppendices.zip

[2] World Wide Web Consortium, Extensible Markup Language (XML) 1.0 (Fifth Edition), http://www.w3.org/TR/xml/, 2008

[3] World Wide Web Consortium, Document Object Model (DOM) Level 1 Specification, http://www.w3.org/TR/REC-DOM-Level-1/, 1998

[4] Simple API for XML, http://www.saxproject.org/, 2004

[5] Gáborné PAP, Péter SZLÁVI, László ZSAKÓ, mikrológia 14, Módszeres programozás: Szövegfeldolgozás, 4. edition, 1995

[6] ELTE, Programming Fundamentals (M1,M2), http://progalapm.elte.hu, 2010

[7] Ricardo A. Baeza-Yates, Teaching algorithms, SIGACT News, 26:4, 51-59, 1995.

Presentation of improved version of guide application for teaching programming fundamentals

László MENYHÁRT
Department of Media & Educational Informatics, Eötvös Loránd University
Budapest, 1117, Hungary

and

Dr. Gáborné PAP
Department of Media & Educational Informatics, Eötvös Loránd University
Budapest, 1117, Hungary

ABSTRACT

One year ago in our previous article we declared that the education of programming for the informatics students at the University must contain the whole process of the development. It was not changed as our experiences that the majority of the students are only interested in creating an operative code somehow. In that article we presented a solution which tried to assist to solve this problem. Our excel-based guidance helped to follow the steps of the whole programming process. We took into consideration the feedbacks, and performed the improvements. This new application supports the complex data types, more sub-tasks and now it is available on the web. This article presents the new web-based system and reports about its welcome.

Keywords: Education, Introductory programming, Algorithm, Specification.

1. INTRODUCTION

The Programming Fundamentals course at Eötvös Loránd University is one of the basic courses for Software Development and Teaching Informatics BSc programs. On this course we follow through the whole process of programming started from creating specification and algorithm, coding, testing, debugging and writing appropriate documentation to the well-functioning application. [2], [3]

The students are only happy to deal with the coding from this process. It is partly understandable because most cases with this experiments and retouching finally they get runnable solution and sense of achievement. But this level is amateur, professional programmers should be on higher level. To cope on their job in a team we must teach them the systematic programming. Our new application gives a hand to this. With using this we get them to pay attention to the specification and algorithm before the coding.

2. DIRECTION OF OUR DEVELOPMENT

Our earlier article presented the ProgFundCppWizard application kit. [6] [7] Our survey showed that the students would enjoy more a web-based and graphical surface. Furthermore we resolved some limitation and implemented new features.

Surface
The most conspicuous change is the surface. The students live in the "world of the web". That is why with switching to web-based platform from the excel-based one we would like to endear using this new ProgrammingFundamentalsWizard (PFW) application.

Reconsider the structure of the tasks
Solving more complex tasks is possible with building from more sub-tasks. The application was implemented to the style of the examination papers and homeworks. These tasks contain common input information and have more questions with their outputs and sometimes extra inputs. So the main function performs the reading data and calling calculating functions steps. So every subtask has its own specification and algorithm.

Complement the missing data types
Unfortunately the previous excel was unable to handle complex data types. Since these are necessary to solve a bit more complicated problems, arrays and records are available now.

Nassi-Shneiderman Diagram (NSD) editors
Following the matter of the course where we use NSD instead of pseudo code the application contain a NSD editor. [1] There are more applications with which NSD can be drawn. These are collected by B. Shneiderman in 2003. [10] Unfortunately more than 50% are not available nowadays. There are some not enough flexible apps however there are some code generator apps as well. Structorizer [11] is not mentioned as a work from an ELTE student, the StukiMania [12]. Last year Menyhárt presented an editor in his paper [17].

3. PROGRAMMING FUNDAMENTALS WIZARD

So this brand new web-based application tries to assist to the students to solve their homeworks or it can be more generic trace. It gives a place to collect the information of the task and edit the NSD of the algorithm. The application is available on URL [14]. HTTPS guarantees the secure communication. The server has only a self-generated certificate that is why user have to accept the warning sometimes. The philosophy of this framework is that with its restriction the students will be forced to think and create an algorithm before the coding and their works will be helped. It is useful for the students because it helps to interpret the tasks. It records the known information in its structure. It is helpful for teachers because the homeworks will be unified, NSDs will be in same appearance and the specification or algorithm of tasks can be collected in digital XML format.

Introduction
The application is available in English and in Hungarian languages. [14] User can switch between the languages at the left upper corner with clicking on the link EN or HU. The brochure of the application is available on URL [13].

Registration and login: Users must be logged in. Login process can be in three different ways: with GMail account using OpenID technology, with INF account for our students and after registration to the system.

In case of login with GMail user must accept on the Gmail page the accessibility to the email address. Name of the user and language information will be used in the automatic registration process.

Our students have an account on inf.elte.hu domain, so they can use the same userid and password with which they can reach the intranet. Automatic registration process will set the full name and Hungarian language.

If somebody did not have an account in the previous environment or did not want to use this account, he or she must register on the site and must log in with the registered email address as the userid and the initial password sent there. The initial password must be changed.

After a success login the user gets to the main page which is the soul of this one-page application.

Structure of the page and the task: The menu is located on the left side of the page while the editor is on the right side.

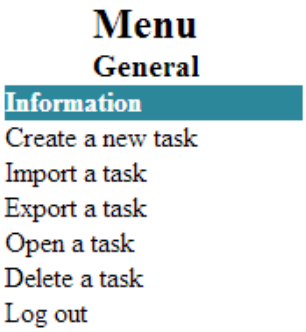

Figure 1: Menu items at first time

The menu is changing dynamically according as the logged-in user's saved tasks, its opening status and how many sub-tasks are in it.
In case of the first time of the usage users do not have saved tasks. Figure 1 shows the menu items at this time.
When the user opens a task the menu items are changed and the name and the identifier of the task appear after the fourth menu item.

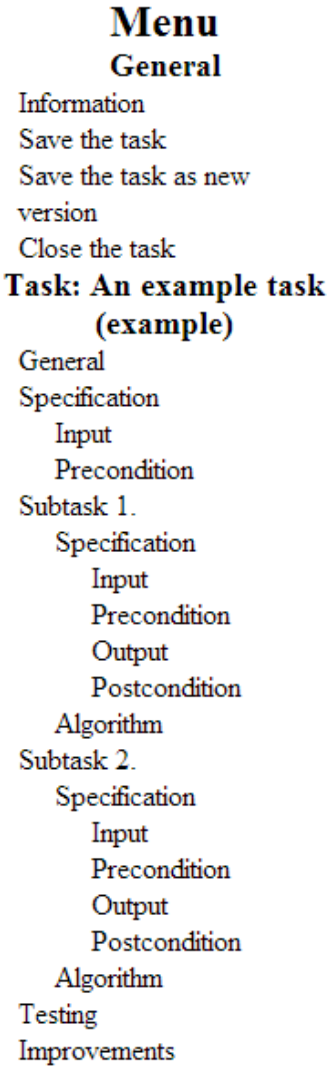

Figure 2: Menu items after opening a task

Figure 2 shows the menu items after opening a task. Menu items from the fifth one effect on the opened task.
One task can contain more sub-tasks. This time additional menu items will appear with its sub-menu under the Subtask 1.

Description of menu and operations is in this section. At first time the following options can be chosen:

Information – With clicking on this item short welcome message and description will appear on the right side.

Create a new task – A new, empty task will be generated and opened immediately.

Import a task – A downloaded - or got from anybody - task can be imported to the system from the user's disk.

Export a task – The file of a task can be downloaded from the server.

Open a task – The user chooses a task from the saved ones which will be opened. This time the menu items will be changed dynamically to the other operations.

Delete a task – User chooses a task from the saved ones which will be removed from the database of the system.

Log out – User leaves the application with this.

Menu items after opening a task

Save the task – Modification of the tasks happens in the memory belong to the session. It will be stored in the database with clicking on this menu. The identifier of task is not changed.

Save the task as new version – The task will be saved with a new automatically generated identifier without deleting the old one.

Close the task – The task should be closed at the end of the work.

General – On the appeared page general information can be stored. Only the short identifier is required because it will be the main part of the name of the task and it will be used at file generation. Long name, text of the task, environment information and author information can be stored here, too.

Specification – Clicking on Specification menu item the control will jump automatically to the next sub-menu: Input. There is another sub menu item: Precondition.

Input and Precondition – PFW was designed special problem solving where there is common part of the input and there are more questions. This page is to store the common data, types, initial values, constant data, type and size of array, record information with its fields. Precondition concerns to the common input data only. Its definition is possible with simple alphanumeric characters, short sentences. Similar way as it can be defined in a Microsoft Excel cell with functions.

Subtask – There can be more subtasks in one task. User can define the identifier of the subtask and its text on this page.

Specification (in a subtask) – Clicking on Specification menu item the control will jump automatically to the next sub-menu: Input. There are other three sub menu items: Precondition, Output and Postcondition.

Input and Output – Gathered input and output data of the subtask can be stored on this page with their name, type, initial value, array and record information.

Precondition and Postcondition – The given subtask's precondition and postcondition should be defined here only.

Algorithm – User can edit the algorithm in NSD format on this page with clicking on each box of the diagram and choosing the proper menu item on the popup menu. The possible operations will be presented in the next paragraph and they are shown on Figure 3.

Testing – Testing information can be stored here. Each row can store one testcase with its input data, name of the test file, expected output, the actual output and whether it passed or failed with short notes if necessary.

Improvements – Here the user can store the further development opportunities.

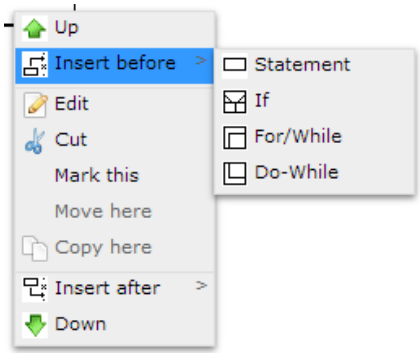

Figure 3: Pop-up menu at editing NSD

Description of operations in the application and the menu items of popup menu can be found here.

Edit – It starts the editing value of the given element. The value will be copied to the right text field or text area where the user can modify it.

Help – Pulling over the mouse to this image short tooltip can be read.

OK – It saves the new value to the server and refreshes the page.

Cancel – This icon rejects the new value at editing and restores the old value.

Cut – This deletes the given element.

Add – It adds a new element with initial value to the list.

Add a new subtask! (link) – This generates a new subtask to the opened task and refreshes the menu.

Delete this subtask! (link) – It deletes the given subtask and refreshes the menu.

Download picture of NSD (button) – PNG image of NSD will be downloaded to the user's computer.

Generate simple CPP code in CBP project (button) – The server generates a Code::Blocks project filled out with the known information and C++ source code is generated from the input, output and algorithm. These files will be packed to a zip file and downloaded from the server to the user's computer. User must continue this implementation with reading data, writing data and other steps.

Generate Word documentation (button) – The server generates the documentation filled out with the known information. Its editing must be continued with screenshoots and other parts.

Editing NSD (popup menu) – At clicking with the mouse right button on a NSD box a popup menu will appear with the following menu items.

Up or Down / – The given box will jump before the previous box or after the next box.

Insert before or after / – A new sub menu will appear with the next items. These algorithm blocks can be inserted before or after the given box. This can be a statement , if condition (two-way fork) , while or for loop or do-while loop .

Edit – The value of the box can be edited in a popup editor window.

Cut – It deletes the given box.

Mark – The given box will be marked for the next two operations.

Move – The marked box will be moved before the given box.

Copy – The marked box will be copied before the given box.

Technologies
The application is implemented in Java and it is running on Glassfish application server. The database is PostgreSQL. It uses OpenID, LDAP and it sends emails. The client is a one-page application which uses AJAX to communicate with the server.
The tasks are stored in the database in XML format. It will be loaded into the memory at opening from where the application gets data with XPath or XSL transformation.
Defining the tasks it uses an own extended language, the Task Markup Language (TML). TML based on AML which was presented in one of my earlier papers [5].

4. QUESTIONS AND ANSWERS

While we were designed and implemented this new guide new questions were drawn up which are answered here.

In which phase should PFW be presented to the students?
It makes no sense to deal with PFW on the first lessons when students learn basic things. It should be presented on those lessons when the subject is about specification, creating algorithm and coding. They got some information about testing and documentation on the lecture so they can try it with PFW on the practice. It presentation one times is important because at first subtask concept is not known but they can meet with it in this application. They can use it without precise explanation. Later they learn about functions and with this they can understand easier the importance of the parameters which is managed by PFW if the specification is well-defined.

Can be the result of the code generation that students will not learn coding?
This question came up at the previous application as well. Now the answer is even more no; because of more reasons. Aim of PFW is much more than automatic code generation. It is rather guide to coding and creating documentation. That is why we recommend this to beginner programmers, but it helps not only their work. [8] At creating algorithm we insist to our principle that it must be language independent without programming language specific expressions. In this way the structure of the algorithm will present in the generated source-code but C++ specific operators (for instance ":=" will be there instead of "=") and other expressions must be changed by the user. The generated code will not contain data reading with checking the preconditions because it is not part of the algorithm. Without implementing these, the application is not runnable. Finally there is no different boxes for while loop and for loop, so students must correct the syntax here, too. So the students must learn coding even if they use PFW.

5. EXPERIENCE WITH THE APPLICATION

Our students started to use this application at the time of writing this article. They learnt only the basic syntax of the programming language. [14] The next season will include the creating algorithm step. That is why we have not enough feedbacks just some positive opinion.

There is a group where the language of the education is English because the students arrived more different countries (England, Brazil, Iran, Kamerun, Macedonia, Germany, Saudi Arabia, Turkey, USA, Vietnam, …). It is especially good that definition of algorithm is not in pseudo code in this group because its strength would be the native language while pseudo code in English language would be too similar to the source code and we would not be capable to enhance its language independent property. [9]

Before this article we surveyed our work with upper-year students who ended this course already. We created two anonymous surveys for two groups. These surveys were published in Google Form format.

Survey – First group
At first those students were questioned who were involved in the previous research last year and entered their email address to further researches. The application was presented for them and they were asked to reply to the following questions. [15]

Questions:

1. Was the server available? (yes / no)
2. In which time-window was the application used? (free text, e.g. between 11 and 13)
3. How satisfied were you with the response time of the server? (fast / appropriate / acceptable / slow / very slow, loaded)
4. Would you have used this tool if you had had the chance to use it during completing the subject? (Yes / No)
5. What do you think about the direction of the development of this web-based, graphical application? (Keep it up! / Another direction would be better. Please

describe proposed developments (7th question)! / It was enough. No more!)
6. What kind of mistakes did you find in the application? (Free text)
7. What kind of improvements would you suggest? (Free text)
8. Other observations: (Free text)

Answers: Last year we got only 9 email address from the 13 students who sent back the answers. They got the questions but only one response arrived. According to this one active student the server was available between 20 and 22 and it was fast. He would use it and suggested some improvements. He personally found us to help in dressing the application to more designed surface.

Survey – Second group
Questions of second group were very similar to the previous year's questions. It was actualized to PFW from ProgFundCppWizard only. [16]

Questions about the home assignments of the Programming Fundamentals subject:
1. How many hours did you spend making the home assignment? (in hours)
2. What percentage of the time was used for making an algorithm A= , creating the code C= and writing the documentation D= ? If its sum is not 100, what did you do in the remaining time?
3. What was the order of making the following parts: algorithm (A), coding (C) and documentation (D)?

Questions about testing the PFW:
4. What do you think about this idea? (It is useless / It is good but the application is very labor-consuming / It is good / It is very good)
5. Do you think that it helps improving the importance of making an algorithm? (No / Partly / Yes)
6. Do you think that it helps making documentation? (No / Partly / Yes)
7. Do you see a danger in it if this application is used by the students? (Free text)
8. Is it confusing that the algorithm must be prepared first? (Yes / No)
9. Would you have used this tool if you had had the chance to use it during completing the subject? (Yes / No)
10. How do you feel, would you have saved any time with this tool when completing your home assignments? (The home assignment would not have been completed. / It would have caused delays./ No / Little / Much)
11. What kind of mistakes did you find in the application? (Free text)
12. What kind of improvements would you suggest? (Free text)
13. Other observations: (Free text)

The evaluation of the questionnaire
The link of the questionnaire was sent to every students who learnt this course earlier. It means more hundred, almost one thousand students. 20-30 minutes would have been enough taking a quick look onto the application and filling out the survey in the defined three weeks when we were waiting for this. Unfortunately only 2 i.e. two students sent their answers. After this we decided that our research will be mandatory part of our course next time.

1. One of them spent only 6 hours with the homework while the other student more than 4 days.
2. Percentages between algorithm, coding and documentation were very different: 5-35-60% and 50-30-20%.
3. Both of them kept the order Algorithm-Code-Documentation.
4. "It is good" and "It is good but the application is very labor-consuming" were the two answers.
6. Making documentation is helped.
7. One student wrote some opinion: „Only that if students could use this on the course Programming Fundamentals and it was not available on other courses it would be difficult for some lazy students. Because easy to get used to a good thing. :) But it would be good if it was available from courses and examination papers via Internet."
8. Starting with algorithm was not annoying restriction.
9. Both of them would have used this application.
10. They could save few-or-more time.
11. Mistakes were no mentioned.
12. There was no suggested improvements.
13. There was no other observation.

We are glad that these two respondents found our work useful and the message about the importance of the algorithm came through. We rely on that this new webapplication will be more interesting in production use on our courses at the current moment of the education.

6. FUTURE DEVELOPMENT

Preconditions and postconditions

As it was mentioned preconditions and postconditions can be defined in simple sentences now, but it would be more exact if MathML was integrated.

Collecting and assessment

Extracting short documentation from the system in PDF format is possible, or sending from here the homework to the defined teacher will be implemented. Preprocessing would be a good feature with which the completely correct and bad solutions could be filtered.

7. REFERENCES

[1] I. Nassi, B. Shneiderman, **Flowchart techniques for structured programming**, ACM SIGPLAN Notices, Volume 8 Issue 8, August 1973, Pages 12 - 26

[2] E.W. Dijkstra, **A Discipline of Programming**, Prentice-Hall, Englewood Cli_s, 1973.

[3] P. Szlávi, L. Zsakó, **Módszeres programozás: Programozási bevezető**, 18. Mikrológia

[4] Sz. Csepregi, A. Dezso, T. Gregorics, S. Sike, **Automatic Implementation of Service Required by Components**, Workshop on Property Verification for Software Components and Services ,PROVECS 2007, http://lina.atlanstic.net/provecs/2007/provecs2007proceedings.pdf

[5] L. Menyhárt, **Can a language be before "the first programming language"?**, Teaching Mathematics and Computer Science, 2011, Volume IX, Issue II, 209-224 ISSN: 1589-7389, http://tmcs.math.klte.hu/Contents/2011-Vol-IX-Issue-II.html

[6] L. Menyhárt, G.né Pap, **Dokumentáció alapú programfejlesztés**; INFODIDACT 2012 konferencia, Zamárdi, Magyarország, 2012.11.15-2012.11.16.

[7] L. Menyhárt; G.né Pap, **How can we get our students to think while we help their work too?: Document based development**; Proceedings of the 7th International Multi-Conference on Society, Cybernetics and Informatics. Konferencia helye, ideje: Orlando, Amerikai Egyesült Államok, 2013.07.09-2013.07.12. Florida: International Institute of Informatics and Systemics (IIIS), 2013. pp. 97-102. (ISBN:ISBN-13: 978-1-936338-83-2)

[8] V. Averbukh, M. Bakhterev, **The analysis of visual parallel programming languages**, ACSIJ Advances in Computer Science: an International Journal, Vol.2, Issue3, No. 4,2013, ISSN : 2322-5157

[9] M. Weise, **A Model for Teaching Informatics to German Secondary School Students in English-language Bilingual Education**, Proceedings of the 6th International Conference ISSEP 2013; Oldenburg, Germany, February 26–March 2, 2013/Diethelm et al. (Eds.)/ Potsdam: Universitätsverlag Potsdam, 2013/ S.127-137

[10] B. Shneiderman, **A short history of structured flowcharts (Nassi-Shneiderman Diagrams)**, University Maryland, 2003, http://www.cs.umd.edu/hcil/members/bshneiderman/nsd/

[11] B. Fisch, **Structorizer**, http://structorizer.fisch.lu/

[12] T. Molnár, **StukiMania**, http://stukimania.hu, 2013

[13] http://xml.inf.elte.hu/2013_14_1/progalap/anyagok/PFW_leiras.pdf

[14] https://157.181.166.134:8181/PFW/index2_EN.jsp

[15] https://docs.google.com/forms/d/1LfhO64yJRFhywHqRBfoJzawK8PBZDizImWkTFnI4HmA/viewform

[16] https://docs.google.com/spreadsheet/viewform?usp=drive_web&formkey=dERsTi1rS1V6OGc3Rzc3cm85YW5KNFE6MA#gid=0

[17] L. Menyhárt, **Nassi-Schneiderman diagram in HTML based on AML**, Acta Didactica Napocensia, 2013, Volume 6, Number 3 pp. 19-26. ISSN: 2065-1430

Pharmaceutical wastewater treatment associated with renewable energy generation in microbial fuel cell based on mobilized electroactive biofilm

Zainab Z. Ismail*
Department of Environmental Engineering, Baghdad University
Baghdad, Iraq

And

Ali A. Habeeb
Department of Environmental Engineering, Baghdad University
Baghdad, Iraq

*Corresponding author (Z.Z. Ismail), Email: zismail9@gmail.com; zismail3@gatech.edu

ABSTRACT

Industrial wastewater generated from pharmaceutical industry generally contains high organic load and the treatment is primarily carried out using biological methods. Anaerobic wastewater treatment is considered as the most cost effective solution for high organically polluted industrial waste streams. However, biotreatment of wastewaters associated with energy recovery seems to be a potential approach for waste treatment and conservation. On the other hand, Microbial fuel cells (MFCs) represent a new bio-electrochemical technology for generating electricity directly from biodegradable organic compounds. This research work aimed to study the potential of industrial pharmaceutical wastewater treatment accompanying with bioelectricity production in microbial fuel cell utilizing mixed cultures immobilized on a packed bed in the anode compartment. A dual-chambered lab scale microbial fuel cells (MFC) have been developed, based on electroactive biofilm attached to activated carbon granules bed. The MFC was fueled with actual pharmaceutical industry wastewater. The MFC was inoculated with anaerobic mixed consortiums, previously acclimated to pharmaceutical wastewater. Results revealed that maximum COD removal effeciency up to 81%, and current density of 342.86 mA/m^2 were observed in this study. Experimental work indicated that the presented microbial fuel cell (MFC) design can be successfully used for simultaneous pharmaceutical wastewater treatment and power generation.

Key words: Microbial fuel cell, Pharmaceutical industry, Biomass, Wastewater, Power generation.

1. INTRODUCTION

The microbial fuel cell (MFC) is a new form of renewable energy technology that can generate electricity from what would otherwise be considered waste [1]. In MFC, microorganisms oxidize organic matter in the anode chamber producing electrons and protons. Electrons transfer via an external circuit to the cathode chamber where electrons, oxygen and protons combine to produce water [2, 3]. Electron transfer from the biofilms to the anode is critical for contaminant removal and electricity generation in MFCs [4]. Electron transfer can occur directly via extracellular redox cofactors and nanowires formation on the anode surfaces

is governed by different factors including: substratum conditions, hydrodynamic features and characteristics of aqueous medium and cell surface properties. Previously reported studies have mentioned the importance of large anode surface area to achieve high power generation. However, a greater extent of bacterial growth should assist in a higher electron transfer to the anode [5]. On the other hand, when wastewater happens uncontrolled, it oozes through to streams, rivers, and subsoil water causing quality deterioration of these media [6]. The wastewater generated from pharmaceutical industry generally contain high organic load and the treatment is primarily carried out using two major types of biological methods; aerobic and anaerobic. However, due to high strength, it is infeasible to treat some pharmaceutical wastewater using aerobic biological processes. As an alternative, an anaerobic process is preferred to remove high strength organic matter. Anaerobic wastewater treatment is considered as the most cost effective solution for organically polluted industrial waste streams. In particular the development of high rate systems, in which hydraulic retention times (HRT) are uncoupled from solids retention times (SRT), has led to a worldwide acceptance of anaerobic wastewater treatment [7].

The main aim of this study was to design and construct an MFC that generate renewable energy from electroactive biofilm by using freshly collected actual pharmaceutical industrial wastewater. The biofilm was mobilized on granular activated carbon particles placed in the anode compartment. The biofilm was originated from an aged anaerobic sludge.

2. MATERIALS AND METHODS

Design of lab scale microbial fuel cell

The MFC was constructed of Perspex material with two different sized-chambers. Dimensions of anodic and cathodic chambers were 20 x 20 x 26 cm and 10 x 10 x 15 cm, respectively. As given in Fig. 1, the cathode chamber was fully submerged in the anode chamber with two opposite sides containing two pieces of cation exchange membrane (CEM), which were sandwiched between two perforated Perspex sheets with a net membrane area of 44 cm^2. The electrodes in each chamber were pierced with copper wires extended outside the MFC to simply connected to an external electrical circuit through which electrons were transported. Approximately 60% of the anode compartment volume was occupied by granular activated carbon (GAC) as a biofilm bearer material, and the remaining 40% was considered as a head space. Cylindrical shaped-granular activated carbon (GAC) of 2.36-4.75 mm diameter and different lengths averaged from 3.5-6 mm were used a biofilm bearer. The chemical composition of GAC was of 90.74% carbon and 9.26% ash content. The porosity of GAC was 45%.

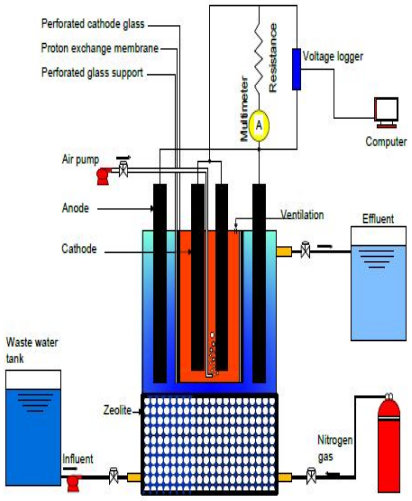

Fig. 1 Schematic diagram of the MFC system

Inoculum and substrate

MFC inoculated with mixed culture collected from the bottom of a secondary settling tank in a wastewater treatment plant at a local pharmaceutical factory, north of Baghdad (Iraq). The MFC was fueled with actual pharmaceutical industrial wastewater collected from the discharge of the same pharmaceutical manufacturing factory.

Process operation

To start up and operate the MFC, one liter of the mixed culture was placed in the anode compartment and was sparged with nitrogen gas for a period of 10 min to maintain anaerobic environment. After 10 days, the MFC was fed with a primarily treated actual pharmaceutical wastewater at a rate of 3 mL/min corresponding to a hydraulic retention time (HRT) of 38 hr. Oxygen concentration was continuously monitored in the anodic compartment, the absence of oxygen was observed. This means that the flow of oxygen from the cathodic to the anodic compartment was negligible and the anode compartment can be considered as anoxic.

During normal operation, anode and cathode electrodes were connected by means of wires and an external resistance of 100 Ω. The voltages between the edges of this resistance were continuously monitored. These voltages were directly related to the current flowing between the electrodes by Ohm law. Fig.2 presents the scheme of the MFC system.

Fig. 2 The Scheme of the MFC system

Analytical analysis and methodologies

Chemical oxygen demand (COD), dissolved oxygen (DO), pH and TDS of the influent and effluent were conducted on a daily basis. The quality of the primarily treated influent to the MFC is given in Table 1. Voltage was continuously measured by voltmeter and data acquisition system and converted to power according to P=I*V, where P power, I current and V voltage. Power was normalized by the total surface area of the anode electrodes. Polarization curves were plotted with the function of current density measured at different resistances ranged from 50 to 3000 Ω. The microbial fuel cells were operated for a period of 52 days.

Table 1 Quality of the actual samples of the Pharmaceutical wastewater

Constituent	Unit	Average Value
COD	mg/L	800
BOD	mg/L	40
pH	-	7.37
TDS	mg/L	355
NO_3^-	mg/L	7.23
SO_4^{-2}	mg/L	138
Cl^-	mg/L	10
PO_4^{-3}	mg/L	2.13

3. RESULTS AND DISSCUSION

Chemical Oxygen Demand (COD) Removal

MFC was continuously operated for 52 days achieving an average and maximum COD removal effeciencies of 72 and 81%, respectively as given in Fig. 3. However, fast removal of COD was observed after 2 days of the MFC start up. This could be attributed to the fact that the inoculation of MFC was originally acclimated to the constituents of the pharmaceutical wastewater.

Average initial COD concentration was 800 mg/L. The observed maximum removal efficiency of COD in the current study was higher than the previously published values of treating industrial wastewaters in MFCs which were 75% for starch wastewater collected from a starch-processing plant [8], and in a very good agreement with the maximum reported efficiency in the range of 62%–92% [9-16].

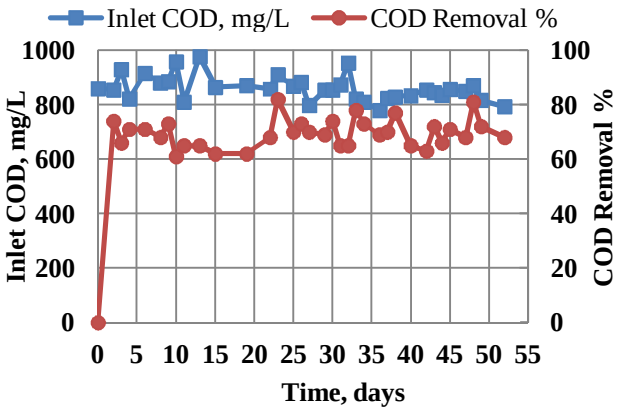

Fig. 3 Profiles of inlet COD (■) and COD removal effeciency (●)

However, the source and type (real or synthetic) of substrate, type and concentration of inoculum, geometric design of microbial fuel cell (MFC), type of electrodes, and other parameters highly affect the organics removal efficiency. However, the overall efficiencies observed for COD removal potentially indicate an effective wastewater treatment process.

Current and power generation

In this study, the MFC system generated maximum stable current of 342.86 mA/ m^2 with a maximum obtained Coulombic efficiency of 21%. These results revealed that the anaerobically developed mixed microorganisms were electrochemically active. For electricity generation, the current increased rapidly at the first day, then fluctuated current values were observed followed by fast increase after 18 days to a maximum constant value of 342.86 mA/ m^2 as shown in Fig. 4.

A wide range of variable resistances from 50 to 3000 Ω was applied. Fig.5 illustrates the polarization curve plot. It is obvious from this plot that the maximum power density and current density are 206 mW/ m^2 and 342.86 mA/ m^2, respectively which were obtained at an external resistance of 100 Ω. These results indicate that in spite of the unpleasant quality of pharmaceutical wastewater to the microorganisms growth and activity, the observed power density for MFC was significantly favorable compared to the power density of 239.4 mW/m^2 at external resistance of 120 Ω reported by Lu et al. (2004) for a MFC fed with starch industry wastewater taking into consideration the favorable quality of starch wastewater to the microorganisms.

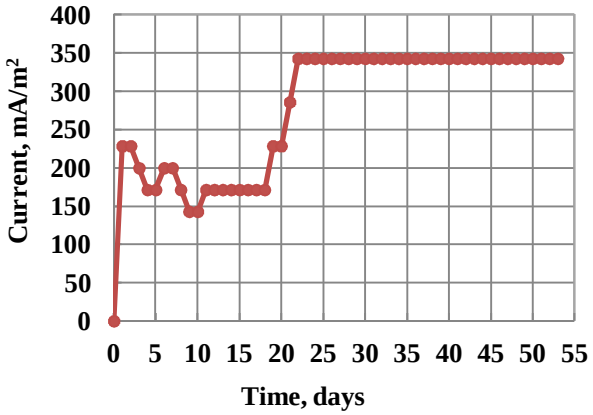

Fig. 4 Current generation profile

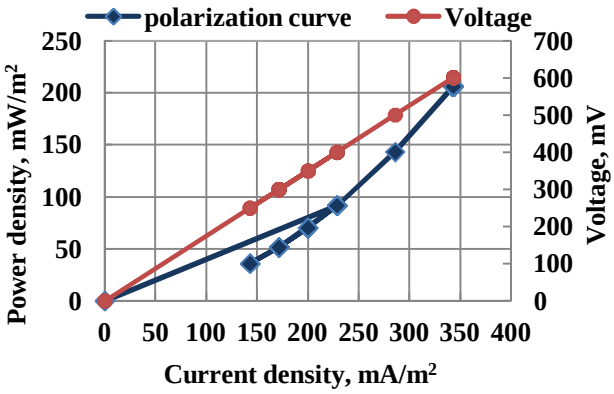

Fig. 5 Polarization curve for the MFC

Effect of external resistances

To investigate the effect of external resistances on the current generation and the corresponding COD removal, the current was recorded with different resistances across the anode and cathode to establish the relationship between the resistance and current. As presented in Fig. 6, at lower external resistance, more COD was removed resulted in a higher current generation.

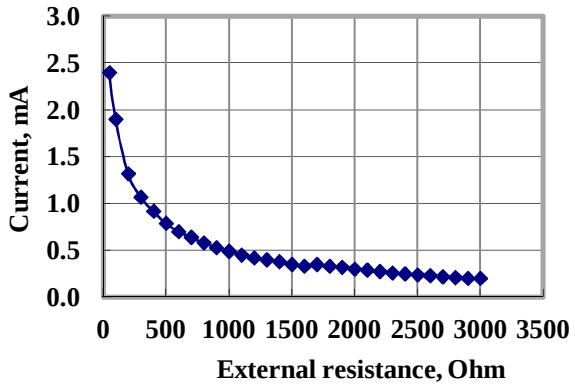

Fig. 6 Current generation with different external resistances for MFC

4. CONCLUSION

This study demonstrated and evaluated the performance of a dual-chambered mediator-less microbial fuel cell catalyzed with anaerobic sludge previously acclimated to pharmaceutical wastewater in which the latter was used to fuel the MFC for simultaneous wastewater treatment and power generation. Approximately 60% of the anode chamber was filled with granular activated carbon (GAC) as a biofilm barrier. However, the biofilms which grow under anaerobic environment and attached to the surfaces of the anode were the main contributors to the electricity generation. Results revealed that maximum COD removal effeciency and power output up to 81% and 206 mW/ m^2, respectively were achieved in this study.

5. ACKNOWLEDGEMENT

This research was supported by the Ministry of Industry and Minerals, State organization for Drug Industries (SDI), Iraq.

6. REFERENCES

[1] P.K. Barua, D. Deka "Electricity generation from biowaste based microbial fuel cells" **International Journal of Energy Information and Communications**, Vol .1, 2010, pp. 77-92.

[2] Z. Li, X. Zhang, Y. Zeng, L. Lei, "Electricity production by an overflow-type wetted wall microbial fuel cell", **Bioresource Technology**, Vol. 100, 2009, pp. 2551-2555.

[3] Z.Z. Ismail, A.J. Jaeel, "Modelling study of an upflow microbial fuel cell catalyzed with anaerobic aged sludge", **International Journal of Ambient Energy**, , 2014, in press.

[4] A. Dumitru, A. Morozan, M. Ghiurea, K. Scott, S. Vulpe, "Biofilm growth from wastewater on MWNTs and carbon aerogels", **Physical Status Solidification Journal**, Vol. 205, 2008, pp. 1484-1487.

[5] U. Karra, S.S. Manickam, J.R. McCutheon, N. Patel, B. Li, "Power generation and organics removal from wastewater using activated carbon nanofiber (ACNF) microbial fuel cells (MFCs)", **International Journal of Hydrogen Energy**, Vol. 38, 2013, pp. 1588-1597.

[6] A. Anatoliy, B. Svetlana, L., Alexandre "Microbial fuel cell based on electroactive sulfate-reducing biofilm", **Energy Conversion and Management**, Vol. 67, 2013, pp. 283-286.

[7]C. Shreeshivadasan, P.J. Sallis, "Application of anaerobic biotechnology for pharmaceutical wastewater treatment", **The IIOAB Journal**, Vol. 2, 2011, pp. 13-21.

[8] B.H. Kim, H.S. Park, H.J. Kim, G.T. Kim, I.S. Chang, J., Lee, N.T. Phung, "Enrichment of microbial community generating electricity using a fuel-cell-type electrochemical cell', **Applied Microbiology and Biotechnology**, Vol. 63, 2004, pp. 672-681.

[9] S.You, Q. Zhao, J. Zhang, J. Jiang, S. Zhao, "A microbial fuel cell using permanganate as the cathodic electron acceptor", **Journal of Power Sources**, Vol. 162, 2006, pp.1409-1415.

[10] S.V. Mohan, S.V. Raghavulu, D. Peri, P.N. Sarma, **"**Bioelectricity production by mediator-less microbial fuel cell under acidophilic condition using wastewater as substrate: Influence of substrate loading rate", **Biosensors and Bioelectronics**, Vol. 92, 2007, pp.1720-1726.

[11] M.A. Rodrigo, P. Canizares, J. Lobato, R. Paz, C. Saez, J.J. Linares, "Production of electricity from the treatment of urban waste water using a microbial fuel cell", **Journal of Power Sources**, Vol. 169, 2007, pp.198-204.

[12] G. Antonopoulou, K. Stamatelatou, S. Bebelis, G. Lyberatos, "Electricity generation from synthetic substrates and cheese whey using a two chamber microbial fuel cell", **Biochemical Engineering Journal**, Vol. 50, 2010, pp.10–15.

[13] M. Rahimnejad, A.A. Ghoreyshi, G. Najafpour, T. Jafary, "Power generation from organic substrate in batch and continuous flow microbial fuel cell operations", **Applied Energy**, Vol. 88, 2011, pp.3999–4004.

[14] Y. Yuan, B. Zhao, S. Zhou, S. Zhong, L. Zhuang, "Electrocatalytic activity of anodic biofilm responses to pH changes in microbial fuel cells", **Bioresource Technology**. Vol. 102, 2011, pp. 6887–6891.

[15] A.E. Tugtas, P. Cavdar, B. Calli, "Continuous flow membrane-less air cathode microbial fuel cell with spunbonded olefin diffusion layer", **Bioresource Technology**, Vol.102, 2011, pp. 10425–10430.

[16] D. Fangzhou, L. Zhenglong, Y. Shaoqiang, X. Beizhen, L. Hong, "Electricity generation directly using human feces wastewater for life support system", **Acta Astronautica**, Vol. 68, 2011, pp.1537-1547.

[17] N. Lu, S-g. Zhou, L. Zhuang, J-t. Zhang, J-r. Ni, "Electricity generation from starch processing wastewater using microbial fuel cell technology", **Biochemical Engineering Journal**, Vol. 43, 2009, pp. 246-251.

Measurement of Flow Properties of Mammalian Blood with Different Hematocrit Values Using Falling Needle Rheometer

Takamasa SUZUKI, Sadao ARAKI and Hideki YAMAMOTO
Department of Chemical, Energy and Environment Engineering, Faculty of Environmental and Urban Engineering, Kansai University, 3-3-35, Yamate, Suita, 564-8680, Osaka, Japan
e-mail: yhideki@kansai-u.ac.jp

Kimito KAWAMURA
R&D Laboratories for Sustainable Value Creation, Asahi Group Holdings, ltd., 1-1-21, midori, Moriya, 302-0106, Ibaraki, Japan

Hiroko AIDA
Equine Research Institute Japan Racing Association, 321-4, Tokami, Utsunomiya, 320-0856, Tochigi, Japan

and

Dominik BERNITZKY, Roberto PLASENZOTTI
Core Unit for Biomedical Research, Medical University of Vienna, Waehringer Guertel 18-20 / AKH1Q, A-1090 Wien, Austria

ABSTRACT

The development of viscometry with high accuracy and quick operation, as well as the establishment of a data evaluation method by pathology are largely required. Especially, the flow properties of human blood are an important factor in the evaluation of blood disease on the medicine, but the method of viscometry and the data collection are not so easy. This study has been described on the viscosity measurement and their evaluations for mammalian blood (rabbit, pig and horse) including human blood. A compact-sized falling needle rheometer (FNR) and a flow analysis method using this device for blood have been developed, and the relationship between the apparent viscosity and physical properties (density, hematocrit value) of blood have also been evaluated. Measured flow properties of blood are evaluated as a flow curve showing the relationship between the shear stress and shear rate. Observed flow curves of mammalian bloods show three typical fluid regions, these are, the Non-newtonian fluid region for a low shear rate range, the transition region and the Newtonian fluid region for a high shear rate range. Flow properties of blood in the Casson fluid region and the apparent viscosity (μ) in the Newtonian fluid region are measured, and they are compared between mammals.

Keywords: Flow property, Viscosity, Mammalian blood, Rheometer and Flow curve.

1. Compact-Sized Falling Needle Rheometer

The flow model of a falling needle in a static fluid according to the above assumptions is given in Fig.1. This model shows that the falling needle falls at a terminal velocity (Ut) in the static fluid introduced into the cylindrical fluid vessel. The fluid vessel diameter is R, and k is the ratio of the needle diameter to fluid vessel diameter. The minute circular cylinder core is assumed as the fluid model for theoretical analysis. The inner diameter and outer diameter of this core are γ and γ +dr, and the total length is L. The shear stresses on the inside and outside surfaces of the minute circular cylinder core are τ and τ +dτ, respectively. The pressures at the top and bottom of the minute circular cylinder core are P_1 and P_2. When the falling needle falls at a terminal velocity in the static sample fluid, the momentums affected on four surfaces of the minute circular cylinder core are balanced with each other, and they are balanced while the needle is falling at the terminal velocity. Therefore, this force balance can be described by the following equation:

$$P_1\left\{(r+dr)^2\pi - r^2\pi\right\} + 2\pi rL\tau = P_2\left\{(r+dr)^2\pi - r^2\pi\right\} + 2\pi(r+dr)L(\tau+d\tau) \quad (1)$$

When $\Delta P = P_1 - P_2$ is less than 0, Eq.1 is arranged as follows:

$$\frac{1}{r}\frac{d(r\tau)}{dr} = \frac{\Delta P}{L} \quad (2)$$

Furthermore, while the needle falls at the terminal velocity in the sample fluid, the force balance of gravity, buoyancy, pressure and shear stress affected on the needle surfaces are given as

$$(\rho_s - \rho_f)g\pi(kR)^2 L + \pi(kR)^2\Delta P = 2\pi kRL\tau_{(r=kR)} \quad (3)$$

In this equation, ρ_f and ρ_s are the fluid and needle density, respectively. The left-hand side first term of Eq.3 is the

force of gravity and buoyancy, and the second term is the force of the pressure difference. The right-hand side term is the shear stress. This balance can be simply described by

$$(\rho_s - \rho_f)g + \frac{\Delta P}{L} = \frac{2\tau_{(r=kR)}}{kR} \quad (4)$$

Figure 1 illustrates the velocity distribution of the sample fluid due to falling of the needle. The amount of fluid (Q) to transfer between the falling needle surface and the container wall due to falling of the needle can be calculated by

$$Q = 2\pi\int_{kR}^{R} ur\,\mathrm{d}r = \pi(kR)^2 U_t \quad (5)$$

Figure 1 shows that the sample fluid around the falling needle is pulled downward with falling of the needle in the static sample fluid. On the other hand, the fluid near the container wall rises with the falling needle. The maximum velocity in the sample fluid is that on the needle surface. The maximum velocity is equal to that of the falling needle velocity. On the other hand, the velocity on the container wall becomes zero according to the above assumptions. Therefore, the boundary conditions of the velocity distribution can be described by

$$u_{(r=kR)} = -U_t \quad (6a)$$

$$u_{(r=R)} = 0 \quad (6b)$$

In order to obtain the relationship between the shear rate and shear stress for the sample fluid, the Eqs. 2, 4, 5, 6a, and 6b and a constitution equation of the sample fluid are used simultaneously for flow analysis [6].

The constitution equation for a Newtonian fluid based on the law of viscosity is given by

$$\tau = \mu\left(\frac{\mathrm{d}u}{\mathrm{d}r}\right) = \mu\gamma \quad (7)$$

where μ is the viscosity, τ is the shear stress, and γ is the shear state. The viscosity of the fluid sample can be calculated by the following equation from combining Eqs.2, 4, 5, 6a, 6b, and 7.

$$\mu = -\frac{(\rho_s - \rho_f)g(kR)^2\left\{(k^2+1)\ln k + 1 - k^2\right\}}{2(k^2+1)U_t} \quad (8)$$

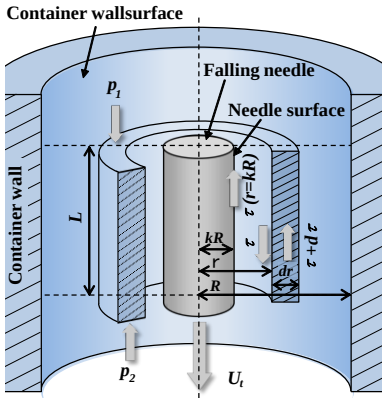

Fig.1 Flow model of the sample fluid in the fluid vessel of falling needle rheometer

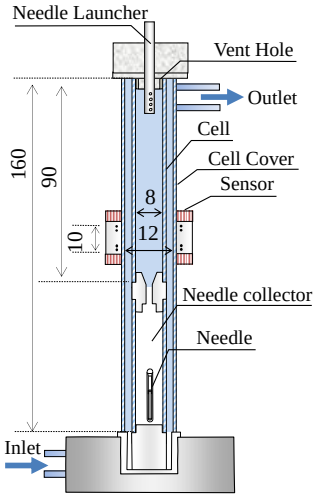

Fig.2 Schematic diagram of the compact-sized falling needle rheometer for measurement of blood viscosity

2. Experimental Method

A schematic photograph of the compact-sized falling needle rheometer for measurement of blood viscosity is shown in Fig. 2. The experimental apparatus consists of vertical double cylindrical vessels (one is a fluid vessel and the other is an insulating vessel cover) made of acrylic material. The cap and bottom of the inner fluid vessel are made of Teflon. The inner fluid vessel for a blood sample is covered with the insulating vessel cover. The temperature of the inner fluid vessel is controlled at 310.15 K using a constant temperature water circulation system. The diameter of the inner fluid vessel is 8 mm, and the height of the vessel is 90 mm. The total volume of the inner fluid vessel is about 4cm^3. A needle collector for the collection of the falling needles is connected to the bottom of the inner fluid vessel via a needle-fluid separator made of Teflon. The needle-fluid separator is a slender cylindrical tube, and its diameter is 2.2 mm, which is similar to the needle diameter (2 mm). Densities of blood are measured by the portable density meter (DMA-35, Anton Paar Co., Ltd.) within an uncertainty of 10^{-4}g•cm^{-3}. The flow analysis is carried out using the observed passing time (terminal velocity) of the falling needles, needle densities, and blood density.

3. Results and Discussion

The observed flow curve for male human, male horse, rabbit and pig blood with anticoagulant is shown in Fig. 3. This flow curve shows a linear relationship between the shear stress and shear rate in a high shear stress range. However, non-Newtonian behavior (Casson behavior) was confirmed in a low shear stress range. The observed flow curve of fresh blood showed the three typical fluid regions, that is, the non-Newtonian fluid region for the low shear rate range, and the transition region and Newtonian fluid region for the high shear rate range.

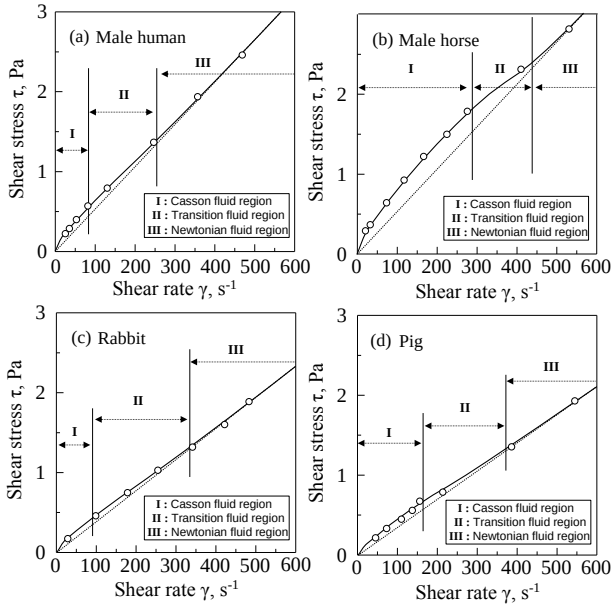

Fig.3-a Flow curve of fresh human blood for male with anticoagulant at 310.15K
Fig.3-b Flow curve of fresh horse blood for male with anticoagulant at 310.15K
Fig.3-c Flow curve of fresh rabbit blood with anticoagulant at 310.15K
Fig.3-d Flow curve of fresh pig blood with anticoagulant at 310.15K

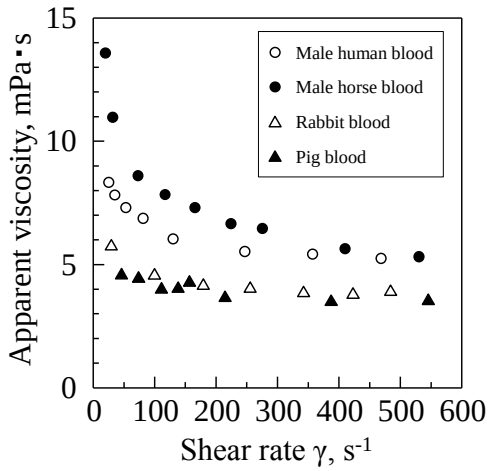

Fig.4 Relationship between apparent viscosity and shear rate for mammalian blood at 310.15K

Figure 4 showed the relationship between the apparent viscosity and shear rate for mammalian blood at 310.15 K. Apparent viscosity at low shear rate range shows higher value than that of high shear rate range. Apparent viscosity for each mammalian blood showed different behavior under the low shear rate range. The rheological parameters that were obtained are listed in Table 1. Apparent horse blood viscosity for the high shear rate range was similar range with human blood. The blood viscosities of pig and rabbit showed lower value than that of human and horse. Blood viscosity and hematocrit value were confirmed the different for each mammalian blood. It was found that the apparent viscosity for blood was closely connected with the hematocrit values.

Table1 Comparison of apparent viscosity, hematocrit value and density of mammalian blood with anticoagulant at 310K

	Density [kg/m^3]	Ht* [%]	Apparent viscosity [mPa ·s]
Male Human	1050.6	43.6	5.374
Male Horse	1053.3	44.0	5.336
Rabbit	1046.9	36.0	3.879
Pig	1037.9	28.0	3.551

* Hematocrit value is the volume percentage of red blood cells included in whole blood.

Table 2 shows the physical properties for healthy mammalian blood that are a mean red blood cell count, a mean corpuscular volume and a hematocrit value. The curvature of flow curve at low shear rate range became large with increasing of the hematocrit value.

Table2 The properties of normal mammalian blood

	Human	Horse	Rabbit	Pig
Red blood cell count (10^4/μL)	430-570 (male) 390-520 (female)	700-1.100	400-800	600-800
Mean corpuscular diameter (μm)	8	5.5	7	6
Mean corpuscular volume (fL)*	83-101	42-47	58-71	38-52
Hematocrit value (%)	40-50(male) 35-45(female)	35-45	28-45	25-40

* The mean corpuscular volume (MCV) is a measure of the average red blood cell volume that is reported as part of a standard complete blood count.

4. Conclusion

A compact-sized falling needle rheometer with quick operation has been developed for the viscometry of mammalian blood with anticoagulant. The measured flow properties of mammalian blood are evaluated as a flow curve, that is, the relationship between the shear stress (τ) and shear rate (γ). The comparison examination of the flow curves for each mammalian blood was carried out. The curvature of flow curves at low shear rate range closely connected with hematocrit value. Value of the apparent viscosity showed horse>human>pig=rabbit. It became clear that the developed falling needle rheometer has high application for viscometry of mammalian blood.

Nomenclature

d	needle diameter, m
g	gravitational acceleration, m·s^{-2}
G	geometric needle constant, 1·m^{-2}
k	ratio of container to needle diameter
kR	needle radius, m
n	fluid index
L	total needle length, m
P_1, P_2	pressure of the upper and lower end of aminute circular cylinder, Pa
ΔP	pressure difference ($\Delta P=P_1-P_2$), Pa
Q	net flow rate of fluid pushed aside by the needle, m^3·s^{-1}
r	radius coordinate, m
R	container radius, m
u	velocity in the system length direction, m·s^{-1}
U_t	terminal velocity of a falling needle, m·s^{-1}
π	circular constant
ρ_f	fluid density, kg·m^{-3}
ρ_s	needle density, kg·m^{-3}
γ	shear rate, s^{-1}
τ	shear stress, Pa
μ	Newton viscosity, Pa·s

References

[1] E.W. Merrill, **Physiol. Rev**. 49, 863 (1969)
[2] M.F. Kiani ,A.G. Hudez, **Biorheology** 28, 65 (1991)
[3] H.Hartert, **Flow Properties of Blood and Other Biological Systems**, Pergamon Press, Oxford, New York & Paris, (1960),pp. 186-192
[4] P. Gaehtgens, **Biorheology** 17, 183 (1980)
[5] H.Yamamoto,K.Kawamura,K.Omura,S.Tokudome, **Int.J.Thermophysics**,31,2361(2010)
[6] H. Yamamoto, **J. Chem .Eng. of Japan** 25, 803 (1995)
[7] M. J.Davis, H. Brenner , **Phys. Fluids** 13, 3086 (2001)
[8] E.G. Wehbeh, T. J. Ui, R. G., **Phys. Fluids** 8, 645 (1993)
[9] J. A. Lescarboura, G. W. Swift, **AIChE J.** 14, 651 (1968)

Use of Computer Vision and Motion Capture Technology to Determine Position of Soccer Robots

Authors: Elmo B. de Faria
University of Mato Grosso
IARA: Intelligence Artificial, Robotics and Automation Groups
http://www.ic.ufmt.br/
elmo@ic.ufmt.br

Juan F. B. Noguera
Polytechnic University of Valencia
www.upv.es
pblanes@ai2.upv.es

Claudia A. Martins
University of Mato Grosso
IARA: Intelligence Artificial, Robotics and Automation Groups
http://www.ic.ufmt.br/
claudia@ic.ufmt.br

Abstract
The propose of this study is to develop hardware and position algorithms completely integrated with the sensorial systems of robots to determine exactly the position of soccer robots in the playing field. These algorithms detail how to configure controllers to determine the movement of robots during the match.
The study initially introduces some concepts of stereo reconstruction and triangulation in Computer Vision approaching, and provides an introduction to the calibration of cameras and types of triangulation. Finally is considers a structure to integrate camera systems with the movements of robots. An Experiment is shown which calculates the distance between robots and yours position in the real world.

1-Introduction
According to Truco and Verri [6] in the visual systems of animals, including man, the process of image formation begins with light rays coming from the outside world and impinging on the photoreceptors in the retina. The process of image formation in computer vision begins with de same light rays entering the camera through an angular aperture, and light intensities are registered (figure 1).

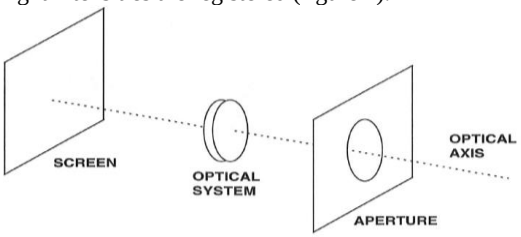

Figure 1- Elements of Imaging Device

1.1 - Camera Model
In the pinhole camera model [6][8], light enter from a scene or a distant object, but only a single ray enters from any particular point. In a physical pinhole camera, this point is then "projected" on to an imaging surface [2]. As a result, the image on this image plane (also called the projective plane) is always in focus, and the size of the image relative to the distant object is given by a single parameter of the camera: it's focal length. In the case our idealized pinhole camera, the distance from the pinhole aperture to the screen is precisely the focal length.

* Sponsored by Babel Program Erasmus Mundus

This is shown in Figure 2, where *f* is the focal length of the camera, Z is the distance from the camera to the object, X is the length of the object, and x is the object's image on the imaging plane. In the figure, we can see from the similar triangles that -x/f = X/Z, where

$$-x = f\frac{X}{Z} \qquad [1]$$

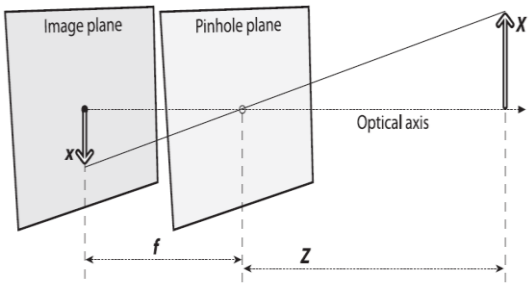

Figure 2- Pinhole Camera Model

The projection of the points in the physical world into the camera can be summarized by the following simple formula:

$$q = MQ \qquad [2]$$

where,

$$q = \begin{bmatrix} x \\ y \\ w \end{bmatrix}, M = \begin{bmatrix} f_x & 0 & c_x \\ 0 & f_y & c_y \\ 0 & 0 & 1 \end{bmatrix}, Q = \begin{bmatrix} X \\ Y \\ Z \end{bmatrix} \qquad [3]$$

Multiplying this out, we find that w = Z, and so, since the point q is in homogeneous coordinates, we should divide through by w (or Z) in order to return to equation [1]. The minus sign disappears because we are now looking at the non-inverted image on the projective plane in front of the pinhole rather than the inverted image on the projection screen behind the pinhole, (Figure 2).

1.2 - Camera Calibration
One of the main goals of computer vision is to understand the visible world by inferring 3D properties from 2D images [6]. In the context of stereo imagery, the first step that needs to be performed in the process of recovering 3D information from 2D

images is known by the term calibration. Camera calibration is the process of computing the internal camera geometric and optical characteristics, and modelling the relationship between 2D images and the 3D world. Many types of calibration methods are presented in available literature. Available literature suggests that they can be grouped into three main categories: traditional methods, self-calibration and active-motion based methods. The former method, the one that will be reviewed, is performed by observing a calibration object whose exact geometry in 3D space is known with precision. This method provided by Zhang [2] is of particular research interest, since it provides similar methodology to the one implemented by OpenCV platform, as well a common ground for data comparison.

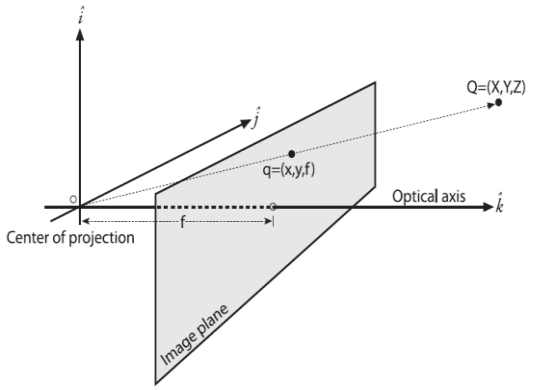

Figure 3 - Point Position in Real Space

The calibration object used in this study is a classic flat grid of alternating black and white squares that is usually called a "chessboard"(even though it need not have eight squares, or even an equal number of squares, in each direction), (Figure 4).

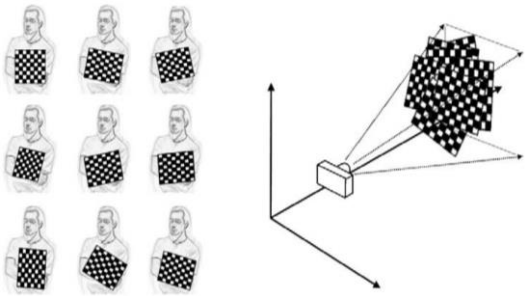

Figure 4- Chessboard Calibration Camera

Let us consider a 3D point in world coordinates $P = (X, Y, Z)^T$. We are assuming that the world reference system is known to readers. This 3D point may coincide with the center of projection of the camera (Although in general it does not need to). We shall let $P_c = (X_c, Y_c, Z_c)^T$ be the coordinates of the same point, this time in the camera reference frame, with $Z_c > 0$ if the point is to be visible. The origin of the camera frame is its center of projection, and the Z axis is the optical axis. The extrinsic parameters of the camera are then the translation vector and the rotation matrix that effect the transformation from the world point to the same point in the frame of reference of the camera [12]:

$$\begin{bmatrix} X_c \\ Y_c \\ Z_c \end{bmatrix} = R \begin{bmatrix} X_w \\ Y_w \\ Z_w \end{bmatrix} + T \qquad [5]$$

where,

$$\begin{aligned} X_c &= r_{11}X + r_{12}Y + r_{13}Z + T_x \\ Y_c &= r_{21}X + r_{22}Y + r_{23}Z + T_x \\ Z_c &= r_{31}X + r_{32}Y + r_{33}Z + T_x \end{aligned} \qquad [6]$$

Are the intrinsic parameters,

$$f_x = \frac{f}{s_x} \qquad [7]$$

is the focal length in effective horizontal pixel size units

$\alpha = \frac{s_x}{s_y}$, the aspect ratio

(o_x , o_y) , the coordinates of the image center, and

k_1 , the radial distortion coefficient.

Combining the equations, we obtain:

$$\begin{aligned} x - o_x &= -f_x \frac{r_{11}X + r_{12}Y + r_{13}Z + T_x}{r_{31}X + r_{32}Y + r_{33}Z} \\ y - o_y &= -f_y \frac{r_{21}X + r_{22}Y + r_{23}Z + T_y}{r_{31}X + r_{32}Y + r_{33}Z} \end{aligned} \qquad [8]$$

Where $f_y = \frac{f}{s_y}$ assuming that the location of the image center (o_x , o_y) is known and that radial distortion can be ignored, the difficulty that presents itself to estimate f_x , α , R, and T from image points $(x_i,y_i)^T$ which are the projection of N known world points $P_i=(X_i,Y_i,Z_i)^T$ obtained from the calibration pattern, in world coordinates.

This point in the image plane reference frame is:

$$\begin{bmatrix} x \\ y \end{bmatrix} = \begin{bmatrix} \frac{-fX_c}{s_x Z_c} + o_x \\ \frac{-fY_c}{s_y Z_c} + o_y \end{bmatrix} \qquad [9]$$

1.3- Reconstruction by Triangulation

Simple reconstruction by triangulation is possible if the intrinsic and extrinsic parameters of the stereo system are known. Let us assume that we have a perfectly undistorted, aligned, and measured stereo rig as shown in Figure 5: two cameras whose image planes are exactly coplanar with each other, with exactly parallel optical axes (the optical axis is the ray from the center of projection) that are a known

distance apart, and have equal focal lengths $f_l = f_r$. Also, let us assume for now that the principal points c_x left and c_x right have been calibrated to have the same pixel coordinates in their respective left and right images. A principal point is where the principal ray intersects the imaging plane. This intersection depends on the optical axis of the lens.

The image plane is rarely aligned exactly with the lens and so the center of the image is almost never exactly aligned with the principal point. With a perfectly undistorted aligned stereo rig and known correspondence, the depth Z can be found from the similar triangles; the principal rays of the images begin at the centers of projection O_l and O_r and extend through the principal points of the two image planes at c_l and c_r

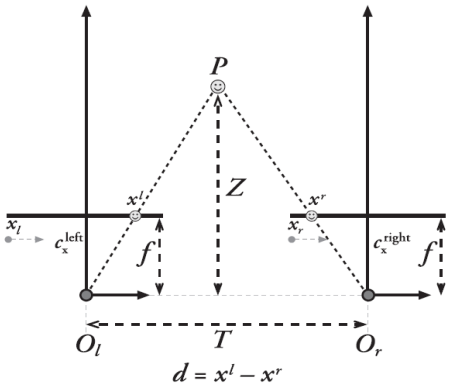

Figure 5 – Stereo Images Par

In this case, taking x_l and x_r to be the horizontal positions of the points in the left and right imager (respectively) the depth is inversely proportional to the disparity between these views, where the disparity is defined simply by $d = x_l - x_r$. This situation is shown in Figure 5, where we can easily derive the depth Z by using similar triangles. Referring to the figure 5, we have:

$$\frac{T-(x^l-x^r)}{Z-f}=\frac{T}{Z}\Rightarrow Z=\frac{fT}{x^l-x^r} \qquad [10]$$

Since depth is inversely proportional to disparity, there is obviously a nonlinear relationship between these two terms. When disparity is near 0, small disparity differences make for large depth differences. When disparity is large, small disparity differences do not change the depth by much. The consequence is that stereo vision systems have high depth resolution only for objects relatively near the camera. Figure 6 shows the 2D and 3D coordinate systems for stereo vision. Like in a right-handed coordinate system, if you point your right index finger in the direction of X and bend your right middle finger in the direction of Y, then your thumb will point in the direction of the principal ray. The left and right imager pixels have image origins at upper left in the image, and pixels are denoted by coordinates (x_l, y_l) and (x_r, y_r), respectively.

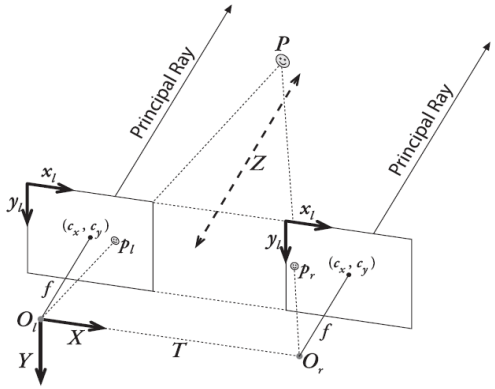

Figure 6 - Stereo Coordinate System

The center of projection is at O_l and O_r and principal rays intersect the image plane at the principal point (c_x, c_y). After mathematical rectification, the cameras are row-aligned (coplanar and horizontally aligned), displaced from one another by T, and of the same focal length f. Mathematically it is possible to find image projections and distortion maps that will rectify the left and right images into a frontal parallel arrangement. When designing your stereo rig, it is best to arrange the cameras approximately frontal parallel and as close to horizontally aligned as possible. This physical alignment makes mathematical transformations more manageable. The mathematical alignment can produce extreme image distortions and so reduce or eliminate the stereo overlap area of the resulting images. Thus we, need synchronized cameras. This is a major problem for many cameras viewing in live images. With epipolar geometry, it is possible to have located corresponding points on the two or more stereo pairs of cameras. This geometry derives from Essential and Fundamental Matrix for stereo systems.

3-Laboratory Implementation

This study presents two experiments in techniques to locate robots in the soccer field. The first presents results for two cameras in stereo systems to calculate the distance to the robots with a marker calibrator. In the second we propose a structure with six cameras for locating robots in the field during a game of soccer. These methods and materials are shown above, [9]. The robot used is the NAO standard platform league for the ROBOCUP, shown in figure 7.

NAO is a programmable, 58cm tall humanoid robot with the following key components:

- Body with 25 degrees of freedom (DOF) whose key elements are electric motors and actuators
- Sensor network, including 2 cameras, 4 microphones, sonar rangefinder, 2 IR emitters and receivers, 1 inertial board, 9 tactile sensors, and 8 pressure sensors
- Communication devices, voice synthesizer, LED lights, and 2 high-fidelity speakers

- Intel ATOM 1,6ghz CPU (located in the head) that runs a Linux kernel and supports Aldebaran's proprietary middleware (NAOqi)
- Second CPU (located in the torso)
- 27,6-watt-hour battery that provides NAO with 1.5 or more hours of autonomy,.

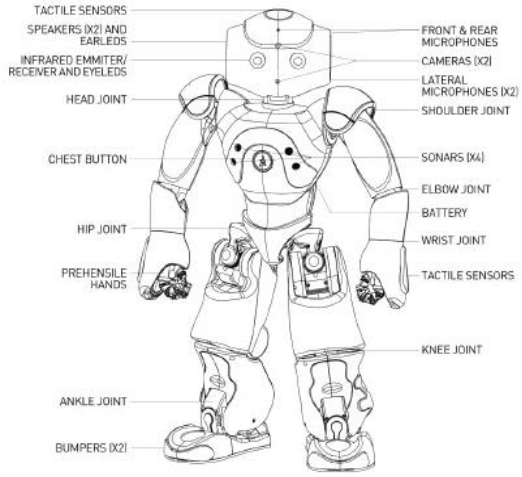

Figure 7 - NAO Soccer Robot Platform

The cameras for this experiment are the optitrack V100-R2, with specifications:

- Pixel Size : 6 µm × 6 µm
- Imager Size : 4.5 mm × 2.88 mm
- Imager Resolution : 640 × 480(0.3 MP)
- Frame Rate: 25, 50, 100 FPS
- Default Lens: 4.5mm F#1.6
    - Horizontal FOV: 46°
    - Vertical FOV: 35°

The calibration of cameras is done with OpenCV algorithms using the chessboard model shown in Figure 8. In this image OpenCV provides a convenient method for handling this common task. The function cvDrawChessboardCorners() draws the corners found by cvFindChessboardCorners() onto an image that you provide. If not all of the corners are found, the available corners will be represented as small red circles. If the entire pattern is found, then the corners will be painted in different colours (each row will have its own colour) with connected bylines representing the identified corner order.

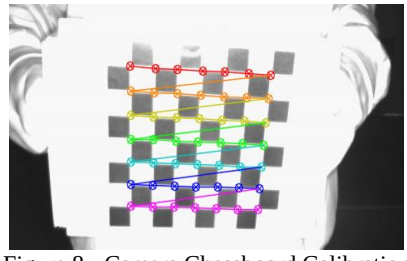

Figure 8 - Camera Chessboard Calibration

After the calibration process, other functions can use like, Stereo Correspondence and Stereo Calibration, both of which are tested in this project. A general diagram of the robotic system and the calibrated cameras is shown in figure 9. In this instance, only one robot is used to calculate the distance of the marker for future estimates of real positions in the soccer field. The robots have a constant height; in this case the Z coordinate for word systems is 60cm. To determine different positions in this axis, the bar marker is used and different distances are obtained. The positions and height of cameras up the center of the soccer field (reference XYZ in real world terms) are known. The systems propose working in real-time. This means that, when a robot walks the distance measured changes and the new position is calculated. The data are used to correct de position of the robot and to validate the embedded algorithms. These algorithms are often is a strategic player in the real game as simulated on desktops and in exhaustive tests.

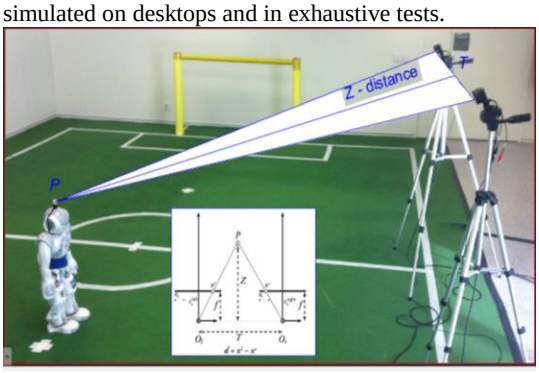

Figure 9 - General Schematic

Figure 10 illustrates in detail the image and object identification of a marker on the head of a robot. This marker is a reflective infrared object. The cameras detect this marker and convert it into XY positions for Left and Right images. Objects witch are not reflective are not detected and are discarded. Note that for both cameras 0 and 1 only de marker is detected other elements in view are ignored.

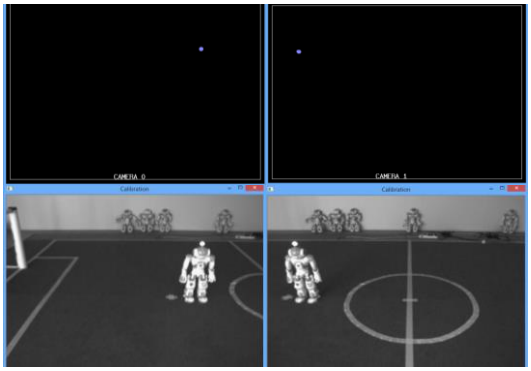

Figure 10 – Robot Image in Camera Identification

In order to estimate the distance in different height levels, a marker calibrator is used. Figure 11 shows the marker and the distance Z0, Z1, Z2 and Z3 for the stereo system.

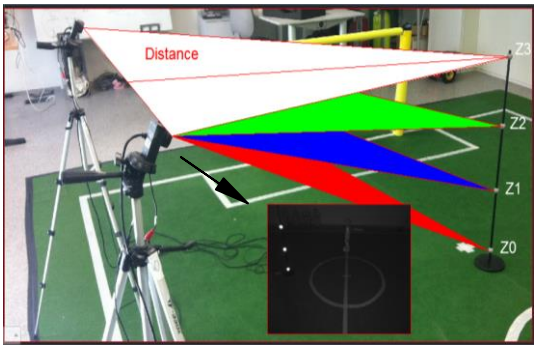

Figure 11 – Calculation of Distance and 3D Position

In another test, six cameras are used to estimate the position of robots in a simulated game of soccer. For this situation there is a new arrangement as shown in Figure 12.

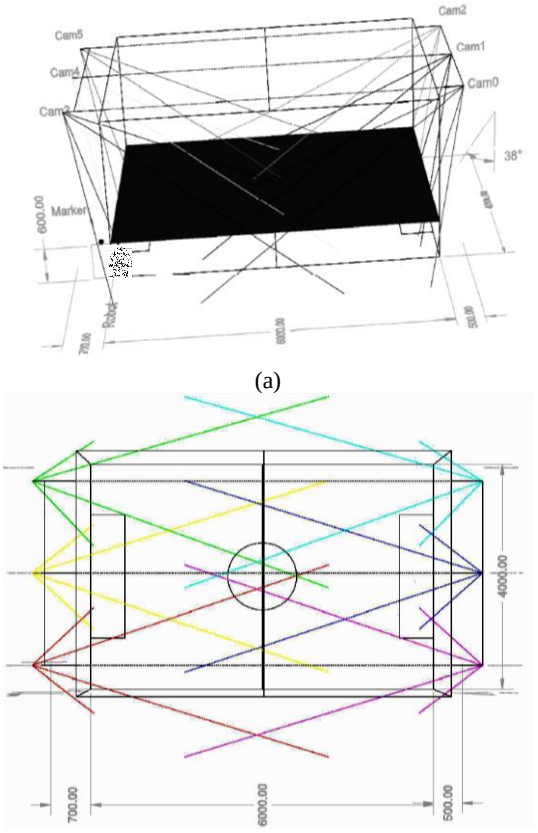

(a)

(b)

Figure 12 – (a) Reference Position System for Two Teams in a Game of Robot Soccer. (b) Top View.

All cameras are synchronized and a computer identifies and triangulates the positions of two teams of soccer robots (6 robots). This information is obtained and filed in a data file system. These files stay to be read for the robots team, [10][11].

3 - Results

Table 1, shows the estimated distance to four markers for the arrangement shown in Figure 11. The column "Calculated" shows the values obtained by calculating distance with triangle algebra. The column "Results" shows the values obtained directly from the reconstructed algorithms for triangulation. The percentage error is shown in the last column of the table.

Distance	X cam0	X cam1	Calculated	Results	Error (%)
Z0	77.02	582.18	2332.38	2545.00	2.13
Z1	60.76	599.09	2193.17	2388.00	1.95
Z2	42.59	617.42	2088.06	2236.22	1.48
Z3	22.60	636,71	2022.37	2093.76	0.71

Table 1 – Distance Results

Figure 13(a) shows the results of the calculations of distance. The data source is shown in Figure 14. The error is around 2.5% for this test. In a system like that in Figure 12, where six cameras are used, many cameras provide many different positions for markers. In this case it is possible to do calculate an average value for data and reduce the error. Figure 14 shows the software development for this project. The platform is Windows, and Visual Studio, C++ is the language used.

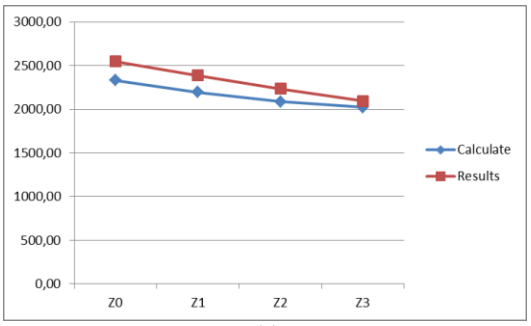

(a)

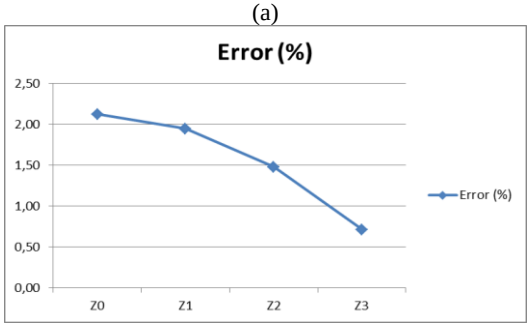

(b)

Figure 13 – (a) Distance From Position of Markers ; (b) Errors in Calculated Distances

4. Conclusions

The results obtained from the laboratory experiments show that this system is able to determine the position of robots in a soccer field. It is clear that position is more precise for robots near the center of cameras. Like in equation [8] the relation of disparity ($d = x_l - x_r$) is inversely proportional to depth. There is clearly a non-linear relationship between these two terms. When disparity is near 0, small disparity differences

make for large differences in depth. When disparity is large, small disparity differences much. The consequence is that stereo vision systems have high depth resolution only for objects relatively near to the cameras. Figure 13-(b) clearly demonstrates that errors are minor for markers near to cameras, and major for markers far from of cameras. This is less of a problem when many cameras are used because an average result can be used. Another process under investigation is the use of Neural Networks to estimate the 3D real position for robots in the soccer field.

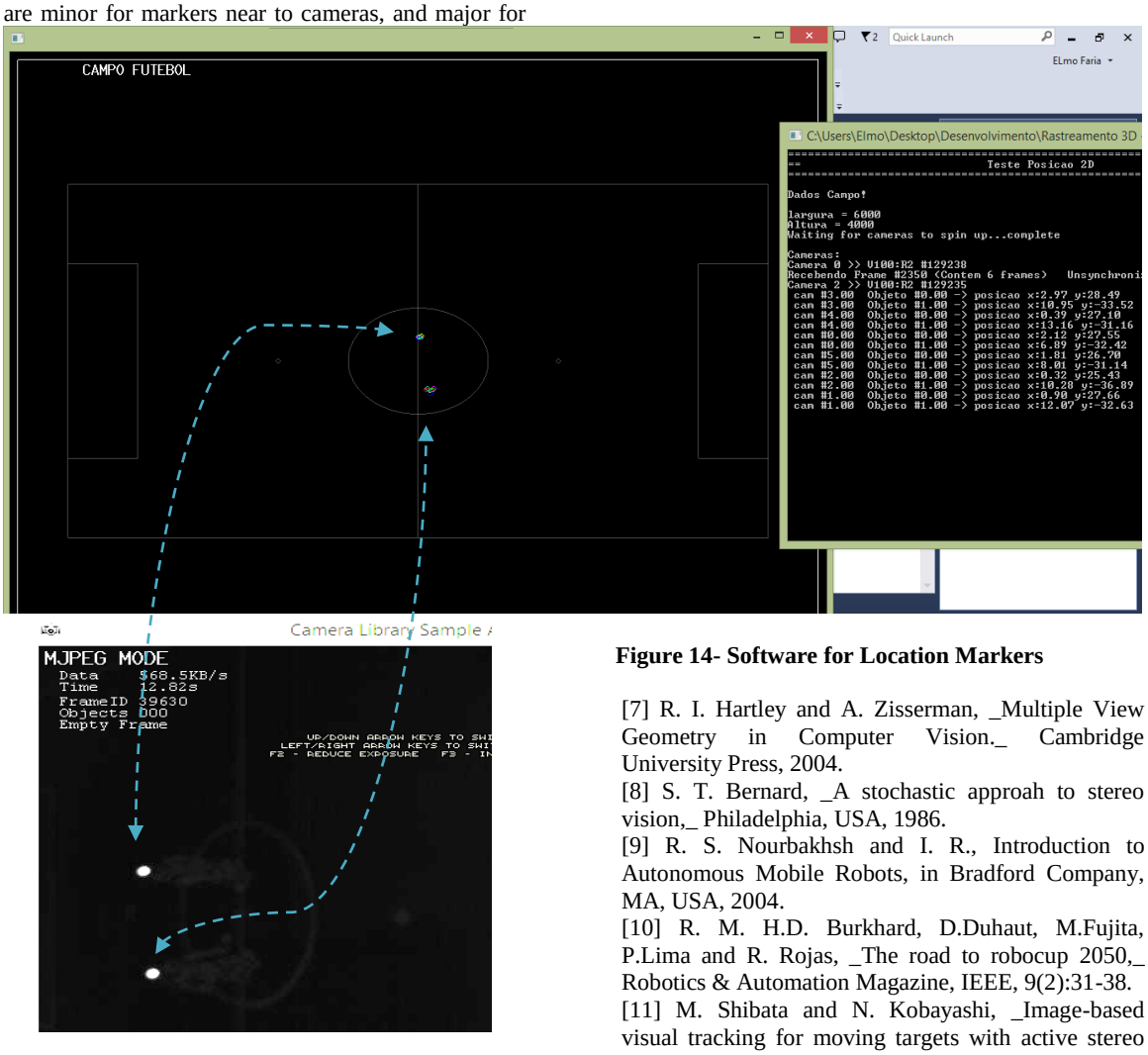

Figure 14- Software for Location Markers

5-Bibliography and References

[1] Okko H. Bosgra, Huibert Kwakernaak and Gjerrit Meinsma, “Design Methods for Control Systems”, 2009.

[2] G. Bradski and A. Kaehler. Learning OpenCV. O'Reilly Media, Inc., Sebastopol, CA, _rst edition edition, 2008.

[3] G. Burdea and P. Coi_et. Virtual Reality Technology. John Wiley & Sons, Inc, Hoboken, New Jersey, second edition edition, 2003.

[4] K. Kirby, J. Forlizzi, R. Simmons. Affective social robots. Robotics and Autonomous Systems, 2010.

[5] J. Shi and C. Tomasi. Good Features To Track. Technical report, IEEE Conference on Computer Vision and Pattern Recognition, June 1994.

[6] E. Trucco and A. Verri. Introductory Techniques for 3-D Computer Vision. Prentice Hall, Inc., Upper Saddle River, New Jersey, edition, 1998.

[7] R. I. Hartley and A. Zisserman, _Multiple View Geometry in Computer Vision._ Cambridge University Press, 2004.

[8] S. T. Bernard, _A stochastic approah to stereo vision,_ Philadelphia, USA, 1986.

[9] R. S. Nourbakhsh and I. R., Introduction to Autonomous Mobile Robots, in Bradford Company, MA, USA, 2004.

[10] R. M. H.D. Burkhard, D.Duhaut, M.Fujita, P.Lima and R. Rojas, _The road to robocup 2050,_ Robotics & Automation Magazine, IEEE, 9(2):31-38.

[11] M. Shibata and N. Kobayashi, _Image-based visual tracking for moving targets with active stereo vision robot, in SICE-ICASE, 2006. International Joint Conference, 2006, pp. 5329_5334.

[12] J. K. Yi Ma, Stefano Soatto and S. S. Sastry, _An Invitation to 3-D Vision, from images to geometric models._ in Springer, 2006.

[13] P. M. David Gallup, Jan-Michael Frahm and M. Pollefeys, Variable baseline/resolution stereo,_ 2008.

[14] S. M. Nixon, Feature Extraction in Computer Vision and Image Processing.

[15] R. I. Hartley., _Theory and Practice of Projective Rectification._ International Journal of Computer Vision, 35(2): 115-127, 1999.

[16] C. . Z. Z. Loop, _Computing Rectifying Homographies for Stereo Vision,_ in IEEE Conference on Computer Vision and Pattern Recognition, Colorado, USA, 1999.

[17] OpenCV. (Open Source Computer Vision Library). [Online]. Available: www.opencv.org.

Cooperative broadcast scheme for VANETs in OFDM wireless networks

Katsuhiro Naito
Faculty of Information Science, Aichi Institute of Technology,
1247 Yachigusa, Yakusa Cho, Toyota, 470-0392, Japan
E-mail: naito@pluslab.org
Kazuo Mori, and Hideo Kobayashi
Department of Electrical and Electronic Engineering, Mie University,
1577 Kurimamachiya, Tsu, 514-8507, Japan
Email: {kmori, koba}@elec.mie-u.ac.jp

***Abstract*— Dissemination of Emergency Safety Messages is an important function in Inter-Vehicle Communication to realize safety applications. Therefore, short delay dissemination and reliable delivery are required in Vehicular ad-hoc networks. In this paper, we have focused on the physical layer of DSRC, and have proposed a cooperative communication scheme based on OFDM modulation. Our cooperative communication scheme can realize simultaneous transmission of a same OFDM signal from some difference vehicles. From the simulation results, we can show that our scheme can achieve short dissemination delay in urban environment by simultaneous transmission.**

***Keywords*— DSRC, IEEE 802.11p, VANET, IVC, OFDM, Cooperative Communication**

I. Introduction

Vehicular ad-hoc networks (VANETs) have been focused as fundamental networks for several Intelligent Transport System (ITS) services such as collision avoidance, peer-to-peer communication, etc [1], [2]. Vehicles in VANETs construct a temporal network autonomously for Inter-Vehicle Communication (IVC). Therefore, many researches based on ad-hoc networks have been proposed for VANETs. On the contrary, dynamics of network topology due to high movement of vehicles and strict requirements for delay and reliability are special characteristics in VANETs comparing to general ad-hoc networks.

The dominant standard in VANETs is Dedicated Short-Range Communications (DSRC)[3], which uses a 5.9 GHz licensed band. In the DSRC-based IVC, multi-hop transmission is required to support large dissemination range (500 - 1000m) because a high frequency signal is not suitable for Non-Line Of Sight (NLOS) situation due to large size obstacles, buildings etc.[4], [5] Therefore, many routing protocols for VANETs have been proposed[6]. However, almost all routing protocols suffer from the high movement of vehicles, and some researchers consider the effective flooding mechanism for VANETs because it is suitable for dynamic topology change situation[7], [8]. Additionally, high frequency signals tend to be attenuated severely when Line Of Sight (LOS) is not guaranteed because they cannot penetrate obstacles such as large size trucks, buildings etc [9].

It is well known that multi-hop dissemination based on the flooding mechanism causes serious contention and collision, which become more serious when many messages are generated by multiple sources. Unfortunately, vehicles in VANETs generally transmit Periodic Beacon Messages (PBM) including vehicle's status information, e.g. position, speed, and direction. Therefore, all applications should assume large background traffic due to PBMs. Additionally, Emergency Safety Messages (ESM) should be disseminated within 500m range in a real-time manner ($\leq$ 100ms) [10] because ESMs are used for safety application such as collision avoidance etc [11], [12]. As the results, more effective dissemination mechanism is required to realize the requirement in VANETs.

IEEE 802.11p is well known as the physical layer for DSRC, which employs Orthogonal Frequency Division Multiplexing (OFDM). OFDM is a modulation technique, which is employed in IEEE 802.11a, g, WiMAX, and LTE systems [13]. In OFDM systems, receivers can demodulate some same OFDM signals within a guard interval (GI) period because OFDM receivers can remove Inter-Symbol Interference (ISI) completely by selecting a clear signal part without ISI. The authors focus on the physical modulation techniques to solve difficulty of efficient dissemination mechanisms for VANETs

in this paper because we have considered the cooperative communication system based on OFDM[14].

This paper proposes the cooperative communication system for VANETs. The new idea of this paper is employing multiple transmission of same OFDM signals to disseminate information effectively because same OFDM signals can be demodulated in OFDM when the signals arrive within a GI period. From the simulations, we evaluate the performance of our cooperative communication system in VANETs comparing to a basic flooding mechanism, and clarify that our system can be realizing the short dissemination delay and scalability in urban environment for VANETs.

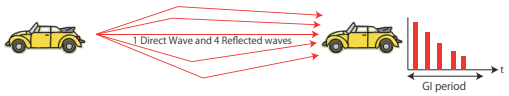

Fig. 1. OFDM communication.

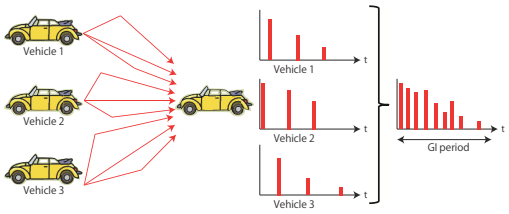

Fig. 2. Cooperative communication.

II. OFDM Cooperative Communication

A. Overview

OFDM is the one of the multi-carrier modulation scheme that employs various sub-carriers for data transmission. The benefit in OFDM is high tolerance for multi-path fading by adding a guard interval (GI) because OFDM receivers can mitigate ISI effect by clipping out a clear signal part without overlapped adjacent signal parts. Therefore, OFDM is recently used in various wireless communication systems, eg. WiFi, WiMAX, LTE etc. IEEE 802.11p for VANETs also employs OFDM because it is an extended standard based on IEEE 802.11a.

Fig. 1 shows the symbol transmission in OFDM systems. Generally, a transmitter copies the end part of the OFDM symbol and adds it as a GI. Then, it transmits the GI part and the OFDM symbol part together. At a receiver, some reflected waves generally arrive with the directed wave. The multiple reflected waves depend on a channel impulse response. These reflected waves generally cause inter-symbol interference in wireless systems because the adjacent signals overlapped each other. However, OFDM receivers can demodulate the OFDM symbol when the maximum delay of the reflected waves is within the GI period because the receivers can clip out the whole OFDM signal without ISI by cut the GI period off.

The idea of the proposed cooperative communication is to employ simultaneous transmission of same OFDM signals because same OFDM signals can be deemed as multiple signals in a multi-path fading environment. Therefore, some vehicles in the cooperative communication transmit a same OFDM symbol at same instance like as Fig. 2. Therefore, a receiver can receive a direct wave and some reflected waves from different transmitters, and can demodulate these waves when they arrives within the GI period. The benefits of our cooperative communication scheme are achieving effective usage of wireless resources by transmitting an OFDM symbol simultaneously and obtaining a route diversity gain by transmitting from different vehicles. As the results, our scheme can realize a short dissemination delay and a high delivery ratio.

B. Flowchart

Fig. 3 is the flowchart of the media access control in the cooperative communication. The challenge in the cooperative communication for multi-hop networks is how to synchronize a transmission timing among transmitters autonomously. Therefore, the time synchronization is sometimes difficult because some method requires a bit synchronization. On the contrary, the proposed cooperative communication based on OFDM requires time synchronization in a GI period, which is 1,600 [ns] in IEEE 802.11p. Therefore, the requirement for the time synchronization is not strict comparing to the conventional work.

In the proposed media access control, we employ a Carrier Sense Multiple Access/Collision Avoidance (CSMA/CA) as a basic control method, and extend it to support a group CSMA/CA among transmitters because nodes should handle various packets from different sources. Generally, CSMA uses a random back-off period to distribute transmission timing of each node autonomously. Hence, nodes select a different random back-off period and transmit a packet at different timing according to the selected back-off period. In the proposed media access control, each vehicle should select a same random back-off period to synchronize a same OFDM signal autonomously. The procedures of the proposed scheme are described as follows.

- The procedures start when vehicles receive a packet from neighbor vehicles.

- Vehicles confirm the packet forwarding history to avoid a redundant forwarding because we assume message dissemination for ESM and avoid the forwarding loop of the packet.
- Vehicles initialize the Back-Off Index (BOI) that determines the maximum number of contention window size CW_{max}, where CW_{min} is the minimum number of contention window size. CSMA/CA generally handles the BOI value according to retransmission process. However, this paper uses the initial BOI value because retransmission for the assumed ESM dissemination is not performed.
- Vehicles calculate the maximum number of contention window size according to the initialized BOI value. The maximum number of contention window size denotes the interval period for the back-off period (BOP). The BOP is generally selected randomly with uniform distribution in CSMA/CA. But, is is selected randomly with the next process in the proposed media access control.
- We can select a random value consciously because random value is generally generated by a predefined random sequence in software. Therefore, Vehicles in the proposed cooperative communication generate a random value with the source ID, the hop count information and the sequence number of data packets for each vehicle as random seeds. Hence, vehicles can obtain a unique random value according to the source ID, the hop count information and the sequence number of data packets, and vehicles that receive the same OFDM signal can select the same random back-off periods. As the results, each vehicle can synchronize the transmission timing among neighbor forwarding vehicles autonomously. The benefits of this procedure are that vehicles can synchronize a transmission timing autonomously and they can distribute a transmission timing according to a received packet information.
- Vehicles sense a channel status after the selection of the initial BOP value and select two operations: retrying channel sensing for a busy status and checking the BOP value for an idle status.
- Vehicles start to transmit the OFDM signal when the BOP value is zero. Otherwise, they decrease the BOP value and wait for the transmission timing.

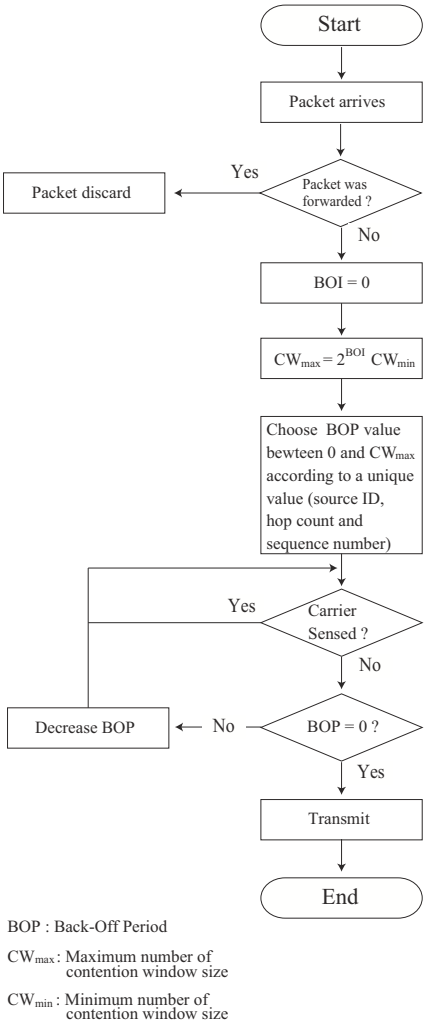

Fig. 3. Flowchart of cooperative communication.

III. Numerical results

We perform the simulation to evaluate the performance of the conventional CSMA/CA and the proposed cooperative communication by QualNet. As the application, we assume emergency safety service such as collision avoidance. Therefore, one of vehicles transmits an ESM to whole vehicles in the simulation area. In the simulation, the flooding mechanism is used to disseminate ESM to the whole network because several routes over streets are required due to many buildings.

Fig. 4 is the assumed urban area map. There are two big avenues and eight small streets in the map. The length of each avenue and street is 750 [m]. One hundred vehicles are randomly located for each avenue, and twenty vehicles are randomly located for each street. Therefore, 360 vehicles are located in the map. During the each ESM transmission, all vehicles do not move because the movement is especially

TABLE I

SIMULATION PARAMETERS.

Simulator	QualNet
Simulation time	730 [s]
Simulation trial	10 [times]
Simulation Area	750 [m] × 750 [m]
Wide of avenue	45 [m]
Wide of street	20 [m]
Number of vehicles	360 [vehicles]
Vehicle velocity	static
Size of ESM	100 [Byes]
Traffic of ESM	0.6, 0.75, 1, 1.5, 3, 6 [ESM/s]
Communication device	IEEE 802.11p
Transmission rates	6 [Mbps]
Transmission power	19 [dBm]
Channel frequency	5.9 [GHz]
Antenna gain	0 [dB]
Antenna type	Omni directional
Antenna height	1.5 [m]
Propagation path loss model	Two-ray ground reflection model
Wireless environment	AWGN

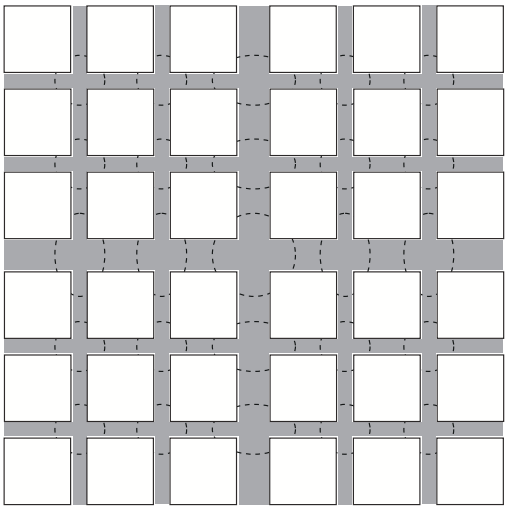

Fig. 4. City map in simulations.

small within the transmission period. We change the traffic rate of ESM from 0.6 to 6 [ESM/s]. The detail simulation parameters are shown in Tab. I.

Fig. 5 shows the dissemination delay performance. The results of CSMA/CA show that the delay in the same avenue is longer than that in the same street because the avenues have a lot of vehicles comparing to the streets. Additionally, the delay increases according to the traffic increase because more wireless resource is required for flooding process. The delay in the cross avenue and street is longer than those

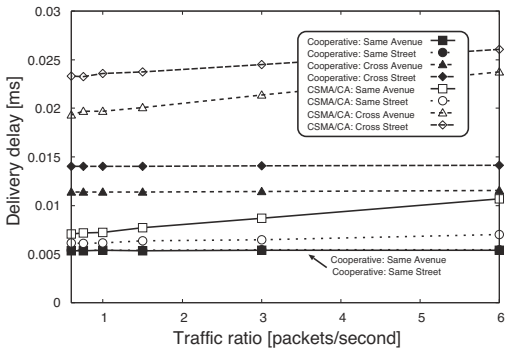

Fig. 5. Delay performance.

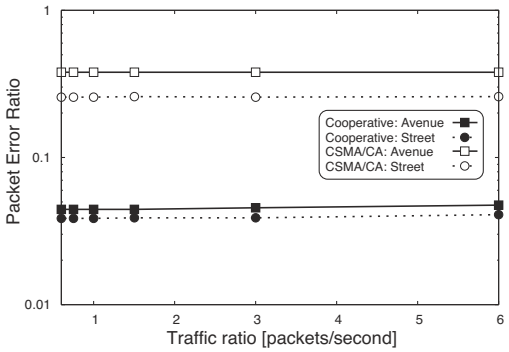

Fig. 6. Packet error ratio.

in the same avenue and the same street because LOS is difficult to be realized due to buildings. The results of the cooperative communication scheme show that the delay in the same avenue is almost same in the same street because some vehicles can transmit a same ESM simultaneously. Therefore, the delay does not increase according to the traffic increase. Moreover, the delay in the cross avenue and the cross street can be reduced comparing to those with CSMA/CA because our scheme can reduce the required wireless resource and can reduce forwarding delay.

Fig. 6 is the packet error ratio performance. The results of CSMA/CA show that the packet error ratio in the avenues is larger than that in the streets because the density of vehicles in the avenues is higher than that in the streets. Therefore, more packet collisions occur in the avenues. From the results of the cooperative communication scheme, we can find that the packet error ratio is quite smaller than that with CSMA/CA because vehicles can transmit a same OFDM packet simultaneously and can decode the packet within the GI period successfully. Hence, a lot of packet transmission do not cause

a big interference to reception of packets.

Fig. 7 is the definition of packets in the proposed cooperative communication. In these figures, vehicle 1 and vehicle 6 transmit their own data packet. Vehicles 2, 3 and 4 forward the packet from vehicle 1. As the results, vehicle 5 can receive 4 packets. In this paper, we define the packet type based on the effect to the communication. At first, the packet from vehicle 4 arrives at vehicle 5 at first. Therefore, we define this packet as a first packet. Then, vehicle 5 receives the packet from vehicle 3. This packet arrives at vehicle 5 within GI period, and does not cause any interference to the packet from vehicle 4. We define this packet as a duplicated packet. The packet from vehicle 2 arrives at vehicle 5 after GI period. This packet causes an interference to the packets from vehicle 3 and 4. Therefore, we classify this packet as a non-duplicated packet even in the packet data is same. Finally, the packet from vehicle 6 is the different packet from vehicle 1. We define this packet as an interference packet because it causes interference to the packets from vehicle 2, 3 and 4.

Fig. 8 shows the interference packet reception performance. From the results, we can find that the performance of CSMA/CA is the large number of packet receptions and that of the cooperative communication is the small number. This is because, many packets over CSMA/CA operation cause a big interference to communication. On the contrary, small number of packets over the cooperative communication cause a small interference because vehicles can reduce transmission period by transmitting a same OFDM packet simultaneously. Additionally, the reception ratio of the cooperative communication increases slowly according to the increase of the traffic. The reason is the remained wireless resource also reduces according to the traffic increase, and the probability of simultaneous transmission of different packets will also increase.

Fig. 9 shows the duplicated packet reception performance in the cooperative communication. This type of packet is defined in the proposed scheme, not in CSMA/CA because duplicated packets also cause an interference in general wireless systems. From the results, various duplicated packets are received in the proposed scheme. The multiple receptions of duplicated packets can improve the packet reception ratio by increasing the reception power and the diversity effect. Finally, we can find that our proposed media access control can handle accurate synchronization of packet transmission autonomously.

Fig. 10 is the packet reception performance of non-duplicated packets in the cooperative communication. This

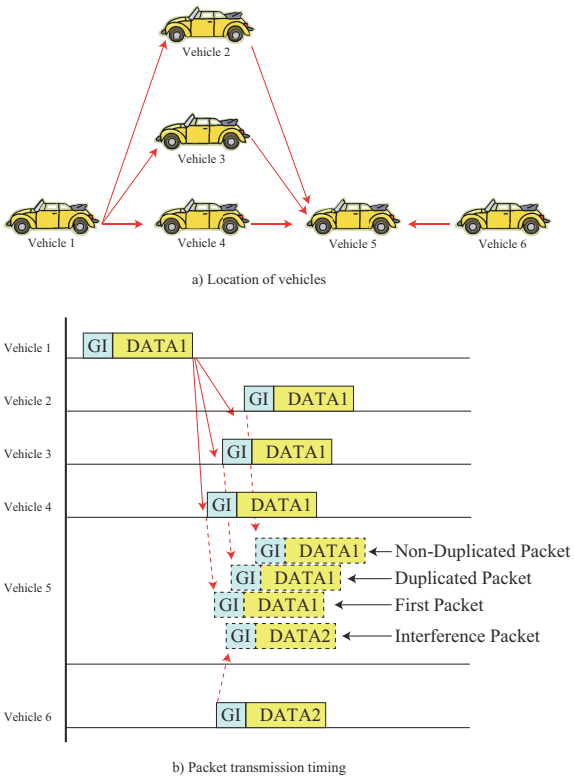

Fig. 7. Definition of packet types.

type of packet is also defined in the proposed scheme. From the results, we can find that the number of non-duplicated packets is the small number. The non-duplicated packets occur when subset of forwarding vehicles delay the transmission timing due to an interference from neighbor vehicles. However, we can obtain the benefit of the simultaneous transmission because the number of non-duplicate packets is especially smaller than that of the duplicated packets.

IV. Conclusion

This paper has focused the characteristics of OFDM communication scheme, and has proposed the cooperative communication for VANETs. In the evaluation, we can find that our proposed synchronization scheme performs well to achieve the cooperative communication by selecting a random back-off period. Additionally, our cooperative communication scheme can achieve short dissemination delay for whole area including a same street and cross streets in VANETs.

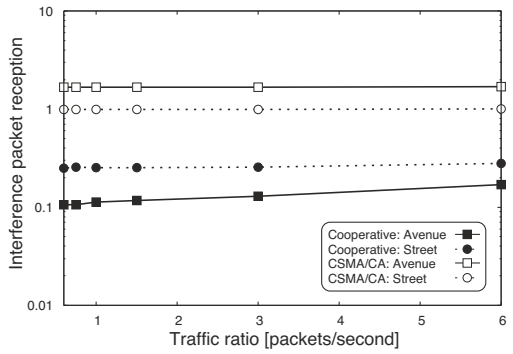

Fig. 8. Interference packet reception.

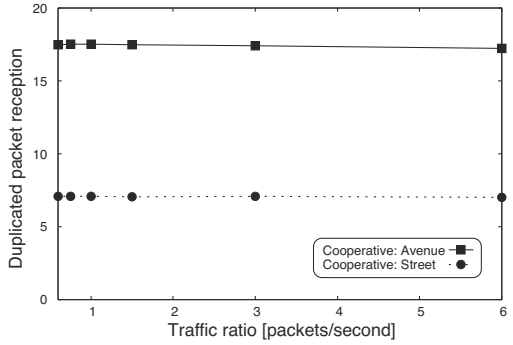

Fig. 9. Duplicated packet reception.

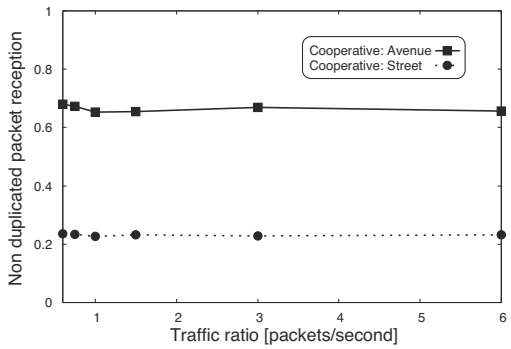

Fig. 10. Non-duplicated packet reception.

ACKNOWLEDGMENT

This work is supported in part by Grant-in-Aid for Young Scientists (B)(23700075) and Grant-in-Aid for Scientific Research (C) (26330103) Japan Society for the Promotion of Science (JSPS).

REFERENCES

[1] V. Naumov, R. Baumann, T. Gross, "An evaluation of inter-vehicle ad hoc networks based on realistic vehicular traces," ACM MobiHoc '06, pp. 108–119, May 2006.

[2] J. Mittag, F. Thomas, J. Härri, and H. Hartenstein, "A comparison of single- and multi-hop beaconing in VANETs," ACM VANET '09, pp. 69–78, Sep. 2009.

[3] IEEE Standard for Information Technology Telecommunications and Information Exchange Between Systems Local and Metropolitan Area Networks Specific Requirements; Part 11: Wireless LAN Medium Access Control (MAC) and Physical Layer (PHY) Specifications; Amendment 6: Wireless Access in Vehicular Environments, IEEE Std. 802.11p, Jul. 2010.

[4] Rex Chen, Jin Wen-Long and A. Regan, "Broadcasting safety information in vehicular networks: Issues and Approaches", IEEE Networks, vol.24, Issue 1, pp.20–25, Jan. 2010.

[5] G. Resta, P. Santi and J. Simon, "Analysis of Multi-Hop Emergency Message Propagation in Vehicular Ad Hoc Networks", ACM MOBIHOC 2007.

[6] M. Naghshvar and T. Javidi, "Opportunistic Routing with Congestion Diversity in Wireless Multi-hop Networks," in Proc. of the IEEE Conference INFOCOM 2010, Nov. 2010.

[7] C.-F. Chiasserini, R. Gaeta, M. Garetto, M. Gribaudo and M. Sereno, "Efficient Broadcasting of Safety Messages in Multihop Vehicular Networks", IEEE IPDPS 2006.

[8] F. J. Ros, P.M. Ruiz and I. Stojmenovic, "Acknowledgment-based Broadcast Protocol for Reliable and Efficient Data Dissemination in Vehicular Ad-hoc Networks", IEEE Transactions on Mobile Computing, vol.11, issue 1, pp.33–46, Jan. 2012.

[9] R. Meireles, M. Boban, P. Steenkiste, O. Tonguz, J. Barros, "Experimental study on the impact of vehicular obstructions in vanets," in Vehicular Networking Conference (VNC), Dec. 2010, pp. 338–345.

[10] The CAMP Vehicle Safety Communications Consortium, "VSC-A Task 3 Final Project: Identify Intelligent Vehicle Safety Applications Enabled by DSRC", Technical Report, Mar. 2005.

[11] Zhe Wanget and M. Hassan "How Much of DSRC is Available for Non Safety User?", Proc. ACM VANET 2008 pp. 23 – 20, 2008.

[12] J. Yin, T. ElBatt, G. Yeung, B. Ryu, S. Habermas, H. Krishnan and T. Talty, "Performance Evaluation of Safety Applications over DSRC Vehicular Ad Hoc Networks", Proc. ACM VANET, pp. 1–9, 2004.

[13] IEEE Standard for Information Technology Telecommunications and Information Exchange Between Systems Local and Metropolitan Area Networks Specific Requirements; Part 11: Wireless LAN Medium Access Control (MAC) and Physical Layer (PHY) Specifications, Mar. 2012.

[14] K. Naito, K. Mori and H. Kobayashi, "OFDM cooperative flooding mechanisms for Multi-hop networks," The 5th International Multi-Conference on Engineering and Technological Innovation (IMETI 2012), Jun. 2012.

Implementation of IPv4/IPv6 Translation Mechanisms for BIS and NAT64 Router

Katsuhiro Naito
Faculty of Information Science, Aichi Institute of Technology,
1247 Yachigusa, Yakusa Cho, Toyota, 470-0392, Japan
E-mail: naito@pluslab.org
Keisuke Sugita, Yuta Inoue, Kazuo Mori, and Hideo Kobayashi
Department of Electrical and Electronic Engineering, Mie University,
1577 Kurimamachiya, Tsu, 514-8507, Japan
Email: {kmori, koba}@elec.mie-u.ac.jp

***Abstract*— IPv6 addresses will be only assignable address in the near future because IPv4 addresses are almost exhausted. Therefore, almost all operation systems can support IPv6 communication. On the contrary, some conventional applications do not still support IPv6 addresses and users will suffer from the unavailability of IPv6-oriented applications. As the results, translation mechanisms for IPv4-oriented applications are still required in practical usages. Bump-In-the-Stack (BIS) mechanism is a candidate smooth transition method from IPv4 to IPv6 networks because it allows hosts to communicate with other hosts through IPv6 networks using existing IPv4-oriented applications. In this paper, we have designed a kernel module for IPv4/IPv6 translation mechanisms for Linux OS, and have implemented it with Linux Netfilter functions. The developed translation mechanism supports a host operation, where the hosts can communicate by IPv4 address over IPv6 networks, and a router operation, where hosts can communicate by IPv4 address via the developed router. From the experimental results, our implementation can realize high throughput without overhead of translation.**

***Keywords*— Bump-In-the-Stack; NAT64; Kernel module; Address translation; Linux; Router.**

I. Introduction

The Asia-Pacific Network Information Center (APNIC) had announced that the APNIC pool for IPv4 address range had reached its final /8 IPv4 address block [1]. This means that IPv6 address range will be only available in the near future for new address assignment.

IPv6 is the well known network layer protocol for the next generation Internet and its address space is 128 bit. Almost all network venders have tried to implement an IPv6 stack in recent products. Therefore, Internet infrastructures are becoming to support IPv6 communication. On the contrary, some conventional IPv4 applications do not support IPv6 due to suspend of maintenance, expensively rewrite cost for IPv6, etc. The authors consider that the replacement from IPv4 to IPv6 is not easy because IPv4 devices and services have continued to be widespread. Hence, network address translation (NAT) mechanisms will be required to communicate between IPv4 and IPv6 networks [2], [3].

One of the solution for these issues is a translation mechanism between IPv4 and IPv6 addresses [4]. Dual-stack lite requires an IPv6 access network and tunnels between a host and a Network Address Port Translation (NAPT) 44 device, which is operated by service providers [5]. The idea of the dual-stack host is to transfer IPv4 packets through the tunnel between the host and the NAPT 44 device. Therefore, IPv4 packets can be routed through the tunnel even if the access network is IPv6. Additionally, the host can send its IPv6 traffic because its access network is IPv6. Generally, the dual-stack lite requires hosts to be assigned both IPv4 and IPv6 address. Therefore, the assignment of IPv4 address will be difficult in the near future because new IPv4 addresses will have been exhausted.

NAT64 and NAT-PT [6], [7], [8] are translation mechanisms where the host runs only IPv6. They are called large-scale NATs (LSNs) or carrier grade NATs. Recent NAT64 devices can serve a translation function to 10,000 subscribers, but their scalability will be limited due to the expansion of network traffic. In addition, the translations have several technical issues [9].

We have developed the host translation mechanism based on Bump-In-the-Stack (BIS) approach, which allows hosts to communicate with other IPv6 hosts using existing IPv4 applications [10]. Our fundamental implementation of the address translation mechanism can achieve high throughput performance by packet processing in kernel space. In this paper, we have implemented the translation mechanism for DNS messages in kernel space. Additionally, our implementation supports address translation for a host and a network. We

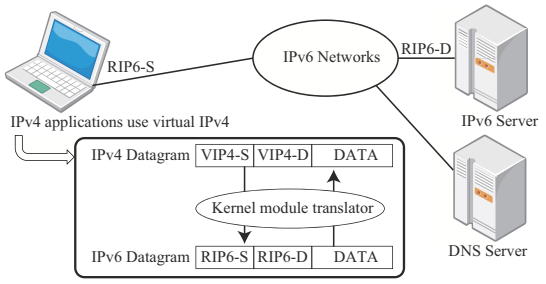

Fig. 1. Overview (Host based translation).

employ Linux netfilter [11] to handle packets in Linux kernel. Therefore, our developed kernel module can be installed easily without any modification of Linux kernel code. From the numerical results, we can find that our implementation can achieve high throughput by processing packets in kernel space.

II. Host based translation mechanism

A. Overview

Fig. 1 shows the overview communication of the host based translation between IPv4 and IPv6 addresses. According to the BIS mechanisms, we employ a virtual interface based on tun/tap on the host for a virtual IPv4 address, which is used by IPv4 oriented applications. Therefore, each IPv4 application creates an IPv4 datagram with a virtual IPv4 source address and a virtual IPv4 destination address. The virtual IPv4 destination address is assigned based on a DNS 'AAAA' reply message, and is informed by a DNS 'A' reply message. In the translation module, the IPv4 datagram is converted into the IPv6 datagram with a real IPv6 source address and a real IPv6 destination address.

Fig. 2 shows the system model of host based translation. The functions are classified into the address translation function and the DNS message translation function. The kernel module can handle a socket buffer by using Linux netfilter function. Therefore, the developed kernel module can be easily installed without any modification of kernel code.

B. Virtual Interface

IPv4-oriented applications require an IPv4 address to use an IPv4 socket. In the proposed system, the system prepares a virtual network interface with a virtual IPv4 address. The virtual IPv4 address is used as a source address in the IPv4-oriented applications.

The proposed implementation uses tun/tap interface to create a virtual network interface. Tap is well known software emulation of ethernet devices and tun is also software emulation of a network layer. Therefore, tap interface is usually used to create a bridge interface and tun interface is used for creating network tunnels. On the contrary, the purpose of the virtual interface in the proposed implementation is to assign a virtual IPv4 address for IPv4 applications. Therefore, the virtual interface does not receive any packets from IPv4 applications because the developed kernel module hooks all packets from IPv4 applications to the virtual interface. As the results, we can employ both tun/tap interface as the virtual interface.

C. Packet hook mechanism

The developed kernel module employs Netfilter framework in Linux, which is a packet manipulation framework. Netfilter provides a set of hook functions for exchanging a socket buffer between the Linux network stack and a kernel module. Therefore, the kernel module can register its own callback functions when packets traverse the respective hook points, and it can send back the packets to the network stack. Netfilter is a useful framework because these kernel modules can modify packet information without any modifications of Linux kernel code.

The developed kernel module uses four hook points such as NF_INET_LOCAL_OUT, NF_INET_LOCAL_IN, NF_INET_POST_ROUTING and NF_INET_PRE_ROUTING. NF_INET_LOCAL_OUT and NF_INET_LOCAL_IN are the hook points for outbound packets and inbound packets for IPv4-oriented applications respectively. NF_INET_POST_ROUTING and NF_INET_PRE_ROUTING are the hook points for outbound packets and inbound packets for physical network interfaces.

D. Assignment of virtual IPv4 address

IPv4-oriented applications require two IPv4 addresses such as an IPv4 source address and an IPv4 destination address to construct a connection. The IPv4 source address $VIP4-S$ is assumed to be predefined and is assigned to the virtual network interface. The IPv4 destination address $VIP4-D$ should be selected according to a real IPv6 address. Therefore, the kernel module assigns $VIP4-D$ corresponding to the real IPv6 address $RIP6-D$ when a DNS reply message is received. The virtual IPv4 address range is assumed to be a private address space, and is used internally in the operating system.

E. Translation of DNS messages

- Resolution of Fully Qualified Domain Name (FQDN)
  In the proposed mechanism, all IPv4-oriented applications use the DNS mechanism to solve an IP address from FQDN when they start communication. Therefore, the DNS resolver creates a DNS A query message to solve the target FQDN.

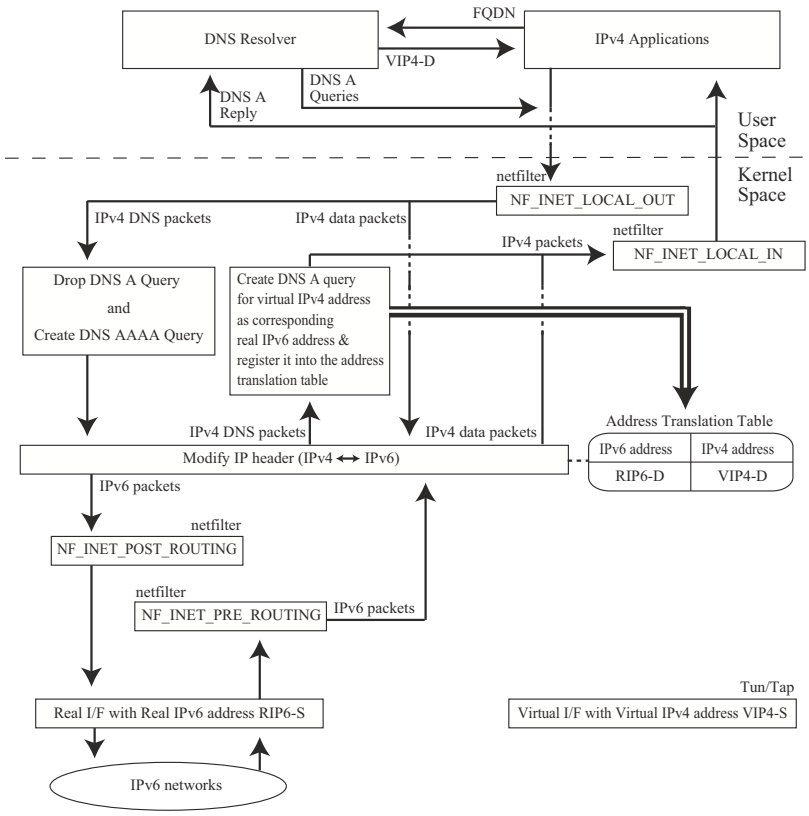

Fig. 2. System Model (Host based translation).

- Translation from DNS A query to AAAA query
  The host should transmit a DNS AAAA query message to solve the FQDN because the real interface has only IPv6 address. Therefore, the kernel module translates the DNS A query message to the DNS AAAA query message.
- Creation of a virtual IPv4 address
  The kernel module should assign a new virtual IPv4 address corresponding to the real IPv6 address in the DNS AAAA reply message. Therefore, it checks the DNS AAAA reply message from IPv6 networks, and creates a new virtual IPv4 address for the DNS A reply message.
- Registration of the IPv4/v6 address pair
  The information about the pair of virtual IPv4 address and the real IPv6 address is used to translate a header information between IPv4 and IPv6. Therefore, the information is registered into the address translation table.
- Response of virtual IPv4 address
  The kernel module creates the DNS A reply message corresponding to the DNS AAAA reply message and the pair information in the address translation table. Therefore, the DNS resolver can receive the DNS A reply message including the virtual IPv4 address for the target FQDN. As the results, the IPv4-oriented application can obtain a virtual IPv4 address without any modifications in the application code. The IPv4-oriented application can communicate with the IPv6 host using the virtual IPv4 source address $VIP4-S$, paired with the virtual IPv4 destination address $VIP4-D$, while the host can communicate with the IPv6 server host using the real IPv6 source address $VIP6-S$, paired with the real IPv6 destination address $VIP6-D$.

F. Translation of IPv4/IPv6 addresses

The kernel module handles transmitted IPv4 packets from IPv4 applications as a socket buffer in Linux network stack, and translates the IP header format because IPv4 and IPv6 have a different packet structure. The translation is performed to the socket buffer of each packet directly. Therefore, the translation overhead is small because memory copy is not required.

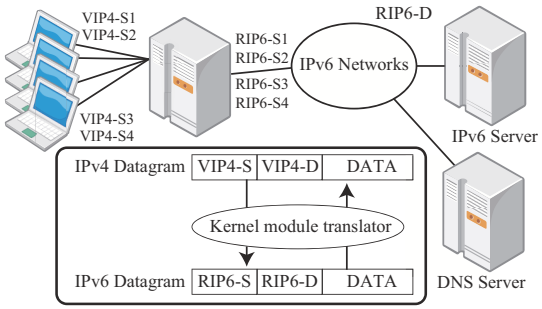

Fig. 3. Overview (Router based translation).

III. Router based translation mechanism

A. Overview

Fig. 3 shows the overview communication of the router based translation between IPv4 and IPv6 networks. The router based translation generally requires scalability because it can support many client IPv4 hosts. Our translation procedures are implemented in Linux kernel space. Therefore, our implementation design is suitable for the router based translation, which requires high throughput performance. In the router based translation, a virtual IPv4 source address is assigned to each client by Dynamic Host Configuration Protocol (DHCP) or manually. The translation router has many real IPv6 source addresses corresponding to the virtual IPv4 source addresses. Similar manner in the host based translation, the translation router assigns a virtual IPv4 destination address based on a DNS 'AAAA' reply message, and informs it by a DNS 'A' reply message. As the results, each client creates an IPv4 datagram with an assigned virtual IPv4 source address and an informed virtual IPv4 destination address. The translation router translates the IPv4 datagram to the IPv6 datagram with the real IPv6 source address and the real IPv6 destination address.

Fig. 4 shows the system model of the router based translation. The developed kernel module also employs Netfilter framework in Linux. The developed kernel module uses two hook points such as NF_INET_POST_ROUTING and NF_INET_PRE_ROUTING. NF_INET_POST_ROUTING and NF_INET_PRE_ROUTING are the hook points for outbound packets and inbound packets for physical network interfaces. Therefore, the kernel module can handle the packet between these hook points.

B. Assignment of virtual IPv4 address

The router based translation mechanism should assign a virtual IP address to each client host. The assignment process can be achieved by DHCP or manually. The developed router has many IPv6 addresses corresponding to each virtual IP address and one IPv4 address for a gateway address. The host set the gateway address as the default gateway. Therefore, all IPv4 packets can be received by the developed router. The virtual IPv4 address range is assumed to be a private address space, and is used internally in the local network.

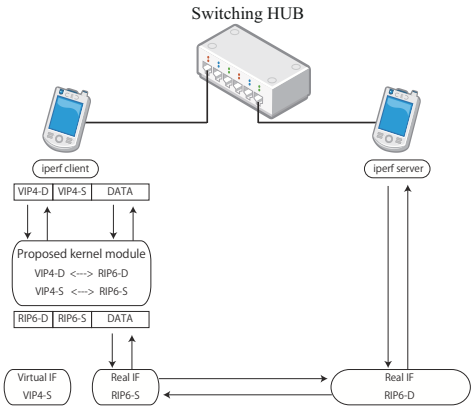

Fig. 5. Experimental model (Host based translation).

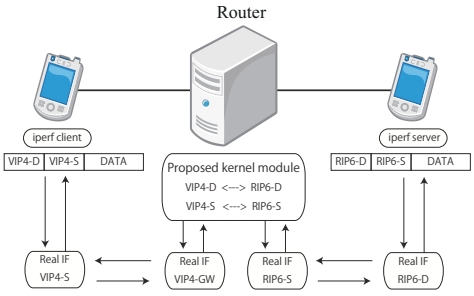

Fig. 6. Experimental model (Router based translation).

C. Translation of IPv4/IPv6 addresses

The difference between the host based translation and the router based translation is information in the address translation table. In the host based translation, a virtual IPv4 source address is fixed because the address is assigned to the virtual network interface. On the contrary, each client host in the router based translation has its own virtual IP address. Therefore, the router should manage the virtual IPv4 addresses for source and destination addresses and the real IPv6 addresses for source and destination addresses respectively.

IV. Experimental results

We have performed the experimental trials to evaluate the performance of our implementation. Figs. 5 and 6 show the evaluation models of the host based translation and the router based translation respectively. In the experiment, two hosts

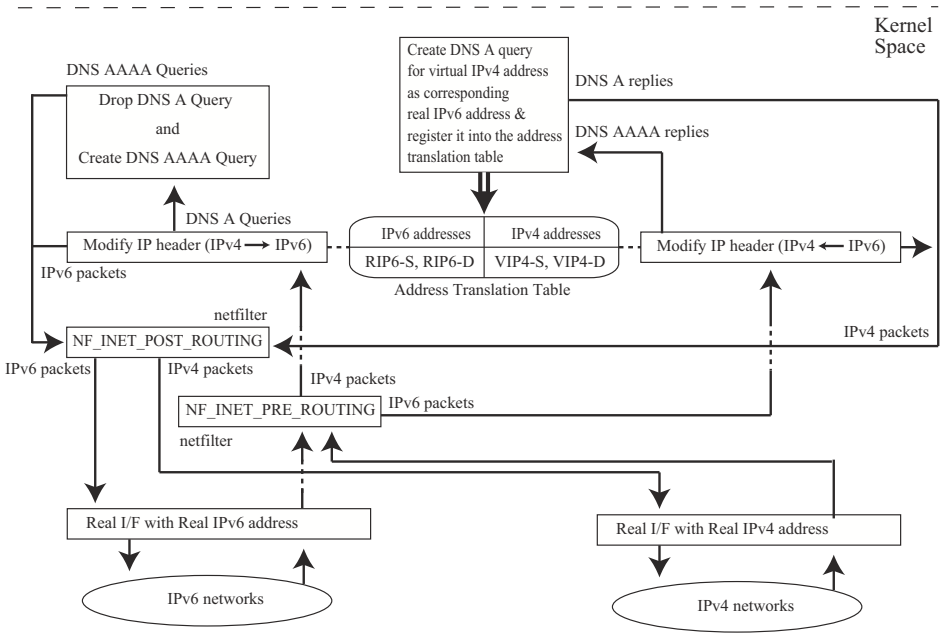

Fig. 4. System Model (Router based translation).

TABLE I

PERFORMANCE EVALUATION PARAMETERS.

OS	Linux
Distribution	Ubuntu 10.04
Kernel version	linux-2.6.32-24-generic
CPU	Intel Pentium 4 2.40GHz
Memory	512 MBytes
Network	Ethernet 100Mbps
Application	iperf
Size of transferred data	100 MBytes
Transport protocol	TCP
Number of measurement	10

TABLE II

TRANSLATION DELAY FOR DNS MESSAGE.

Proposed	Default IPv6
843.3 [μs]	793.1 [μs]

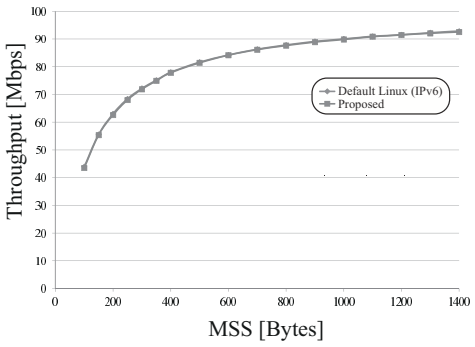

Fig. 7. Throughput (Host based translation).

communicated with each other through the developed kernel module. In the trials, we used iperf [12], which is the well-known network benchmark tool. The virtual interface was constructed by tun during the measurements in the experiment of the host based translation. Throughput overhead may depend on Maximum Segment Size (MSS) size because the ratio of header size to total packet size will be larger when the MSS size decreases. Therefore, we evaluated the throughput of certain sizes of MSS. As the comparison, we have evaluated the throughput performance of IPv4 and IPv6 communication with default Linux kernel without the developed kernel module. Details of the evaluation parameters are given in Table I.

Fig. 7 shows the throughput performance of the host based translation. The results show that the throughput of our implementation and that of general Linux OS are almost same because our translation processing is performed in the kernel space. Therefore, there is no overhead due to memory copy between the user space and the kernel space. The reason for reducing of throughput at small MSS size is the overhead of the IP header.

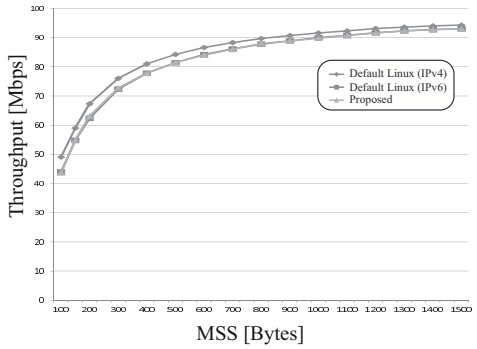

Fig. 8. Throughput (Router based translation).

Fig. 8 shows the throughput performance of the router based translation. The results show that our implementation can realize high throughput performance even if the packet forwarding is required as a router function. In the practical usage, many client hosts will be connected to the router to communicate with IPv6 networks. The overhead with increasing of client hosts is searching process for the address translation table. However, the overhead will be small because the implementation of the searching process employs hashing method. From the results, we can find that our implementation can achieve the best throughput of the hardware by processing in kernel space.

Tab. II shows the translation delay of DNS message. The delay in the evaluation includes the DNS resolver processing, the translation delay in the proposed mechanism, the network propagation delay and DNS server processing. Therefore, the translation delay is about 50 [μs]. From the results, we can find that the overhead of the DNS translation is not big because DNS resolution is performed only at an initial phase of communication.

V. Conclusion

This paper extends our translation mechanisms to support BIS and NAT64 router functions. Our implementation is designed as Linux kernel module by using Linux netfilter function. Therefore, our kernel module is easy to install to Linux kernel without modification of Linux OS, and achieves high throughput performance by processing packets in kernel space. From the experimental trial, we can find that our implementation can realize the best performance of the hardware.

Acknowledgment

This work is supported in part by Grant-in-Aid for Young Scientists (B)(23700075) and Grant-in-Aid for Scientific Research (C) (26330103) Japan Society for the Promotion of Science (JSPS).

References

[1] http://www.apnic.net/publications/news/2011/final-8, retrieved: Dec., 2011.
[2] D. Wing, “Network Address Translation: Extending the Internet Address Space,” IEEE Internet Computing, Vol. 14, No. 4, pp. 66 – 70, July-Aug. 2010.
[3] E. Nordmark and R. Gilligan, “Basic Transition Mechanisms for IPv6 Hosts and Routers,” IETF RFC 4213, Oct. 2005.
[4] Y. Xia, B. S. Lee, C. K. Yeo, and V. L. S. Seng, “An IPv6 Translation Scheme for Small and Medium Scale Deployment,” 2010 Second International Conference on Advances in Future Internet (AFIN), pp. 108 – 112, Jul. 2010.
[5] A. Durand, R. Droms, J. Woodyatt, and Y. Lee, “Dual-Stack Lite Broadband Deployments Following IPv4 Exhaustion,” IETF draft, May 2011.
[6] M. Bagnulo, P. Matthews, and I. van Beijnum, “NAT64: Network Address and Protocol Translation from IPv6 Clients to@IPv4 Servers,” IETF draft, Mar. 2009.
[7] G. Tsirtsis and P. Srisuresh, “Network Address Translation - Protocol Translation (NAT-PT),” IETF RFC 2766 Feb. 2000.
[8] F. Baker, X. Li, C. Bao, and K. Yin, “Framework for IPv4/IPv6 Translation,” IETF draft Aug. 2010.
[9] C. Aoun and E. Davies, “Reasons to Move the Network Address Translator - Protocol Translator (NAT-PT) to Historic Status,” IETF RFC 4966, Jul. 2007.
[10] K. Tsuchiya, H. Higuchi, and Y. Atarashi, “Dual Stack Hosts using the ”Bump-In-the-Stack” Technique (BIS),” IETF RFC 2767, Feb. 2000.
[11] http://www.netfilter.org, retrieved: Dec. 2011.
[12] http://iperf.sourceforge.net, retrieved: Dec. 2011.

Enhanced MAC-based Efficient Message Authentication Scheme over VANET

Taeho Shin
Department of Computer Engineering, Kyungil University
Kyungbuk, Korea

Jaeyoon Jung and Hyunsung Kim*
***(Corresponding Author) Department of Cyber Security, Kyungil University**
Kyungbuk, Korea

and

Sung-Woon Lee
Department of Information Security, Tongmyong University
Busan, Korea

ABSTRACT

Vehicular ad-hoc network (VANET) provides various services for vehicles through wireless communications. Rhim recently proposed a MAC-based efficient message authentication scheme for VANET. However, this paper shows that Rhim's scheme is not secure against replay attack and proposes an enhanced scheme to solve the problem in Rhim's scheme.

Keywords: VANET, Message Authentication, Session Freshness, and Security.

1. INTRODUCTION

Vehicular ad-hoc network (VANET) provides various services for vehicles through the communications of vehicular to vehicular (V2V) and vehicular to infrastructure (V2I) in order for vehicles to operate in a safe and comfortable way. Since vehicles engaging in VANET receive many services, they can run with safety and efficiency. Offering and using various services require safe and reliable V2V and V2I communications, and therefore many studies on the subject have been conducted [1-3]. The security mechanisms in VANET should provide correctness of sender of message and integrity of the transmitted messages. Furthermore, privacy should be also provided in VANET focused on the identity and location of vehicles [4]. Most of the existing researches used a public key based encryption system to provide secure and reliable communications. However, according to dedicated short range communication (DSRC) protocol on VANET, a vehicle should transmit and identify many messages within a short time so that a great number of operations take place. Moreover, when a vehicle is required to communicate with a server, the DSRC is notable to guarantee the connection with the server at all times.

Recently, Rhim proposed a MAC-based efficient message authentication scheme over VANET to address the problem which is that public key based authentication scheme causes large operations [5].

However, this paper shows that Rhim's scheme is not secure against replay attack and proposes an enhanced scheme to solve the problem in Rhim's scheme, which is message authentication code (MAC) based authentication scheme using symmetric keys. The proposed scheme uses tamper resistant hardware (TRH) with symmetric key cryptosystem due to the symmetric key based authentication scheme does not provide broadcasting authentication. The proposed scheme makes all vehicles of a group maintain the same symmetric key, which is protected through TRH, to provide broadcasting authentication. Any issued symmetric keys should be regularly updated for the security reason. To update the keys, our system uses a different communication from DSRC in the process of issuing and updating symmetric keys, which does not guarantee that a vehicle can always communicates with a server [6]. The proposed scheme provides privacy in which the messages transmitted by a vehicle do not include any identification information of the vehicle. Furthermore, it does not only meet all security requirements of VANET including message authentication, integrity, non-repudiation, and conditional anonymity, but also satisfy all requirements for strong privacy protection, including anonymity and unlinkability.

2. REVIEW OF RHIM'S SCHEME

This section reviews Rhim's MAC-based efficient message authentication scheme, which is composed of vehicle registration phase, message authentication phase, group key updating phase, vehicle identification phase and group key request phase, and provides security analysis focused on the message authentication phase of Rhim's scheme. Table 1 defines notations used in this paper.

Table 1. Notations

Notation	Description
VID	Vehicle's real identity
PID	Vehicle's pseudo identity
T	Timestamp
K_G	Group key
K_V	Individual vehicle's secret key
$MAC_K()$	Message authentication function by using the key K
$\{M\}_K$	Symmetric key encryption by using the key K

2.1 Rhim's Scheme

It is assumed in Rhim's scheme that vehicle tamper resistant hardware (TRH) has previously physical identity received from the on board unit (OBU) and individual vehicle received from the trusted authority (TA) is stored. The operation of TRH is an agreed to stop the TRH KILL message is present.

[Vehicle registration phase]
This phase is required only once for a vehicle V to register to a certain group as follows :

R1) V submits $\{VID, T\}_{KV}$ and VID to GTA to join a group governed by it, where $\{VID,T\}_{KV}$ denotes that VID and T are encrypted by using the key K_V.
R2) After receiving the message from V, GTA checks it's vehicle list, revocation list, and new vehicle list. It finishes the protocol if VID is in the revocation list. It stores the vehicle information into the vehicle list and transmits new registration notification message to TA only if VID is in the new vehicle list. After receiving the message from GTA, TA informs the new registration notification message to all GTAs and GTA removes the vehicle information from the new vehicle list.
R3) GTA decrypts the message $\{VID, T\}_{KV}$ by using K_V stored in the new vehicle list and check integrity of VID. It transmits $\{PID, K_G, T\}_{KV}$ and T to V if the integrity check is successful.
R4) After receiving the message from GTA, V decrypts the message $\{PID, K_G, T\}_{KV}$ by using K_V and checks the integrity of T. It stores PID and K_G into TRH only if the integrity check is successful.

[Message authentication phase]
This phase is for the message authentication between vehicles in a same group.

A1) Sender V_i computes $\mu=MAC_{KV}(M)$ and $MAC_{KG}(M||\mu)$.
A2) It broadcasts M, μ and $MAC_{KG}(M||\mu)$.
A3) After receiving the message, receiver V_j computes $MAC_{KG}(M||\mu)$ by using the received M and μ and the stored K_G, and checks the integrity of the received $MAC_{KG}(M||\mu)$. It authenticates the message only if the integrity check is successful. Otherwise, it destroys the message.

[Group key updating phase]
This phase is performed regularly in a certain time-interval based on the timer on TRH to update group key as follows :

U1) V sends $\{PID, T\}_{KV}$ and PID to GTA.
U2) After receiving the message from V, GTA checks it's vehicle list, revocation list, and new vehicle list. It finishes the protocol if PID is in the revocation list. It updates the database table with new PID' and K_G' and transmits $\{PID', K_G', T\}_{KV}$ to V.
U3) After receiving the message from GTA, V decrypts the message $\{PID', K_G', T\}_{KV}$ by using K_V and checks the integrity of T. It replaces PID and K_G into PID' and K_G' on TRH only if the integrity check is successful.

[Vehicle identification phase]
This phase is to check the identification of the message sender by GTA.

I1) GTA checks the identification of the message by verifying M in $MAC_{KV}(M)$ using the vehicle key in the vehicle list.
I2) It informs VID to TA for the revocation of the vehicle if the vehicle needs to be revoked.
I3) TA informs VID to all GTAs for the revocation and each GTA adds VID to the revocation list.

[Group key request phase]
This phase is invoked if a vehicle moves from a group to another one.

M1) When a vehicle enters into an overlapped area between groups, V in GTA_1 sends $\{PID, T\}_{KV}$ and PID to GTA_2.
M2) After receiving the message from V, GTA_2 sends PID to GTA_1 via secure channel.
M3) GTA_1 sends VID, PID and K_V to GTA_2 via secure channel.
M4) After receiving the message from GTA_1, GTA_2 checks VID. It finishes the protocol if VID is in the revocation list. Otherwise, it checks the integrity of PID by decryption the message $\{PID, T\}_{KV}$ from V by using the received K_V from GTA_1.
M5) GTA_2 sends $\{PID', K_G', T\}_{KV}$ and T to V only if the integrity check is successful.

2.2 Security Analysis of Rhim's Scheme

Rhim argued that his scheme is strong against security threats but his scheme is weak against replay attack due to the lack of freshness in the message. The replay attack is a form of network attack in which a valid data transmission is maliciously or fraudulently repeated or delayed by an adversary.

Sender V_i broadcasts $\{M, \mu, MAC_{KG}(M||\mu)\}$ to neighbor vehicles at A2 in the message authentication phase. The integrity of the message is only depending on the checking of M and μ from $MAC_{KG}(M||\mu)$. However, this message is weak against the replay attack because the message does not provide any way to provide freshness. That means that there is no way to reject the message if an attacker captures and retransmits the message. Thereby, neighbor vehicles could not detect the replay from any attacker. This is enough to make neighbor vehicles to be confused.

3. ENHANCED MAC-BASED MESSAGE AUTHENTICATION SCHEME

This section proposes an enhanced MAC-based message authentication scheme to solve the replay attack problem in Rhim's scheme. The enhanced scheme also is composed of five phases including vehicle registration phase, message authentication phase, group key updating phase, vehicle identification phase and group key request phase as shown in Fig. 1 to Fig. 5. However, we will only focus on the message authentication phase in detail because all other phases should be the same.

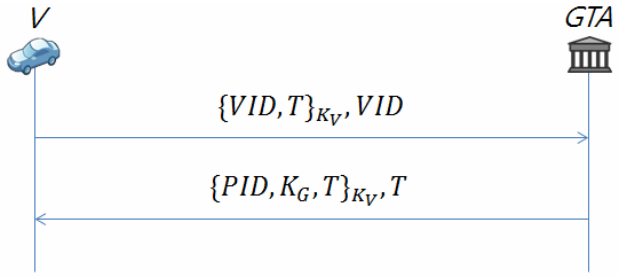

[Fig. 1] Vehicle registration phase

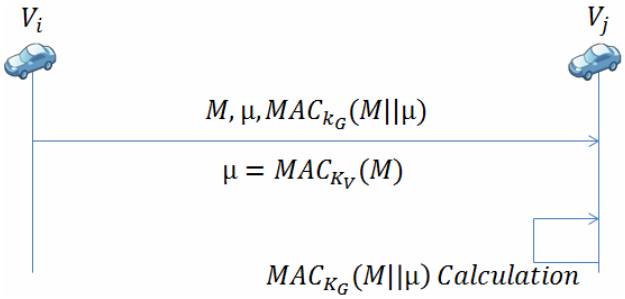

[Fig. 2] Message authentication phase

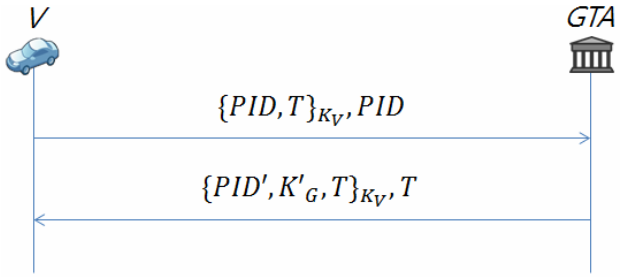

[Fig. 3] Group key updating phase

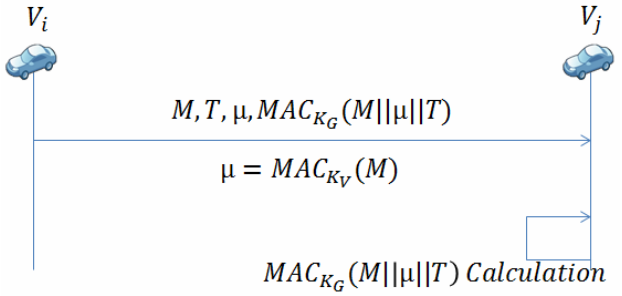

[Fig. 4] Vehicle identification phase

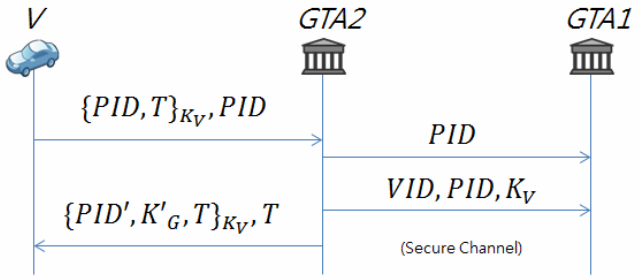

[Fig. 5] Group key request phase

[Message authentication phase]
The way to solve the replay attack is to provide freshness in the message. The basic format of this phase is very similar with the Rhim's one but we could add timestamp to provide the freshness of the message. This phase is for the message authentication between vehicles in a same group.

MA1) Sender V_i computes μ=$MAC_{KV}(M)$ and $MAC_{KG}(M||\mu||T)$.
MA2) It broadcasts M, μ, T and $MAC_{KG}(M||\mu||T)$.
MA3) After receiving the message, receiver V_j computes $MAC_{KG}(M||\mu||T)$ by using the received M and μ and T and the stored K_G, and checks the integrity of the received $MAC_{KG}(M||\mu||T)$. It authenticates the message only if the integrity check is successful. Otherwise, it destroys the message.
MA4) The freshness of T is checked by performing T'-$T \leq \Delta T$, where T' is the current system clock of V_i and ΔT is the expected time interval of a transmission delay. If T in the message has a valid time interval, integrity check is successful.

4. SECURITY ANALYSIS

This section provides security analysis focused on the message authentication, replay attack resilience, and privacy focused on the anonymity and untraceability.

[Safety Message Authentication]
The message authentication is provided by using message authentication code in each sessions' message, $MAC_{KG}(M||\mu||T)$. It is the message digest from the combination of the message M, the MAC μ of M, and the clock T. The vehicle could form a secure message Msg={ M, μ, T, $MAC_{KG}(M||\mu||T)$}. Upon receiving the message, each checks the validity of T and the integrity of $MAC_{KG}(M||\mu||T)$. If they are successful, the receiver believes that the message is secure.

[Resistance to Replay Attacks]
Replay attack is a form of network attack in which a valid data transmission is maliciously or fraudulently repeated or delayed. This is carried out either by the originator or by an adversary who intercepts the data and retransmits it, possibly as part of a masquerade attack. The proposed scheme uses system clock T and message authentication code to against from the replay attack. Sender V_i broadcasts {M, μ, T, $MAC_{KG}(M||\mu||T)$} to neighbor vehicles at MA2 in the message authentication phase. The integrity of the message is depending on the system clock and $MAC_{KG}(M||\mu||T)$. There is no way to form the proper message to an attacker without knowing K_G even if he (she) could intercept and know the information of M, μ and T from the transmitted message. Thereby, our scheme could provide security against the replay attack by provide freshness of the message.

[Resistance to Privacy Attacks]
Privacy is the ability of an individual or group to seclude themselves or information about themselves and thereby express themselves selectively [7]. There are two issues related with the privacy in security concern, which are anonymity and untraceability. The proposed scheme uses *PID* instead of *VID*, which changes in each session regularly. Thereby, an attacker could not know the identity of the sender by just intercepting the messages. Furthermore, there are no relations between sessions from a specific participant due to the usage of K_G and K_V, respectively. So, an attacker could not get any relations between sessions. That's why our scheme could provide privacy.

5. CONCLUSIONS

This paper showed that Rhim's scheme is not secure against replay attack and proposed an enhanced MAC-based message authentication scheme to solve the problem in Rhim's scheme. The proposed scheme uses symmetric keys and based on TRH. The proposed scheme provides privacy in which the messages transmitted by a vehicle do not include any identification information of the vehicle. Furthermore, it does not only meet all security requirements of VANET including message authentication, and conditional anonymity, but also satisfy all

requirements for strong privacy protection, including anonymity and unlinkability.

6. ACKNOWLEDGEMENTS

This work was supported by the National Research Foundation of Korea Grant funded by the Korean Government (MEST) (NRF-2010-0021575) and also was supported by the National Research Foundation of Korea Grant funded by the Korean Government (MEST) (NRF-2011-0008890).

7. REFERENCES

[1] H. Hartenstein, K, Laberteaux, **VANET Vehicular Applications and Inter-Networking Technologies**, Wiley, 2009.

[2] S. Al-Sultan, M. M. Al-Doori, A. H. Al-Bayatti, H. Zedan, "A comprehensive survey on vehicular Ad Hoc network", **Journal of Network and Computer Applications**, http://dx.doi.org/10.1016/j.jnca.2013.02.036, 2013.

[3] H. Kim, "Routing Scheme based on Vehicle Density and Expected Expiration Time over VANET", **Journal of Security Engineering**, Vol. 9, No. 5, 2012, pp. 459-468.

[4] D. A. Rivas, J. M. Barceló-Ordinas, M. G. Zapata, J. D. Morillo-Pozo, "Security on VANETs: Privacy, misbehaving nodes, false information and secure data aggregation", **Journal of Network and Computer Applications**, Vol. 34, No. 6, 2011, pp. 1942-1955.

[5] W. W. Rhim, **A Study on MAC-based Efficient Message Authentication Scheme for VANET**, M. S. Thesis, Hanyang University, 2012.

[6] http://en.wikipedia.org/wiki/Dedicated_short-range_communications.

[7] http://en.wikipedia.org/wiki/Privacy.

Development of Infrastructure for Precise Time Transmission

Vladimir SMOTLACHA
CESNET
Prague, Czech Republic

and

Josef VOJTECH
CESNET
Prague, Czech Republic

ABSTRACT

The paper describes the optical infrastructure for highly precise time transfer in the Czech Republic. It interconnects atomic clocks and supports time comparison between them. Specific issue is the bidirectional optical amplification required for some of time transfer methods. The paper presents our experiments with distributed optical amplification.

Keywords: Time transfer, optical network, optical amplifiers, atomic time.

1. INTRODUCTION

Very accurate timing is essential in many areas of human activity, for example in metrology, navigation, geodesy, astronomy including radio-astronomy, earth survey, seismology, fundamental physics, etc. Traditional radio frequency transmission of accurate time over satellites, for example GPS (Global Positioning System) is reaching its limits. More accurate TWSTFT (Two Way Satellite Time and Frequency Transfer) method is very expensive as it requires a dedicated channel at a geostationary satellite. However, optical transfer over fiber link can provide even better accuracy and stability and is becoming subject of intensive research. There were developed techniques utilizing one-way transfer or two-way transfer in either single fiber or pair of fibers. We can observe increased number of both theoretical studies and practical field implementations.

This paper describes design of dedicated optical infrastructure for time and frequency transfer (TF-infrastructure) in the Czech Republic. The TF-infrastructure uses resources provided by existing Czech academic network CESNET. The network utilizes DWDM (Dense Wavelength-Division Multiplexing) technology which provides end-to-end optical path and eliminates conversion from optical to electrical domain and vice versa. It allows us to implement time and frequency transfer at physical layer in dedicated optical channels that are isolated each to other.

2. MOTIVATION

The design of TF-infrastructure is based on our preliminary experience with time transfer between Czech and Austrian national time and frequency laboratories UFE and BEV [1], whose regular operation has started in August 2011.

TF-infrastructure is designed as a heterogeneous platform that covers many current and near future tasks of involved organizations. The goals include:

- Time transfer from deployed Cesium primary standards and Hydrogen masers to the national time and frequency laboratory in UFE. Higher number of these interconnected clocks will improve accuracy and stability of UTC(TP), the national approximation of UTC time scale.
- Comparison of the national approximation of UTC with that one in neighboring countries.
- Checking of accuracy and stability of other connected atomic clocks.
- Distribution of accurate time and stable frequency to demanding users.
- Obtaining of experience with the coherent frequency transfer as a preliminary activity aimed at intended building of optical clock.

Fig. 1 shows current state of the TF-infrastructure: it joins four organizations that operate atomic clocks and another two organizations that use atomic time scale or frequency from remote source. The topology is determined by existing DWDM network extended by dedicated dark fiber links. The TF-infrastructure includes also links to neighboring countries Austria and Poland. The link to BEV in Vienna is in use and connectivity to the Polish network is ready for future usage, for instance setting up time transfer channel to Polish laboratories GUM (Warsaw) or AOS (Borowiec).

3. TIME TRANSFER METHOD

Basic idea is following: two adapters (A and B) transfer their local time to opposite site. They are connected either by a bidirectional optical link (single fiber), or a pair of unidirectional fibers. In the first case, there must be used two different wavelengths, while it is preferred the same wavelength in both directions in the second case. Each adapter is provided by 1PPS (1 Pulse per Second) signal from local clock and has an output representing received 1PPS signal from the opposite site. Time interval counter (TIC) measures the interval x_A (resp. x_B) between local and remote 1PPS. The schematic is shown in Fig. 2.

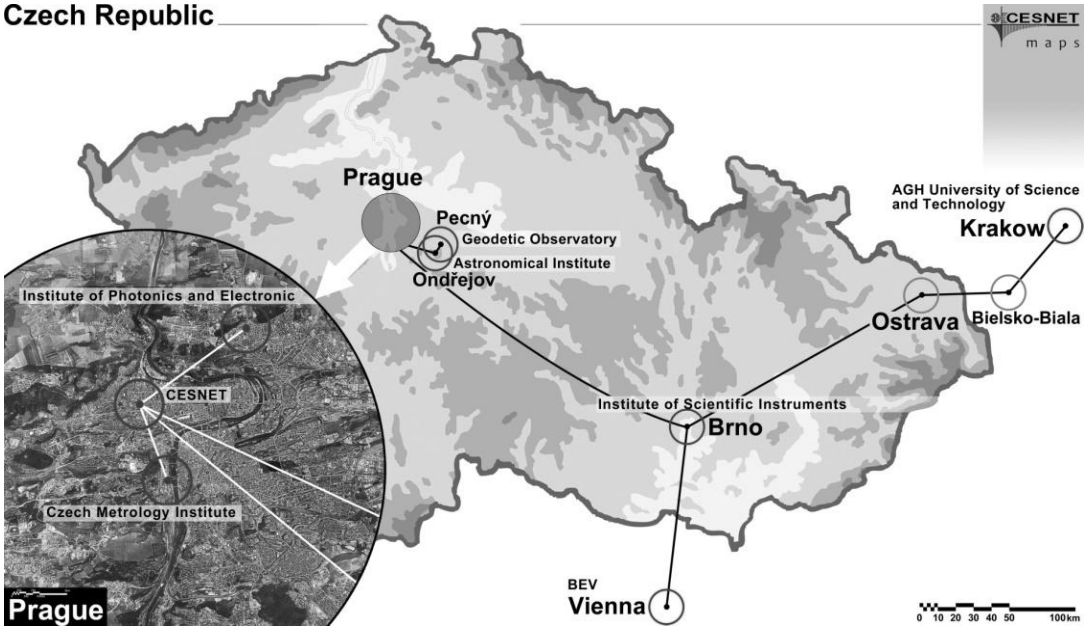

Figure 1 Map of the TF-infrastructure

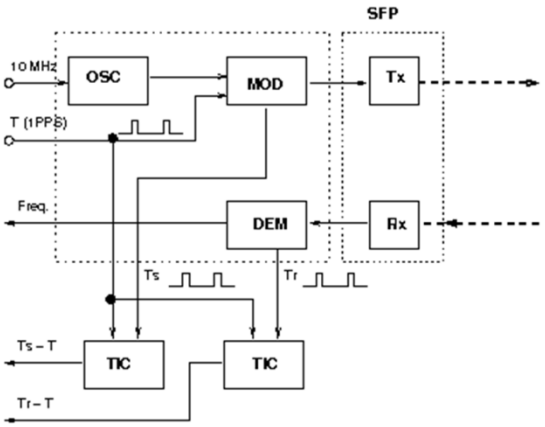

Figure 2 Time transfer adapter

On a fiber pair with identical physical length and wavelengths, the delay in both directions equals: $\delta = \delta_{AB} = \delta_{BA}$. In real network, the fiber length in both directions slightly differs (e.g. due to patch cords in switching boards, fibers compensating the chromatic dispersion), introducing delay asymmetry Δ:

$$\Delta = \delta_{BA} - \delta_{AB}. \quad (1)$$

The delay asymmetry Δ has to be measured by an independent method and is subject of system calibration.

In case of single bidirectional fiber, the physical length is equal, however the propagation delay, which is done by the refractive index, depends on the wavelength. The delay difference can be estimated by Eq. (2):

$$\Delta = D_{fiber} \cdot \Delta\lambda \cdot L. \quad (2)$$

D_{fiber} is fiber chromatic dispersion coefficient, $\Delta\lambda$ is wavelength difference and L is physical length of the fiber. Eq. (2) allows us to avoid calibration of the transfer system, however its uncertainty must be considered. The uncertainty of Δ depends on several other physical effects, e.g. polarization mode dispersion, thermal dependency of refractive index of directionally disjoint paths (patchcords and filters), thermal dependency of fiber chromatic dispersion coefficient, and filters central wavelength thermal dependency. Detailed analysis is done for instance in [2].

Regardless of single fiber or fiber pair setup, the clock offset Θ_{AB} is calculated using the same formula:

$$\Theta_{AB} = (x_A - x_B - \Delta) / 2. \quad (3)$$

Values x_A and x_B are measured every second. These data are than processed, for instance to reduce white phase noise introduced by time interval counters.

4. TECHOLOGY

The TF-infrastructure physical topology is a star with center in CESNET point of presence in Prague, while the transport layer topology is a star having center in Institute of Photonics and Electronics (UFE). Both localities are interconnected by DWDM link providing 16 bidirectional channels. Links between CESNET and involved organizations utilize the available technology, in most cases it is a combination of commercial and open DWDM transmission systems:

- Pair of channels (with the same wavelength in both directions) in an operational DWDM optical network.
- Pair of DWDM channels with different wavelengths in single fiber bidirectional transmission system.
- Pair of DWDM channels (both uni- and bi-directional) in experimental links.

- Dark fiber – usually the last mile in the urban area.

Despite this heterogeneous physical layer, the transport layer provides parameters required for accurate time transfer. Currently, channels for time transport in operational network are amplified by the same unidirectional amplifiers that are used for standard data channels. We also test several types of bidirectional amplifiers. Once deployed, these amplifiers will be dedicated only for time (resp. frequency) transfer. In future, we plan to install these new amplifiers also in the CESNET backbone links.

Our adapters for time transfer utilize standard SFP (resp. SFP+) transceivers, which guaranties compatibility (e.g. wavelength stability and optical power) with data service in shred fibers.

Optical link UFE – BEV

The link between UFE (Prague) and BEV (Vienna) is 550 km long and has an attenuation of 137 dB. It represents the longest link in TF-infrastructure. It utilizes reserved wavelength in CESNET optical data network, which is equipped by Cisco ONS 15454 in segment Prague – Brno, respectively by CzechLight Open DWDM system in segment Brno – Vienna. The "last mile" between network PoP (Point of Presence) and institute in both Prague and Vienna uses rented dark fiber. All optical amplifiers are EDFA (Erbium-doped Fiber Amplifier). The setup is shown in Fig. 3.

Optical link CESNET – VUGTK

Typical example of TF-infrastructure is a fiber shared for both and standard data service (N x 10Gb/s) and time transfer between CESNET and VUGTK (Geodetic Observatory in Pecny) as is depicted in Fig. 4. The geographical distance between both sites is 35.2 km. The main part of the line is represented by a 78 km long single fiber which has an attenuation of about 21.2 dB. The link setup reserves four unamplified wavelengths in ITU grid for time transfer and supports up to 16 amplified DWDM wavelengths for standard 10Gbit/s Ethernet data channels. Time transfer wavelengths are available at connectors of ADD/DROP filters - Fig. 4.

The direction CESNET to VUGTK uses channel #38 (1546.92 nm) of the ITU grid, the opposite direction uses channel #39 (1546.12 nm). The link CESNET - VUGTK is considered a pilot implementation of the TF-infrastructure.

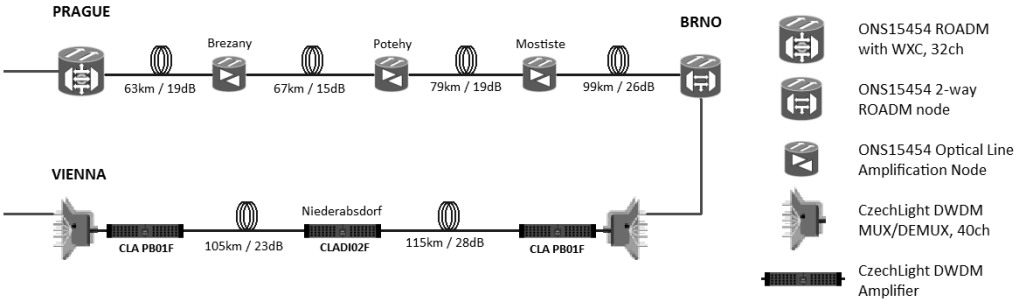

Figure 3 Link UFE - BEV

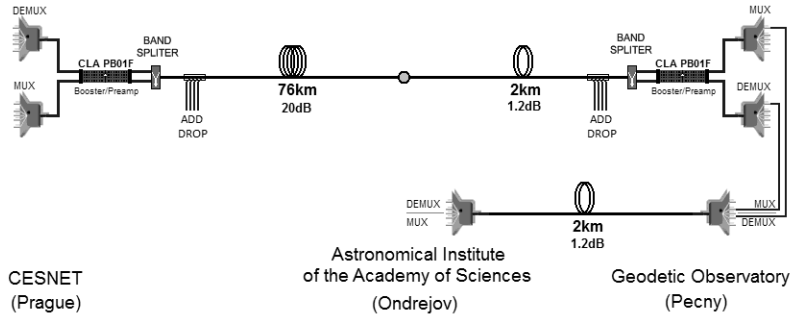

Figure 4 Link CESNET - VUGTK

5. PERFORMANCE

Time transport between CESNET and VUGTK utilizes single bidirectional fiber, therefore symmetrical change of propagation delay, e.g. temperature dependence of refractive index cancels in the first order. Similarly cancels influence of possible change of the fiber physical length, for example when the provider replaces a patch cord in the switch board. As different wavelength is used in both directions, there exists corresponding propagation delay difference which might be evaluated. We provided this analysis in [3] – the result is 1.16 ns. This value represents the systematic offset and must be used in calculation of time transfer.

Fig. 5 and Fig. 6 provide comparison of optical time transfer with GPS based methods in term of TDEV for both UFE – BEV and CESNET – VUGTK. Graphs confirm smaller noise of

optical time transfer compared with both PPP and Common View methods. Noticeable white phase noise is about 3 times lower in case of CESNET – VUGTK time transfer. The reason is the symmetry of the optical path due to single fiber without any optical amplifiers.

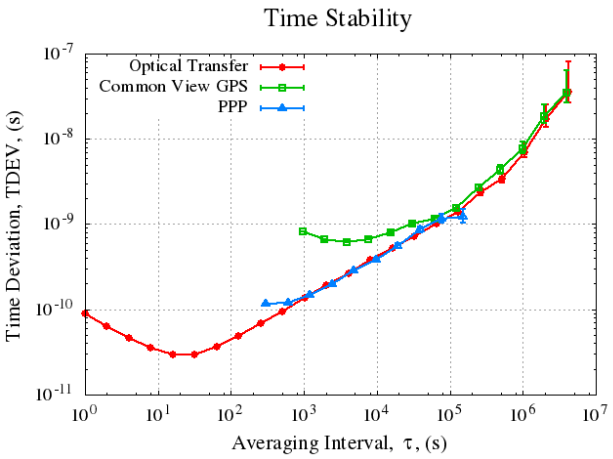

Figure 5 UFE - BEV time transfer stability

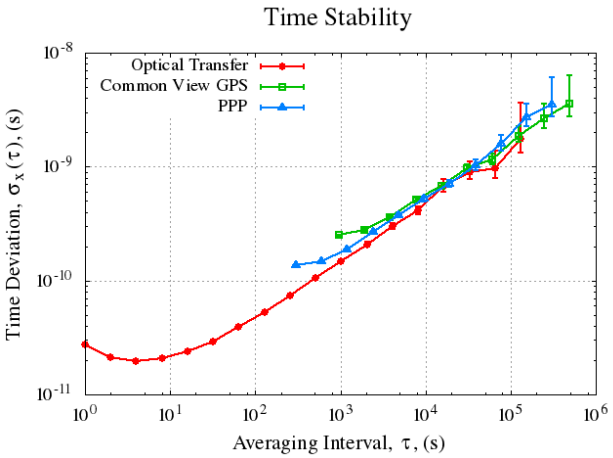

Figure 6 CESNET - VUGTK time transfer stability

6. OPTICAL AMPLIFIERS

Optical amplifiers are important elements of any long distance transmission when attenuation exceeds basic power budget of transmitter/receiver pair. Bidirectional time and frequency transfer in single fiber is always preferred over unidirectional transfer in a pair of fiber threads. However, it introduces an issue of bidirectional symmetrical amplifiers in order not to lose advantage of path symmetry. In case of time transfer, quasi-bidirectional amplification might be acceptable when supported by specific arrangements, e.g. as much as possible equal arrangement for disjoint parts of the path [3]. Unfortunately, this does not apply for frequency transfer or for time transfer with best available precision.

We decided to use fully symmetrical configuration of optical path including amplifiers in our TF-infrastructure whenever it is possible to deploy it. We performed tests of bidirectional Erbium Doped Fiber Amplifiers (EDFAs) from three different vendors in laboratory setup using fiber spools with 100 km of G.652 fiber. Example of such setup for 200 km is shown in Fig. 7. We achieved transmission distance of 500 km in setup of 4 EDFA and 5 fiber spans, each of 100 km [4]. Unfortunately, it is uncommon to keep such distance symmetry between amplifiers in field implementation.

Discrete vs. distributed amplifiers

Identical path for both directions is necessary for keeping low delay uncertainty regardless of temperature changes or other environmental influences as previously mentioned. Any unidirectional equipment in the optical path (e.g. pair of unidirectional amplifiers) is a source of asymmetry and therefore possible difference of delays in both directions. It implies that not only the fiber itself but also the other optical components including amplifiers must be bidirectional.

When we designed the infrastructure, we initially considered discrete bidirectional amplifiers, as EDFA (Erbium-doped Fiber Amplifier) or SOA (Semiconductor Optical Amplifiers) Both these types of bidirectional amplifiers were already described and experimentally in time transfer applications [4].

Usage of discrete bidirectional amplifiers suffers from a drawback: The amplifiers should be deployed equidistantly, i.e. in distances corresponding to the same value of signal attenuation in order incoming signal from both directions has the same power. Otherwise, the weaker signal experiences smaller gain and suffers from higher OSNR (Optical Signal to Noise Ratio) [5]. In practical setup, such condition might be difficult or even impossible to satisfy due to problems with housing and maintenance.

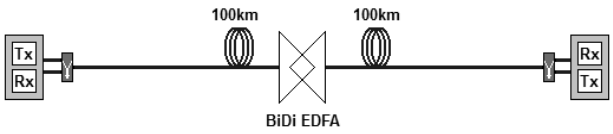

Figure 7 Discrete bidirectional amplifier deployment

We tested and evaluated another approach, the utilization of distributed Raman amplifier, where the amplification is happening directly in the transmission fiber. Raman gain happens in every fiber, and arises from the power transfer from one optical beam to another which is downshifted in frequency, i.e. upshifted in wavelength. It is non-resonant phenomena so the gain bandwidth is broad over 40 THz with maximum close to 13.2 THz. In long reach transmission band of 1550 nm, it corresponds to 100 nm approximately [6]. Based on these facts, we have chosen the pump wavelength of 1450 nm. Experimental laboratory setup is shown in Fig 8. Adapters operating on wavelengths of 1546.12 nm and 1546.92 nm are connected by 200 km fiber according to specification G.652D spooled on totally four reels. Raman sources are bound into the line at its both ends.

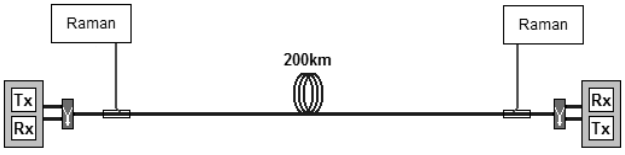

Figure 8 Pair of Raman amplifiers deployment

7. CONLUSIONS

We achieved error-free operation (Bit Error Ratio better than 10E-12) on distance of 200 km for Raman pump output power ranging from 250 mW to 475 mW. It matches line output powers from -28 dBm to -16 dBm and thus on-off gain from 14,7 to 26 dB. Measured dependence of on-off gain on pump power is shown in Fig 9.

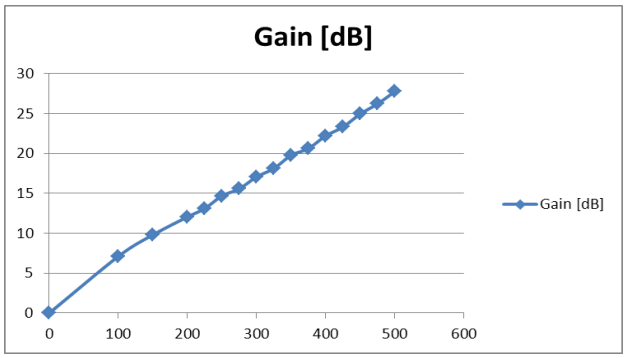

Figure 9 On-off gain of distributed amplifiers

We experimentally verified time transfer over 200 km long amplified fiber line, with the same paths for both ways of time transfer. All necessary equipment was located only in terminal ends of the line. According to our knowledge, this is the first time reported precise time transmission over optical fiber using distributed Raman amplification.

Further advantage of this method is the achieved gain, which is by up to 5 dB higher than gain achieved with discrete amplifiers because discrete amplifiers suffer from gain saturation caused by unwanted lasing.

8. ACKNOWLEDGMENTS

This work was supported by the Ministry of Education, Youth and Sport of the Czech Republic as part of the CESNET Large Infrastructure project LM2010005 and by the grant TA01011105 from Technology Agency of the Czech Republic.

9. REFRENCES

[1] V. Smotlacha, J.Vojtech, A. Kuna, "Two-way optical time and frequency transfer between IPE and BEV", **European Frequency and Time Forum (EFTF)**, 23-27 April 2012, Gothenburg, pp. 375–378, 2012.

[2] L. Sliwczyzski, P. Krehlik, A. Czubla, L. Buczek, M. Lipinski, "Dissemination of time and RF frequency via a stabilized fibre optic link over a distance of 420 km", **Metrologia**, Vol. 50, No. 2, 2013, pp. 133–145.

[3] V. Smotlacha, J. Vojtech, A. Kuna, "Optical Infrastructure for Time and Frequency Transfer", **Joint UFFC, EFTF and PFM Symposium**, 21-25 July 2013, Prague, pp. 481–484, 2013.

[4] V. Smotlacha, J. Vojtech, A. Kuna, **"**Time and frequency Transfer Infrastructure**"**, In proceedings of **Precise time & Time intervals systems (PTTI)**, 2013.

[5] L. Sliwczyzski, P. Krehlik, A. Czubla, L. Buczek, M. Lipinski, **"**Frequency Transfer in Electronically Stabilized Fiber Optic Link Exploiting Bidirectional Optical Amplifiers", **IEEE Transactions in Instrumentation and Measurement**, Vol. 61, No. 9, 2013, pp. 2573-2580..

[6] M. N. Islam **"**Raman Amplifiers for Telecommunications", **IEEE Journal of Selected Topics in Quantum Electronics**, Vol. 8, No. 3, 2002.

Model and Architecture of Mobile Electronic Voting

Sandra I. Bautista Rosales
Departamento de Posgrado, Escuela Superior de Cómputo - Instituto Politécnico Nacional
Ciudad de México, C.P. 07738, México

Chadwick Carreto Arellano
Sección de Estudios de Posgrado e Investigación, Escuela Superior de Cómputo - Instituto Politécnico Nacional
Ciudad de México, C.P. 07738, México

Eduardo Bustos Farías
Departamento de Investigación, Escuela Superior de Cómputo - Instituto Politécnico Nacional
Ciudad de México, C.P. 07738, México

Luis Enrique Hernández Olvera
Departamento de Ciencias e Ingeniería de la Computación, Escuela Superior de Cómputo - Instituto Politécnico Nacional
Ciudad de México, C.P. 07738, México

ABSTRACT

Democracy is a field in which the advancement of technology has impacted through electronic media such as perforated cards, optical scanners, digital and biometric electronic voting machines, among others, converging into what has been called "electronic voting" . There are countries that have implemented this type of voting by electronic voting models that conform to the laws of each and consider only specialized devices for the reception of suffrage. However, although there are many technological advances in the emission and reception of the vote, has not been considered a model that can be applied to mobile devices that gives voters the opportunity to cast its ballot from wherever they are located and with the certainty that procedural safeguards and principles of the vote will be respected.

Keywords: Electronic voting, Security, Mobile Wireless Networks, Authentication, digital sign, mobile devices.

1. INTRODUCTION

With the advancement of new technologies of information and communication, especially the Internet, it has potentialized the flow of information that has reached impressive levels and has come to produce social changes.

These changes have caused democracy transforms that electoral processes are included in the flow of information and facilitate decision-making; and so everything contributes to consider the inclusion of electronic voting [2].

There are countries that have introduced electronic voting in different electoral processes according to various voting models adhere to the political system of each. However, all these models include specialized voting devices at the reception of the vote and has not been considered opt for own user devices, such as mobile devices, to cast their vote.

Moreover, the continued advancement of mobile devices and connectivity capabilities to wireless networks allows users to be in touch anytime, anywhere; which brings us to one of the main challenges that must meet all electronic voting conducted by this means, that is, provide security when sending data through the air, which is one of the propagation channels more insecure to transmit, so it is necessary to use appropriate security models to meet this need [10]. This is the reason why this work is focused on developing a Model and Architecture of Mobile Electronic Voting which allows the user to cast their vote through a process of identification and authentication via your mobile device, from anywhere which are as long as it has an Internet connection.

The remainder of the paper is organized as follows. Section II provides a theoretical framework which will address some of the most important concepts for this work. In Section III defines the problem statement. The proposed security model that solves such problem is raised in section IV, the Section V gives the model infrastructure (Architecture) for the functioning of the Mobile Electronic Voting Model, in Section VI gives a case study overview developed to test the benefits of the model. Finally, Section VII concludes the paper and defines future work.

2. THEORETICAL FRAMEWORK

The vote being public or secret expression of a preference to one or more options [1], it can be said that electronic voting (EV) has the same objective, except that electronic devices are used to do it so it can identify two aspects of the same [2]:

a) EV in broad meaning: it's all election mechanism in which the electronic media or any technology used in the different stages of the electoral process, namely effective act of voting.
b) EV in meaning strict: the very act in which the issuer of the deposited vote or express their will through electronic means (electronic voting) or any other receiver technology suffrage.

Given this classification, this paper will consider the electronic voting in the broad sense, which leads to define some basic concepts for this.

There are various electronic voting systems currently are already used in different countries, mainly Western ; generally three types of hosts and a fourth [2] in the process will be adopted by more recent are identified. The above systems are:

1. In a punch card. The voter receives a card, which must pierce your choice by means of an apparatus. This system is somewhat problematic in that the accuracy of drilling depends on the user and could not properly count each card perforation. This is an obsolete system, but still continues to use.
2. By an optical reading machine. The voter makes marks with a pen on a ballot, so that later they can be inserted into a reader device and the vote counted. The voter does not come into direct contact with technology, but your ballot.
3. By direct recording devices. Use similar devices to an ATM, the voter preference set through a touch screen or a keyboard. Maybe the same device can record the vote or the vote is recorded on external media. After voting, the voter uses his card by way of a traditional ballot, inserting it in an urn, which in turn will be a magnetic card reader device, and perform the count.
4. Remote Electronic Voting. It is one that provides the voter should not travel to the polling station to cast their vote and through the network (may be internal or from any platform connected to Internet).

Will this last type of system which takes into account the proposed voting model.

Security in general, refers to compliance with the security services listed below [3]:

- Confidentiality. Ensures that private information can be accessed only by authorized entities.
- Data integrity. Refers to data protection so that cannot be modified, destroyed or lost in a malicious or accidental.
- Authentication. It is related to the identification data or service identities. Authentication of an entity is to confirm your identity, that is, a check that is who they claim to be. Authentication data concerning the validity of data, meaning the integrity of the same.
- No rejection. Ensures that the sender of some information cannot refuse / deny content transmitted or that the recipient cannot deny receipt or content.

The ***digital signature*** is a mathematical scheme that guarantees privacy of conversation, data integrity, the authenticity of the message / digital sender and sender non-repudiation [4]. You can also say it is a cryptographic method that associates an identity, whether a particular person or team to a message sent via network transmission.

Blind signature is a kind of digital signature produced for messages that are kept hidden from the signer and therefore a third entity requesting the signature [5]. This concept was introduced by Chaum in order to ensure anonymity in electronic payment systems [6], but now also been given use of electronic voting systems. Blind signatures require two entities, the user who requested the signature and the signatory who signs the message.

Generally, an electronic Internet voting should cover all the functional requirements of the electoral process and the security needed to protect themselves from potential attacks from the network. Some of the essential requirements are as follows [5]:

- *Authentication*: only the voters included in the voter list will be allowed to cast their vote.
- *Anonymity* and no coercion, no one should be able to determine the value of the vote or link it to the voter.
- *Uniqueness*: no voter should vote more than once.
- *Monitoring and auditing*: it must be possible to verify that the end of the electoral process, all the votes were counted correctly.

Other requirements given by [7] are:

- *Accuracy*: Avoid that the vote cast is altered, duplicated or deleted by anyone. Every legitimate vote should be counted correctly.

- *Simplicity*: The voting process should be as simple as possible. In other words, a user-friendly interface of e-election and does not need to learn complex techniques and any additional equipment.

3. PROBLEM STATEMENT

Technological advances coupled with cryptographic techniques have been a factor in the gradual integration of electronic voting in the traditional voting systems. The Internet and various electronic devices facilitate the capture, transmission and reception of the vote, thus providing a more convenient and efficient process for all participants.

However, the new voting system which is derived from electronic voting, that is, the remote e-voting also carries certain problems or additional risks that already exist in the traditional system. For example, user authentication, and it must be identified to have the respective permits and in turn vote to remain anonymous when casting their vote.

Another problem comes from considering the Internet as the primary means of transmission, it is necessary to implement security schemes for electronic voting system that provide security and privacy to voters.

Since usually the vote is captured electronically and sent to an electronic ballot to be posted at the end of the voting period, the audit becomes another problem, since there is no guarantee that those votes that are being stored are not altered while choosing ends.

At present there are many protocols and electronic voting

schemes ranging according to certain voting patterns. For example, " A verifiable electronic voting scheme Internet " [7] provides an outline of how to monitor the voting process, specifying 4 phases, namely phase registration, authentication, voting and counting, also proposes five entities participants: Voters, Certificate Authority, authentication Centre, Centre for Monitoring and counting center, being the greatest contribution of this work verifiability.

Another paper entitled "A Secure Electronic Voting Protocol for the General Elections" [8] proposed a voting center consists of four steps which navigate through five modules.

A third protocol is "A Limited Voting Mechanism based Key Exchange Protocol" [9], it makes use of blind signature protocol and the Diffie - Hellman for key exchange between the voter and the server authenticated responsible for receiving the message for the vote. One disadvantage of this protocol is that it does not allow the voter to verify that their vote has been properly counted.

In Table I we can see the comparison of the different models proposed voting.

TABLE I.
MODEL COMPARISON OF ELECTRONIC VOTING

	Protocolos			
Requirements	**Protocol of Liaw [8]**	**Protocol of Chang-Lee [9]**	**Protocol of Chun-Ta Li [7]**	**proposed Model**
precision	✓	✓	✓	✓
ease	X	✓	✓	✓
Attached to the Law	✓	✓	✓	✓
verifiability	✓	X	✓	✓
Privacy	✓	✓	✓	✓
Scheme on Internet	✓	✓	✓	✓
Based on wireless networks	not specified	not specified	not specified	✓
They see mobile devices	X	X	X	✓

4. PROPOSED MODEL

With electronic voting models that have been proposed so far, we can see that most take into account specific places so that voters go to cast their vote and / or contemplated dedicated to receiving and vote count devices. It is true that there are already models posed for a scheme based on Internet, but their descriptions in the type of communication that are vague or employ almost nil and such models focus primarily on the effective act of voting, rather than on the specifications and protocols that must be followed to make use of a wired or wireless network.

As for security, most of the proposed protocols use relatively simple authentication mechanisms, i.e. smart cards and / or verification that the voter was previously registered in a database, so it is necessary to use of different authentication mechanisms to ensure the reliability of the voting system.

Moreover, the models already proposed electronic voting only mention that the various government entities must participate and monitor the voting process to succeed, but these models do not contain a section on the legislative part which is applied in each of democratic nations.

The importance of carrying electronic voting to a mobile framework is of vital importance, as it would provide voters a model much more convenient for them to vote, making use of the benefits they provide their own mobile devices, i.e., allowing cast their vote from anywhere where they are (and a wireless network is available), without having to travel to a place where some specialized in receiving or vote counting devices are.

The proposed model is an alternative that could be taken in many democratic countries, as well as provide benefits to voters to break geographical barriers, it is also convenient for the agencies responsible for managing the entire voting process, as avoid unnecessary expenses (paper, pens and even specialized devices that can be very expensive) and most of the efforts could focus on ensuring system security and voter.

The Mobile Electronic voting model proposed, consisting of four layers as shown in Figure 1:

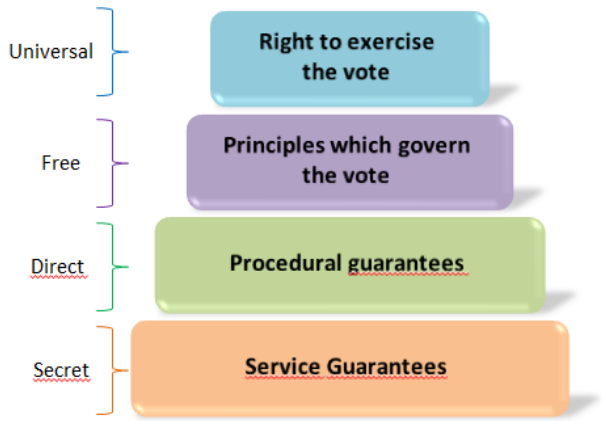

Figure.1 Proposed Model of Mobile Electronic Voting

Each layer focuses on various aspects and phases in the voting process and also help to meet the characteristics of the traditional voting, then describes each:

A. ***Faculty or right to exercise the vote:*** It refers primarily to the process of registering voters who meet the basic qualifications for voting, that way they will be granted a username and password for later use them in the voter identification process.
B. ***Principles which govern the vote:*** In this layer the voter authentication process specified, to be held by the Electronic Signature and the implementation of RSA encryption algorithm to authenticate via their mobile device, and specify the principles of the vote, such as the universal, free, equal and secret suffrage, to name a few.

C. ***Procedural guarantees:*** This layer involves the issuance of documents, certificates, such as user authentication certificate; legislative aspects governing the voting process and the rules are defined in accordance with the laws of the country or the organizer of the vote are also specified.

D. ***Service guarantees***: In this layer the guarantees that must be met each procedure specified in the vote are specified, e.g. transparency, verification of authentication, verification of votes cast by a digital certificate, the integrity of the information, secure communication in sending data through the implementation of the AES algorithm, among others.

5. INFRASTRUCTURE AND ARQUITECTURE

The infrastructure consists of the set of elements necessary for the operation of the model described thus infrastructure can be described as follows:

- User ID: This will be provided by a user and password.
- User authentication: Will be established by means of the electronic signature.
- Organism Validator: Will be responsible for verifying that the user is who he claims to be by means of an electronic signature, and the agency must keep a record of the accesses made by the user.
- Secure access to the service: It will develop an encryption algorithm to shield the data transmission channel (air).

To design the architecture, it was based on this infrastructure to determine where each layer Architecture Model is implemented as shown in Figure 2:

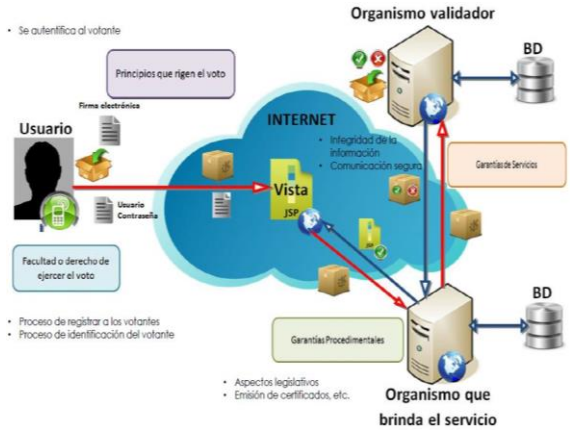

Figure 2. Description of each layer of the model in the proposed architecture.

6. CASE STUDY

To verify the performance of Electronic Voting Model, it has a case study consisting of a Mobile Electronic urn that will be implemented on the architecture described above.

The case study consists of two applications: a Mobile and Web. Roughly Mobile application includes the following:

- User registration
- Request verification code
- Request for username and password to access
- Casting of Votes
- Issuance of a disagreement

The web application is oriented toward the Directors and Auditors, who may perform the following actions:

- Manage users
- Manage events voting
- View events

Register a new user (voter) and the area shown in Figure 3 to access the mobile app:

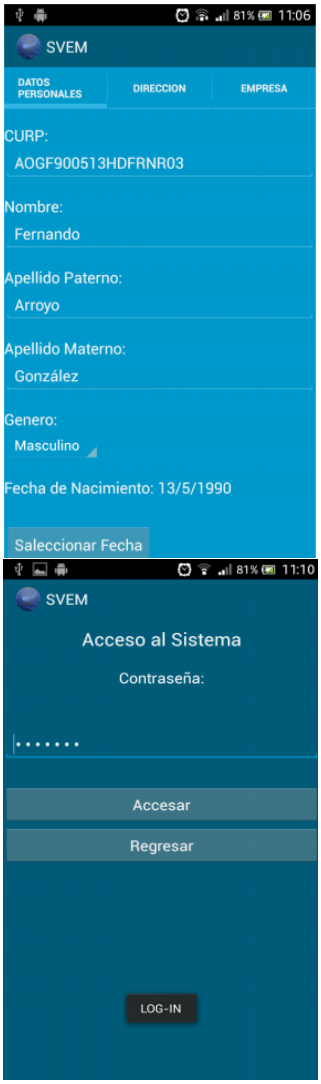

Figure 3. Register a new user (voter) and Login.

In Fig. 4 the query shows the completed ballot.

Figure 4. Query shows the completed ballot.

7. CONCLUSIONS AND FUTURE WORK

The proposal and progress of an Electronic Voting Model applied mainly to Wireless Networks and Mobile Systems described in this paper. As can be seen, the model is based on a four-layer model to cover different aspects to be considered in the Electronic Voting. Intended as a contribution not only to ensure the identification and authentication of the voter, but also seeks to protect the identity of the user and the security of the votes cast. Furthermore, with the implementation of the model in Architecture transparencies throughout the whole process and not only to provide finalize the vote.

Currently we are working on validating the mechanism of authentication users Urn Mobile Electronics (case study) which is a part of a Security Model in Mobile Networks that electronic signature of the user to operate [12] and user application on the Android operating system.

ACKNOWLEDGEMENTS

The authors of this study thank ESCOM and AMITE for the facilities provided for the development of this work.

REFERENCES

[1] Real Academia Española, Diccionario de la lengua española, 22ª ed. 2010. [Online] Available in: <http://lema.rae.es/drae/>. [Consulted September 12th. 2012].

[2] Téllez Valdés, Julio. El voto electrónico, México, Tribunal Electoral del Poder Judicial de la Federación, 2010. [Online] Available in: <http://www.te.gob.mx/documentacion/publicaciones/Temas_selectos/14_voto.pdf> [Consulted October 04th. 2012].

[3] F. Rodríguez-Hernríquez, N.A. Saquip, A. Díaz Pérez, C. K. Koc. Cryptographic Algorithms on Reconfigurable Hardware (Signals and Comminication Technology). Springer Verlag, New York, Inc., 2006.

[4] Kaur, R. Digital Signature. Guru Nanak Dev University, India. International Conference on Computing Sciences, 2012.

[5] M. de L. López García. Diseño de un protocolo para votaciones electrónicas basado en firmas a ciegas definidas sobre emparejamientos bilineales. Centro de Investigación y Estudios Avanzados del Instituto Politécnico Nacional. México, 2011.

[6] D. Chaum, R. L. Rivest and A. Sherman. Crypto 82 in Advances in Cryptology 1981 to 1997, Vol. 1440 of Lecure Notes in Computer Science, p. 13-19. Springer Berlin, 1999.

[7] Chun-Ta Li, Min-Shiang Hwang, Yan-Chi Lai. A verifiableElectronic Voting Scheme over the Internet. Sixth International Conference on Information Technology: New Generations, Las Vegas Nevada, April 2009.

[8] H. T. Liaw. A secure electronic voting protocol for general elections. Computers & Security, 2004.

[9] C.C. Chang and J. S. Lee. An anonymous voting mechanism based on the key exchange protocol. Computers & Security, 2006.

[10] Mudhakar Srivatsa. Who is Listening? Security in Wireless Networks. IEEE-International Conference on Signal processing, Communications and Networking, Madras Institute of Technology, Anna University Chennai, India, pp. 167-172, 2008.

[11] Gentles, Donovan and Sankaranarayanan. Biometric Secured Mobile Voting. Kingston, Jamaica, 2011.

[12] Hernández O. Luis E. Modelo de Seguridad para Redes Aplicado a Dispositivos Móviles. Escuela Superior de Cómputo, Instituto Politécnico Nacional, 2013.

[13] L. Bass, P. Clements, R. Kazman, Software Architecture in Practice, 2nd Edition, Addison Wesley, 2003.

Image-inspired Approach of Literal Node Identification in Linked Open Data

Takahiro Kawamura
and Shinichi Nagano
Corporate Research & Development Center,
Toshiba Corp.
Kawasaki, 212-8582, Japan

Akihiko Ohsuga
Graduate School of Information Systems,
University of Electro-Communications,
Tokyo, 182-0021, Japan

ABSTRACT Linked Open Data (LOD) is starting to spread for the creation of innovative service. In LOD, each node represents a Uniform Resource Identifier (URI), and then LOD sets of different domains are connected and merged as the LOD cloud in the world. However, even in DBpedia which is a de facto hub of LOD, 5% of the values are literal (string without URI). Therefore, we proposes a method of identifying literal nodes that have the same meaning to facilitate cross-domain search. Interdisciplinary point of our method is that it is inspired by a winner of computer shogi (Japanese chess) contest, in which records of games are regarded as figures. Thus, our method regards part of th LOD graph as a block image, and extracts image features based on Scale-Invariant Feature Transform (SIFT), which is a well-known method in computer vision. In learning experiments for determining identities of literal pairs, we successfully classified about 17,000 literal pairs extracted from DBpedia with F-measure of 99%.

Keywords: Linked Open Data, LOD, Literal Matching, Ontology Alignment, Image Feature, Computer Shogi

1. INTRODUCTION

The goal of this paper is to connect literals (string values without URI) of triples $< Resource, Property, Value >$ as much as possible, and to create "linked" data of the original meaning. DBpedia, which represents part of Wikipedia, is currently a *de facto* hub of LOD in the world, but according to our research approx. 5% of the values in DBpedia are literals. Since the literal becomes a terminal node, and we need to rely on regular expression matching, we cannot trace the links in the LOD graphs during searches. Therefore, in order to determine the identity of literal values and support data linkage, we propose a method for matching literal values using LOD graph structures. These initiatives will be applied for cross-domain search through links in LOD. Literal matching corresponds to "name identification," which is a traditional but important problem in system integration (SI) projects. It is also similar to instance matching in ontology alignment, although the matching target is not an instance (resource in LOD) but a value.

The novelty of this paper is that the proposed method regards the target literal and surrounding information in LOD as a block image, and extracts image features around the literal. Then, it determines the identity of the literals through similarity discrimination of two images. The reason for adopting the image processing technique is inspiration from great progress of recent computer shogi, in which records of games are regarded as figures, and a game is played to make a good figure in the record [1]. Thus, the contribution of this paper is the introduction of a new feature in Linked Data integration.

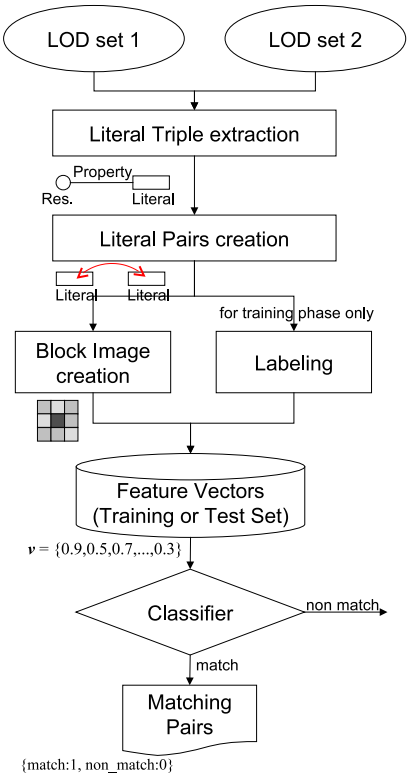

Fig. 1. Workflow of literal matching

2. IMAGE FEATURE EXTRACTION FROM LOD

The workflow of literal matching is shown in Fig.1. First, we define the literal matching as a binary classification problem of the possible literal combinations (pairs) between two LOD sets, based on the related work [2]. Then, we propose a method to construct the feature vector based on Scale-Invariant Feature Transform (SIFT) [3], which is a well-known method in computer vision. SIFT extracts local features for each key point in an image. The area surrounding a key point is divided into 4×4 blocks, with each block providing illumination changes (gradient) of 8 orientations per 45 deg., and then a vector with 128 dimensions is created in SIFT algorithm.

Fig.2 illustrates a method of generating a block image from two LOD graphs. We select properties and resources connected from two literal values for comparison, and another two properties and values connected from the above resources, and then generate a grayscale image of 3×3 blocks by calculating

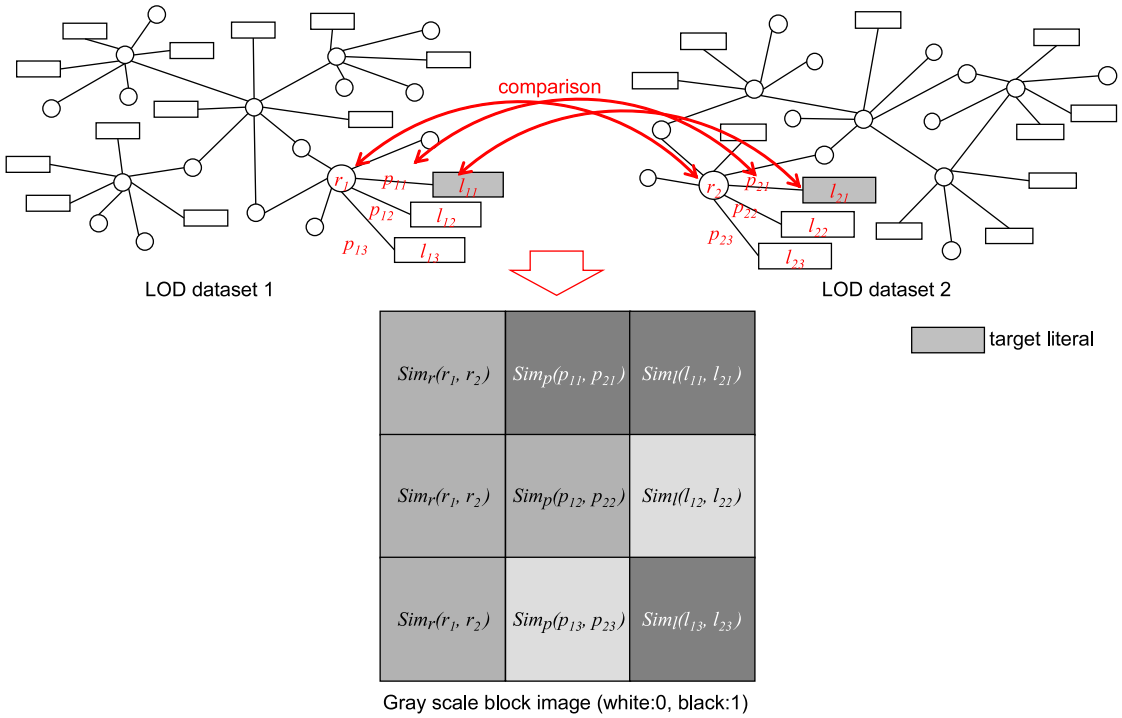

Fig. 2. Image generation from LOD

each similarity Sim_l, Sim_p, Sim_r. Each block has a value $[0, 1]$, where 1 represents black. Regarding the selection of another two properties and values, if we find that the above two resources have common properties, we alphabetically select two properties and their values as the second and the third row. If they don't have common properties, we select the two most similar properties and their values. Thus, we attempt to generate an image with specified regularity. The similarities Sim_l, Sim_p, Sim_r are composed of string similarity and semantic similarity and defined as follows:

$$\begin{aligned} Sim_l(l_{1i}, l_{2j}) =& \alpha\ StringSim(l_{1i}, l_{2j}) \\ &+\beta\ SemanticSim(l_{1i}, l_{2j}) \end{aligned} \tag{1}$$

$$\begin{aligned} Sim_p(p_{1i}, p_{2j}) =& \gamma\ StringSim(p_{1i}, p_{2j}) \\ &+\delta\ SemanticSim(p_{1i}, p_{2j}) \end{aligned} \tag{2}$$

$$\begin{aligned} Sim_r(r_1, r_2) =& \epsilon\ StringSim(r_1, r_2) \\ &+\zeta\ SemanticSim(r_1, r_2) \end{aligned} \tag{3}$$

$$StringSim(S1, S2) = \frac{|S1 \cap S2|}{|S1 \cup S2|} \tag{4}$$

$$SemanticSim(S1, S2) = \begin{cases} 1.0 & \text{if} \quad \text{S1 = S2} \\ 0.75 & \text{else if} \quad \text{S1 is } \textit{Synonym} \text{ of S2} \\ 0.5 & \text{else if} \quad \text{S1 is } \textit{Hypernym} \text{ or } \textit{Hyponym} \text{ of S2} \\ 0.25 & \text{else if} \quad \text{S1 has same } \texttt{namespace} \text{ as S2} \\ 0.0 & \text{else} \end{cases} \tag{5}$$

l_{ij}, p_{ij}, r_{ij} mean identifiers of a literal node, a property and a resource, respectively. Also, parameters $\alpha, \beta, \gamma, \delta, \epsilon, \zeta$ satisfy $0 \leqq \alpha, \beta, \gamma, \delta, \epsilon, \zeta, \alpha + \beta, \gamma + \delta, \epsilon + \zeta \leqq 1$. These parameters depend on problems to be solved, but we set 0.5 for each in the next section. $StringSim$ is a Jaccard coefficient, and $SemanticSim$ corresponds to a simplified calculation of the similarity indicator based on path lengths between two classes in ontology matching. Also, $S1, S2$ are strings, and are regarded as sets of characters in $StringSim$. To determine *Synonym*, *Hypernym*, *Hyponym*, we refer to the external ontologies, and we use WordNet and Japanese WordNet in the next section.

The intuitive meaning of this image is representation of contextual information on the graph. That is, the image represents the connection of semantic contents on the graph. For example, if the literals are synonyms with different notations and their semantic similarity cannot be determined by ontology, then the image that has high similarities in each block except for a block of the literals like Fig.3(a) can be expected. In contrast, the block of the literals will have high similarities, but most of the other blocks will have low similarities in the case of homonyms with the same notation like Fig.3(b). In this manner, we represent the similarities of the target nodes and

surrounding links and nodes as an image, and characterize the connection of meaning in the graph.

Finally, we regard a target literal value as a key point in the image, and construct the feature vector from the similarity changes of the adjacent 9 blocks. Unlike SIFT, no orientation is set and an absolute value of the similarity at the key point is included as a basis. The feature vector $\boldsymbol{v}$ is represented by the following equation.

$$\begin{aligned} \boldsymbol{v} =& Sim_l(l_{11}, l_{21}) + \Delta_{p1} + \Delta_{r1} \\ & \Delta_{l2} + \Delta_{p2} + \Delta_{r2} \\ & \Delta_{l3} + \Delta_{p3} + \Delta_{r3} \\ \Delta_{li} =& (Sim_l(l_{1i}, l_{2i}) - Sim_l(l_{1(i-1)}, l_{2(i-1)})) \\ \Delta_{pi} =& (Sim_p(p_{1i}, p_{2i}) - Sim_l(l_{1i}, l_{2i})) \\ \Delta_{ri} =& (Sim_r(r_1, r_2) - Sim_p(p_{1i}, p_{2i})) \quad (i = 1, 2, 3) \end{aligned} \tag{6}$$

In SIFT, the gradient is taken as the feature in order to absorb the difference in illuminance values by lighting etc. In the comparison of LOD sets, if both sets are written in the same schema (property definitions), the similarities of the links and nodes surrounding the matching literals are expected to change at a high level, although they are expected to change at a lower level as a whole in the case of sets with different schemas. Therefore, in order to absorb the difference in the relative level of the similarity between the LOD sets to be compared, the proposed method does not use the absolute values of Sim, but the differences from adjacent blocks (similarity gradient) as the training data for generic features.

3. CLASSIFICATION EXPERIMENT ON LITERAL PAIRS

Unlike in the case of instance matching, we could not find any public research tool to perform a comparison for literal matching on LOD. We thus compared the proposed method with a simple string matching of literal values as a baseline method.

A. Experimental Setting

For literal matching between LOD sets with the same schema, we first extracted triples $(N = 8,504)$ that have literal values, from the resources in the "JPOP" (Japanese pop music) category of DBpedia Japanese, and created literal pairs $((N^2 - N)/2 = 36,154,756)$. We then selected 17,391 pairs, excluding the pairs obviously not matching such as time and location, and manually marked the literal matching to them TRUE or FALSE.

Next, we calculated the image feature described in the previous section for each of the above-mentioned pairs. We used an ensemble learning method, Random Forest [4], as the classifier, and then evaluated with 10-fold cross-validation. Other research on instance matching [2] indicated that Random Forest surpasses other methods owing to the nature of the problem. There are 10 decision trees, each of which randomly takes 4 features and unlimited depth of the tree. The algorithm of each tree is an implementation (modified REPTree) based on C4.5.

B. Comparison with baseline method

We first show the results of the baseline method and the proposed method for the same schema sets. As a baseline method, we used string comparison of literal values with Jaccard coefficient jcc. Table 1 shows the matching results, in which TRUE and FALSE mean matching pairs and non-matching pairs, respectively.

Table 1. CLASSIFICATION RESULT OF STRING COMPARISON

	$jcc > 0.7$		$jcc > 0.9$	
	Precision	Recall	Precision	Recall
TRUE	0.614	0.580	0.828	0.547
FALSE	0.988	0.990	0.987	0.997

As a result, FALSE indicates that both precision and recall have high scores. Since the matching pairs are only about 3% of all the pairs, if we strictly determine the identities of the pairs, and raise the accuracy of the majority FALSE, then we can easily raise the total accuracy. Moreover, comparison of the results of TRUE in the case of $jcc > 0.7$ and $jcc > 0.9$ indicates that if we strictly determine the string matching, we can also easily raise the precision of TRUE. However, the recall of TRUE decreased, and we lost many matching pairs as a result. Therefore, we can understand that solving the problem of literal matching will involve raising the recall of TRUE without decreasing the precision by separately looking at the results of TRUE and FALSE.

Table 2. CLASSIFICATION RESULT OF IMAGE FEATURES

	Precision	Recall	F-Measure
TRUE	87.5	82.6	85.0
FALSE	99.5	99.7	99.6
Weighted Avg.	99.2	99.2	99.2

Next, in Table 2 we present the result using the proposed method. As a result, we found that the proposed method improved the recall of TRUE 25 points compared with the case of $jcc > 0.7$, improving the precision 5 points compared with the case of $jcc > 0.9$. In addition, the weighted average according to the number of pairs including FALSE resulted in over 99% precision, recall and F-measure.

4. RELATED WORK

First, research on instance matching can be divided into approaches depending on domain (dataset) knowledge to raise accuracy, and domain-independent approaches that dispense with the need to prepare training data for each domain. The former research is Rong et al.[2], in which instance matching is defined as a binary classification problem and determined by a learning method. However, they also utilize a transfer learning method, TrAdaBoost [5], to reduce the training data depending on a domain. ObjectCoref [6] introduces a self-learning framework that repeatedly finds pairs of specific properties and values for training data reduction. This research also provides useful guidance for literal matching. The latter research is RiMom [7]. In regard to domain-independent approaches, most research combines several features, for instance string similarity such as Jaccard coefficient, cosine, TF/IDF and Levenshtein distance, and semantic similarity such as WordNet and inverse functional property, and also structural similarity without any learning method. RiMom can suggest

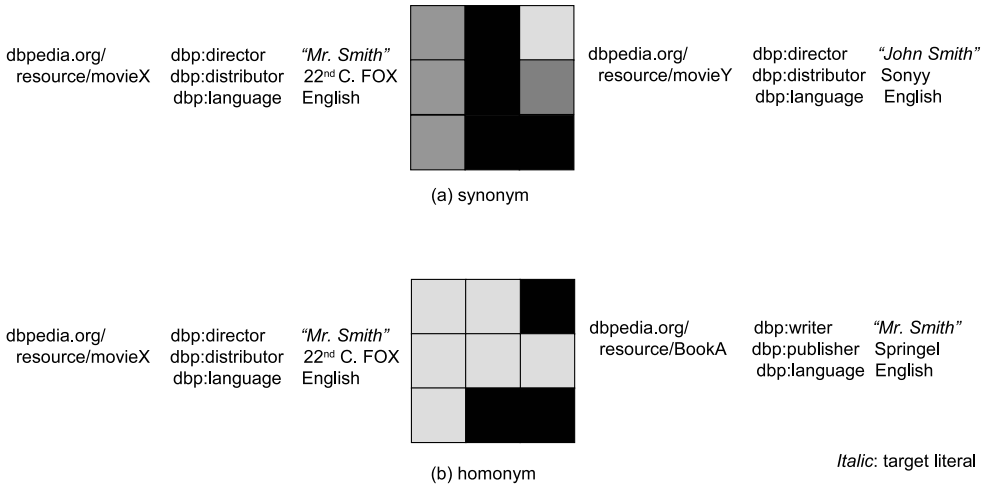

Fig. 3. Example features of synonym and homonym

the proper combination of features according to the dataset characteristics.

Literal matching is a problem similar to instance matching, but an independent problem. Literal matching matches several nodes that are not instances (resources in LOD), if they indicate the same entity in the real world. This problem remains even after performing instance matching and property matching [8]. For example, even if movie resources A and B are matched by instance matching and 'author' property of A and 'writer' property of B are matched by property matching, in the case that there are two author/writer in the movie the problem that which node indicates which author/writer remains. There is also a case that 'director' property of a movie resource and 'writer' property of a book resource indicate the same person. In this case, the nodes of the same person cannot be found after instance matching. In regard to technical aspect, although instance matching can utilize semantic and structural similarity of properties and nodes connected to the instance as features, literal matching is for a terminal node that only connects to a property, and then needs to define a new feature.

First, we introduce Apache Solr that is used for name identification in SI projects, since we could not find research similar to literal matching of LOD. Narrowly conceived, name identification means confirming the consistency of customers' information for financial institutions and administrative organizations, whereas broadly conceived it usually refers to data cleansing. Frameworks such as Solr calculate word similarity using TF/IDF etc., and then suggest words that might have the same meaning. Developers visually confirm the words and register them in a dictionary. In the early stage of the Semantic Web, freedom from word ambiguity was considered advantageous, but nowadays if users search for "dentist" on the web, "dental clinic" is also included in the results owing to such frameworks. However, synonyms with totally different notations are not suggested by using word similarity. Moreover, homonyms with the same notations cannot be distinguished by dictionary registration.

Also, in social tagging research, J.J. Jung proposed multilingual tag analysis using several co-occurrence patterns. [9] identifies user community of similar lingual practice for discovering tag correspondences, and then expands queries by referring to the correspondences for retrieving better results in tag-based information retrieval systems. Tag correspondence corresponds to literal matching pair in our paper. It, however, tries to organize a set of multilingual tag pairs which have meaningful relationships without dictionaries, although we refer to the external ontologies for the calculation of semantic similarity.

5. CONCLUSION AND FUTURE WORK

This paper addressed literal matching to determine identities of literal values in LOD. Then, we proposed a novel method to extract image features from LOD, inspired by computer shogi. We then confirmed that it successfully classified the pairs with F-measure of 99%. We intend to apply it to other domains.

REFERENCES

[1] T. Obata, T. Sugiyama, K. Hoki, and T. Ito: "Consultation Algorithm for Computer Shogi: Move Decisions by Majority", Computers and Games, Vol. 6515, pp. 156–165, 2011.

[2] S. Rong, X. Niu, E. W. Xiang, H. Wang, Q. Yang, and Y. Yu: "A Machine Learning Approach for Instance Matching Based on Similarity Metrics", Proc. of 11th Int'l Semantic Web Conf. (ISWC), pp. 460-475, 2012.

[3] D. G. Lowe: "Object recognition from local scale-invariant features", Proc. of Int'l Conf. on Computer Vision (ICCV), 1999.

[4] L. Breiman: "Random Forests", Machine Learning, 45(1), 2001.

[5] W. Dai, Q. Yang, G. Xue, Y. Yu: "Boosting for transfer learning", Proc. of 24th Int'l Conf. on Machine Learning (ICML), pp. 193-200, 2007.

[6] W. Hu, J.Chen, G. Cheng, Y. Qu: "Objectcoref & falcon-ao: results for oaei2010", Proc. of 5th Int'l Workshop on Ontology Matching (OM), CEUR Workshop Proceedings, Vol. 689, 2010.

[7] J. Li, J. Tang, Y. Li, Q. Luo: "Rimom: A dynamic multistrategy ontology alignment framework", IEEE Transactions on Knowledge and Data Engineering, Vol. 21, No. 8, pp. 1218-1232, 2009.

[8] K. Gunaratna, K. Thirunarayan, P. Jain, A. Sheth, and S. Wijeratne: "A Statistical and Schema Independent Approach to Identify Equivalent Properties on Linked Data", Proc. of 9th Int'l Conf. on Semantic Systems (I-SEMANTICS), pp. 33-40, 2013.

[9] Jason J. Jung: "Cross-lingual query expansion in multilingual folksonomies: A case study on Flickr", Knowledge-Based System, Vol. 42, pp. 60-67, 2013.

Bio-Inspired Trust and Reputation Model Investigations over Hops Coefficient Factor in Static and Dynamic Wireless Sensor Networks.

Vinod Kumar VERMA,
Department of Computer Science & Engineering, SLIET,
Longowal, Punjab - 148106, India

ABSTRACT

Resource utilization requires a substantial consideration for a trust and reputation model to be deployed within a wireless sensor network (WSN). In the evaluation, our attention is focused on the effect of hops coefficient factor estimation on WSN with bio-inspired trust and reputation model (BTRM). We present the state-of-the-art system level evaluation of accuracy and path length of sensor node operations for their current and average scenarios. Additionally, we emphasized over the energy consumption evaluation for static and dynamic mode of BTRM-WSN model. The performance of the hops coefficient factor for our proposed framework is evaluated via analytic bounds and numerical simulations.

Keywords: Wireless sensor network, BTRM-WSN, accuracy, path length, energy.

1. INTRODUCTION

Wireless sensor networks, with its services, have changed our life in the last few years. In fact, we are using it as a way to access numerous domain services and applications such as defense equipments, ecological and habitat monitoring, industrial process control, home automation, weather forecasting, health care system, traffic control, civilian applications etc. Wireless sensors are small size devices equipped with radio transceivers and low power batteries. Typical features of sensor node include power, storage and low cost computational capability hardware [1-2]. A wireless sensor network is intended to sense, collect, processes and transmit event specific information in order to accomplish a distributed domain task. Moreover wireless sensor networks [3-4] are the type of networks where the resultant is fully based on the sensor nodes cooperation. A wireless sensor network consists of a group of sensors or nodes connected through a linked mechanism to accomplish a distributed sensing task. Wireless sensor networks can be deployed in the conditions which are severe from the physical deployment point of view. Security aspect becomes the contemporary field of research in wireless sensor network and gaining more and more attention from scientists and researchers to proceed further [5]. Usually wireless sensor networks are deployed in an open informant where the probability of an adversary [6] always remains more than in a closed environment. There are numerous proposals to detect an adversary node in the wireless sensor networks. Traditional means to protect a network include cryptography specific techniques and methodologies. Availability of cryptographic solutions redresses the issues like authentication, authorization, confidentiality and integrity but the requirements of wireless sensor networks are more diverse than the traditional security policies. Complex computations in the cryptography strategies [7] becomes its major drawbacks and made these policies unsuitable to be deployed in wireless sensor network which constitutes severe power constraints. For the all set of services, trust is advisable and represents a key requirement that should be considered as a mandatory criterion for any application developer. Many efforts have been done so far to address the issue of trust and reputation management in several environments. Thus, for instance, a number of trust and reputation models have been proposed in the literature ranging from peer-to-peer networks [8-10], to wireless sensor networks (WSNs) [11-14], to (mobile) ad hoc networks [15-17], to multi-agent systems [18,19], or even to vehicular-to-vehicular networks [20-22]. Recently, trust and reputation management finds its place in some popular fields such as cloud computing [23-25], identity management and identity federation [26-28], Web services [29-31], and the Internet of Things [32]. Hence, it is remarkable that the wider coverage and acceptance as well as a range of scenarios makes a trust and reputation model very useful and adequate. It is appropriate to mention at this stage that some authors have already applied bio-inspired algorithms in order to perform such trust and reputation management. Some examples are Quality of Service-based Distance Vector Protocol [33], AntRep [34], Time-based Dynamic Trust Model [35] (which make use of ant colony systems [36] and ant colony optimization [37]), which further leads Bio-inspired Trust and Reputation Model for WSN (BTRM-WSN) [38]. Some of the contributors exploited the benefits of fuzzy logic and fuzzy representation which leads to to the development of models such as Comprehensive Reputation-Based Trust Model With Fuzzy Subsystems [39], A Fuzzy Reputation Agent System [40], or Pervasive Trust Management [41]. An initiative towards linguistic fuzzy logic enhancement of a trust mechanism for distributed networks was proposed by Gomez Marmol et al. [42]. We selected bio-inspired trust and reputation model for investigations in terms of accuracy, path length and energy consumption. This research focuses on the hops coefficient factor based issue and exhibits our analysis in the extremely critical environment.

Section 2 presented the BTRM-WSN trust and reputation model in wireless sensor networks. Section 3 highlights our motivation for research work. Section 4, illustrated the problem definition and system model. Section 5 describes the detailed design of our experimental setup. Simulation results and validations are presented and discussed in Section 6. Finally, conclusions are made in Section 7.

2. BTRM-WSN TRUST AND REPUTATION MODEL

This trust model for wireless sensor networks (WSN) is based on the bio-inspired algorithm of ant colony system [36-38][43-44]. In this model, most trustworthy path leads to find the most reputable service provider in a network. WSN launches a set of artificial agents while searching for a most reputable service

provider. In order to carry out a decision about next sensor, a probability is given to each arc by the following expression:

$$pk(r,s) = \begin{cases} \frac{[\tau_{rs}]^{\alpha}[\eta_{rs}]^{\beta}}{\sum[\tau_{ru}]^{\alpha}[\eta_{ru}]^{\beta}} & if\ s \in Jk(r); \\ otherwise & 0 \end{cases} \quad (7)$$

The following equation represents modification of the ants pheromone trace.

$$\tau_{s1s2} = (1 - \varphi)\tau_{s1s2} + \varphi\, \Omega \quad (8)$$

where $\Omega = (1+(1 - \varphi)(1- \tau_{s1s2}\ \eta_{s1s2}))\ \tau_{s1s2}$ denotes the convergence value of τ_{s1s2} and φ represents a parameter controlling the amount of pheromone. The best path found by all ants is given by

$$\tau_{rs} = (1-\rho)\tau_{rs} + \rho\left(1 + \tau_{rs}\eta_{rs}Q\left(S_{Global_{Best}}\right)\right)\tau_{rs} \quad (9)$$

where $Q(S_{Global\_Best})$ denotes path quality. The quality of the S_k paths can be measured as the average of all the edges belongs to that path.

$$Q(S_k) = \frac{\tau k}{\sqrt{Length(S_k)}}\%A_k \quad (10)$$

where $\%A_k$ denotes the percentage of trustworthy paths. The punishment or rewards of the path leading to the selected peer is given by

$$\tau_{rs} = (\tau_{rs} - \varphi \times df_{rs})\frac{Sat}{df_{rs}} \quad (11)$$

The distance factor joining the link between sensor *r* and *s* is given by the following equation.

$$df_{rs} = \sqrt{\frac{df_{rs}}{\mathrm{L}(S_k)(\mathrm{L}(S_k) - d_{rs} + 1}} \quad (12)$$

3. MOTIVATION FOR CURRENT WORK

To effectively exhibits and analyze the performance of a trust and reputation model remains the top priority for the wireless sensor network system. An optimal trust and reputation model can enhance the performance of the overall system, but the wireless sensor network system may not be dependent on the same. A single parameter in trust and reputation modeling strategy may give the best result for one instance, but we have to deploy such an efficient trust and reputation modeling strategies that provide optimal results in data dissemination. The improper assessment strategy may overload the entire network and consume more resources both in terms of energy and computation which result in the entire system performance degradation. There always remains dire influence of the parameters like hops coefficient, sensor augmentation and resource utilization factor in trust and reputation model of the entire operating environment when evaluating a specific wireless sensor network. The goal remains there is to carefully choose and examine the trust and reputation modeling strategies for the identification of parameters responsible for optimal information dissemination without compromising any constraints than expected outcome. Therefore, a typical realization should be required to identify the parameter contribution towards the scope of a particular trust and reputation model strategy for the wireless sensor networks.

4. PROBLEM DEFINITION AND SYSTEM MODEL

In our analysis, we consider hundred networks composed of fifty sensor nodes each for hundred scenarios in a two dimensional fields. Sensor nodes in a cluster with a specific radio range transmit the data to the cluster head and then the base station within the entire network. Network deployment focuses on hops coefficient and path length factor in the specified conditions. Although any trust and reputation sensor node strategy can be used in our model, we utilized BTRM-WSN trust and reputation model for our proposed framework. Accordingly, for static and dynamic wireless sensor network with trust and reputation model strategy mentioned above, we are concerned in finding the following two problems. (i) What is the influence of hops coefficient factor over fixed coverage area on static and dynamic communication mode of wireless sensor networks, (ii) How the BTRM-WSN trust and reputation model affect the parameters like accuracy, resource utilization and energy consumption in the said WSN system.

5. DETAILED SETUP

We focused on three parametric aspects namely: accuracy, path length and energy consumption for information dissemination in wireless sensor networks. For this, we have developed the unmitigated scenario pinpointing two main targets. Firstly, we are interested to find the value of three above mentioned parameters for stationary wireless sensor networks. We want to know the summation of all the node operations with sensor augmentation and resource utilization factor parameter. Lesser path length of node operation always given due attention as it consumes fewer resources and exhibits more efficiency. Secondly, we want to make an estimation of the sensor value variation effects on communication performance in correlation with two trust and reputation models. Finally, we made the comprehensive evaluation of energy consumption with static wireless sensor network in our proposed framework. We designed a wireless sensor network template using the following parameters. 15% of all nodes in a randomly created WSN acted as clients and the rest of 85% nodes acted as servers. 5% of the nodes acted as relay servers not offered any services and acted as relay nodes. The radio range of the nodes set at 12 hops to its neighbors. We consider a scenario where the percentage of malicious servers remained 30% which specify the indispensable condition for our WSN framework evaluation. We set the minimum and maximum number of sensors 50 that creates a WSN. Sensor nodes belonging to our developed networks spread over the area of 100 m × 100 m. A total of hundred networks were examined hundred times and the final result reflects the average value of all the networks. The process of searching trustworthy server was conducted hundred times for each network. Table 1 displays the summary of parameters deployed in our model.

Table 1 Scenario Parameters

Scenario Options	*Value*
% Client	*15*
% Relay Sever	*5*
% Fraudulent Server	*30*
Radio Range	*12*
Delay	*0*
Number Execution	*100*
Number of Network	*100*
WSN Area	*100 m × 100 m*
Minimum Number of Sensors	*50*
Maximum Number of Sensors	*50*
Hops Coefficient Factor	*0.1 - 1.0*
Node Orientation	*Static , Dynamic*

Figure 1 shows the setup of our simulation. In the simulation window, yellow dots denotes client nodes, green dots represent the benevolent nodes, red dots show malicious node, blue dots

depicts relay nodes and black dots exhibit idle nodes respectively.

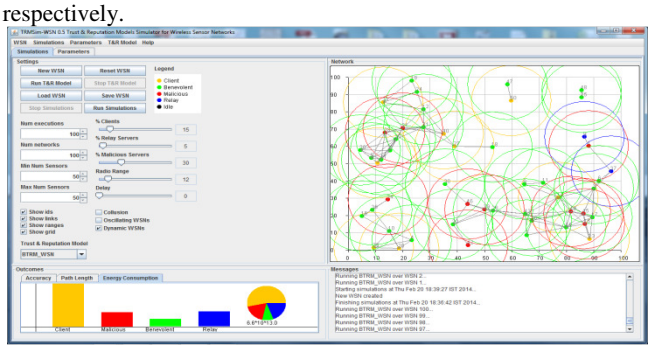

Figure 1 Simulation Scenario

6. ANALYTICAL RESULTS AND VALIDATIONS

This section enables us to implement and evaluate trust and reputation models for different wireless sensor network modes. We used Java based event driven TRMSim-WSN simulator [45] version 0.5 for wireless sensor network allowing the researchers to simulate and represent random network distributions and provides statistics of different data dissemination policies including the provision to test the different trust and reputation model strategies. Numerous decisions like static or dynamic or oscillating networks, a combination of dynamic and oscillatory networks, the percentage of fraudulent nodes, the percentage of nodes acting as clients or servers, etc. can be implemented as well as tested over it. The proposed model is tested on BTRM-WSN trust and reputation models with extreme conditions. We reported a comprehensive analysis based on hops coefficient factor and resource utilization factor over static and dynamic wireless sensor networks. We gathered data for three metrics namely accuracy, path length and energy consumption. The outcome of the simulations will be subject to the following subsections.

6.1 Accuracy Investigations

The term accuracy in the trust and reputation models may be defined as the selection percentage of trustworthy nodes. We calculated the accuracy from two viewpoints namely: current and average. Initially, we calculated current accuracy corresponds to static and dynamic WSN mode as shown in figure 2. Static WSN mode exhibits less zigzag behavior than dynamic WSN mode. In case of static WSN mode the current accuracy remained more stable as compared to dynamic mode. The reason behind the same is complex computation for accuracy calculation in dynamic WSN mode. Next we calculated average accuracy which depicts approximately similar behavior as we noticed in case of current accuracy. At the beginning and at the ending instance, average accuracy outperforms current accuracy as shown in figure 3. This is because of the fact that current accuracy reflects the resultant of one event whereas the average accuracy depicts the summation of all the events. One common observation we noticed that the accuracy reflect incremental behavior as we increase the hops coefficient values in BTRM-WSN trust and reputation model. This shows a good agreement with the results reported in reference [46]. An initiative towards the description of energy consumption analysis for different trust and reputation models was proposed in reference [46]. We enhanced this evaluation towards a bit intricate assessment by incorporating hops coefficient factor, resource utilization and energy evaluation aspect in our scenario.

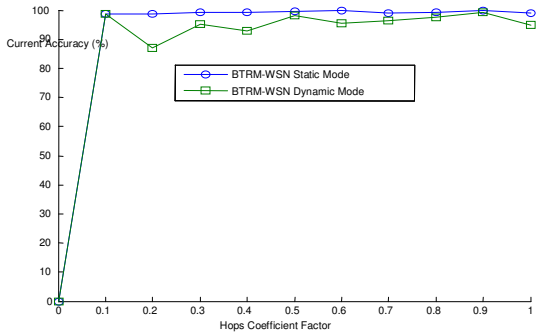

Figure 2 - Current accuracy versus hop coefficient factor in BTRM-WSN model

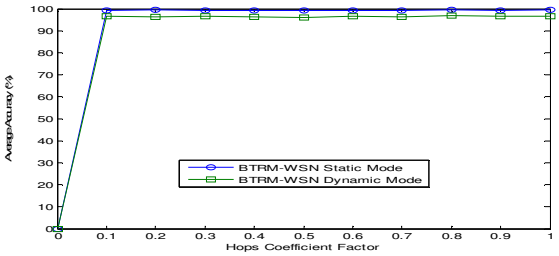

Figure 3 - Average accuracy versus hop coefficient factor in BTRM-WSN Model

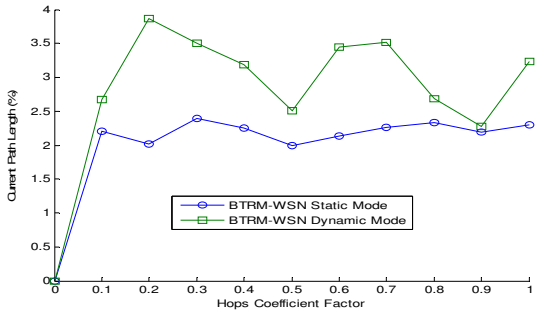

Figure 4 - Current path length versus hop coefficient factor in BTRM-WSN Model

Further we observed average path length which shows steady behavior than current path length as reported in figure 5. One common thing we analyzed that the dynamic WSN consumes more resources than the static WSN in both types of path length values.

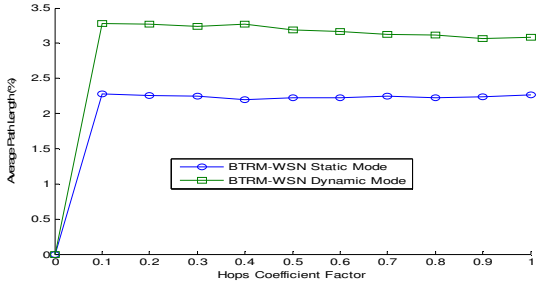

Figure 5 - Average path length versus hop coefficient factor in BTRM-WSN Model

We also observed that the Static WSN mode is more prone towards resource utilization than dynamic WSN mode. We proposed a more robust framework subsuming different WSN

nodes versus hops coefficient and resource utilization on a single platform. Verma et al. [47] presented scalability impact on the wireless sensor network. We extended this scalability concept to a further extent by adhering the hops coefficient towards the evaluation of BTRM-WSN trust and reputation model which makes our proposal more robust. Moreover Xiong et al. [48] reported peer to peer trust and reputation based model for structured peer to peer networks. including strategies for its implementation and evaluation in decentralized environmental conditions. Especially for unstructured peer to peer networks based on parameters was suggested by Chen et al. [49]. We enhanced the contribution to a certain extent by hops coefficient, path length and energy consumption parameters for wireless sensor network evaluation making our investigation more rigorous and real time.

6.4 Energy Concerns

Lastly we focused on the average energy consumption for BTRM-WSN trust and reputations model. A comparative analysis from the energy consumption aspect is shown in figure 6.

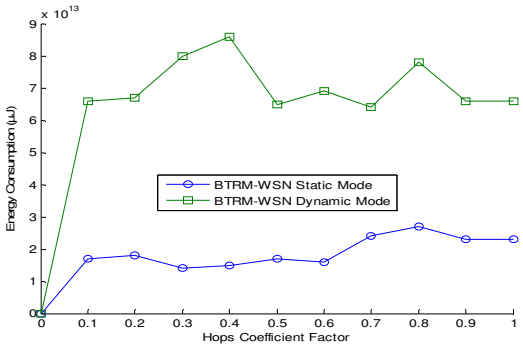

Figure 6 - Energy consumption versus hop coefficient factor in BTRM-WSN Model

We observed that the energy consumption increases with the increase in the hops coefficient factor in a zigzag manner. In case of static WSN, energy consumption exhibits gradual incremental behavior and remains maximum for the hops coefficient value 0.8 and minimum for 0.1. For the dynamic WSN mode, energy consumption remains highest at the hops coefficient value 0.4 and lowest for 0.1. Marmot. F et al. [50] reported a comparative analysis of the energy consumption with respect to sensors specific aspects. In our proposal, we extended this concept towards a more robust evaluation with the static and dynamic WSN mode.

7. CONCLUSIONS

This paper concluded the influence of hops coefficient factor on the BTRM-WSN trust and reputation models in wireless sensor networks. We have observed the effect of hops coefficient factor for static and mode of WSN. It is evident from the simulation that there is a strong relationship in between hops coefficient factor and resource utilization on the WSN modes of trust and reputation model evaluation. We evaluated a wireless sensor network framework with reference to three performance metrics namely: accuracy, path length and energy consumption viewpoint. We estimated accuracy and path length in terms of overall percentage of the functionality whereas energy consumption in terms of millijoule specifically for sensor node operations. We stressed on three major directions. Firstly, we evaluated accuracy, path length and energy consumption for BTRM-WSN trust and reputation model. Secondly, we investigated the entire framework for hops coefficient factor evaluation on above stated trust and reputation model and lastly the same model is deployed for the overall evaluation of a static and dynamic wireless sensor network. We observed that with the increment in the hops coefficient factor value reflects their strong affection and correlation in static and dynamic WSN modes. We can predict with our investigations that more the hops coefficient value better will be the probability of accuracy, optimal resource utilization and more energy consumption by the wireless sensor network system. Further we also estimated that static WSN can have more probably of accuracy, optimal path length and lesser energy consumption than the dynamic WSN mode. In the future, we would like to work towards additions on newer trust and reputation models for the wireless sensor network domain.

8. REFERENCES

[1] A. Alkalbani, T. Mantoro, and A. O. Md Tap, " Improving the Lifetime of Wireless Sensor Networks Based on Routing Power Factors", NDT , IEEE UAE Conference , Dubai, UAE, April 2012.

[2] H.Chen, H.Wu, X. Zhou, and C. Gao, "Reputation-based Trust in Wireless Sensor Networks", International Conference on Multimedia and Ubiquitous Engineering (MUE'07), 0-7695-2777-9/07.2007.

[3] Chee-Yee Chong, Srikanta P. Kumar "Sensor Networks: Evolution, Opportunities and Challenges" proceeding of the IEEE. Vol. 91, No. 8, pp.1247-56 August 2003.

[4] IF Akyildiz, W Su, Y Sankarasubramaniam, E Cayirci, A survey on sensor networks. IEEE Commun Mag. 40(8), 102–114 (2002). doi:10.1109/ MCOM.2002.1024422.

[5] Jim Esch, "A Survey of Trust and Reputation Management Systems in Wireless Communications" Proceedings of the IEEE | Vol. 98, No. 10, October 2010, Digital Object Identifier: 10.1109/JPROC.2010.2060252.

[6] J. Hurt, Y. Lee, H. Yoont, D. Choi, and S. Jin, "Trust evaluation model for wireless sensor networks," in Proceedings of the 7th International Conference on Advanced Communication Technology (ICACT '05), pp. 491–496, Phoenix Park, Republic of Korea, February 2005.

[7] Q. Jing, L. Y. Tang, and Z. Chen, "Trust management in wireless sensor networks," Journal of Software, vol. 19, no. 7, pp. 1716–1730, 2008.

[8] Kamvar S, Schlosser M, Garcia-Molina H. The EigenTrust algorithm for reputation management in P2P networks. Proceedings of the International World Wide Web Conference (WWW), Budapest, Hungary, 2003.

[9] Xiong L, Liu L. PeerTrust: supporting reputation-based trust in peer-to-peer communities. IEEE Transactions on Knowledge and Data Engineering 2004; **16**(7):843–857.

[10] Zhou R, Hwang K. PowerTrust: a robust and scalable reputation system for trusted peer-to-peer computing.Transactions on Parallel and Distributed Systems 2007; **18**(4):460–473.

[11] Boukerche A, Xu L, El-Khatib K. Trust-based security for wireless ad hoc and sensor networks. Computer Communications 2007; **30**(11–12):2413 –2427.

[12] Dhurandher SK, Misra S, Obaidat MS, Gupta N. An ant colony optimization approach for reputation and quality-

ofservice- based security in wireless sensor networks. Security and Communication Networks 2009; **2**(2):215-224.

[13] Kim TK, Seo HS. A trust model using fuzzy logic in wireless sensor network. Proceedings of World Academy of Science, Engineering and Technology, vol. 32, 2008; 69–72.

[14] Zhang Z, Ho PH, Nat-Abdesselam F. RADAR: A reputation-driven anomaly detection system for wireless mesh networks. Wireless Networks 2010; **16**:2221–2236.

[15] Omar M, Challal Y, Bouabdallah A. Reliable and fully distributed trust model for mobile ad hoc networks. Computers and Security 2009; **28**(3–4):199 –214.

[16] Buchegger S, Le Boudec JY. A robust reputation system for P2P and mobile ad-hoc networks. Proceedings of the Second Workshop on the Economics of Peer-to-Peer Systems, Cambridge MA, USA, 2004.

[17] Almenárez F, Marín A, Campo C, García C. PTM: a pervasive trust management model for dynamic open environments. Privacy and Trust, First Workshop on Pervasive Security and Trust, Boston, USA, 2004.

[18] Sabater J, Sierra C. REGRET: reputation in gregarious societies. In Proceedings of the Fifth International Conference on Autonomous Agents, Müller JP, Andre E, Sen S, Frasson C (eds). ACM Press: Montreal, Canada, 2001;194–195.

[19] Songsiri S. MTrust: a reputation-based trust model for a mobile agent system. In Autonomic and Trusted Computing, no.4158 in LNCS Third International Conference, ATC 2006. Springer: Wuhan, China, 2006; 374–385.

[20] Breuer J, Held A, Leinmller T, Delgrossi L. Trust issues for vehicular ad hoc networks. 67th IEEE Vehicular Technology Conference (VTC2008-Spring), Singapore, 2008.

[21] Raya M, Papadimitratos P, Gligor V, Hubaux JP. On data-centric trust establishment in ephemeral ad hoc networks. Proceedings of IEEE INFOCOM, Phoenix, AZ, USA, 2008.

[22] Lo NW, Tsai HC. A reputation system for traffic safety event on vehicular ad hoc networks. EURASIP Journal on Wireless Communications and Networking 2009; **2009**:1–10.

[23] Takabi H, Joshi JBD, Ahn GJ. Security and privacy challenges in cloud computing environments. IEEE Security and Privacy 2010; **8**:24–31. DOI: 10.1109/MSP.2010.186.

[24] Wang S, Zhang L, Wang S, Qiu X. A cloud-based trust model for evaluating quality of Web services. Journal of Computer Science and Technology 2010; **25**(6):1130-1142. DOI: 10.1007/s11390-010-9394-1.

[25] Hwang K, Kulkarni S, Hu Y. Cloud security with virtualized defense and reputation-based trust management. Eighth IEEE International Conference on Dependable, Autonomic and Secure Computing, Chengdu, China, 2009;717–722, DOI: 10.1109/DASC.2009.149.

[26] Gómez Mármol F, Girao J, Martínez Pérez G. TRIMS, a privacy-aware trust and reputation model for identity management systems. Elsevier Computer Networks Journal 2010; **54**(16):2899–2912. DOI: 10.1016/j.comnet.2010.07.020.

[27] Mohan A, Blough DM. AttributeTrust - a framework for evaluating trust in aggregated attributes via a reputation system. In Proceedings of the 2008 Sixth Annual Conference on Privacy, Security and Trust, 2008; 201–212. DOI: 10.1109/PST.2008.28.

[28] Windley PJ, Daley D, Cutler B, Tew K. Using reputation to augment explicit authorization. In Proceedings of the 2007 ACM workshop on Digital identity management, DIM '07, 2007; 72–81.

[29] Conner W, Iyengar A, Mikalsen T, Rouvellou I, Nahrstedt K. A trust management framework for service-oriented environments. Proceedings of the 18th International Conference on World Wide Web, WWW '09, 2009; 891–900, DOI: 10.1145/1526709.1526829.

[30] Malik Z, Bouguettaya A. RATEWeb: Reputation Assessment for Trust Establishment among Web services. The VLDB Journal 2009; **18**(4):885–911. DOI: 10.1007/s00778-009-0138-1.

[31] Bianculli D, Jurca R, BinderW, Ghezzi C, Faltings B. Automated dynamic maintenance of composite services based on service reputation. Proceedings of the 5th International Conference on Service-Oriented Computing, ICSOC '07, 2007; 449–455. DOI: 10.1007/978-3-540-74974-5_42.

[32] Sachin B, Parikshit M, Antonietta S, Neeli P, Ramjee P. Proposed security model and threat taxonomy for the Internet of Things (IoT). In Recent Trends in Network Security and Applications, Third International Conference, CNSA 2010, Communications in Computer and Information Science vol. 89, Natarajan M, Selma B, Nabendu C, Dhinaharan N (eds): Chennai, India, 2010; 420–429.

[33] Dhurandher SK, Misra S, Obaidat MS, Gupta N. An ant colony optimization approach for reputation and quality-ofservice-based security in wireless sensor networks. Security and Communication Networks 2009; **2**(2):215-224.

[34] Wang W, Zeng G, Yuan L. Ant-based reputation evidence distribution in P2P networks. In GCC, Fifth International Conference on Grid and Cooperative Computing. IEEE Computer Society: Changsha, Hunan, China, 2006; 129–132.

[35] Zhuo T, Zhengding L, Kai L. time-based dynamic trust model using ant colony algorithm. Wuhan University Journal of Natural Sciences 2006; **11**(6):1462–1466.

[36] Dorigo M, Stützle T. Ant Colony Optimization. Bradford Book: Cambridge, MA, 2004.

[37] Cordón O, Herrera F, Stützle T. A review on the ant colony optimization metaheuristic: basis, models and new trends. Mathware and Soft Computing 2002; **9**(2–3):141–175.

[38] Gómez Mármol F, Martínez Pérez G. Providing trust in wireless sensor networks using a bio-inspired technique.Telecommunication Systems Journal 2011; 46(2):163–180.

[39] Tajeddine A, Kayssi A, Chehab A, Artail H. PATROL-F-a comprehensive reputation-based trust model with fuzzy subsystems. In Autonomic and Trusted Computing, no.4158 in LNCS Third International Conference, ATC 2006. Springer: Wuhan, China, 2006; 205–217.

[40] Carbó J, Molina JM, Dávila J. Trust management through fuzzy reputation. International Journal of Cooperative Information Systems Mar 2003; **12**:135–155.

[41] Almenárez F, Marín A, Campo C, García C. PTM: a pervasive trust management model for dynamic open environments. Privacy and Trust, First Workshop on Pervasive Security and Trust, Boston, USA, 2004.

[42] GómezMármol F, Gómez Marín-Blázquez J,Martínez Pérez G. Linguistic fuzzy logic enhancement of a trust mechanism for distributed networks. Proceedings of the Third IEEE International Symposium on Trust, Security and Privacy for Emerging Applications (TSP-10), Bradford, UK, 2010; 838–845. DOI: 10.1109/CIT.2010.158.

[43] Dorigo, M., & Gambardella, L. "Ant colony system: a cooperative learning approach in the traveling salesman problem".IEEE Transaction on Evolutionary Computing, 1(1), 53–66.1997.

[44] Dorigo, M., Gambardella, L., Birattari,M., Martinoli, A., Poli, R.,& Stützle, T. (2006). Ant colony optimization and swarm intelligence in LNCS: Vol. 4150. 5th international workshop, ANTS 2006. Brussels: Springer, 2006.

[45] Félix Gómez Mármol, Gregorio Martínez Pérez, "TRMSim-WSN, Trust and Reputation Models Simulator for Wireless Sensor Networks", IEEE International Conference on Communications (IEEE ICC 2009), Communication and Information Systems Security Symposium, Dresden, Germany, 14-18 June 2009.

[46] A. S. Alkalbani, A.O. Md. Tap, T. Mantoro "Energy Consumption Evaluation in Trust and Reputation models for Wireless Sensor Networks", 5th International Conference on Information and Communication Technology for the Muslim World, 2013.

[47] Vinod Kumar Verma, Surinder Singh, N.P Pathak., "Analysis of scalability for AODV routing protocol in wireless sensor networks", Optik-International Journal of Light and Electron Optics .Sciencedirect, (2013), http://dx.doi.org/10.1.016/j.ijleo.2013.07.041.

[48] L. Xiong and L. Liu, "PeerTrust: Supporting Reputation-Based Trust for Peer-to-Peer Electronic Communities," IEEE Trans. Knowledge and Data Eng., vol. 16, no. 7, pp. 843-857, 2004.

[49] S. Chen Y. Zhang G. Yang ,"Parameter-estimation based trust model for unstructured peer-to-peer network's" IET Communication, 2011, Vol. 5, Issue 7, pp. 922–928 & The Institution of Engineering and Technology 2011, www.ietdl.org doi: 10.1049/iet-com.2010.0619

[50] Go´mez Ma´rmol F, Martı´nez Perez, G. Providing trust in wireless sensor networks using a bio-inspired technique. In Proceedings of the networking and electronic commerce research conference, NAEC'08. Lake Garda, Italy; Sep 2008.

CFD Study of Regional Air-conditioning System in Room

Nguyen Anh TUAN
Ministry of Science and Technology
Hanoi, The Socialist Republic of Vietnam
and
Huy Bich NGUYEN
Nong Lam University
Hochiminh city, The Socialist Republic of Vietnam
and
K. D. HUANG
Vehicle Engineering Department, National Taipei University of Technology
Taipei, R.O.C, Taiwan

ABSTRACT

The regional air conditioning mechanism (RACM) can control the airflow in the workroom for the purpose of achieving a regional steady-state temperature. With this concept, each staff in a different area of the location can be satisfied with respect to their own local environment. The RACM was constructed of a main duct inlet-outlet round ports. The numerical simulation of many cases in a symmetrical two dimensional (2-D) instead of 3-D could save computing time and still maintain the physical properties of the system were conducted in this study with varying relative distance between inlet and outlet port, inlet port height, and outlet port height to obtain the optimal airflow and temperature distribution and thermal comfort indices in occupied zone. Based on low intake airflow velocity magnitude, the laminar model has been investigated for numerical simulation of airflow in different 9 cases. A solution-adaptive mesh refinement is brought to refine and coarsen model to enable the physical feature of the flow field to be better resolved. The CFD simulation results predicted that the RACM could successfully establish a regional air-conditioning cell, an individual personal-comfort, and RACM inferred more energy efficient than a typical air conditioning system. The concepts in this study are relevant to all kinds of regional air conditioning in any enclosed space.

Keywords: Energy-saving, Regional air conditioning, Airflow management

1. INTRODUCTION

In a highly developed life, more and more people are seeking for a comfortable living conditions. Air conditioning has become a popular comfort providing device for two decades. It has become a need for everyone, whether in an office or any closed space especially for warm and wet climate as in Taiwan. People are looking for an independent temperature zone controlled in a workroom that can be more pleasant, comfortable, healthy, and safety, energy efficient. In these opinions, a theory of personalized air conditioning systems has been showed and rightly remains a central concern in designing intelligent workplaces since the early 1990s [1].

Zeng and Kacsmarczyk [2] investigated personalized ventilation systems (PVS), whose design allows each occupant to control his/her air flow direction, temperature and select options according to their personal thermal comfort demands. In their study they showed that the perceived air quality of PVS is superior to the conventional mixing ventilation system given the same amount of supply air.

Cho et al. [3] presented a personal environment module (PEM), which was constructed of two diffusers connected by flexible ducts, a main fan, a mixing box with two variables, speed fans and filters. The PEM as an alternative air conditioning system for improving thermal comfort in workspaces has been studied. Comparisons with a typical under floor (UFAC) system were conducted. The advantages of the PEM are not only that it can be controlled flexibly and easily, but also that it offers significant potential for improving thermal comfort in workspaces.

Fanger et al. [4-6] proposed that personalized ventilation can improve occupant's thermal comfort, the perceived air quality and decrease the intensity of SBS symptoms as compared to mixed ventilation. Occupants will use the provided individual control of airflow rate and positioning of the air terminal device to obtain their preferred micro-environment in rooms where the air temperature is within the range recommended by indoor climate standards. They recommend development of more efficient air terminal devices.

Murakami et al. in 2007 [7] proposed a new system to control air-conditioning systems, lighting systems, etc. via occupants' requests. That system collects occupants' requests from their own personal computers and controls the air-conditioning system with logic balances the needs of occupants and energy consumption. The Logic for Building a Consensus was used and could be adjusted according to operating strategies such as energy-saving or occupants' satisfaction with their environment. The results of experiments show that this interactive system could save 20% more energy compared with controlling an air-conditioning system at a constant 26 ^{0}C.

Tuan [8] further studied and analyzed the concept of regional air conditioning in the workroom using RACM modules. Based on three case studies, the numerical simulations showed that the airflow occupation appeared to provide the best thermal comfort according to occupants' preferences and also reduced much of the energy loss for systems if intake air velocity was set at 0.8 m/s. Other simulation results have also been presented by the authors [9], who investigated steady state flow and heat transfer within a modeled room using the RACM setup. Many different parameters were studied with different inlet air temperatures, air supply flow rates, outlet vacuum pressures and outlet port positions. Relative to the optimizing building's energy saving, ensuring the occupants' comfort, and preserving air quality in conventional air-conditioning, there were some studies that were pointed out that such as: Novel evaporative cooling system with an automatic wind and automatic wind-tracking device, the origination, development and current status of chilled ceiling, displacement and combination systems for energy savings are discussed [10–12]. The numerical simulation of airflow in room with chilled ceilings and ceiling-mounted devices were shown and analyzed to improve energy-efficient and comfortable condition of air-conditioning system [13]. Although much work has been done to date, more studies need to be conducted to ascertain the effect of air conditioning systems in contributing to energy thrift. In this paper, the numerical predictions of regional air conditioning mechanism in a room were study are useful for the prediction of the temperature and velocity

Nomenclature

T	temperature
h_1	inlet port height
h_2	outlet port height
g	gravity acceleration
ρ	density of fluid
t	time
v	velocity magnitude
τ_{ij}	is stress tensor
P	pressure
L	height of RACM
d	diameter of RACM
F_i	external body forces
h	height of model room
D	diameter of model room
L_1	distance between inlet port and floor
L_2	distance from floor to outlet port
e	internal energy
E	total energy
H	specific enthalpy
	X, Y Cartesian coordinates
β	thermal expansion coefficient
ε	turbulence kinetic energy dissipation rate
μ	dynamics viscosity
ϕ	dependent variable
I	number of interactions
S_m	the mass added to the continuous phase
S_h	includes heat of any other volumetric heat sources

air flow distribution conducted in several research groups. The results of this in the room by using RACM. The RACM could create a circulation air flow zone within which the desired level of high thermal comfort is achieved. This topic could be of benefit to manufacturers by predicting the necessary characteristics to fabricate a real RACM product to be produced for use in the real world.

2. SYSTEM ANALYSIS

The RACM is a personal cooling system, which is integrated by air-conditioning, a blower fan, a regional air conditioning system, a suck fan and two dampers, as shown in Fig. 1. The main air-conditioning supplies air cooling to RACM by the blower fan. The RACM can turn on a circulation airflow zone. During operating process, the cooling air will channel through the damper, regulate the cooling air and activate the occupied zone to generate a comfortable zone according to the opening angle of damper. The cooling air will direct to RACM, where the cooling air will exchange the heat with occupied zone in the room, after that the cooling air was suck back to the main air conditioning by a suck fan with the aim of recycling the cooling air from occupied zone. Thus, this system can not only satisfy thermal comfort occupants' required, but also significantly reduce the energy consumption of the air conditioning system.

3. MODELING METHOD

3.1. Physical and mathematical model

A regional air conditioning mechanism (RACM) is located in the centre of the virtual room. An upper round part has been designed for air inlet and a lower round part has been

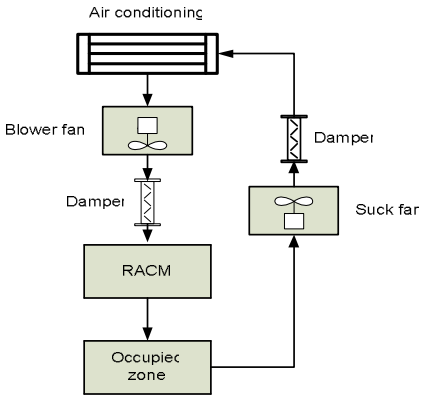

Fig. 1 Construction of RACM in room

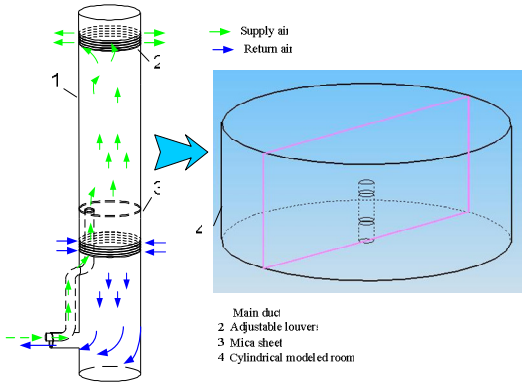

Fig. 2 The RACM system in cylindrical room

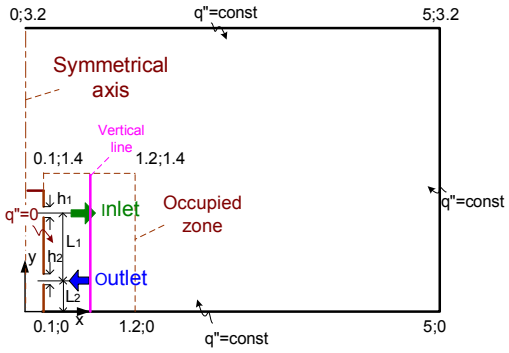

Fig. 3 Physical model of the simulated room

designed for air outlet on the main pipe of the RACM module. The RACM is connected to the central cooling system by pipes as shown in figure 2. The distributed cooling air at occupied zone also was regulated by adjustable louvers on inlet port and outlet port to create the most comfortable occupancy. To improve the air flow distribution feature for space for human occupancy the adjustable louvers were fastened on inlet and outlet. Above part of fan blow and below part of fan suck were separated by a mica sheet to eliminate the effect on each other between two hot and cool fluid flows. The RACM enable the occupants to satisfy with respect to their own thermal comfort demands. Since the RACM is placed in the centre of a cylindrical room, the surrounding space is a symmetrical plane, thus, the simulations were analyzed in a symmetrical plane 2D model instead of a 3D model. This 2D simulation was applied to save computing time while still maintaining the physical

properties of the model as presented in Fig. 3. Moreover, the use of a 2-D model enables a higher quality and density of numerical mesh geometry. The initial unstructured mesh system was applied to discretise the model and high density mesh at the inlet and the outlet flow region using Gambit software [15]. A computational model of the room with a RACM module was constructed using the CFD software of FLUENT Inc. (Fluent 6. 3). After simulation running one time, using solution-adaptive refinement such as gradient adaption of temperature, the model can be refined by adding cells at occupied zone to enable the physical feature of the independent temperature field to be better resolved and coarsen the rest of model room. When adaption is used properly, the resulting mesh is optimal for the flow solution. In other words, computational resources are not wasted by the inclusion of unnecessary cells in the rest of model, as in the structured grid approach. Therefore, the mesh quality of gradient adaption seems to better than initial mesh in the same laminar viscous model, and then the gradient adaption has been chosen for further simulation. Thus, the mesh had 11555 elements in total.

3.2 Simulation method

Assumptions are made with respect to the simulation of this study as follows:
(1) Newtonian fluid
(2) Unsteady state
(3) Effects of gravity and buoyancy are considered
(4) Uniform air velocity at the outlet
(5) Laminar flow

3.3. Governing equations

There are three groups of basic equations, which are derived from there basic physics laws of conservation. The mass conservation, momentum conservation and energy conservation are results in the continuity respectively. Since the flow in an air conditioning mechanism cell is laminar flow [14], the laminar viscous model has been chosen for investigation. The standard wall function was used in the simulation of near-wall treatment. In the simulation including the radiation model, the radiation heat transfer between walls was computed by switching the discrete ordinates (DO) model [14].

The conservation equations for laminar flow are presented: The mass conservation equation, or continuity equation, can be written as follows:

$$\frac{\partial p}{\partial t}+\frac{\partial}{\partial x_i}(\rho u_i)=S_m \qquad (1)$$

Momentum conservation equations can be written as follows:

$$\frac{\partial}{\partial t}(\rho u_i)+\frac{\partial}{\partial x_j}(\rho u_i u_j)=-\frac{\partial p}{\partial x_i}+\frac{\partial \tau_{ij}}{\partial x_j}+\rho g_i+F_i \qquad (2)$$

The stress tensor τ_{ij} is given by

$$\tau_{ij}=\left[\mu\left(\frac{\partial u_i}{\partial x_j}+\frac{\partial u_j}{\partial x_i}\right)\right]-\frac{2}{3}\mu\frac{\partial u_l}{\partial x_l}\delta_{ij}$$

The conservation for energy is written as follows:

$$\frac{\partial}{\partial t}(\rho E)+\frac{\partial}{\partial x_i}(u_i(\rho E+p))=\frac{\partial}{\partial x_i}\left(k_{eff}\frac{\partial T}{\partial x_i}-\sum_j h_j{}' J_{j'}+u_j(\tau_{ij})_{eff}\right)+S_h \qquad (3)$$

Where t is time, is the mass density, is the flow velocity, p is the fluid pressure. The source S_m is the mass added to the continuous phase from the dispersed second phase and any user-defined sources, is stress tensor (described above), and and F_i are the gravitational body force and external body viscous dissipation, respectively. S_h includes heat of any other volumetric heat sources, h is sensible enthalpy [14]. forces in the (i) direction, three term on the right hand side of Equation (3) represent energy transfer due to conduction, species diffusion, and to solve these equations, initial and boundary condition must be specified around the boundary of system. Because the equations are highly nonlinear, they are not solvable by explicit, closed-form analytical methods. The numerical finite volume method as used in Fluent has been used for solving the equations. The domain is discretized into cell or elements and nodal points are defined. Upon solution of the equations, the values of the dependent variables are known at the nodal points [14].

Table 1 Flow boundary condition and geometrical parameters of RACM inlet and outlet

Names	V_{in} (m/s)	T_{in} (K)	P_{out} (Pa)	L_2(m)	Cases
	0.3	293	-4	0.5	1
Group 1	0.4	293	-4	0.5	2
	0.5	293	-4	0.5	3
	0.3	293	-2	0.5	4
Group 2	0.4	293	-2	0.5	5
	0.5	293	-2	0.5	6
	0.3	293	-2	0.3	7
Group 3	0.4	293	-2	0.3	8
	0.5	293	-2	0.3	9

3.4. Boundary conditions

The air flow equations were solved for the selected conditions for air inlet and outlet and wall boundaries. The velocity and temperature of inlet air as well as the negative outlet pressure were chosen for all nine cases as indicated in Table 1. Heat flux of vertical, ceiling, floor wall was 3 W/m^2. The surfaces of the walls of the respectively. F_i also contains others model-dependent source terms such as porous-media and user-defined sources, k_{eff} is the effective conductivity, the first room were assumed to have an absorptivity of 0.85. Adiabatic wall condition was chosen for RACM walls. The distance between inlet port and floor surface (L_1) was 1.3 m. RACM height (L) and diameter (d) was 1.5 m and 0.2 m, respectively. The inlet height port (h_1), outlet port height (h_2) was 0.08 m. The temperature inlet of 20 ^{0}C was set for the model in the overall simulations.

3.5. Impact of physical and geometrical parameters on RACM

In order to investigate the impact of the in-outlet parameters of RACM on the distribution of airflow in the room, nine cases were conducted and were divided into three groups of three cases each. Both groups one and two had the same geometry parameters, but were placed under different negative outlet pressure conditions as shown in Table 1. Meanwhile group three considers the change of distance between room surface and outlet port (L_2), and other parameters are the same as group 2. Each case in the same group has a different cooling air inlet velocity as depicted in Table 1.

4. THERMAL COMFORT INDICES

The thermal environment required for occupants in a room can be calculated by using:

(i) General thermal comfort - PMV (Predicted Mean Vote), PPD (Predicted Percentage of Dissatisfied occupants) and operative temperature T_0.

(ii) Local thermal comfort - vertical air temperature profiles, temperature and velocity field, drafts.

4.1. Operative temperature

Following the ISO (International Organization for Standardization [16]), the operative temperature is influenced by the air temperature and the mean radiant temperature given by:

$$T_o = A \bullet T_{oz} + (1 - A) \bullet T_{mr}$$

Where T_{oz} is the air temperature of the occupied zone and Tmr is the mean radiant temperature. Where the relative velocity is less than 0.2 m/s or where the difference between the mean radiant and the air temperature is small (< 4 ^{0}C), the operative temperature can be calculated with sufficient approximation as the mean value of air and the mean radiant temperature (A =5) [15]. This means that mean radiant temperature and air temperature are equally important for the level of thermal comfort in a zone. According to ASHREA–55, the values of operative T_0 shall be between 23 ^{0}C and 26 ^{0}C when applied to mainly sedentary occupants' summer cooling period.

The difference in the vertical air temperature between the feet and the head must be considered when determining conditions for acceptable thermal comfort. The vertical temperature profiles are a function of sedentary occupant height. One measure indicates that the most comfortable thermal environment is achieved when air temperature at head level is lower than temperature of floor surface level. Following the ISO 7730 [15], the vertical air temperature difference between 1.1m and 0.1 m (head and ankle level) shall be less than 3 ^{0}C. Occupants' feet will feel uncomfortable when they come into contact with floor surfaces that are of too high or too low a temperature. In international standards, it is recommended that the range of the floor surface temperature shall be 19–29 ^{0}C in the occupied zone where sedentary occupants wear normal shoes [16].

4.2. Predicted mean vote (PMV)

The thermal comfort of the occupied zone is another important issue. The thermal comfort of the occupied zone can be predicted by calculating the PMV proposed by Franger [5]. Man's thermal sensation is mainly related to the thermal balance of his body as a whole. This balance is influenced by physical activity and clothing, as well as the environmental parameters: air velocity, air temperature, mean radiant temperature (MRT), relative humidity of the air. One measure points out that high thermal comfort is achieved when the PMV index is in the range of $-0.5 < PMV < +0.5$ [16].

5. RESULTS AND DISCUSSION

Based on the theory that the airflow convection effect is much stronger than the diffusion effect, this aim of this research is to limit the air energy to a certain region by means of creating a circulation cell. The inlet flow speed acts as the inertia and negative outlet pressure provides the centrifugal force to form a circulation cell. Therefore, the RACM can make the office room into a region with different temperature sections without any partitions. In this study, a total of nine simulations set in a hypothetical summer cooling period were carried out by using FLUENT. The simulated room has dimensions of 3.2 m height (h) and 10 m diameter (D) as shown in Fig 2. The left corner of the modeled room (length = 0.1–1.2 m; height = 0–1.4 m) is intended to correspond to the occupied zone of the room.

5.1. Temperature and velocity field

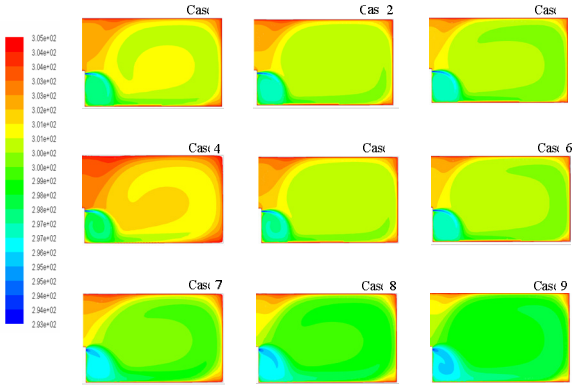

Fig. 4 Air temperature distribution in room with RACM installation

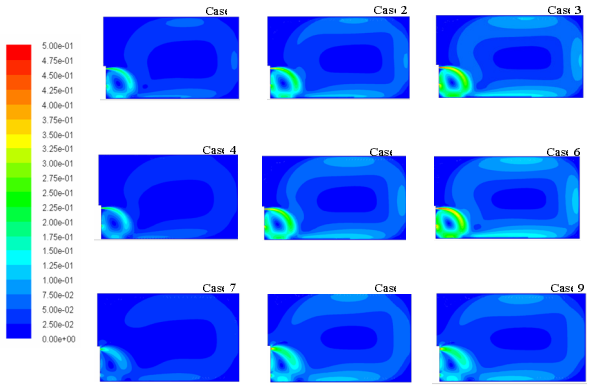

Fig 5. Air velocity distribution in room with RACM installation

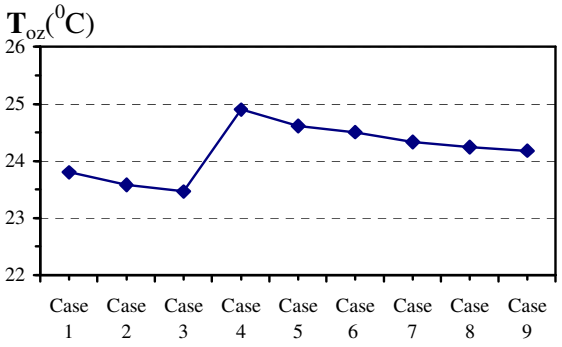

Fig 6. Mean temperature variation of occupied zone

CFD simulations of temperature and velocity distributions in an unsteady state during a five hundred second simulation were carried out for all three groups. Figures 4 and 5 depict the thermal environment in the modelled room. As depicted above, the corner of the left side corresponds to the occupied zone. It is apparent from these figures that the RACM can be a circulation cell in an occupied zone. This is to be expected because the cool inlet flow speed acts as the inertia and negative outlet pressure provides the centrifugal force needed to form a circulation cell.

It can be found the difference of the distribution pattern in the occupied zone between group one (corresponding to cases one, two and three) and group two (corresponding to cases four, five and six) as change negative outlet pressure (P_{out}). While in group three (corresponding to cases seven, eight and nine) impacts on the outlet position (L_2) create the temperature and velocity field in comparison with that of groups one and two. It is also seen from the figures that the circulation airflow zone is less uniform in group three as the outlet position is

moved down to L_2 = 0.3 m. The average air temperature in these zones is in the range 23.86–24.89 ^{0}C as shown in Fig. 2. and is lower than that of the rest zone of the room, two thermal environment areas are created in the room as observed in Fig .5. The average air velocity in these zones is in the range 0.091–0.164 m/s as shown in Fig. 7. This is the criterion for weak wind, which is the most comfortable velocity magnitude to occupant as observed in Fig .4. To summarize, the distribution patterns in Figs 4 and 5 show that an occupant is more likely to feel comfortable at the corner left side in the room with RACM. The circulated distribution flows around the occupied zone and the type of temperature and velocity profiles guarantee a suitable thermal environment for the occupants' demands. The energy loss increases as air inlet velocity increase and if the air inlet velocity is set lower than the recommended value of 0.3 m/s, the circulation airflow cell can not be established. Presumably the reason for this is that the air inlet kinetic energy is not sufficiently high enough for the cooling air to reach as far as the underneath outlet part and the surface floor to create a circulation airflow zone. Therefore, to create the circulation airflow zone, the cooling air supply should be more than the recommended value.

5.2. Operative Temperature

Occupied zone temperature and MRT were computed by Fluent. The temperature at occupied zone decrease with increasing Vin in the same group as shown in Fig. 6. This is because of the increase of cooling inlet airflow. Moreover, the Toz in the group 2 will increase as the outlet vacuum pressure decreases. Presumably, because lower sucked outlet pressure appears, thus, the cooling circulation in the group 2 is not concentrate as much as in the group 1. Meanwhile, the Toz in the group 3 will decrease as decrease the outlet port position in comparison with that of group 2. The reason for this is that more cooling circulation concentrated at occupied zone. Fig. 6. shows that the increase of mean radiant temperature with increasing V_{in} are because of the increase of potential energy of inlet cooling air. These results were used for calculating the operative temperature as presented in Fig. 7. These temperaturescould provide a high thermal environment within the occupied zone given the acceptable operative temperature is between 23 ^{0}C and 26 ^{0}C in a summer cooling period [15].

5.3. Predicted mean vote (PMV)

The temperature at occupied zone and MRT and assumed to be 50% in the room, clothing insulation is 0.5 clo and metabolic level is assumed to be 1.0 met for sedentary occupants during summer conditions. Most of the PMV values for the RACM module are higher than -0.5 as the allowable PMV index is in the range of $-0.5 < PMV < +0.5$. Except for cases two and three, the PMV offers the lower potential with PMV<-0.5.

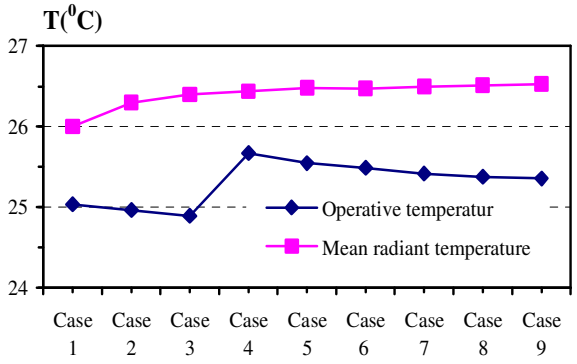

Fig 7. Operative temperature and mean radiant temperature variation of occupied zone

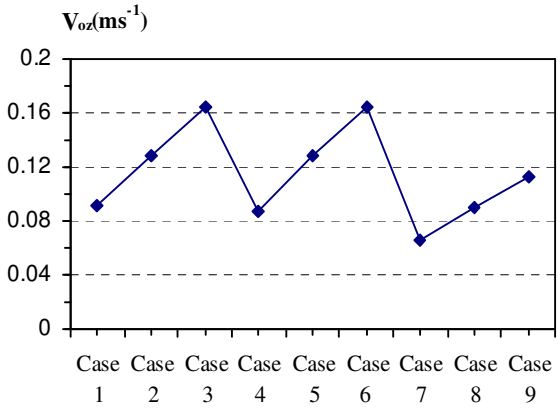

Fig 8. Mean velocity variation of occupied zone

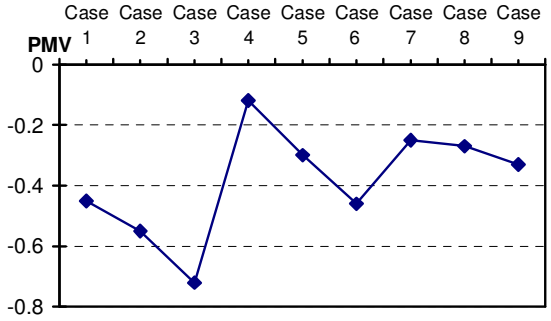

Fig 9. PMV Variation of occupied zone

Presumably because high air inlet velocity value and high sucked outlet pressure appear in these two cases, theirs are out of the criteria range. It is also predictable from figure 9 that the PMV offers a higher potential for thermal comfort as the cooling supply air inlet velocity decreases in each research group.

6. CONCLUSIONS

Numerical predictions of distribution patterns in a room with regional air conditioning mechanism (RACM) are reported that show:

An air-flow circulation cell can easily be formed. The inlet flow speed acts as the inertia and the outlet vacuum pressure provides the centrifugal force to form a circulation cell.

Air convection dominates inside the cell; cells only air diffusion takes place; there is no mixing effect. Since the convection effect of airflow is much stronger than diffusion, the energy and concentration can basically be kept inside the cell. Therefore the regional air-conditioning mechanism can be successfully established.

The operative temperature results provided a good thermal environment for the occupied zone in the range of 24.89-25.66 ^{0}C this meets the operative temperature requirement of between 23 ^{0}C and 26 ^{0}C during a summer cooling period.

The thermal comfort PMV index has shown higher potential with groups two and three, whereas the value in the case of group one is lower. In addition, the PVM index effect increases as cooling supply air loads are decreased for each research group.

This concept can be applied to any closed air-conditioning environment such as in a bus, a train and a factory, etc.

ACKNOWLEDGMENT

This work was supported by The National Foundation for Science and Technology Development (NAFOSTED), The Socialist Republic of Vietnam.

REFERENCES

[1] C.W. Churchman, **The Design of Inquiring Systems**, New York: Basic Books Inc. Pub., 1971.

[2] J. Ivari, "A Paradigmatic Analysis of Contemporary Schools of IS Development", **European Journal of Information Systems**, Vol. 1, No. 4, 1991, pp. 249-272.

[1] R.J. Caddirey, **The intelligent building- an ASHAE opportunity**, ASHREA transaction, No. 1, 1988, pp. 925-933.

[2] Q. Zeng, J. Kaczmarczyk, A. Melikov, P.O. Fanger, **Perceived air quality and thermal sensation with personalized ventilation system,** Proceedings of 8th International Conference of Air Distribution in Rooms-Room Vent 2002, 2002, pp 61–64.

[3] S.H. Cho, W.T. Kim, **Thermal characteristics of a personal environment modules task air conditioning system: an experimental study**, Energy Conversion and Management, No.42, 2001, pp. 1023–1031.

[4] A.K. Melikov, **Personalized ventilation**, Indoor Air, No. 14, 2004, pp. 157–167.

[5] P.O. Fanger, **Indoor air quality in the 21st century: search for excellence**, Indoor Air 2000, 10, pp. 68–73.

[6] J. Kaczmarczyk, A.K. Melikov, and P.O. Fanger, **Human response to personalized ventilation and mixing ventilation, Indoor Air**, No. 14, 2004, pp. 17–29.

[7] Y. Murakami, et al, **Field experiments on energy consumption and thermal comfort in the office environment controlled by occupants" requirements from PC terminal**, Building and Environment, No. 42, 2007, pp. 17– 27.

[8] N.A. Tuan, T.C. Liu, K.T. Tseng, **An air conditioning energy-saving mechanism**, the 19th international symposium on Transport Phenomena, Reykjavik, (2008).

[9] N.A. Tuan, K.T. Tseng, **A numerical of regional air conditioning mechanism**, IEEE International Conference on Sustainable Energy Technologies, 2008.

[10] D. Faulkner, W. J. Fisk, D. P. Sullivan, D. P. Wyon, **Ventilation efficiencies of task/ambient conditioning systems with desk-mounted air supplies**, Indoor Air, No. 9, 1999, pp. 273–81.

[11] J. Niu, N. Gao, M. Phoebe, H. Zuo, **Experimental study on a chair-based personalized ventilation system**, Building and Environment No. 42, 2007, pp. 913□25.

[12] W. Sun, K.W. Tham, W. Zhou, N. Gong, **Thermal performance of a personalized ventilation air terminal device at two different turbulence intensities**, Building and Environment No. 42, 2007, pp. 3974□83.

[13] S. Wantanabe, A. Melikov, G. Knusdsen, **Design of an individually controlled system for an optimal thermal microenvironment**, Building and Environment No. 45, 2010, pp. 549□58.

[14] FLUENT 6.3, Fluent Inc, Lebanon, NH 03766, USA: FLUENT Inc. 2006.

[15] GAMBIT 2.4. User guide, all volumes. Lebanon, NH 03766, USA: FLUENT Inc., 2007.

[16] Thermal Environmental Conditions for Human Occupancy, ANSI/ASHRAE standard 55–1992.

AUTHORS INDEX